STUDIES IN

VANADIUM CHEMISTRY

*

by

MD. ABDUS SALAM

B.Sc. (Hons.), M.Sc., University of Rajshahi, Bangladesh

*

A Thesis presented for the Degree of Doctor of Philosophy

Department of Physical and Inorganic Chemistry

The University of Adelaide

Awarded 28th July 1986.

JUNE 1986

STUDIES IN VANADIUM CHEMISTRY

SUMMARY

The chemistry of vanadium in the +4 oxidation state is dominated by the very stable $[V=O]^{2+}$ grouping. This 'vanadyl' moiety acts as a coordination centre forming many stable mononuclear complexes with a variety of ligands. The research project explores some other less well known aspects of the chemistry of the element, in particular, the formation of dimeric vanadyl complexes and the ability of V^{4+} to form chelate complexes not containing the oxo group. An important aspect of the preparative work has been the identification of the type of chelating ligands which stabilize these less common types of vanadium complexes.

The synthetic work on the dimeric alkoxo-bridged oxovanadium(IV) complexes of the type $[VO(AA)(OR)]_2$ has established that such complexes can be formed with a restricted type of bidentate ligands (AA = anion of β-diketone or o-hydroxy aldehyde or ketone) and with primary or secondary alkoxide bridges. The dimeric nature of $[VO(acac)(OMe)]_2$ has been confirmed by its X-ray crystal structure determination. Similar dimeric structures are postulated for all the prepared complexes on the basis of their sub-normal magnetic moments, mass spectra and their characteristic E.S.R. spectra and other spectroscopic properties. In a number of complexes the study of the magnetism over an extensive range of temperature has permitted the calculation of J, the coupling between the unpaired electron on each of the two vanadyl centres as well as understanding the mechanism of the magnetic exchange in these dimers.

The novel non-vanadyl vanadium(IV) complexes of the type VL_2 have been prepared from three types of dinegative tridentate ligands, L^{2-} which are: (a) Schiff bases of aroylhydrazines with β-diketones or o-hydroxy aromatic carbonyl compounds,

(b) Schiff bases of o-aminophenols with the same carbonyl compounds and

(c) 2,2'-dihydroxyazoarene dyes.

In all cases the ligands are planar, with the donors ⁻O N O⁻ forming a five- and a six-membered chelate rings. The crystal structures of four of these VL_2 complexes with different ligand systems show their general preference for the uncommon trigonal prismatic geometry which have been discussed explicitly in terms of d^1-electronic configuration, ligand geometry and the bite sizes of the chelate rings. The unusual stabilization of the V^{4+} ion in the absence of the oxo function in the VL_2 complexes may be attributed to π-electron donation from four strongly basic phenolic and/or enolic oxygen donors in a flattened tetrahedral arrangement provided by two dinegative tridentate ligands. These complexes show strong LMCT bands in the visible region and characteristic E.S.R. spectra.

A number of VO^{2+} and VO^{3+} complexes containing the same L^{2-} have been prepared in an attempt to elucidate the reaction mechanism of the formation of VL_2. With type (a) ligands, reaction of equimolar amounts of $VOCl_2$ and LH_2 has been found to give readily oxidizable $(VOL)_2$ or VOLHCl from which in turn the vanadium (+5) complexes VOL.OR and $(VOL)_2O$ have been prepared. In these complexes, as the crystal structures of VO(Bzac-BH).OEt and $[VO(Bzac-BH]_2O$ show, the vanadium has a square pyramidal coordination. The monomeric $V^{IV}OLHCl$ can be used to form mixed ligand complexes of the type VLL'.

The electrochemical study of VL_2 complexes showing a reversible V^{IV}/V^{III} wave in the region (-)0.050 - (-)0.400 V vs S.C.E. can be used as an aid to identify and characterize such complexes.

'With all these present bis-tridentate non-vanadyl vana-dium(IV) chemistry being known, it is now not inappro-priate to strongly re-state Floriani's[64] conclusion that the classic statement concerning the low reactivity of VO^{2+} must be revised.' -

STATEMENT

This thesis contains no material which has been accepted for the award of any other degree or diploma in any University, and to the best of my knowledge and belief, contains no material previously published or written by another person, except where due reference is made in the text of the thesis.

(MD. ABDUS SALAM)

ACKNOWLEDGEMENTS

ABBREVIATIONS

The abbreviations listed below have been used throughout the text of this thesis.

acac	Acetylacetone	Me	Methyl
Bzac	Benzoylacetone	Et	Ethyl
dbm	Dibenzoylmethane	Pr^n	n-Propyl
HNP	2-Hydroxy-1-napthaldehyde	Pr^i	iso-Propyl
HAP	2-Hydroxyacetophenone	Bu^n	n-Butyl
Sal	Salicylaldehyde	Bu^2	sec-Butyl
BH	Benzoylhydrazine	Ph	Phenyl
SalH	Salicyloylhydrazine	Bz	Benzyl
OAP	o-Aminophenol	EtOMe	2-Methoxyethyl
3-am-2-nap	3-Amino-2-napthol	EtOEt	2-Ethoxyethyl
β-nap	β-napthol	LiOAC	Lithium acetate
Erio T	Eriochrome Black T	AA	Bidentate ligand

The abbreviations for the dibasic tridentate Schiff base ligands (LH_2) were derived from those of the component aldehyde/ketone and the amine, e.g. the Schiff base derived from condensation of acetylacetone and benzoylhydrazine was abbreviated as acac-BHH_2; that from benzoylacetone and salicyloylhydrazine as Bzac-$SalHH_2$; that from 2-hydroxy-1-napthaldehyde and o-aminophenol as HNP-$OAPH_2$; etc. The tridentate azo dyes were also abbreviated using abbreviations of the diazonium and the coupling components, e.g. the azo dye derived from coupling of diazonium salt of o-aminophenol and β-napthol was abbreviated as OAP-β-nap; etc. These tridentate ligand abbreviations are given in Section 6.5 after the name of each ligands.

I.R.	Infrared	br	broad
UV	Ultraviolet	sh	shoulder
N.M.R.	Nuclear Magnetic Resonance	m	medium
E.S.R.	Electron Spin Resonance	s	strong
B.M.	Bohr Magenton	ms	medium strong
nm	nanometer	w	weak

CONTENTS

CHAPTER   1

INTRODUCTION

1.1   COORDINATION CHEMISTRY OF VANADIUM

The number of publications in the inorganic literature concerned with the chemistry of vanadium is rather small compared to other transition metals. This is in part due to its limited involvement in bioinorganic chemistry as compared to the extensive roles of other metals, especially iron and copper in a number of key physiological and numerous essential proteins and enzymes. Only in recent years, there has been some interest in the biochemistry and physiology of vanadium[1], compounds of biological significance, especially vanadyl(IV) porphyrins[2].

One of the interesting features of vanadium chemistry lies in its being an early transition metal and its capacity to exhibit oxidation states ranging from -1 to +5 with the high oxidation +5 and +4 states being the most stable. Particularly stable is the +4 oxidation state which is the most common for vanadium and not often found in the other first series transition metals. The complexes of vanadium vary widely in their redox properties from those of vanadium(V) which are generally oxidising to those of vanadium in the +2 and lower states which are strongly reducing.

Because of its isotopic composition [mass numbers 50(0.24%) and 51(99.76%)], the mass spectra of the vanadium complexes can be easily interpreted and are of great help in synthetic work. The presence of only one d electron in the +4 oxidation state, combined with a nuclear spin of 7/2, gives rise to easily resolvable eight-line electron spin resonance spectra which are of great value in studying the chemistry of this state.

1.2   OXOVANADIUM(IV) COMPLEXES

The chemistry of vanadium is dominated by the stable vanadium(IV) - oxo species commonly referred to as the vanadyl, VO^{2+} entity. The VO bond is essentially a double bond which involves π-bonding through donation of charge from the filled $2p_\pi$ orbitals of the oxo ligand into the vacant $3d_{xz}$ and $3d_{yz}$ orbitals on vanadium. It is this transfer of electronic charge to the high oxidation V^{4+} centre which stabilizes the VO^{2+} entity and enables it to act as a discrete coordination centre. The most characteristic feature of the oxovanadium(IV) complexes is the sharp and strong $V = O$ stretching frequency observed[3] in their infrared spectra at 985 ± 50 cm^{-1}, corresponding to a $V = O$ force constant of $k = 7.0 \pm 0.7$ md/A°. This $\nu V = O$ serves as a diagnostic tool for identification of the vanadyl oxygen in the oxovanadium(IV) complexes.

The oxovanadium(IV) ion is probably the most stable diatomic oxocation known and it forms an extensive range of anionic, cationic and neutral complexes with a variety of ligands[4-9]. These complexes generally exhibit five coordination which may be increased to six by accepting a ligand in the vacant site trans to the vanadyl oxygen. However, some recent work[10-14] has shown that the sixth ligand may have a cis arrangement with respect to the vanadyl oxygen as was found in the crystal structures of $VO(acac)_2$.4-phenylpyridine by Caira et al.[12] and $[VO(bipy)_2Cl]^+$ by C.J. Hawkins[14]. Caira et al.[10] suggested on the infrared evidence that the $VO(acac)_2$.B (B = several substituted pyridines) could be classified into either cis or trans isomers depending on the pyridine substituent. Similar suggestions have been made[11] for the $VO(AA)_2$.4-methyl-pyridine N-oxide adducts (AA = anion of acetylacetone, benzoylacetone or dibenzoylmethane).

The $V = O$ stretching frequency is quite sensitive to the nature of the cis or trans ligand. Donors that increase electron density on the metal ion by transferring charge into the same d orbitals of vanadium as the oxo ligand reduce its acceptor properties towards O, thus lowering both the V-O multiple

bond character and the infrared stretching frequency. The VO^{2+} entity is so stable that it has a discrete existence in compounds in the solid state, in fused state, in solution and in the vapour state[4]. The inertness of the oxo ligand is reflected by its very slow exchange rates[15,16], in contrast to the rates of donor atoms at the other positions which are comparable to those in other +2 cations[17].
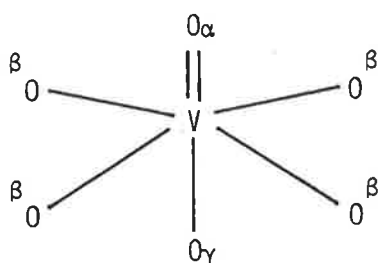
Oxygen	Position	Residence Time (sec)
α	Vanadyl	$\simeq 1.8 \times 10^4$
β	Equatorial	1.35×10^{-3}
γ	Trans	$\simeq 10^{-11}$

Figure 1.2.1: O^{17} exchange for $VO(H_2O)_5^{2+}$ in aqueous solution at room temperature.

The coordination of VO^{2+} is often compared with that of Cu^{2+} in which, due to Jahn-Teller effects, the principal coordination sites are the corners of a square plane.

1.2.1 OXOVANADIUM(IV) CHELATES WITH O AND/OR N-DONOR AROMATIC OR QUASI-AROMATIC LIGANDS

In most of these complexes, the ligands are β-diketones or aromatic 2-hydroxyaldehydes or ketones, or the Schiff bases derived from their condensation with a variety of amines such as hydrazines, alkanolamines, o-hydroxy arylamines and diamines. Such Schiff bases may act as bidentate, tridentate or tetradentate ligands.

(a)   BIDENTATE LIGANDS

β-diketones (AA<u>H</u>), having at least one hydrogen on the α-carbon atom and capable of exhibiting keto-enol tautomerism[18] react with VO^{2+} to form $VO(AA)_2$ complexes, in which the vanadium replaces the enolic hydrogen thereby shifting the keto-enol equilibrium in favour of the enol form. These metal-β-diketonates, with six-membered chelate rings, exhibit aromatic behaviour. For example, substitution of the α-proton bears a close resemblance to various electrophilic substitution reactions in the benzene ring[19]. The β-diketones and o-hydroxyaldehydes or ketones exhibit high pK_a values, give rise to planar chelate rings and can act as pπ donors to form $VO(AA)_2$ or related Schiff base complexes. An advantage of these ligands is their numerous substituent derivatives with varying electron-withdrawing capabilities which can be correlated to the stability, bonding, electrochemical and stereochemical properties of their complexes.

The X-ray crystal structure determinations of $VO(acac)_2$[20] and $VO(Bzac)_2$[21] show a five coordinate square pyramidal arrangement with the vanadium atom lying ~ 0.5Å above the plane formed by the four singly-bonded oxygen atoms of the diketone ligand. The extensive reviews by Selbin[4,5] summarize the chemistry and properties of many such $VO(AA)_2$ complexes. Many of them form six coordinate adducts with Lewis bases like ammonia, pyridine, bipyridyl and phenanthroline[10,11,22-24].   Recently the E.S.R.[25], magnetic properties[26] and electrochemistry[27] of such complexes have attracted interest.

The chemical reactions of these complexes were investigated with considerable attention only after 1960[19] with an objective of exploring new preparative methods for a variety of their derivatives. Interests in the $VO(AA)_2$ type complexes in the present study are their use to prepare (i) some alkoxo-bridged vanadyl dimers of the type $[VO(AA)(OR)]_2$, containing only one such (AA) ligand per vanadium in which the square pyramidal structure is completed by the bridging alkoxo groups, and (ii) some non-oxo vanadium(IV) complexes of the type VL_2 containing some Schiff base ligands formed <u>in situ</u> by the

reactions of the VO(AA)$_2$ with aroylhydrazines under appropriate conditions (Chapter 3.1.2).

(b) TRIDENTATE SCHIFF BASES

Because of the great synthetic flexibility of Schiff base formation, many ligands of diverse structural type have been synthesized by condensing various ketones or aldehydes with different amines, such as diamines, alkanolamines, hydroxyarylamines, hydrazines, etc. Schiff bases derived from β-diketones, or o-hydroxyaldehydes or ketones, and aroylhydrazines have keto-enol tautomeric equilibrium associated with the β-diketone as explained above and the aroyl-hydrazine part[28]. The extensive delocalization over both systems favour enol-ization to a greater extent than the individual components giving rise to a potentially dinegative ligand. It is also possible to obtain the Schiff bases, in situ, during reactions of some metal aldehyde or ketone complexes with suitable NH$_2$- containing compounds. In certain cases[29,30] this is the only way to obtain the desired ligand. In the present work, such reactions were used advantageously, especially with acetylacetone-hydrazone complexes where attempts to prepare the Schiff base by condensing acetylacetone with benzoylhydrazine resulted in the formation of a cyclized product. A large number of Schiff base complexes of oxovanadium(IV) with a variety of donor atoms have been reported[4-9,31]. L. Sacconi[32] prepared and studied a number of VO - Schiff base complexes of general formula [X-Salen-N(R)(R')]$_2$VO in which V is coordinated to two identical Schiff bases, and [(X-Sal)(X-Salen-N(R)(R')]VO, in which V is linked to one salicylaldehyde and one Schiff base (X = H, 5,6-benzo- or 5-chloro- and R = CH$_3$, H, C$_2$H$_5$, C$_6$H$_5$, etc.). The authors believe that the Schiff bases behave as bidentate ligands coordinating through the oxygen and the imine nitrogen in the former case and as tridentate ligands in the latter complexes.

However, the present study is confined to the dinegative Schiff bases (LH$_2$) which have the ability to protonate the vanadyl oxygen giving rise to

uncharged $V^{IV}L_2$ type complexes. Vanadyl(IV) complexes of such ligands are known and conform to two types, viz. the VOLX, where, X is a mono or bidentate ligand and the dimeric $(VOL)_2$ complexes which are characterized by their subnormal magnetic moments and most of which contain the dibasic tridentate ligands having O͡N͡O or O͡N͡S donor atoms. Zelentsov[33-35] prepared some VO-complexes of the Schiff bases derived from 5-R-salicylaldehyde and 5-R'-ortho-aminophenol (R = H , R' = H, Cl, Br and R = NO_2, R' = Br). Ginsberg et al.[36] prepared these as well as some new complexes with substituted Schiff bases where, R = H, R' = H, CH_3, Cl, Br, NO_2; R = Cl, R' = H, Cl and R = NO_2, R' = H, Br, NO_2. On the basis of the magnetic data, they suggested a dimeric structure. Similar dimeric structures were proposed by several workers[37-39] for the oxovandium(IV) complexes of the various Schiff bases derived from 2-hydroxy-1-napthaldehyde and 4-R', 5-R substituted o-aminophenols. Similar complexes of Schiff bases derived from salicylaldehyde or substituted salicyl-aldehyde and 1-napthylmethylamine[40] or o-hydroxybenzylamine[41] or alkanola-mines[42,43] were also proposed on the basis of their infrared, electronic and E.S.R. spectral data and subnormal magnetic moments, to have dimeric configur-ations. Unfortunately, no crystal structure on any of this type of dimers has yet been determined probably because of the difficulty in growing suitable crystals due to their insolubility or instability in solution[44]. The elect-ronic spectra of many of these insoluble complexes were obtained by reflect-ance from the solid or as a mull and were interpreted in terms of the Ballhausen-Gray orbital scheme[45]. Also most E.S.R. spectra of the above dimers were obtained with solid undiluted powders[6].

Although Dua et al.[46] reported some oxovanadium(IV) complexes of some tridentate benzoylhydrazones and characterized them as oxovanadium(IV) dimers, we believe from our study (Chapter 4) that these compounds were really (hydrazonato)oxovanadium(V) alkoxides or at best a mixture of this and little VO(IV) monomer.

(c) QUADRIDENTATE SCHIFF BASES

This type of ligand is of less interest to our work because such ligands are well-suited to square pyramidal coordination and hence are less likely to form non-oxo vanadium(IV) chelate complexes. Quadridentate Schiff bases derived from salicylaldehyde and polymethylenediamines react with oxovanadium (IV) sulphate to give complexes of formula $[VO(OC_6H_4CH = N-C\ R'\ R''\ (CH_2)_{n-1}-N = CH\ C_6H_4O)]$ (n = 2, R', R'' = H or CH_3; n = 3-10, R' = R'' = H)[47]. The ligand bis(5-methyl-2-hydroxypropiophenone)ethylenediamine complexes with VO^{2+} [48,49]. The Schiff bases derived from β-diketones, e.g. 2,4-pentanedione, 2-methoxophenylbutane-1,3-dione or 2-methoxophenylpentane-1,3-dione with 1,2-diaminoethane also give mononuclear complexes with VO^{2+} [50,51].

1.3 NON-VANADYL VANADIUM(IV) COMPLEXES

As has been stated earlier, the stable VO^{2+} is present as a discrete unit in a wide variety of complexes[4,5,7] a great many of which exhibit square-pyramidal coordination. Six coordination complexes of the simple V^{4+} ion in which the vanadium is not attached to a doubly bonded oxygen atom are rare, especially with chelating ligands. The non-oxo complexes are common with chlorine as the donor atom and with some sulphur containing chelating ligands having shorter bites.

Octahedral $[V(en)_3]F_4$, VF_6^{2-} and VCl_6^{2-} were reported in the mid-sixties[7]. The widely studied vanadium(IV) halides[7] of the type VX_4 (most studied compounds are with X = Cl) are found to be unstable, extremely reactive and rapidly hydrolysed in water to give vanadyl complexes. In most other protonic solvents, e.g. ammonia, amines, alcohols, etc. an incomplete hydrolysis occurs resulting in the product VCl_2S_2 [7] (S = deprotonated solvent). VCl_4 forms mostly octahedral adducts with one or two ligand molecules attached through oxygen-, sulphur-, selenium-, nitrogen-, phosphorus- and arsenic-donors[7,52,53]. An interesting eight coordinated adduct with bidentate o-phenylenebisdimethylarsine, $[VCl_4.2\ diars]$ is known to possess a dodecahedral

structure[54]. Compounds of the type $V(OR)_4$ [55,56] are also unstable and highly susceptible to hydrolysis.

In contrast to VX_4 type complexes, the tris non-vanadyl complexes of bidentate sulphur donor ligands, such as dithiolenes[57] possessing generally trigonal prismatic geometry are stable to hydrolysis. The tris-(cis-1,2-diphenylethane-1,2-dithiolato)vanadium(IV), $V(S_2C_2Ph_2)_3^{2-}$ possesses a distorted trigonal-prismatic coordination[58,59]. The structure of $[(CH_3)_4N]_2$ $[V(S_2C_2(CN)_2)_3]$ (where, $S_2C_2(CN)_2^{2-}$ = maleonitriledithiolate ion) shows a distorted coordination geometry[60] intermediate between a trigonal prism and an octahedron. It has been suggested that eight coordination vanadium(IV) complexes of some bidentate dialkyl dithiocarbamates, e.g. $[V(S_2CN Et_2)_4]$ have a dodecahedral[61] configuration. $V(dtpa)_4$ and $V(dta)_4$ [where, $dtpa^-$ and dta^- are the dithiocarboxylates $C_6H_5-CH_2CSS^-$ and CH_3-CSS^- respectively] have been shown to be dodecahedral in structure[62].

Floriani et al.[63,64] recently reported the preparation of some novel six coordinated octahedral VCl_2L_4 (where, L_4 = an O,N donor tetradentate or two bidentate ligands) type complexes by the reaction of the corresponding VOL_4 complexes with $SOCl_2$. These dichloro derivatives are very sensitive to hydrolysis and regenerate the starting oxovanadium(IV) complexes. That is, the two Cl atoms can reversibly replace the oxo function,

$$VOL_4 \underset{H_2O}{\overset{SOCl_2}{\rightleftharpoons}} VCl_2L_4$$
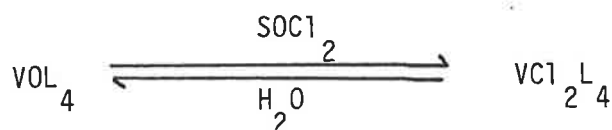
These VCl_2L_4 type complexes can also be prepared directly from VCl_4 and the ligand. For example, $[V(Salen)Cl_2]$ (Salen = N,N'-ethylenebis(salicyliden-iminato) anion) can be obtained from VO(Salen) and $SOCl_2$ as well as from the direct reaction of VCl_4 and $SalenH_2$ [64]. PCl_5 can also be used as a deoxygenating agent instead of $SOCl_2$.

An X-ray analysis shows the $[V(Sal-N-Bu)_2Cl_2]$ molecule to be octahedral[64] with elongation along the Cl-V-Cl direction. The $[V(Sal-N-R)_2Cl_2]$ (R = Bu^n,

PhCH$_2$, Ph, p^{Cl}C$_6$H$_4$) complexes can be used as precursors of other substituted complexes and organovanadium(IV) compounds in which the V–C bond is stabilized by Schiff base ligands[65]. Following Floriani's method, A. Jezierski and J.B. Raynor[66] prepared a number of six-coordinated VX$_2$L and VX$_2$L'$_2$ (X = Cl, Br) type complexes and measured their E.S.R. spectra. The reaction of SOX$_2$ or (COX)$_2$ (X= Cl or Br) with oxovanadium(IV) porphyrinates gives the very reactive dihalo derivatives[67] which are remarkable because they can act as precursors of low-valent vanadium porphyrins. Most recently, M. Tirant and T.D. Smith[68] studied some reactions of the bis(salicylaldehydehydrazone) vanadium(IV) dichloride with some aromatic and heterocyclic amines and obtained in each case the complex of the type V(SalH)$_2$(aminato)$_2$ (SalH = salicylaldehyde hydrazone) formed by the elimination of the reactive chlorine anion as hydrogen chloride.

Van Dreele and Fay[69] reported V(diketonato)$_2$X$_2$ type complexes before Floriani. They also reported the first cationic complexes, [V(dik)$_3$]$^+$Y$^-$(dik = acac or dpm; Y = FeCl$_4^-$ or SbCl$_6^-$) prepared by reaction of V(dik)$_2$Cl$_2$ with Lewis acids FeCl$_3$ or SbCl$_5$.

The first report of non-vanadyl complexes with bidentate oxo-ligands was in 1971 when Henry, Mitchell and Prue[70] prepared the tris-chelated complexes of vanadium(IV) with 1,2-dihydroxybenzene (catechol, cat) and its substituted derivatives of the type Tl$_2$[V(RC$_6$H$_3$O$_2$)$_3$] (R = H, 3-Me, 4-Me, 3-MeO). They suggested an octahedral structure for the complex ion, V(RC$_6$H$_3$O$_2$)$_3^{2-}$ which later was found to be true when Cooper, Koh and Raymond[71] determined the crystal structure of the complex [Et$_3$NH]$_2$[V(cat)$_3$].CH$_3$CN. Some studies of the (Et$_3$NH)$_2$[V(4-X-cat)$_3$] (X = H, NO$_2$, 4-t Bu), Ba[V(cat)$_3$] and (Et$_3$NH)$_2$[V(2,3-Nap)$_3$] (2,3-Nap = anion of 2,3-dihydroxynapthalene) have been carried out in the laboratories of A.A. Diamantis[72].

Diamantis in 1976 discovered the novel VL$_2$ (L^{2-} = a dinegative tridentate O N O donor ligand) type six-coordinated non-vanadyl vanadium(IV) complex, bis[pentane-2,4-dionebenzoylhydrazonato (2-)] vanadium(IV), in which the V has
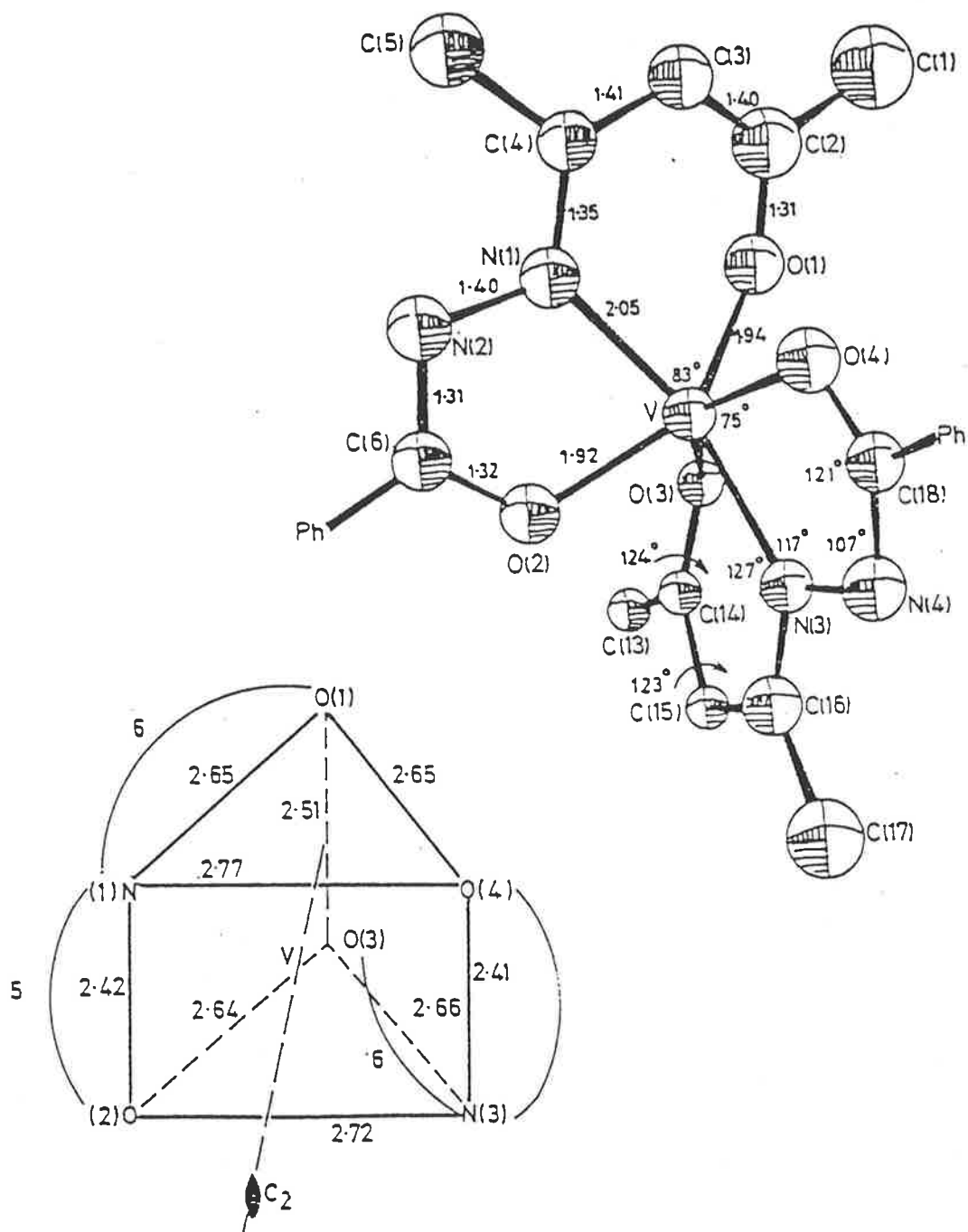
Figure 1.3.1: The crystal structure of V(acac-BH)$_2$.

the unusual trigonal prismatic geometry[73]. Later, in the same laboratory, D. Fairlie[74] and I.W. Roberts[75] prepared V(Bzac-BH)$_2$ and V(Sal-BH)$_2$ respectively. The most interesting feature of these stable VL$_2$ type complexes are the elimination of the oxo function of the vanadyl(IV) species and the subsequent formation of a six-coordinate complex with the trigonal prismatic geometry (Figure 1.3.1). The ligand acac-BH forms a 5-membered and a 6-membered chelate ring and the bite of the former ring (see Figure) is the smallest of any 5-membered ring reported. The trigonal prismatic coordination geometry was attributed to this small bite with the 5-membered chelate rings occupying two of the short edges of the T.P.

1.4 OXOVANADIUM(V) COMPLEXES

The chemistry of vanadium(V), like that of vanadium(IV), is also dominated by the presence of the vanadyl, VO^{3+} group and all the vanadium(V) compounds encountered in this project are of this type. In strongly acid aqueous solution, cis-dioxo VO_2^+ group also exists and many salt and complexes containing this grouping have been characterized crystallographically[76,79]. Vanadium in its +5 state has a d^0 ground state and its complexes are coloured because of their ligand to metal charge-transfer bands.

VOCl$_3$ undergoes several addition reactions to give five or six coordinated addition complexes of the types VOCl$_3$.L [80,81] and VOCl$_3$.2L with a variety of oxygen or nitrogen donor ligands, L [7,82,83]. In these complexes, VOCl$_3$ acts as an acceptor. Depending on the reaction conditions, VOCl$_3$ undergoes solvolytic reactions with ligands containing a replaceable hydrogen atom to give various substitution products, e.g. VO(OMe)$_3$, VOCl$_2$(OMe), VOCl$_2$(OEt), VOCl(OEt)$_2$, VOCl$_2$(acac), VOCl(acac)$_2$ [7,83] and VOCl(N-phenylbenzohydroxamato (-1))[84]. An X-ray crystal structure study of VO(OMe)$_3$ [85] shows that the molecule consists of dimeric units linked in linear polymer chain through one of the μ-alkoxo group giving the vanadium atom an octahedral coordination.

The alkoxo (OR) complexes of the type $VO(OR)L_n$ in which the other positions are occupied by bidentate[86,87] or tridentate[88,89] or quadridentate ligands are also known[88]. The crystal structure of oxoisopropoxobis(8-hydroxyquinolinato)vanadium(V), $VO(OPr^i)(oxine)_2$ [86] shows that the vanadium atom in this molecule is octahedrally complexed.

A few oxo-bridged complexes are known in which the structure

$$\begin{array}{c} O \\ \parallel \\ V \text{---} O \text{---} V \\ \phantom{V \text{---} O \text{---}} \parallel \\ \phantom{V \text{---} O \text{---}} O \end{array}$$

is present with, the other coordination positions of each V atom being occupied by a variety of ligands such as two bidentate, N,N-diethylhydroxylamino $(ONEt_2)$ groups[90], two bidentate 8-quinolinato groups[91] and one tridentate 2-(2'-hydroxyphenyl)-iminomethylphenato group[92] and their crystal structural studies showed the central vanadium atom to be 6,6 and 5-coordinated respectively. In the case of $[VO(ONEt_2)_2]_2O$, the μ-O can be replaced by $C_2O_4^=$ yielding the complex $[VO(ONEt_2)_2]_2C_2O_4$ [93] in which, as proposed by the authors, the $VO(ONEt_2)_2$ groups are bridged by the tetradentate μ_4-oxalato ligand thereby causing a seven coordination environment around each V atom.

The μ-oxo complexes react reversibly with alcohol to give the monomeric alkoxo compound (94) according to the equation,

$$L_2V(O)\text{-}O\text{-}(O)VL_2 + 2\ ROH \rightleftharpoons 2\ VO(OR)L_2 + H_2O.$$
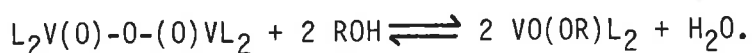
The reaction is formally analogous to the esterification of a carboxylic acid anhydride.[94a]

1.5 OUTLINE OF RESEARCH AIMS

The vanadyl, V = O, moiety with a charge of +2 acts as a coordination centre forming many stable mononuclear complexes with a variety of ligands. The major aim of this research project was to explore some other, less well-known aspects of the chemistry of the element, in particular the ability of V^{4+} to form complexes not containing the oxo group and the formation of dimeric vanadyl complexes. An important aspect of the preparative work has been the identification of the type of chelating ligand which stabilizes these less common types of vanadium complexes. The main project of this research is

divided into three sections.

(i) ALKOXO-BRIDGED OXOVANADIUM(IV) COMPLEXES

Although several dialkoxo-bridged Cu(II), Cr(III) and Fe(III) complexes are known[95-97], no such complexes of VO(IV) had been reported. The aim of this project was to prepare a range of 5-coordinate alkoxo-bridged oxovanadium(IV) complexes of the form $(AA)VO(OR)_2VO(AA)$ involving different mononegative bidentate ligands ($AA\underline{H}$) of varying sizes and electron withdrawing capacities and to examine some of their properties, especially their spectroscopic properties with the aim of gaining an understanding of their electronic structures and bonding. Of particular interest was the study of the magnetic exchange interaction between the two bridged centres over an extended temperature range. The determination of a single crystal X-ray structure of $[VO(acac)(OMe)]_2$ was undertaken with the aim of establishing the type of dimerization involved for which there was evidence from other experimental studies. However, during the course of our detailed investigation of these complexes, there appeared a report[98] of the crystal structure of the same compound.

(ii) BIS-TRIDENTATE NON-VANADYL VANADIUM(IV) COMPLEXES

The first trigonal prismatic non-vanadyl vanadium(IV) complex of the type VL_2 with dinegative tridentate pentane-2,4-dionebenzoylhydrazone as the ligand ($L\underline{H}_2$) was discovered in this laboratory by A.A. Diamantis[73], this which originated a novel field as to the possibility of eliminating the oxo function of the stable V = O group thus having available all six coordination positions to make simple V(IV) chelates. The aim of the present study was to extend research on this type of complexes and to investigate the range and type of dibasic tridentate ligands capable of forming such complexes. The other aims of this project were (a) to study the geometry of the coordination in these novel complexes, (b) to study the mechanism of the formation of these complexes, (c) to investigate the possibility of the formation of mixed ligand

VLL' type complexes, (d) to study their various spectroscopic properties, and (e) to study their detailed electrochemical behaviour and see if this could be used to characterize their formation and as a possible analytical tool.

(iii) COMPLEXES OF OXOVANADIUM(IV) AND (V) WITH TRIDENTATE LIGANDS

The aim of this section was to study the intermediates in the formation of VL_2 complexes. Tridentate ligands, L, are known to form monomeric VOLX [X = H_2O, ophen or $(py)_2$] [37] or $(VOL)_2$ type dimers[6]. The latter are easily oxidizable[92], especially in solution. Our intention was to see whether such VOLX or $(VOL)_2$ complexes occur as intermediates in our system with the hydrazone Schiff base ligands by using preparative and spectroscopic techniques. The secondary aim was to study the oxidation products of the type $V^VOL.OR$ and $(V^VOL)_2O$ which were readily formed from $(VOL)_2$. Of particular interest was their structures and physicochemical properties especially in comparison /in relation to the coordination of L in the VL_2 complexes.

C H A P T E R   2

ALKOXO-BRIDGED   OXOVANADIUM(IV)   DIMERS

2.1   GENERAL INTRODUCTION

The vanadyl(IV) entity, VO^{2+}, forms numerous monomeric complexes with a variety of ligands[4,5,7-9]. Although a number of dimeric oxovanadium(IV) complexes of tridentate ligands are known[6], no such dimeric complexes containing aromatic or quasi-aromatic bidentate ligands have been reported. The interest in the dialkoxo-bridged oxovanadium(IV) complexes containing mononegative bidentate ligands arose when Diamantis[99], on refluxing $VO(acac)_2$ in ethanol, in the presence of phenylhydrazine, accidentally discovered the product $[VO(acac)(OEt)]_2$ in studying the reactions of $VO(acac)_2$ with various substituted hydrazines. Later studies established the product, $[VO(\beta-diketonato)(OR)]_2$, to contain two bridging alkoxo groups. Dimeric alkoxo-bridged compounds of other transition metals, such as Cu(II), Cr(III) and Fe(III) are well characterized[95-97,100-104]. These are prepared,

(i) By direct reaction of the appropriate metal salt and the bidentate ligand in the stoichiometric ratio in an excess of the desired alcohol in the presence of a base[96-97,103]. The Fe(III) complexes[103] were obtained by the oxidation of such a mixture containing the Fe(II) salt. In the case of the Cu(II) complexes[101] the ligand used in excess acted as a base, or

(ii) By bridging two metal centres, already attached to the bidentate ligands, in EtOH in the presence of a base[96]. In some cases, a coordinated ligand molecule provided the base making available the coordination positions needed for the bridging group[103,104].

Bradley et al.[105], in their book on metal alkoxides, described a few vanadium(IV) alkoxides of the type $V(OR)_4$ and a vanadyl(V) alkoxide, $VO(OMe)_3$. These compounds contain both bridging and terminal alkoxo groups. Although a number of analogous Ti(IV) alkoxides have been well-studied structurally, no crystal structure of any vanadium(IV) alkoxide is known. Molecular weight determinations show that vanadium tetramethoxide is trimeric, tetraethoxide is dimeric, whereas the tetra-n-propoxide, n-butoxide and n-amyloxide show average degree of association of 1.38, 1.31 and 1.27 respectively[55]. These compounds are easily hydrolysable.

For the present project, a number of $[VO(AA)(OR)]_2$ type dimers have been prepared by treating $VO(\beta\text{-diketonato})_2$ in appropriate dry and oxygen-free alcohol with phenylhydrazine. Alternative synthetic procedures not utilizing phenylhydrazine have also been developed. A metathesis reaction procedure has been successfully used to prepare the higher alkoxo-bridged dimers.

An interesting aspect of dimeric complexes is the magnetic couplings of the unpaired electrons on the component metal ions. Dimeric complexes are convenient model compounds for studying such magnetic interactions. Magnetic studies of various ligand bridged dimers involving metal-metal interactions have been useful in understanding certain features of the chemistry of metalloproteins and enzymes[106-108]. Hodgson[100] reviewed a number of halogen-, hydroxo- and substituted hydroxo- (including alkoxo-) bridged dimers of the first series transition metals and described mechanisms of magnetic couplings of the unpaired electrons in them. The presence of an unpaired electron on each vanadium atom in $[VO(AA)(OR)]_2$ makes the dimer a suitable system for such magnetic studies. A determination of their magnetic behaviour over an extended range of temperature, together with their spectroscopic and structural investigations was undertaken so as to characterize fully the dimer system. However, during the course of our detailed investigations of these

dimers, there appeared a report[98] on the structure of $[VO(acac)(OMe)]_2$. Before the appearance of this report, we had already determined the crystal structure of this dimer which we report here for comparison.

2.2   FORMATION OF DIMERIC COMPLEXES

The dimeric $[VO(AA)(OR)]_2$ complexes have been obtained using three general methods, viz. (i) from $VO(\beta-diketonato)_2$ complexes, (ii) direct synthesis from $VOCl_2$ and (iii) the methathesis reaction.

(i)   FROM $VO(\beta-DIKETONATO)_2$ COMPLEXES

Some dimeric $[VO(\beta-diketonato)(OR)]_2$ complexes (Table 2.2.1) were prepared by refluxing $VO(\overline{\beta-diketonato})_2$ and $PhNHNH_2$ (1:1) in the appropriate alcohol, ROH. The reaction did not proceed when other bases, such as Et_3N or LiOAC were used instead of $PhNHNH_2$. This clearly rejected our primary idea that $PhNHNH_2$ simply acted as a base and led to a further investigation of its role. It was found that $PhNHNH_2$ removes one of the ligands from $VO(\beta-diketo-nato)_2$ to form a cyclic 3,5-dialkyl derivative of 1-phenylpyrazole (D.P.P.). For example, the reaction of $VO(acac)_2$ and $PhNHNH_2$ in MeOH to give $[VO(acac)(OMe)]_2$ proceeds according to the equation,

$$2\ VO(acac)_2 + 2\ PhNHNH_2 + MeOH(solvent) = [VO(acac)(OMe)]_2$$

$$+2 \quad \text{(1-phenyl-3,5-dimethylpyrazole)} \quad +\ 4\ H_2O.$$
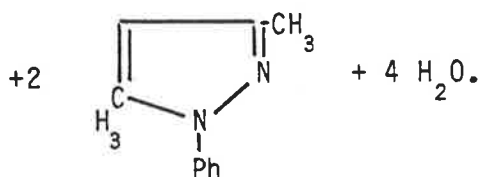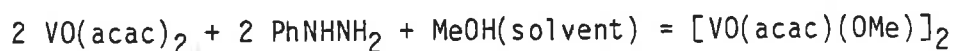
The formation of the heterocyclic product in the above reaction was proved by isolation and determination of its 'H-N.M.R. spectrum which was compared with the product of the reaction between $PhNHNH_2$ and acac$\underline{H}$. The isolation was effected by evaporating to dryness the filtrate of the reaction mixture,

acidifying to decompose any complex left and extracting in $CHCl_3$, and the viscous liquid recovered from it had its 'H-N.M.R. spectrum recorded in $CDCl_3$. The 'H-N.M.R. of the product obtained by drying the reaction mixture of 1:1 acac$\underline{H}$ and $PhNHNH_2$ was also recorded in $CDCl_3$. The τ values (p.p.m.) obtained from these spectra (Table 2.2.2) are comparable with those obtained by Elguero et al.[109]. Most recently, Murray et al.[110], in describing the crystal structure of $(C_5H_9N_2)_4[Mo_8O_{26}]$, reported the in situ formation of the 3,5-dimethylpyrazolium cation, $C_5H_9N_2^+$ during a reaction of $MoO_2(acac)_2$ with benzoylhydrazine in ordinary 'wet' methanol.

TABLE 2.2.1: $[VO(AA)(OR)]_2$ DIMERS PREPARED FROM $VO(\beta\text{-DIKETONATO})_2$ COMPLEXES

NO.	COMPLEX	COLOUR	NO.	COMPLEX	COLOUR
1	$[VO(acac)(OMe)]_2$	Blue	4	$[VO(Bzac)(OMe)]_2$	Green
2	$[VO(acac)(OEt)]_2$	Sky-blue	5	$[VO(Bzac)(OEt)]_2$	Green (Olive)
3	$[VO(acac)(OPr^n)]_2$	Blue	6	$[VO(Bzac)(oPr^n)]_2$	Green (Blue)

TABLE 2.2.2: ^{1}H-N.M.R. DATA (τ VALUES) FOR 3,5-DIMETHYL-1-PHENYLPYRAZOLE (D.P.P.) IN $CDCl_3$

D.P.P. From	^{3}-C$\underline{H}_3$	^{4}-C$\underline{H}$	^{5}-C$\underline{H}_3$
acac$\underline{H}$ + $PhNHNH_2$	7.70	4.01	7.70
$VO(acac)_2$ + $PhNHNH_2$	7.70	4.00	7.70
Literature value[109]	7.71	4.02	7.71

It was observed that the use of two or three-fold molar excess of $PhNHNH_2$ does not affect the reaction or the yield, suggesting that the AA^- in the $[VO(AA)(OR)]_2$ formed is quite stable, in the presence of ROH, to react with $PhNHNH_2$ to give any further D.P.P. This extra stability, at least in the presence of ROH, was further demonstrated when the reaction of $[VO(acac)(OEt)]_2$ with benzoylhydrazine in dry methanol gave the metathesis product, $[VO(acac)OMe)]_2$ instead of the expected $(VOL)_2$ or VL_2 (L = dinegative tridentate pentane-2,4-dionebenzoylhydrazonato anion). In contrast, refluxing of $VO(acac)_2$ with benzoylhydrazine (1:2) in dry methanol under dinitrogen yields the VL_2 complex (Chapter 3). Thus, this reaction of $VO(\beta$-diketonato$)_2$ and $PhNHNH_2$ in ROH was conveniently used to prepare some of the dimers with the lower alcohols (Table 2.2.1). However, such complexes with AA = acac and R = isopropyl or n-, sec- or tert-butyl could not be prepared, probably due to the bulkiness of the alkyl group.

(ii)   DIRECT SYNTHESIS FROM $VOCl_2$

A number of $[VO(AA)(OR)]_2$ complexes (Table 2.2.3), especially with AA = non-β-diketonate ligands such as 2-hydroxy-1-napthaldehyde and 2-hydroxyaceto-phenone were obtained by the direct reaction of AA$\underline{H}$ with $VOCl_2$ in dry ROH and in the presence of a base (Et_3N or LiOAC).

$$2\ VOCl_2 + 2\ AA\underline{H} + 4\ Et_3N + ROH\ (solvent) = [VO(AA)(OR)]_2 + 4\ Et_3NHCl$$
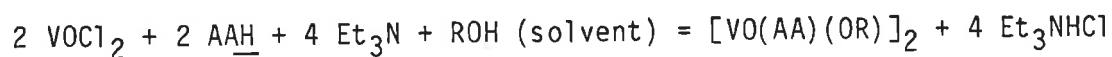
The dimers being extremely sensitive to water, the supplied 50% aqueous $VOCl_2$ solution (B.D.H.) was dried over P_2O_5 under high vacuum for several days until a blue solid mass was obtained. This was dissolved in dry ROH and the V-content determined spectrophotometrically (a_M of VO^{2+} in 1M H_2SO_4 = 17.8 M^{-1} cm^{-1}) and used in all the direct preparations. This method was found to be a successful general method which could be used to form dimeric complexes with ligands other than β-diketones as well as some which could not be prepared by method (i). In all cases, the desired dimeric products of this reaction separated out in a few minutes after proper mixing of the components.

TABLE 2.2.3: $[VO(AA)(OR)]_2$ DIMERS PREPARED DIRECTLY FROM $VOCl_2$

NO.	COMPLEX	COLOUR	NO.	COMPLEX	COLOUR
1	$[VO(dbm)(OMe)]_2$	Apple-Green	5	$[VO(HNP)(oPr^n)]_2$	Green
2	$[VO(dbm)(OEt)]_2$	Green	6	$[VO(HAP)(OMe)]_2$	Olive Green
3	$[VO(HNP)(OMe)]_2$	Green	7	$[VO(HAP)(OEt)]_2$	Green
4	$[VO(HNP)(OEt)]_2$	Apple-Green	8	$[VO(HAP)(oPr^n)]_2$	Olive Green

Also compounds 1, 2, 4 and 5 of Table 2.2.1.

Using this direct procedure, attempts were made to prepare similar dimeric methoxo or ethoxo-bridged complexes with a number of bidentate ligands, such as ethylenediamine,1,2-propanediamine, ethanolamine, o-phenanthroline, glycine, phenylalanine, anthranilic acid, 8-hydroxyquinoline, isopropyledenebenzoylhydrazone, benzaldehydebenzoylhydrazone, dimethylglyoxime, kojic acid and diethyldithiocarbamate. These attempts were unsuccessful because either no pure desired product could be obtained or often some gummy precipitate, mainly of $VO(OH)_n$, appeared or no reaction occurred or some vanadium(V) compounds formed.

(iii) METATHESIS REACTION

The metathesis reaction of the type,

$$[VO(AA)(OR)]_2 + R'OH(solvent) \xrightarrow{\text{Reflux}} [VO(AA)(OR')]_2 + 2 ROH$$
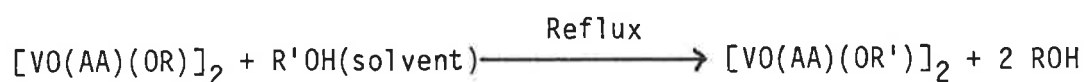
has been most useful in preparing the higher alkoxo-bridged dimers which could not be formed in the pure state by methods (i) and (ii). For example, several attempts to prepare $[VO(acac)(oPr^i)]_2$ dimer in pure form by refluxing (i) $VO(acac)_2$ and $PhNHNH_2$ or (ii) $VOCl_2$, acac$\underline{H}$ and Et_3N in 2-propanol were

unsuccessful. But the metathesis reaction yielded a very beautiful, crystalline product. The use of methoxo- (or ethoxo) bridged dimer as the starting material for the metathesis reaction was preferred, because the small amount of the more volatile alcohol formed during the reaction could easily be driven away by passing a stream of nitrogen through the solution at the end of the reflux. The metathesis reaction does not proceed with very bulky R'OH, possibly due to steric factors. For example, with tert-butanol as the R'OH, only the starting material was isolated. The dimers that were prepared by this method are listed in Table 2.2.4. Some of the starting methoxo- or ethoxo-dimers were only partially soluble in R'OH even under reflux, however, they were completely converted to the -OR'-bridged dimers on reflux. Reactions with solid R'OH such as phenol, p-methoxybenzylalcohol and p-nitrobenzyl-alcohol were carried out in dry toluene in the presence of high excess of the alcohol.

TABLE 2.2.4: $[VO(AA)(OR)]_2$ DIMERS PREPARED BY METATHESIS REACTIONS

NO.	COMPLEX	COLOUR	NO.	COMPLEX	COLOUR
1	$[VO(acac)(OPr^i)]_2$	Blue	11	$[VO(Bzac)(OBz-p^{OMe})]_2$	Green
2	$[VO(acac)(OBz)]_2$	Blue	12	$[VO(Bzac)(OBz-p^{NO_2})]_2$	Green
3	$[VO(acac)(OBz-p^{OMe})]_2$	Blue	13	$[VO(dbm)(OPr^n)]_2$	Olive Green
4	$[VO(Bzac)(OPr^i)]_2$	Olive Green	14	$[VO(dbm)(OPr^i)]_2$	Olive Green
5	$[VO(Bzac)(OBu^n)]_2$	Blue Green	15	$[VO(dbm)(OBz)]_2$	Pale Green
6	$[VO(Bzac)(OBu^2)]_2$	Blue Green	16	$[VO(HNP)(OPr^i)]_2$	Olive Green
7	$[VO(Bzac)(OEtOMe)]_2$	Green	17	$[VO(HNP)(OBz)]_2$	Green
8	$[VO(Bzac)(OEtOEt)]_2$	Green	18	$[VO(HAP)(OPr^i)]_2$	Olive Green
9	$[VO(Bzac)(OPh)]_2$	Blue Green	19	$[VO(HAP)OBz)]_2$	Green
10	$[VO(Bzac)(OBz)]_2$	Green			

Also compounds 3 and 6 of Table 2.2.1 and compounds 5 and 8 of Table 2.2.3.

The dimers of acac⁻ are more soluble in alcohol than those of Bzac⁻ and consequently the benzoylacetonato dimers are separated more quickly and easily from the reaction mixtures. The dimers of dibenzoylmethane, 2-hydroxy-1-napthaldehyde and 2-hydroxyacetophenone, because of their insoluble nature in alcohols, precipitate almost immediately on mixing of the component reactants.

2.3 PROPERTIES AND REACTIONS:

(i) STABILITY

Because of the alkoxo groups, these dimers are extremely sensitive to moisture and are easily hydrolysable in the solid state and in solution in the presence of air. On the other hand, (i) the β-diketones, 2-hydroxy-1-napthaldehyde and salicylaldehyde ligands are known to be stable to hydrolysis because they form $VO(AA)_2$ complexes, whereas, (ii) the 2-hydroxyacetophenone is not. Although VO^{2+} is usually taken to be stable to oxidation, our experience has shown the easy oxidation by air usually resulting in yellow-brown colour due to vanadium(V). For example, the unstable intermediate, $(VOL)_2$ of our VL_2 reaction in alcohol (Chapter 4) oxidizes rapidly, in the presence of air, to the (alkoxo) oxovanadium(V) complex. Also, $VO(acac)_2$ in solution, if allowed to stand for a number of hours, has been reported to change gradually from blue to green to yellow to orange due to its oxidation to a vanadium(V) species[111]. The purity as well as the stability of the prepared alkoxo-bridged dimers depend to a great extent on the dryness of the solvent, ROH and their careful handling in the oxygen-free dry dinitrogen atmosphere. Even a trace amount of moisture can cause formation of significant monomer impurities.

In the solid state, all complexes slowly turn to dark green when exposed to air. The rapidity of this colour change, due to decomposition and oxidation, is an indication of their instability which depends on the nature of the bidentate ligand and the alkoxo group. Complexes with 2-hydroxyacetophenone were found to be the most air-sensitive. That HAPH forms relatively weak

complexes is apparent from the failure to obtain the $VO(HAP)_2$ complex under the following conditions:

(i) $VOCl_2$ + 2 HAP$\underline{H}$ + base $\xrightarrow{\quad EtOH \quad}$ $[VO(HAP)(OEt)]_2$

(ii) $[VO(HAP)(OEt)]_2$ + 2 HAP$\underline{H}$ $\xrightarrow{\quad Toluene \quad}$ Solution goes brown.

No expected reaction.

(iii) $[VO(HAP)(OEt)]_2$ $\xrightarrow[\quad CHCl_3 \quad]{\quad H_2O \quad}$ $VO(OH)_n$
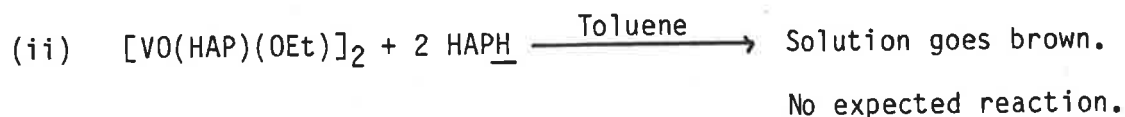
(iv)   Procedure analogous to that for the preparation of $VO(HNP)_2OH_2$

(see Experimental Section) gave brown gummy stuff (V^V).

Graddon[112] and Weber[113] also encountered difficulty in preparing the bis-Cu(II), Co(II) and Ni(II) complexes of this ligand. The general order of air-sensitivity for the various $[VO(AA)(OR)]_2$ complexes appeared to be HAP>HNP>acac>Bzac>dbm when the bidentate ligands were varied keeping the alkoxo group the same. The comparatively high stability of the dibenzoylmethane complexes in the above series is explainable, to some extent, by their low solubility. Factors such as resonance of chelate rings and structural considerations are also important. A number of ligands (many non-aromatic or non-quasi-aromatic) (Section 2.2 (ii)) failed to give such dimeric complexes, probably, because of the extreme unstable nature of the expected dimeric products.

Complexes with bulky alkoxo groups are less stable and this agrees with our observations discussed above relating to the difficulty or failure to prepare them.

The dimers are generally soluble in common organic solvents, e.g. chloroform, dichloromethane, acetone and benzene but their solutions are extremely sensitive to traces of moisture in the solvent which gives the solution a dark cloudy appearance due to the formation of $VO(OH)_2$. In dry solvents, the clear blue or green solution slowly turns dark to dark green to ultimately orange-red when exposed to air. The solutions made by distilling the dry solvent on

to the dimer in carefully degassed containers, stay stable indefinitely. Solutions of the dimer in solvents such as CH_2Cl_2, benzene, etc. are stabilized by the addition of about 5% of the respective alcohol. The above observations are explainable from the following reversible reaction:

$$[VO(AA)(OR)]_2 \; \underset{ROH}{\overset{CHCl_3 + trace\ H_2O}{\rightleftarrows}} \; 2\ [VO(AA)(OH)]^* + 2\ ROH$$

$$VO(AA)_2 + VO(OH)_2$$
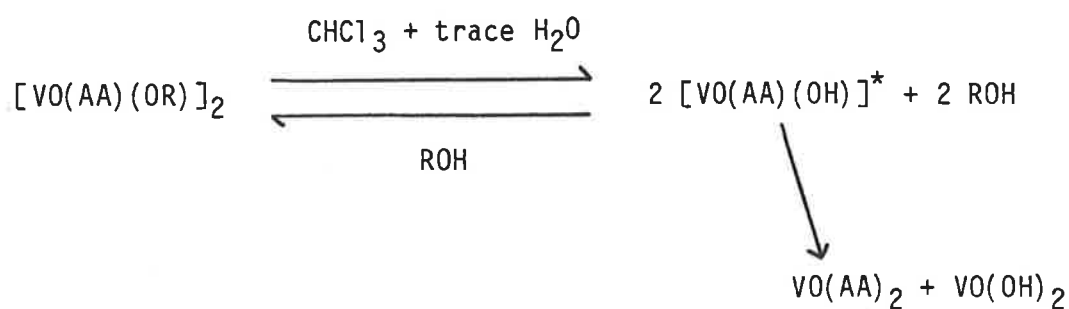
(* Postulated intermediate)

The reaction was established qualitatively for all the bidentate ligands except 2-hydroxyacetophenone. The reaction $[VO(acac)(OMe)]_2 \xrightarrow[H_2O]{in\ CHCl_3}$ $VO(acac)_2 + VO(OH)_2$ was established quantitatively by the following experiment:

Taking extreme care to exclude oxygen, a solution of the complex in distilled, dry and degassed $CHCl_3$ was exposed to an oxygen-free atmosphere of dinitrogen saturated with $CHCl_3$ and H_2O vapour in a desiccator. The initial blue solution started turning dark and in about two hours a dark green precipitate started settling down at the bottom with a supernatent green solution. This precipitate, filtered after 24 hours, was identified to be $VO(OH)_2$. The blue-green mass obtained by evaporating the filtrate was characterized to be $VO(acac)_2$. One equivalent each of the products were obtained from one equivalent of the dimer used.

(ii) REACTIONS

The treatment of $[VO(AA)(OR)]_2$ (except AA = HAP) with the bidentate ligand (AAH) in toluene or dichloromethane results in the formation of the bis $VO(AA)_2$. The same reaction if carried out in alcohol does not proceed. The

explanation must be that -OR is difficult to substitute in the presence of an excess ROH due to the suppression of dissociation of the equilibrium in which an OR group is removed.

Attempts to prepare some mixed ligand complexes by the reaction $[VO(AA)(OR)]_2 + 2 A'A'\underline{H} \rightarrow 2 VO(AA)(A'A')$ were not successful with one possible exception. Refluxing of $[VO(acac)(OEt)]_2$ with Bzac$\underline{H}$ in the molar ratio of 1:2 in toluene resulted in a mixture of $VO(acac)_2$ and $VO(Bzac)_2$ which were separated by fractional crystallization. Similar results were obtained with other β-diketonato systems. The reaction of $[VO(acac)(OEt)]_2$ or $[VO(Bzac)(OMe)]_2$ with HNP$\underline{H}$ in the molar ratio of 1:2 gave a green precipitate of the known compound $VO(HNP)_2.OH_2$ with $VO(acac)_2$ or $VO(Bzac)_2$ in the filtrate. The product was identified by its infrared spectrum and by analysis of its V and ligand contents. It appears that ligands under these conditions are very labile and the more thermodynamically stable products are obtained by a dismutation of the reactants. The reaction of $[VO(acac)OEt)]_2$ with 2-hydroxy-acetophenone in the molar ratio of 1:2, however, gave most probably, VO(acac)(HAP) as evidenced by its V and HAP$\underline{H}$ contents and UV (in 0.5 M H_2SO_4 in 50% aqueous EtOH) and infrared spectra. Because, with this ligand, we were unable to form the complex $VO(HAP)_2$, it seems that the dismutation does not take place but instead the mixed ligand complex is formed. But the compound was unstable and could not be characterized further.

Although $VO(\beta$-diketonato$)_2$ compounds are known to form adducts[10-12] with a variety of bases in their vacant positions, attempts to prepare py-adducts of these dimers were a failure. Addition of pyridine to the degassed $[VO(acac)(OEt)]_2$ in toluene resulted in the decomposition of the dimer. Among the products, we were able to identify $VO(OH)_2$ and $VO(acac)_2.py$. The latter was identified by comparing its electronic spectrum with that of $VO(acac)_2$ in toluene containing pyridine. This demonstrates the lability of the ligand of the dimer to form the most stable compounds.

2.4   X-RAY CRYSTAL STRUCTURE OF [VO(acac)(OMe)]$_2$

The X-ray crystal structure of [VO(acac)(OMe)]$_2$ (Fig. 2.4.1) determined by Diamantis and T. Hambly (*) is identical to that published by Musiani et al.[98]. The crystals were obtained from methanol solution. The bond lengths, bond angles and the deviations of some relevant atoms from some least-squares planes are listed in Tables 2.4.1 - 2.4.3.

The complex consists of methoxo-bridged dimeric [VO(acac)(OMe)]$_2$ units with a crystallographic inversion centre at the middle. Coordination about vanadium approximates a square pyramidal geometry with the vanadyl oxygen occupying the apical site. The two vanadyl oxygens are _trans_ to each other as expected from the siting of the molecule about a centre of symmetry. The V atom is 0.594Å above the plane defined by the four oxygen atoms forming the base of the pyramid. The central cycle defined by the two V atoms and the two bridging O atoms is crystallographically constrained to be planar by the centre and the C(1) of the methyl group lies 0.108Å out of this plane. There is an angle of 44.9° between the planes through the central ring and the acac chelate. The bases of the two edge-sharing square pyramids occupy nearly the same plane. There are no contacts, significantly shorter than the van der Waals radius sum, between the complex molecules.

The V = O(2) distance of 1.586(2)Å shows evidence of multiple bonding and is typical in such structures. The V-O(3) and V-O(4) distances of 1.970(2) and 1.958(2)Å of the terminal oxygens are comparable to the V-O(1) distance [1.965(2)Å] of the bridging oxygen and all these distances are again comparable to the average V-O distances of 1.968 and 1.960Å found in VO(acac)$_2$

Footnote: (*)   As has been stated earlier, during further studies of this family of compounds to reach a reasonably complete chemistry of such complexes, there appeared a report[98] describing structure of this compound.
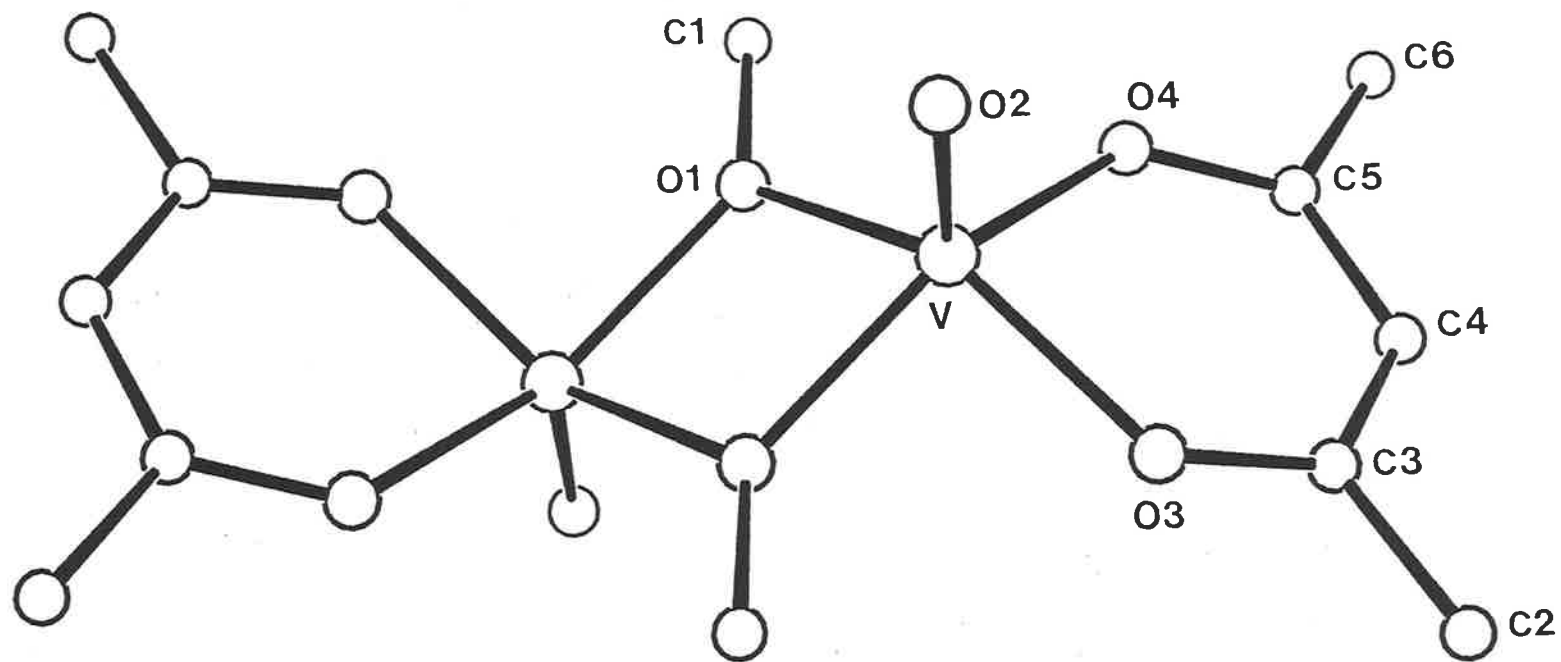
Figure 2.4.1:   The crystal structure of [VO(acac)(OMe)]$_2$.

and $VO(Bzac)_2$ respectively[21], as well as to the average V-O distance of 1.979Å in $V(acac)_3$[114]. The O(3)-V-O(4) and O(1)-V-O(4) angles of 87.1(1) and 87.2(1)° involving respectively the terminal oxygens and the terminal and the bridging oxygens are also comparable to the O-V-O angles (average 87.4°) involving the oxygens of the same acac or Bzac ligand in $VO(acac)_2$ or $VO(Bzac)_2$ as well as to the same (average 88.0°) in $V(acac)_3$. The smaller O(1)-V-O(1^i) angle (75.3(1)°) involving the bridging oxygens in the dimer is due to the relatively shorter distance which is possible between these two oxygens compared to that between the ligand oxygens O(3) and O(4) which is determined by the ligand geometry.

The average C-O and C-C bond distances of 1.282(4) and 1.385(5)Å respectively in the chelate ring indicate the presence of delocalization of the π electrons which probably extends to the metal atoms to form a pseudo-aromatic system. The separation of the V atoms [3.107(1)Å] precludes the possibility of any direct metal-metal bonding.

TABLE 2.4.1: BOND LENGTHS (Å) FOR $[VO(acac)(OMe)]_2$

O(1)	---	V(1)	1.965(2)	O(2)	---	V(1)	1.586(2)
O(3)	---	V(1)	1.970(2)	O(4)	---	V(1)	1.958(2)
V(1)	---	V(1)	3.107(1)	C(1)	---	O(1)	1.419(4)
C(3)	---	O(3)	1.285(4)	C(5)	---	O(4)	1.279(4)
C(3)	---	C(2)	1.486(5)	C(4)	---	C(3)	1.386(5)
C(5)	---	C(4)	1.385(5)	C(6)	---	C(5)	1.494(5)

TABLE 2.4.2: BOND ANGLES (°) FOR $[VO(acac)(OMe)]_2$

O(2)	-	V(1)	-	O(1)	108.6(1)	O(3)	-	V(1)	- O(1)	145.9(1)
O(3)	-	V(1)	-	O(2)	105.2(1)	O(4)	-	V(1)	- O(1)	87.2(1)
O(4)	-	V(1)	-	O(2)	108.0(1)	O(4)	-	V(1)	- O(3)	87.1(1)
V(1)	-	O(1)	-	V(1)	104.7(2)	C(1)	-	O(1)	- V(1)	127.6(2)
O(1)	-	V(1)	-	O(1)	75.3(1)	C(3)	-	O(3)	- V(1)	130.2(2)
C(5)	-	O(4)	-	V(1)	131.1(2)	C(2)	-	C(3)	- O(3)	115.7(3)
C(4)	-	C(3)	-	O(3)	123.7(3)	C(4)	-	C(3)	- C(2)	120.6(3)
C(5)	-	C(4)	-	C(3)	124.3(3)	C(4)	-	C(5)	- O(4)	123.5(3)
C(6)	-	C(5)	-	O(4)	115.1(3)	C(6)	-	C(5)	- C(4)	121.5(3)

TABLE 2.4.3: LEAST-SQUARES PLANES AND THE DISTANCES (Å) OF RELEVANT
ATOMS FROM THE PLANES

PLANE 1: $0.7471x + 0.5840y - 0.3173z = 4.7040$

through $V(1)$, $O(1)$, $V(1^i)$, $O(1^i)$.

$[C(1), - 0.108; O(2), 1.450; O(3), - 1.008; O(4), - 1.082]$

PLANE 2: $0.0623x + 0.9048y - 0.4213z = 4.6356$

through $V(1)$, $O(3)$, $O(4)$, $C(2)$, $C(3)$, $C(4)$, $C(5)$, $C(6)$.

$[O(1), - 0.995; C(1), - 0.992; O(2), 1.516]$

PLANE 3: $0.4369x + 0.8093y - 0.3927z = 4.5250$

through $O(1)$, $O(3)$, $O(4)$, $O(1^i)$.

$[V(1), 0.594; O(2), 2.181; C(1), - 0.042; C(3), - 0.440; C(5), - 0.492]$

PLANE 4: $0.1166x + 0.3663y + 0.9232z = 6.1626$

through $V(1)$, $O(2)$, $V(1^i)$, $O(2^i)$.

$[C(4), - 0.040; C(4^i), 0.040]$

2.5   MASS SPECTRA

Apart from the crystallographic studies, the determination of the mass
spectra is specifically useful in providing direct evidence for dimer
formation. All the dimer complexes gave mass spectra showing the molecular
ion peaks consistent with their dimeric structure complemented thus their
micro-analytical data. An X-ray crystal structure determination of the model
complex, $[VO(acac)(OMe)]_2$ (Section 2.4), showed a dimeric configuration by

bridging through the two methoxo groups, and the similarity in the chemical and spectroscopic properties of the complexes reported in Sections 2.2, 2.7 and 2.8 lead us to believe that they have the same dimeric structures.

All the complexes gave similar fragmentation patterns (Table 2.5.1) consistent with the formulations of the compounds as dimers. Observance of the molecular ion (m/e) peak and loss of OR is a general feature of the spectra. Most interesting is the loss of two OR groups with the retention of a dimeric fragment, $[VO(AA)]_2$. This suggests a structure in which the alkoxo groups are terminal and are not involved in bridging. Such molecules would be expected to lose both alkoxo groups still retaining the dimer structure, at least during the mass spectral experiment. However, the crystal structure of $[VO(acac)(OMe)]_2$ having bridging alkoxo groups clearly rejects such an interpretation.

Because the dimers with the same bidentate ligand but with varying alkoxo groups, on losing two OR groups, give in each case the same mass spectral peaks characteristic of the respective $[VO(AA)]_2$ dimers, it is most likely that dimerization in $[VO(AA)]_2$ occurs through the vanadyl oxygen, possibly $> V\!\!<^{O}_{O}\!\!>V <$, or through some weak V....V interaction, such as $> \overset{O}{V} \cdots \overset{O}{V} <$. However, it is quite unlikely to involve dimerization via the bidentate ligand since the same phenomenon is observed with diverse ligands, such as acacH, BzacH, dbmH, HNPH and HAPH. It appears, therefore, that dimerization in $[VO(AA)]_2$ occurs as a result of a rearrangement following the loss of the alkoxo groups.

With some of the dimers, a special feature of the formation of a fragment, $[VO(AA)]_2O$ with the loss of (OR + R) is observed. Similar fragmentation pattern was also reported[26] for AA = salicyladehyde. A possible structure of this fragment is explainable in terms of oxo-bridging.

TABLE 2.5.1: CHARACTERISTIC MASS SPECTRAL PEAKS FOR THE

[VO(AA)(OR)]$_2$ COMPLEXES

AA=	R=	Molecular Weight	M$^+$	-R	-OR	-OR-R	-2 OR
acac	Me	394.174	394	-	363	-	332
	Et	422.228	422	-	377	-	332
	Pr^n	450.281	450	-	391	-	332
	Pr^i	450.281	450	407	391	348	332
	Bz	546.369	546	455	439	348	332
Bzac	Me	518.316	518	503	487	472	456
	Et	546.369	546	-	501	472	456
	Pr^n	574.423	574	-	515	472	456
	Pr^i	574.423	574	-	515	472	456
	Bu^n	602.474	602	-	529	472	456
	Bu^2	602.474	602	-	529	472	456
	EtOMe	608.421	608	-	532	472	456
	Ph	642.455	642	565	549	472	456
	Bz	670.511	670	579	563	472	456
dbm	Me	642.457	642	627	611	596	580
	Et	670.511	670	-	625	596	580
	Pr^n	698.564	698	-	639	-	580
	Pr^i	698.564	698	-	639	-	580
	Bz	794.652	794	-	686	-	580

AA=	R=	Molecular Weight	M^+	-R	-OR	-OR-R	-2 OR
HNP	Me	538.306	538	-	507	-	476
	Et	566.360	566	537	521	492	476
	Pr^n	594.413	594	-	535	-	476
	Pr^i	594.413	594	-	535	-	476
	Bz	690.501	690	-	583	492	476
HAP	Me	466.240	466	451	435	-	404
	Et	494.294	494	-	449	420	404
	Pr^n	522.347	522	-	463	420	404
	Pr^i	522.347	522	-	463	-	404
	Bz	618.433	618	527	511	420	404

2.6 INFRARED SPECTRA

The Infrared studies of these dimeric complexes are important to (i) demonstrate the presence and examine the effect of coordination on the vibrations of both the non-bridging (AA) and bridging (OR) ligands, (ii) use vibrational frequency of the V = O group as a probe to get an insight into any structural distortions from pure C_{4v} symmetry expected for discrete dimers, or as evidence for interaction between adjacent molecules, (iii) assign vibrational frequencies in comparison to the monomeric $VO(AA)_2$ complexes and (iv) provide supporting evidence for structural similarities in this family of complexes.

Regions of major interest for this particular family of dimers are (i) $\nu V = O$, (ii) $\nu C \cdots O$, $\nu C \cdots C$, $\nu as C \rule[0.5ex]{1em}{0.4pt} O$, etc. for the β-diketonates

and $\nu C = O$ for the hydroxy aromatic carbonyls and (iii) $\nu C \longrightarrow O$ of the bridging alkoxy groups.

(i) $\nu V = O$ REGION

There are three situations in which the $\nu V = O$ may provide structural information about the coordination environment of the vanadyl group. (i) All monomeric VO(IV) complexes incorporating a vacant site trans to the vanadyl oxygen exhibit the $V = O$ stretching frequencies in the region 960 ± 50 cm^{-1} [5] while the attachment of a donor atom to this coordination site reduces this $\nu V = O$ [11,22,24].

(ii) It is expected that, for dimeric complexes, the trans vanadyl groups,

$$
\begin{array}{c}
O \\
\parallel \\
V \overset{\displaystyle -O-}{\underset{\displaystyle -O-}{<\!>}} V \\
\qquad \parallel \\
\qquad O
\end{array}
$$
, should give rise to a symmetric (ideally I.R. inactive or
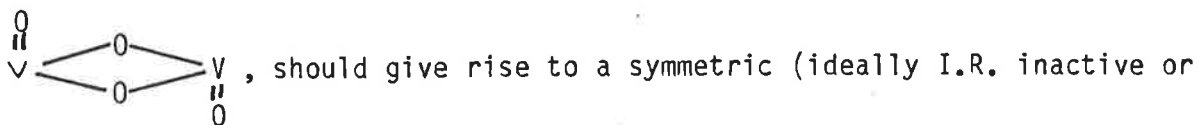
weakly active) and an asymmetric (I.R. active) modes and thus should show two vibrational bands. But little is known about this in the literature. The vanadium atoms in the monomers and these dimers possessing the same coordination symmetry (C_{4v}) should show the $\nu V = O$ in the same region.

(iii) Complexes with ....$V = O$....$V = O$.... polymeric chain interaction or having structural distortion from C_{4v} to D_{3h} show $\nu V = O$ at as low as ~ 850 cm^{-1} [115, 116].

All the alkoxo-bridged oxovanadium(IV) dimers exhibit the $\nu V = O$ (980 - 1000 cm^{-1}) in the expected normal region. This agrees with a C_{4v} symmetry of the vanadium centres in the dimers incorporating a vacant site trans to the vanadyl oxygen and excludes possibilities of any structural distortions or of interactions between the adjacent dimers. Unlike most square-pyramidal monomeric complexes, these dimers, with few exceptions, show characteristic splitting in the bands in the $\nu V = O$ region with a sharp band incorporating a shoulder between 10-20 cm^{-1} on the high or low energy side (Table 2.6.1 and Figure 2.6.1). On occasions further weak bands are observed in the vicinity of the principal $\nu V = O$ stretch. It is not always possible to know whether these bands represent further splitting of the $\nu V = O$ or are due to skeletal

1600   1000   600

cm^{-1}
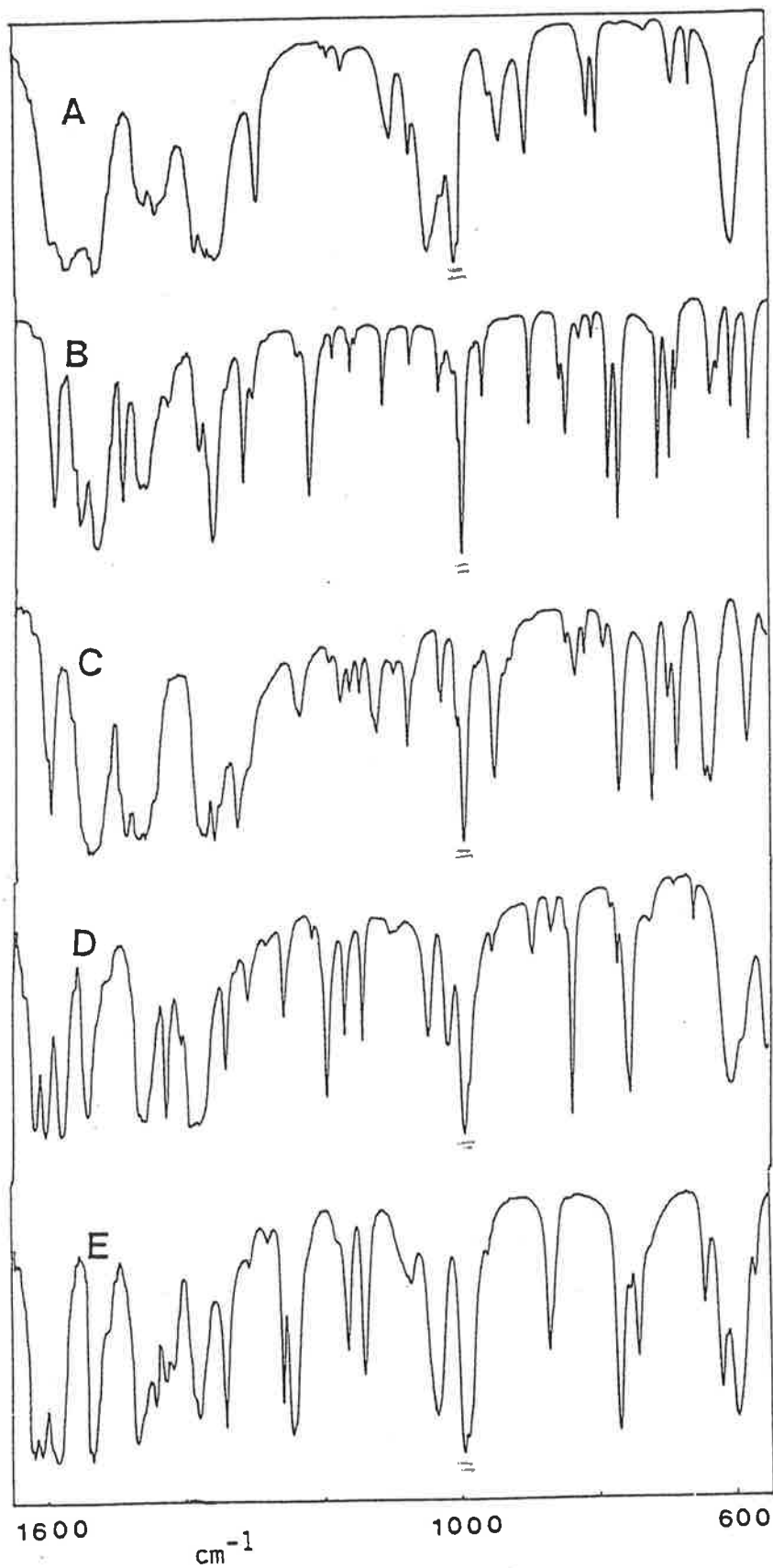
Figure 2.6.1:   Infrared spectra for (A) [VO(acac)(OEt)]$_2$;
(B) [VO(Bzac)(OPh)]$_2$; (C) [VO(dbm)(OPr^i)]$_2$;
(D) [VO(HNP)(OPr^n)]$_2$ and (E) [VO(HAP)(OMe)]$_2$.

$\underset{\displaystyle =}{} \nu_{V=0}$
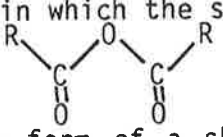
vibrations. In the dimeric structure, the V = O groups are in an essentially identical environment because a virtual centre of symmetry (Section 2.4) is present in such dimers. Therefore, we consider that the observed split in the $\nu V = O$ band arises because of the dimeric nature of these complexes as a result of coupling of the two V = O vibrations. A comparison can be made with the cis $[V{\Large\lessgtr}^O_O]^+$ in which the splitting is $\Delta\nu = 54$ cm^{-1} [77] or with coupling in acid anhydrides, $\begin{smallmatrix} R & & O & & R \\ & \backslash & | & / & \\ & C & & C & \\ & \| & & \| & \\ & O & & O & \end{smallmatrix}$, with $\Delta\nu = 70\text{-}80$ cm^{-1} [117]. The appearance of the split in the form of a shoulder on a peak of half-peak width of about 20 cm^{-1} suggests a $\Delta\nu$ of the order of 10-20 cm^{-1}. Such low $\Delta\nu$ values are

TABLE 2.6.1:   THE V = O STRETCHING FREQUENCIES (cm^{-1}) OF THE [VO(AA)(OR)]$_2$ DIMERS

R ↓ \ AA' =	acac	Bzac	dbm	HNP	HAP
Me	993 s	988) s 984)	1004) 993 s)	994) s 982) 970)	992) s 986)
Et	1003) s 997)	999) 988 s) 977)	998) 989 s) 970)	997) 988) s 970)	990 s) 978)
Pr^n	995 s) 975)	999) 990 s)	1002) 990 s) 980)	990 s) 975) 970)	990 s) 980)
Pr^i	996 s	999) 9905)	1000) 991 s) 970)	990 s	997) 990 s) 980)
Bz	997 s) 988) 983)	998) 9895) 975)	1004) 997 s) 975)	1005) 997 s)	1005) 990 s) 975)
Bu^n	(1005, 993s, 975)				
Bu^2	(992s, 978)				
Ph	(998, 992s, 980)				
EtOMe	999) s, 978 996)				
EtOEt	(1002, 993s, 970)				
Bzac-p^{OMe}	(1004, 997s, 888)				
VO(AA)$_2$*	997	999	997	980**	-

[* For comparison, ** VO(HNP)$_2$OH$_2$]

consistent with the expected low coupling between the two trans V = O groups

linked by two single bonds through two oxygen atoms of the alkoxo groups,

> $\overset{O}{\underset{O}{\overset{\|}{V}}}\underset{O}{\overset{O}{\diagup}}V\overset{}{\underset{\|}{O}}$ <. Ginsberg et al.[36] observed two V = O stretching frequencies

for a few of the dimeric 5-substituted N-(2-hydroxyphenyl)salicylideneimine

complexes of VO^{2+} and they attributed this to unit cell group splitting or to

a crystal packing effect which causes the two vanadium atoms of the dimeric

molecules to be non-equivalent.

Table 2.6.1 suggests that the frequency of the $\nu V = O$ is generally

independent of or does not change significantly with the variation of the

bidentate ligands or the bridging alkoxo groups thus showing similar

structures of these dimers as well as similar environments around the V atoms.

(ii) $\nu s\ C \overset{\cdots}{} O,\ \nu s\ C \overset{\cdots}{} C,\ \nu as\ C \overset{}{} O,$ **etc. and** $\nu\ C = O$ **REGIONS**

The above stretches are important in obtaining information about the

effect of the coordination on the C = O frequencies and the nature of the

bonding in the C = O group. The stretching frequencies of $\nu\ C \overset{\cdots}{} O$,

$\nu s\ C \overset{\cdots}{} C,\ \nu s\ C \overset{\cdots}{} O,\ \nu as\ C \overset{}{} O,\ \delta$ C-H and π C-H regions are diagnostic

for the bonded β-diketonate groups which have a quasi-aromatic structure and

properties. For the hydroxy carbonyl complexes, the ν C = O is the only band

given in the literature as characteristic of the bonded hydroxycarbonyl

ligands.

Rasmussen et al.[118] described the effect of chelation in certain β-dike-

tones which gives rise to a considerable shift of the carbonyl frequency. By

considering the aromatic character of the chelate ring, Bellamy et al.[119]

assigned the higher region band ($\sim$ 1570 - 1600 cm^{-1}) to C $\overset{\cdots}{}$ O stretching and

the lower bands occurring around 1525 cm^{-1} to C $\overset{\cdots}{}$ C stretching modes.

Pinchas et al.[120] on the basis of a study of the I.R. spectra of ^{13}C and ^{18}O

labelled acetylacetonates of Cr (III) and Mn(III) confirmed Bellamy's assign-

ments. They observed significant displacement of the 1570 cm^{-1} band by chang-

ing C = ^{16}O for C = ^{18}O whereas the band at 1515 cm^{-1} was not affected apprec-

iably. This clearly indicated the band at 1570 cm^{-1} to be associated with a vibration mode characteristic of C $\cdots$ O and the one at 1515 cm^{-1} to be a pure C $\cdots$ C band. Similar observations have since been made with various metal-β-diketonate complexes[121-123]. Fay and Pinnavaia[124] measured the infrared spectra of a number of acetylacetonato complexes with various metals and assigned the bands in the regions 1551-1592 cm^{-1} to νs (C $\cdots$ O), 1517-1534 cm^{-1} to νs (C $\cdots$ C), 1333-1397 cm^{-1} to νas (C $\cdots$ O), 1267-1287 cm^{-1} to νas (C - O), 1183-1188 cm^{-1} to δ (C - H) and 760-802 cm^{-1} to π (C - H) stretching modes.

In our dimeric complexes, no band was observed in the regions 1600-1750 cm^{-1} (for β-diketonates) and 1625-1750 cm^{-1} (for hydroxy ketones or aldehydes) indicating that all the carbonyl groups are coordinated. Examples of infrared spectra in the region 1650-600 cm^{-1}, which is the most informative for these dimers are shown in Figure 2.6.1. In agreement with the above assignments, we assign the bands in the regions 1550-1600 cm^{-1}, 1528-1536 cm^{-1}, 1315-1360 cm^{-1}, 1290-1312 cm^{-1}, 1180-1198 cm^{-1} and 770-800 cm^{-1} for the β-diketonato dimers to νs (C $\cdots$ O), νs (C $\cdots$ C), νas (C $\cdots$ O), νas (C - O), δ (C- H) and π (C - H) respectively (Table 2.6.2). For HNP and HAP dimers, we assign the bands in the 1580-1625 cm^{-1} and 1580-1618 cm^{-1} frequency regions to ν C = O (Table 2.6.3). The hydroxy carbonyl compounds contain a number of other bands which are obviously characteristic of the ligand and independent of the alkoxo groups (Table 2.6.4). However, no assignments for these bands are found in the literature. It is evident from Tables 2.6.2 to 2.6.4 that the significant I.R. absorption peaks associated with coordinated β-diketonates and 2-hydroxy-1-napthaldehyde (-1) in both the dimeric [VO(AA)(OR)]$_2$ and the monomeric bis VO(AA)$_2$ complexes are essentially identical which indicates that the A$\underline{A}$H ligands in the dimers are non-bridging. Also Tables 2.6.4 and 2.6.5 illustrate that these band positions are generally independent of the nature or size of the bridging alkoxo groups and no particular effect of R or any reasonable trend in the band positions is observable.

TABLE 2.6.2: ASSIGNMENTS AND COMPARISON OF SOME MAJOR INFRARED PEAKS (cm^{-1}) OF SOME (VO(AA)(OEt)]$_2$ DIMERS AND VO(AA)$_2$ MONOMERS (AA$^-$ = β-DIKETONATES ONLY)

Assignments ↓ \ AA$^-$ =	acac		Bzac		dbm	
	Dimer	Monomer	Dimer	Monomer	Dimer	Monomer
νs C ⋯ O	1596 sh	1592 sh	1592 ms	1592 ms	1602 m	1602)
		1575 sh	1565 sh	1565 sh	1593 ms	1593) ms
	1575 s	1569 s	1550 sh	1550 s	1565 sh	
νs C ⋯ C	1530 s	1530 s	1530 s	1530 s	1530 s	1530 s
νas C ⋯ O	-	1345 msh	1313 m	1312 m	1322 m	1324 ms
νas C - O	1294 ms	1291 s	1297 w	1302 msh	1302 w	1312 msh
					1230 m	1232
δ C - H (deformation)	1185 sh	1190 w	1184 w	1186 w	1187 w	1184 w
π C - H (out of plane bending)	794 ms	800) s 791)	777 ms	780) ms 770)	770 s	765 ms

TABLE 2.6.3: THE C = O STRETCHING FREQUENCIES (cm^{-1}) OF THE [VO(AA)(OR)]$_2$ DIMERS (AA$^-$ = ANION OF HYDROXYALDEHYDE OR KETONE)

AA ↓ \ R=	Me	Et	Pr^n	Pr^i	Bz
HNP	1622 s	1625 s	1622 s	1625 s	1621 s
	1602 s	1605 s	1605 s	1605 s	1604 s
	1580 s	1585 s	1583 s	1585 s	1580 s
HAP	1618) s	1614 s	1612 s	1613 s	1612 s
	1607)	1584s	1585s	1588s	1585 s
	1508 s				1562 sh
VO(HNP)$_2$OH2*	(1623, 1604, 1586)				

* VO(HAP)$_2$ and VO(HNP)$_2$ could not be prepared

TABLE 2.6.4: COMPARISON OF SOME CHARACTERISTIC INFRARED PEAKS (cm^{-1}) (OTHER THAN ν V = O, ν C = O AND ν C - O ALKOXY) OF $[VO(HNP)(OR)]_2$ AND $VO(HNP)_2OH_2$

R	CHARACTERISTIC INFRARED PEAKS										
Me	1540 s	1424 s		1340 m	1308 m	1258 m	1197 m	1170 m	1145 m	833 s	756 s
Et	1547 s	1430 s	1360 sh	1340 m	1310 m	1260 m	1200 s	1170 m	1147 ms	834 s	760 s
Pr^n	1545 s	1430 ms		1342 ms	1310 w	1258 ms	1195 s	1170 s	1143 s	835 s	752 s
Pr^i	1545 s	1430 ms		1340 m	1310 w	1260 m	1200 s	1169 m	1150 w	830 sh	760 s
Bz	1545 s	1428 m		1340 w	1308 w	1255 w	1218 sh	1170 w	1146 w	865 w	755 s
$VO(HNP)_2OH_2$	1541 s	1430 m	1370 ssh	1340 w/m	1308 w	1252 m	1192 s	1169 s	1147 m	832 s	746 s

TABLE 2.6.5: ASSIGNMENTS OF SOME MAJOR INFRARED

PEAKS (cm^{-1}) OF $[VO(Bzac)(OR)]_2$ DIMERS

Assignments	R= Me	Pr^n	Pr^i	Bu^2	Bz	Ph	EtOMe
νs C···O	1620 sh 1589 s 1560 sh 1550 s	1592 s 1563 sh) 1554 ms)	1592 s 1563 ssh) 1554 s)	1590 s 1552 s	1590 s 1550 s	1590 s 1576 sh 1563 sh) 1553 s)	1590 s 1564 sh 1540 s
νs C···C	1536 s	1530 s	1532 s	1530 s	1530 s	1532 s	1530 s
νas C···O	1315 m	1358 s	1352 s	1355 s	1345 s	(1312 s) (1216 s)	1314 s
νas C-O	1291 s	1310 ms	1297 w 1298 w	1274 w	1292 m		1298 ms
δ C-H (deformation)	1180 w	1184 w	1185 w	1185 w 1174 w	1184 w	1196 m	1198 s) 1185 w)
π C-H (out of plane bending)	782 s	780 s	790 w	780 s 765 s	780 s	780 s	770 s

(iii) ν C - O (BRIDGING ALKOXO) REGIONS

Bands due to the C - O stretches of the coordinated alkoxo groups appear in the form of one or more strong absorptions in the 800-1200 cm^{-1} region[103], the exact positions of which are dependent upon the nature of the particular alkoxo group. For polynuclear Ti(OEt)$_4$, Ta(OEt)$_5$ and Nb(OEt)$_5$ complexes, Barraclough et al.[125], from experiments on hydrolysis of the alkoxides, assigned two C - O modes in the regions 1028-1040 cm^{-1} and 1064-1070 cm^{-1}, the former being associated with the bridging and the latter with the terminal ethoxo gruop. Lynch et al.[126] in studying some transition metal (Ti, Zr, Hf, etc.) isopropoxides reported the corresponding absorptions for the isopropoxy group at 1120-1140 cm^{-1} and 1160-1175 cm^{-1}.

The appearance of a single peak at 1030-1050 cm^{-1} in [(AA)$_2$Fe(OMe)]$_2$ (AA = acac, Hexafluoro-acac, DPM) dimers[103,104] was assigned to the C - O stretch of the bridging methoxo group. In the ethoxo-bridged dimers the absorption is at about 1050 cm^{-1} [103]. The strong absorption at 1120 cm^{-1} for [(DPM)$_2$Fe(OPr^i)]$_2$ [103] was assigned to the C - O stretch of the isopropoxo group. For the sec-butoxo dimer, [Fe(hfa)$_2$OCH(CH$_3$)CH$_2$CH$_3$]$_2$ [104], the band at 1000 cm^{-1} was assigned to the butoxo C - O stretch.

The ν C - O bands due to the bridging alkoxo groups of the present [VO(AA)(OR)]$_2$ complexes (Table 2.6.6) have been assigned by taking into consideration the aforementioned literature values for various metal alkoxides and alkoxo-bridged dimers and of the alcohols themselves. To confirm the positions of the ν C - O bands of the bridging alkoxo groups in the dimers, hydrolysis (partial and complete) reactions were performed on some of these dimers and their infrared spectra measured. Because of the sensitivity of these dimers towards moisture, their partial or complete hydrolysis occurs readily to give a mixture of VO(AA)$_2$ and VO(OH)$_n$ and a reduced amount or none of the dimer. The progress of the reaction was followed by recording the intensity of the ν C - O band as well as some other bands characteristic of the alkoxo group. For partial hydrolysis, the dimer was stirred in aqueous-

TABLE 2.6.6: INFRARED FREQUENCIES (cm^{-1}) CHARACTERISTIC OF THE

$\nu C - O$ (ALKOXO) OF THE $[VO(AA)(OR)]_2$ DIMERS

R ↓ / AA=	acac	Bzac	dbm	HNP	HAP
Me	1032 s	1031 s	1037 m	1035 s	1030 s
Et	1044 s	1035 m	1047 m	1042 s	1040 s
Pr^n	1047 s	1041 s	1046 m	1046 m	1045 m
Pr^i	1120 s	1115 s	1121 m	1113 ms	1120 ms
Bz	1034 m	1013 m	1028 m	1033	1032) w 1023)
Bu^n		1030 ms			
Bu^2		1014 s			
Ph		1162 m			
EtOMe		1125 s			

$CHCl_3$ for half to about three minutes and a portion of the $CHCl_3$ extract was then evaporated to dryness (on the vaccum line) and the infrared spectra of the residue recorded. For complete hydrolysis, the dimer, in the same solvent, was heated for about 15 minutes and the $CHCl_3$ evaporated off. The $VO(AA)_2$ was separated from $VO(OH)_n$, by washing with water and its $CHCl_3$ extract evaporated to dryness to obtain $VO(AA)_2$. The particular band reducing in intensity or disappearing on hydrolysis (Figure 2.6.2) was assigned to ν C - O of the alkoxo group by comparing its position with the ν C - O (strongest absorption) of the respective free alcohol. Some neighbouring bands other than the ν C - O that do not occur in the $VO(AA)_2$ were thus assigned as due to the particular alkoxo group. For example, the usually strong absorption appearing at 1035-1047 cm^{-1} in the $[VO(AA)(OEt)]_2$ dimers is assigned to a C - O stretch of the bridging ethoxo group on the basis of the C - O stretch near 1050 cm^{-1} in primary alcohols, and also by comparison with
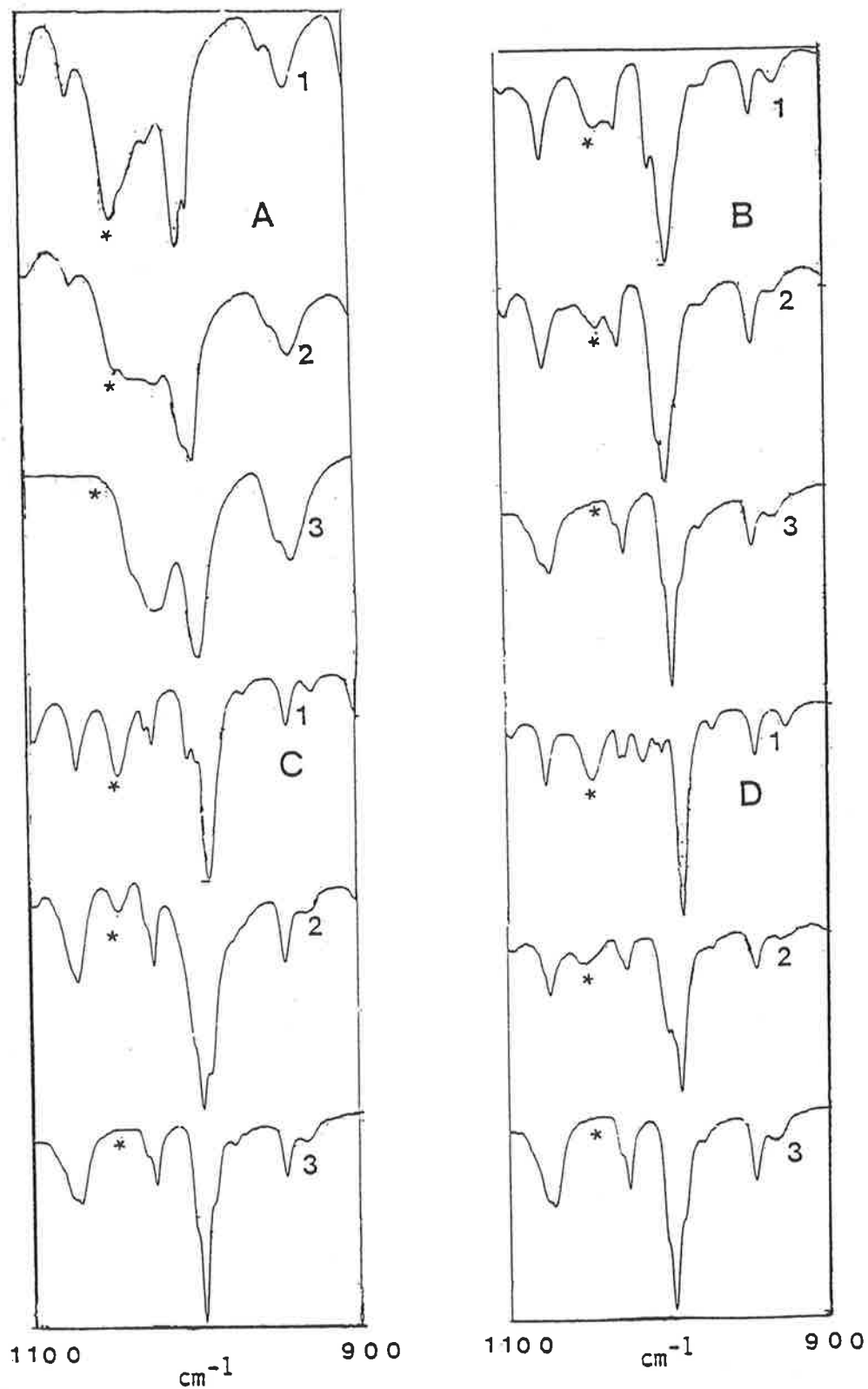
Figure 2.6.2: Infrared spectra showing reduction in intensity or disappearance of the $\nu C - O$ alkoxy band (*) on hydrolysis. (A) $[VO(acac)(OEt)]_2$; (B) $[VO(dbm)(OMe)]_2$; (C) $[VO(dbm)(OEt)]_2$ and (D) $[VO(dbm)(OPr^n)]_2$. [1, 2, 3 denote the spectrum taken before hydrolyis, on partial hydrolysis and on complete hydrolysis, respectively].

the symmetric νC - O at 1042 ± 5 cm^{-1} in R$_2$Sn(OEt)$_2$ [127].The additional neighbouring bands at ~ 1095, ~ 1070, ~ 889 and ~ 867 cm^{-1} are considered characteristic vibrations of the ethoxo group corresponding to absorptions at 1081, 1050 and 876 cm^{-1} in ethanol and are comparable with bands characteristic of some ethoxo complexes[103,104,127].

Table 2.6.6 shows that the band position due to ν C - O of a particular alkoxo group is generally independent of the nature of the bidentate ligands but dependent on the nature of the alkyl group. The ν C - O increases from methoxo to isopropoxo and the ν C - O for methoxo and benzyloxo (OCH$_2$C$_6$H$_5$) are generally the same.

2.7 ELECTRONIC SPECTRA

(i) SPECTRA OF VANADYL COMPLEXES

Several models are available to interpret the electronic spectra of vanadyl complexes of idealized or distorted square-pyramidal geometry. Furlani[128], Feltham[129] and Jorgensen[130] independently used elementary crystal field models to explain the energy level scheme for the vanadyl complexes. Based only on the Cαv symmetry of VO^{2+} alone, Furlani's calculations could not account for all the observed levels. Jorgensen's scheme, based on a tetragonal VO(H$_2$O)$_5^{2+}$ molecule ion with axial destabilization, could only qualitatively account for the 'crystal field' part of the spectrum. These simple crystal field models were also inadequate to explain the observed magnetic properties of some VO^{2+} compounds. To overcome these inadequacies of the simple crystal field model, Ballhausen and Gray[45] developed an energy level scheme (the B-G scheme) by considering the bonding in the molecule ion VO(H$_2$O)$_5^{2+}$ in terms of molecular orbitals which was able to account both for the 'crystal field' and the 'charge transfer' spectra of VO(H$_2$O)$_5^{2+}$ and related vanadyl complexes. They considered particularly the existence of considerable oxygen to vanadium π-bonding which is responsible for the charge transfer

features of the electronic spectrum of $VOSO_4.5\ H_2O$. Room temperature spectral data from various literature sources[4] fit the Ballhausen and Gray scheme well. Their M.O. bonding scheme also explains the resistance of VO^{2+} to protonation. With the oxygen 2p orbitals used for π-bonding, only the non-bonding spσ hybrid orbital is available for protonation which has considerable 2s character and is energetically unsuited for bonding purposes. They could also explain the paramagnetic resonance 'g' factors and the magnetic susceptibilities of vanadyl complexes in terms of their M.O. calculations. Their orbital transformation scheme for the metal and ligand orbitals in C_{4v} symmetry and the molecular orbital scheme for $VO(H_2O)_5^{2+}$ are given in Table 2.7.1 and Figure 2.7.1 respectively. Of $VO(H_2O)_5^{2+}$, one of the water molecules was considered to be <u>trans</u> to the oxo ligand resulting in a C_{4v} symmetry. The order of the energy levels established by them for this symmetry is:

$$b_2\ (d_{xy}) < e\ (d_{xz},\ d_{yz}) < b_1\ (d_{x2-y2}) < a_1\ (d_{z2})$$

Spectral assignments of some oxovanadium(IV) complexes are given in

TABLE 2.7.1: ORBITAL TRANSFORMATION SCHEME IN C_{4v} SYMMETRY[4 5]

REPRESENTATION	METAL ORBITALS	LIGAND ORBITALS
a_1	$3d_{z2} + 4s$	σ_5
	$4s - 3d_{z2}$	$\frac{1}{2}\ (\sigma_1 + \sigma_2 + \sigma_3 + \sigma_4)$
	$4p_z$	σ_6
e	$3d_{xz},\ 3d_{yz}$	$\pi_5\ (2px,\ 2py)$
	$4px,\ 4py$	$\frac{1}{\sqrt{2}}\ (\sigma_1 - \sigma_3),\ \frac{1}{\sqrt{2}}\ (\sigma_2 - \sigma_4)$
b_1	$3d_{x2-y2}$	$\frac{1}{2}\ (\sigma_1 - \sigma_2 + \sigma_3 - \sigma_4)$
b_2	$3d_{xy}$	

Table 2.7.2 giving the approximate energy regions for the transitions. The main features of the spectra of vanadyl complexes are strikingly similar; a band (band I) at about 13,000 cm^{-1} for the electron transition $e_{\pi}^{*} \leftarrow b_2$ or
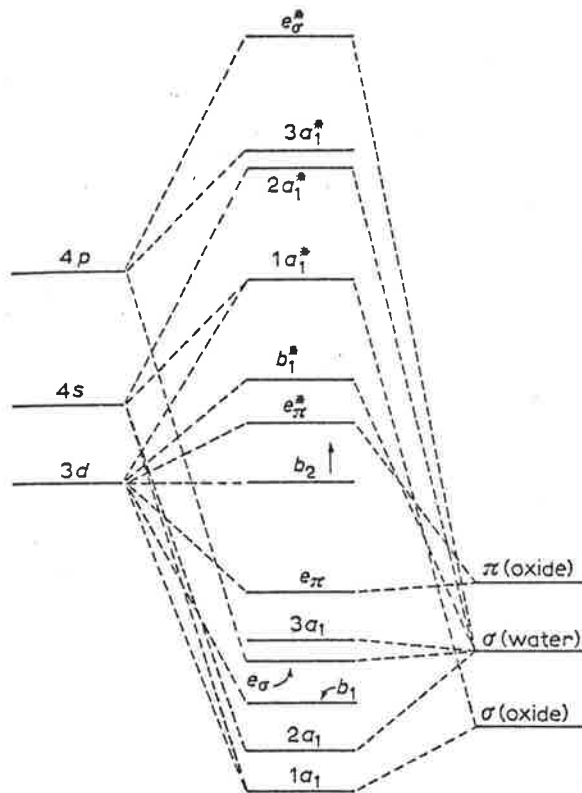
Figure 2.7.1: Energy level diagram for $VO(H_2O)_5^{2+}$ according to Ballhausen and Gray.

TABLE 2.7.2: BAND ASSIGNMENTS FOR SOME VO^{2+} COMPLEXES
ACCORDING TO THE B - G SCHEME[45]

C O M P L E X	BAND POSITIONS (X 10^{-3} CM^{-1})			
	BAND I	BAND II	BAND III	a
	$^2E(1) \leftarrow {}^2B_2$	$^2B_1 \leftarrow {}^2B_2$	$^2A_1 \leftarrow {}^2B_2$	b
	$e_\pi^* \leftarrow b_2$	$b_1^* \leftarrow b_2$	$1a_1^* \leftarrow b_2$	c
	$xz,yz \leftarrow xy$	$x^2-y^2 \leftarrow xy$	$z^2 \leftarrow xy$	d
$VO(acac)_2$ [111]	14.0	17.0		
$VO(enta)^{2-}$ [45,130]	12.8	17.2	29.8	
$VO(oxalate)_2^{2-}$ [45,130]	12.6	16.5	29.4	
$[VO(dl\text{-}tartrate)]_2^{4-}$ dimer[131]	13.4	18.6	23.1	
VO^{2+} complex[4,132] (general)	12-15	15-18	22-30	

a: Band number   c: Electronic energy levels

b: B-G M.O. assignments   d: Transitions between d orbitals

$^2E(1) \leftarrow {}^2B_2$, followed by a second band (band II) at about 17,000 cm^{-1} due to the electron transition $b_1^* \leftarrow b_2$ or $^2B_1 \leftarrow {}^2B_2$. Often the third band (band III) at 20,000-30,000 cm^{-1} is either not observed (presumably because it is buried beneath a much more intense charge transfer band which often sets in at about 30,000 cm^{-1}), or it is seen as a shoulder on that band and is assigned to the transition $^1a_1^* \leftarrow b_2$ or $^2A_1 \leftarrow {}^2B_2$. All higher energy bands up to 50,000 cm^{-1} are also assumed to be charge transfer in origin or are due to intraligand transitions.

The value of 10 Dq is obtained directly from the $b_1 \leftarrow b_2$ transition. And the parameters Ds and Dt specifying the degree of the tetragonality present in the field can be calculated[45,133] from the transitions,

$$e \leftarrow b_2 = (-3\ Ds + 5\ Dt) \quad\ldots\ldots\ldots\ldots\ldots(1)$$

$$b_1 \leftarrow b_2 = 10\ Dq \quad\ldots\ldots\ldots\ldots\ldots\ldots\ldots(2)$$

$$a_1 \leftarrow b_2 = (10Dq - 4\ Ds - 5\ Dt) \quad\ldots\ldots\ldots(3)$$

To explain the electronic spectra of complexes of lower symmetry and at low temperatures, Selbin et al.[111,134,135] proposed different assignments to those of the above B-G scheme. According to their proposal, the observed band I of the B-G scheme contains three bands assigned as (i) $dxy \rightarrow dx^2\text{-}y^2$, (ii) $dxy \rightarrow dxz$ and (iii) $dxy \rightarrow dyz$, band II becomes (iv) $dxy \rightarrow dz^2$ and band III becomes (v) the fifth band, arising from the first charge transfer transition $e\pi^b \leftarrow b_2$. The spectrum of VO(acac)$_2$ [111] shows two bands at 14,000 and 17,000 cm^{-1}: the first of these is split into three components at low temperature and the total of four bands have been interpreted as d-d transitions in C_{2v} symmetry.

Subsequent work using more refined M.O. calculations on VO(H$_2$O)$_5^{2+}$ [136] and VOCl$_4^{2-}$ [137] and on certain vanadyl complexes of C_{2v} symmetry[138,139] confirmed

the relative energy order of the B-G scheme as:

$$d_{xy} < d_{xz} < d_{yz} < d_{x2-y2} < d_{z2}$$

with the dxz and dyz orbitals being non-degenerate in the lower symmetry cases. However, it has been pointed out that although the relative order of the orbitals is the same, the removal of some of the more drastic B-G assumptions and approximations changes the energy gaps between the levels considerably. Consequently, in the absence of low temperature spectra, an interpretation of band I as given by the B-G scheme should be treated cautiously because there is a possibility of its being an envelope of up to three transitions.

(ii) SPECTRA OF DIMERIC COMPLEXES

The only previous work on electronic spectra of dimeric vanadyl complexes is that of L.J. Theriot et al.[37,43,140], Syamal[41] and Havinale[40]. They examined the spectra of several [VO(O N O)]$_2$ complexes for which they assumed dimeric structures on the basis of subnormal magnetic moments (cf. Section 1.2.1). Such spectra are, of course, very relevant to the compounds which are the subject matter of this Chapter. Because of their insolubility, these dimeric complexes were examined in nujol mulls and occasionally in pyridine solution. The spectra were described as being dominated by strong charge transfer bands at about 25,000 cm^{-1} with up to three other bands appearing as shoulders, which were assigned mostly according to the B-G scheme. However, such assignments are based on not well-resolved spectra in the solid state and, although reasonable, can only be considered as tentative.

The electronic spectra of most of the [VO(AA)(OR)]$_2$ dimeric complexes presented in this Chapter were determined in chloroform solution and the energy of the principal bands and their assignments are summarized in Table 2.7.3. Most of these spectra were determined from compounds in which the bidentate AA is acac, Bzac and dbm. However, only a limited number of spectra was determined with the other ligands because of their low solubility and

their instability in chloroform solutions, unless extremely rigorous conditions are followed. For the same reasons, molar absorptivities were only determined in few cases. Examples of spectra, together with those of the corresponding monomeric $VO(AA)_2$ complexes are shown in Figures 2.7.2 to 2.7.4. However, when AA is HNP, the spectra are not strictly comparable because only the hydrate, $VO(HNP)_2.OH_2$ could be obtained. As mentioned earlier, $VO(HAP)_2$ could not be prepared.

A three-band spectrum is obtained for the $[VO(acac)(OR)]_2$ dimers, whereas, in the other $[VO(AA)(OR)]_2$ complexes, there is an additional band in the ultra-violet region. On the basis of the square-pyramidal (C_{4v}) geometry for each vanadium centre and following the energy level scheme by Ballhausen and Gray[45], the two bands at about 15,000 and 17,00 cm^{-1} are assigned to the electronic transitions $e\pi^* \leftarrow b_2$ or $^2E(1) \leftarrow {}^2B_2$ (d_{xz}, $d_{yz} \leftarrow d_{xy}$) and $b_1^* \leftarrow b_2$ or $^2B_1 \leftarrow {}^2B_2$ ($d_{x2-y2} \leftarrow d_{xy}$) respectively. According to the B-G scheme, there should be a third band between 23,000 cm^{-1} and 30,000 cm^{-1} due to the transition $1a_1^* \leftarrow b_2$ or $^2A_1 \leftarrow {}^2B_2$ ($d_{z2} \leftarrow d_{xy}$). This band is most often masked by, or appears as a shoulder on, an intense charge transfer band present in the region. Such shoulders are detectable in the spectra of the $VO(AA)_2$ complexes (e.g. curves 1 in Figures 2.7.2 - 2.7.4). In the dimer complexes, because the charge transfer band is shifted to the longer wave lengths, such shoulders are only seen in a few cases, such as curve 4 in Figure 2.7.2 and curves 3 and 4 in Figure 2.7.4. The additional bands appearing at 33,000-38,000 cm^{-1} are due to intraligand transitions associated with the presence of aromatic rings.

Considering the energy of the bands and their molar absorptivity values (Table 2.7.3), the spectra of the dimers are similar to that of the corresponding $VO(AA)_2$ monomers. Figures 2.7.2 - 2.7.4 clearly indicate the similar patterns in the dimer spectra in complexes with the same AA and varying OR groups. However, the spectra of dimers have small but consistent characteristic differences from those of the monomers. The $VO(AA)_2$ monomers show two distinct absorption maxima in the visible region, whereas the dimer spectrum
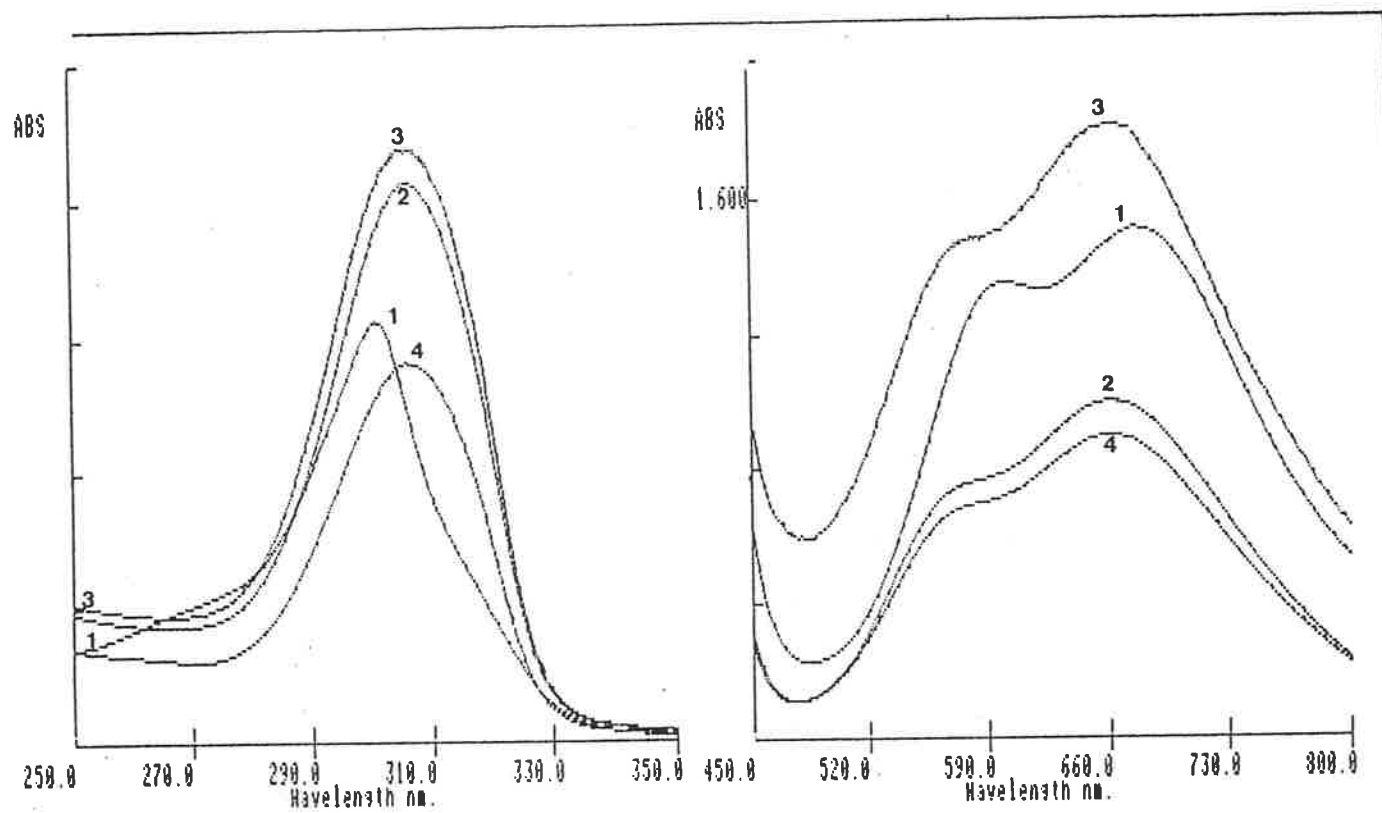
Figure 2.7.2: Electronic spectra (in CHCl₃/N₂) of 1. VO(acac)₂;
2-4. VO(acac)(OR)]₂ with R = Me(2), Et(3) and Bz(4).
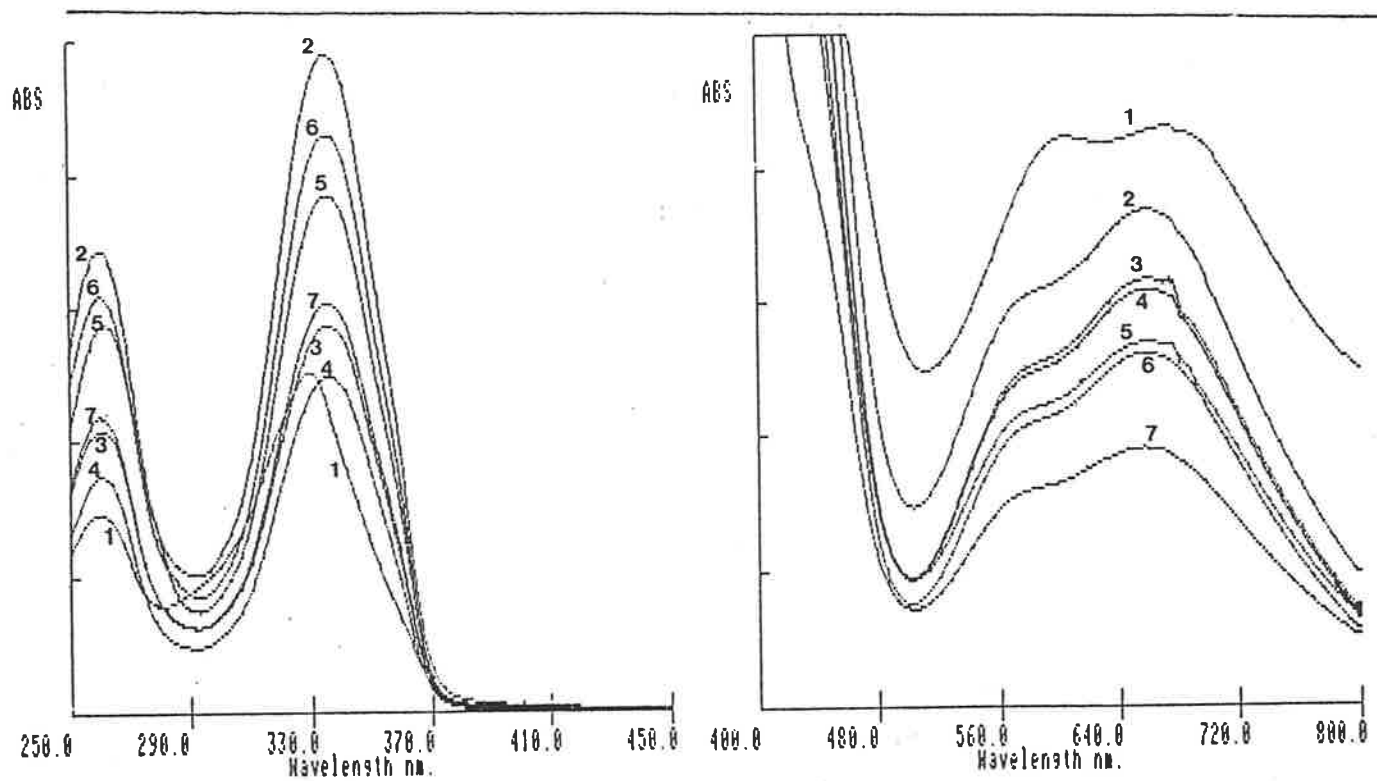
Figure 2.7.3: Electronic spectra (in $CHCl_3/N_2$) of 1. $VO(Bzac)_2$; 2-7. $[VO(Bzac)(OR)]_2$ with R = Me(2), Pr^n(3), Bu^2(4), Ph(5), EtOMe(6) and Bz(7).
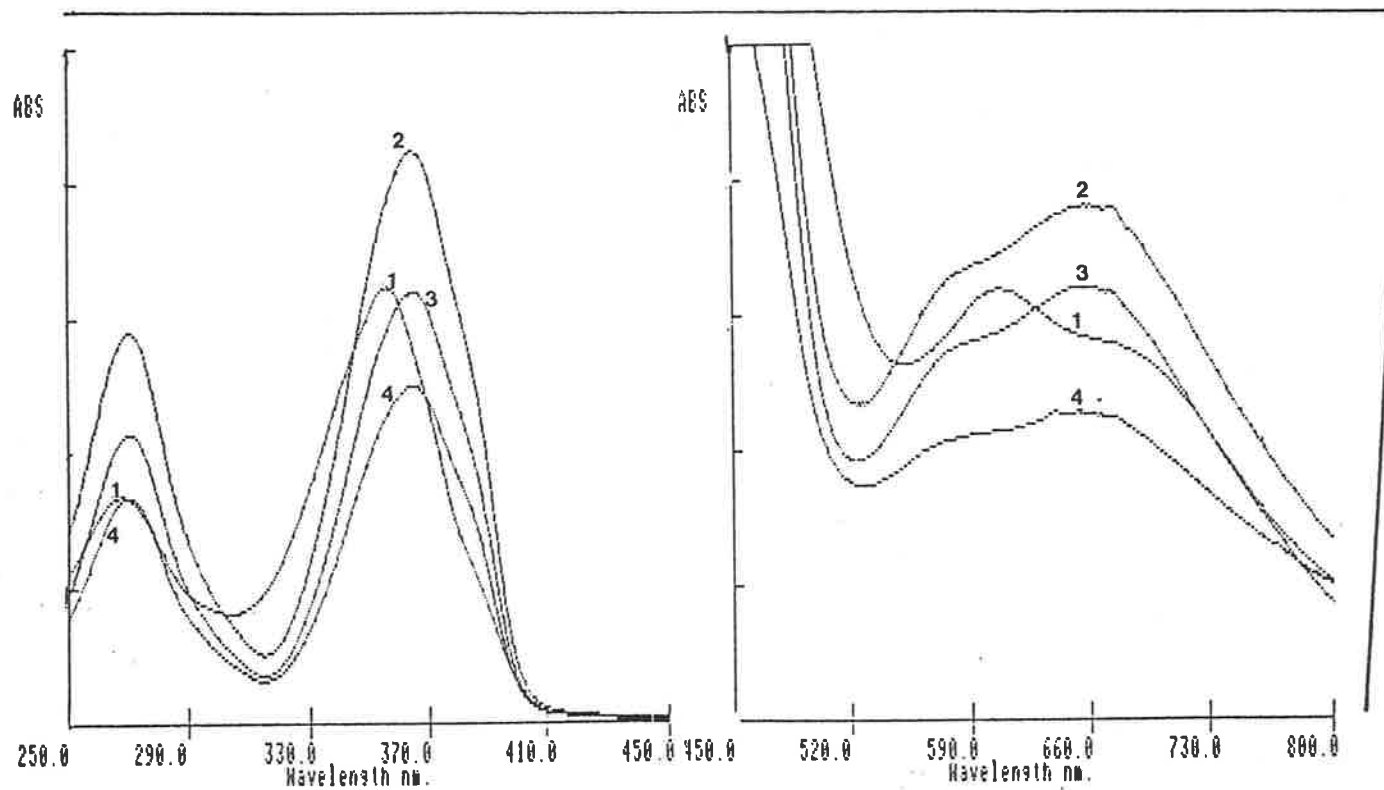
Figure 2.7.4: Electronic spectra (in $CHCl_3/N_2$) of 1. $VO(dbm)_2$; 2-4. $[VO(dbm)(OR)]_2$ with R = Et(2), Pr^n(3) and Bz(4).

TABLE 2.7.3: ELECTRONIC SPECTRAL DATA AND BAND ASSIGNMENTS FOR
$VO(AA)_2$ AND $[VO(AA)(OR)]_2$ COMPLEXES.[*] (SOLVENT = $CHCl_3$;
'a' DENOTES 95% CH_2Cl_2 5% EtOH)

	BAND POSITIONS ($\times 10^{-3}$ CM^{-1}) (MOLAR ABSORPTIVITIES ($M^{-1}cm^{-1}$) ARE SHOWN IN PARENTHESES)			
COMPLEX	BAND I $e_\pi \leftarrow b_2$	BAND II (br.sh in dimers) $b_1^* \leftarrow b_2$	BAND III C.T. ($1a_1^* \leftarrow b_2$)	BAND IV C.T./Intraligand
$VO(acac)_2$	14.8 (42)	16.8 (38)	33.2 (1.37 x 10⁴)	
$[VO(acac)(OMe)]_2$	15.1 (54)	17.2 (43)	32.7	
$[VO(acac)(OEt)]_2$	15.1 (53) 15.2ᵃ (55)	17.2 (41) 17.3ᵃ (44)	32.7 (1.97 x 10⁴)	
$[VO(acac)(OBz)]_2$	15.1	17.2	32.7	
$VO(Bzac)_2$	14.8 (54)	16.5 (53.5)	30.3 (2.86 x 10⁴)	38.8 (1.78 x 10⁴)
$[VO(Bzac)(OMe)]_2$	15.2 (65)	17.2 (54)	29.8	38.3
$[VO(Bzac)(OEt)]_2$	15.1 (64) 15.2ᵃ (68)	17.1 (54) 17.1ᵃ (56)	29.8 (3.35 x 10⁴)	38.3 (2.35 x 10⁴)
$[VO(Bzac)(OPr^n)]_2$	15.2	17.1	29.8	38.3
$[VO(Bzac)(OBu^2)]_2$	15.2	17.1	29.8	38.3
$[VO(Bzac)(OPh)]_2$	15.2	17.1	29.8	38.3
$[VO(Bzac)(OEtOMe)]_2$	15.2	17.1	29.8	38.3
$[VO(Bzac)(OBz)]_2$	15.1	17.1	29.8	38.3
$VO(dbm)_2$	14.9 (64)	16.5 (58)	28.1 (3.91 x 10⁴)	37.3 (2.08 x 10⁴)
$[VO(dbm)(OEt)]_2$	15.2 (88)	17.2 (77)	27.5 (4.72 x 10⁴)	36.9 (3.43 x 10⁴)
$[VO(dbm)(OPr^n)]_2$	15.2	17.2	27.4	37.0
$[VO(dbm)(OBz)]_2$	15.2	17.2	27.5	37.0
$[VO(HNP)(OPr^n)]_2$	15.5	17.1	25.0	29.1, 33.3
$[VO(HAP)(OBz)]_2$	15.0	18.1	25.9	30.8, 36.4

* The spectra of some of the less stable complexes were not determined.

consists of two broad bands, which are not clearly separated and with the higher energy band appearing as broad shoulder on the other. All absorption maxima in the visible region in the case of dimers appear at slightly higher energies (290-340 cm^{-1} for band I and 430-750 cm^{-1} for band II) with respect to that for the monomers. This somewhat higher energy of the dimer d-d bands suggests that the crystal field produced by the two alkoxo oxygens is stronger than that due to the bidentate ligands. Thus, in the [VO(acac)(OR)]$_2$ complexes it is about 430 cm^{-1}, in [VO(Bzac)(OR)]$_2$ complexes, 620 cm^{-1} and in the [VO(dbm)(OR)]$_2$ complexes about 750 cm^{-1} stronger than in the respective monomers. These estimates are based on the B-G scheme which indicates 10 Dq with band II [cf. Section (i)]. If, however, one accepts the assignments given by Selbin[111] these values would be stronger by 300, 400 and 290 cm^{-1} respectively. Such comparisons are not possible for [VO(HNP)(OR)]$_2$ and [VO(HAP)(OR)]$_2$ complexes. The three diketonato ligands and HAP appear to produce a similar crystal field, however, HNP produces a significantly stronger crystal field by about 500 cm^{-1}. In the ultra-violet region, the dimer peaks appear at lower energy levels (about 400-600 cm^{-1}) with respect to that of the monomers.

Table 2.7.3 indicates that the molar absorptivity values of the dimer and the monomer are of the same order and are consistent with the d-d transitions in the visible region (20-45 $M^{-1} cm^{-1}$ per vanadium centre) and with the charge transfer and/or intraligand transition in the UV region [(1-3) x 10^4].

The separation between bands I and II gives a measure of the difference between the crystal field in the Z and in the X and Y directions[133]. As is evident from the Figure below, the smaller the separation the greater is the tetragonal distortion. The fact that the gap between band I and band II is greater in the dimers than in the monomers (e.g. by about 100 cm^{-1} in [VO(acac)(OR)]$_2$, about 300 cm^{-1} in [VO(Bzac)(OR)]$_2$ and about 470 cm^{-1} in [VO(dbm)(OR)]$_2$ dimers) suggests that the tetrogonal distortion is less in the dimers. This is in agreement with the qualitative observation that the

stronger field due to the alkoxo groups will increase the field in the xy
plane and hence reduce the tetragonal distortion. There are schemes which
permit the calculation of parameters which give a quantitative measure of this
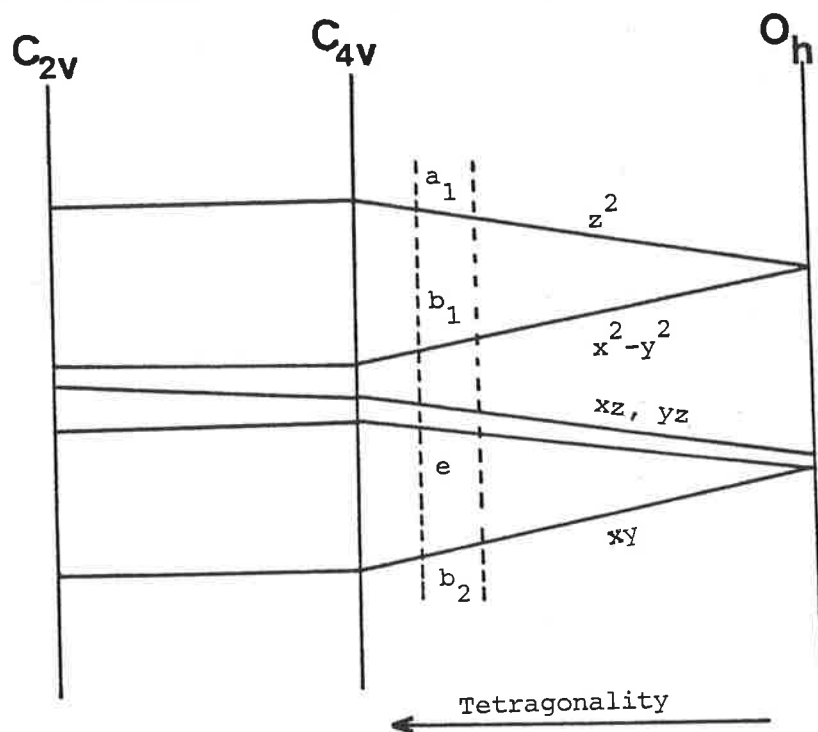
d-orbital splittings in fields of varying symmetry as a
result of varying CF effects. The dotted lines bracket
the approximate region observed in this work.

distortion[45,141,142]. However, these values are heavily dependent on the
energy of band III [133] due to $1a_1^* \leftarrow b_2$ transitions which cannot be determined
accurately in these dimeric complexes for its being masked by the intense
charge transfer band.

The width of bands I and II is difficult to determine because they appear
as a composite band. An estimate can be obtained by measuring the half-height
distance between the position of band I and the low energy contour. Such
estimates suggest that the bands in the dimers are about 200-300 cm^{-1} broader
than in the monomers. From the magnetic studies, a J value of about 100 cm^{-1}
has been obtained for the splitting of the ground state. Although this may be
fortuitous, it is consistent with a splitting of this order in the energy

levels of the d orbitals in the dimeric structures.

In conclusion, the visible and the UV spectra of the dimers are consistent with the proposed structures showing a great similarity to the spectra of the monomeric species and differing only in a slightly stronger crystal field and marginally greater band width.

2.8   ELECTRON SPIN RESONANCE SPECTRA

(i)   INTRODUCTION

The E.S.R. measurements are useful in the study of the dimeric complexes, especially in establishing the dimeric nature of such complexes. Compared to the usually sharp E.S.R. signals for monomeric complexes, because of spin relaxation the dimers show broad features around the mid-field region. The dimers generally exhibit two features, a broad line in the midfield ($g \sim 2$) region for $\Delta M_S = \pm 1$ transition which is often masked or mixed with strong and sharp features due to monomer impurities which exhibit hyperfine splitting. The appearance of a line in the half-field ($g \sim 4$) region for the $\Delta M_S = \pm 2$ 'forbidden' transitions, indicating the presence of triplet-state, confirms the existence of the principal dimer complex. The above features character-istic of dimeric behaviour of the complexes are observable in both powdered solid, in solution and in frozen solution E.S.R. spectra.

Although the half-field absorption at $g \sim 4$ is always a clear indication and proof of the presence of the dimer species, in most cases the admixture of monomer and dimer signals makes it difficult to interprete the mid-field spectra at $g \sim 2$, as even a trace amount of monomer impurity can affect the E.S.R. spectra significantly. Similar observations have been reported by other workers. For example, analytically pure $[Cu_2(Me_5\text{-}dien)_2(N_3)_2](BPh_4)_2$ even after recrystallization[143] showed the monomeric impurity features markedly even though it has little effect on the bulk magnetic susceptibil-ity. Not only the sharp monomer lines dominate the first derivative spectra but attempts to enhance the spectrum by lowering the temperature increase the

sensitivity of the monomeric species while at the same time decrease the population of the triplet state of the antiferromagnetically coupled dimer. In the present alkoxo-bridged dimer systems the effect of the monomer impurity is much more pronounced because of the very high instability and ease of hydrolysis of these dimers. The features, due to the dimer, are generally poorly resolved as expected, because of dipole-dipole broadening.

At liquid nitrogen temperature, the dimer complexes of polycrystalline solid state[42,43,144] or as frozen solution[106,143,145-147] often show hyperfine splittings of the half-field line giving in many cases $2(I_1 + I_2) + 1$ lines which provide further and conclusive evidence for the existence of the principal dimers. In some cases, hyperfine splittings of the $\Delta M_s = \pm 1$ high-field region are also observed[42,143] at liquid nitrogen temperature. This additional hyperfine splitting feature of the dimers is not observed in many individual cases[42,43].

(ii) PREVIOUS RELATED STUDIES

Although a small number of dimeric vanadyl complexes have been studied by E.S.R. methods[6], there has been an extensive solution studies of dimeric copper complexes which also serve as a useful model for our system. Lippard et al.[106] observed clearly the seven-line $[2(3/2 + 3/2) + 1;$ for Cu, $I_1 = I_2 = 3/2]$ hyperfine splitting for the $\Delta M_s = \pm 2$ transition at ~ 1500 G, characteristic of a dimer system, in both the powdered solid at low temperature and in frozen solution of an imidazole-bridged copper complex. Belford et al.[131,146] observed in the g = 2 region a 15-line E.S.R. spectrum for the vanadyl tartrate complexes in solution which they attributed to electron exchange between the two vanadium nuclei $[2(7/2 + 7/2) + 1 = 15]$ constituting a dimer. Their observation of the half-field (g ~ 4) 'forbidden' transitions for all the tartrate (d-, l-, dl-) complexes confirmed the existence of triplet-state binuclear species in these complexes in solution. The E.S.R. spectra of a number of dimeric vanadyl complexes of tridentate ligands were measured in the

polycrystalline solid state[42,43,144] where some of the dimers exhibited the half-field spectra at ~ 1600 G. The low temperature solution E.S.R. studies of some porphyrin dimers of oxovanadium(IV) showed weak absorption at the half-field region and hyperfine splitting in the mid-field region[2] and (for others) the hyperfine splittings in the mid-field as well as in the low-field regions[148].

(iii) RESULTS AND DISCUSSION

(a) POWDERED SOLIDS

All powdered solid E.S.R. spectra of the $[VO(AA)(OR)]_2$ complexes with varying AA and OR groups (some are shown in Figure 2.8.1) are similar in nature and show absorptions in two regions, viz. (i) in the mid-field region (~ 3000 G) a generally very broad feature encompassing a field of about 1500 G with a superimposed narrower feature (width 280-300 G) and (ii) a weak absorption in the half-field region. The relative intensity of the half-field (g ~ 4) region is unpredictable and is about 2-5% of the broad mid-field absorption. The absorptions in the mid- and half-field regions are different from those of the powdered monomer. Similar mid- and half-field spectra are also observed at low temperatures. The intensity of the half-field absorption follows the intensity of the broad feature. As may be seen from the pairs of spectra A, B and C in Figure 2.8.1, there is no any correlation of the effect of temperature with the spectra.

All the spectra have similar shapes and features at room and low temperatures. The broad mid-field and weak half-field absorptions, which are not present in the monomer spectra, can be taken as evidence for the presence of a dimer structure. The broadness of the features and the absence of hyperfine splitting are due not only to intramolecular spin-spin relaxation but also to intermolecular interactions involving both dimers and/or monomers. For example, the spectrum of $VO(acac)_2$ in powdered form shows an unsplit single feature of about 300 G. It is, therefore, not possible to interpret the
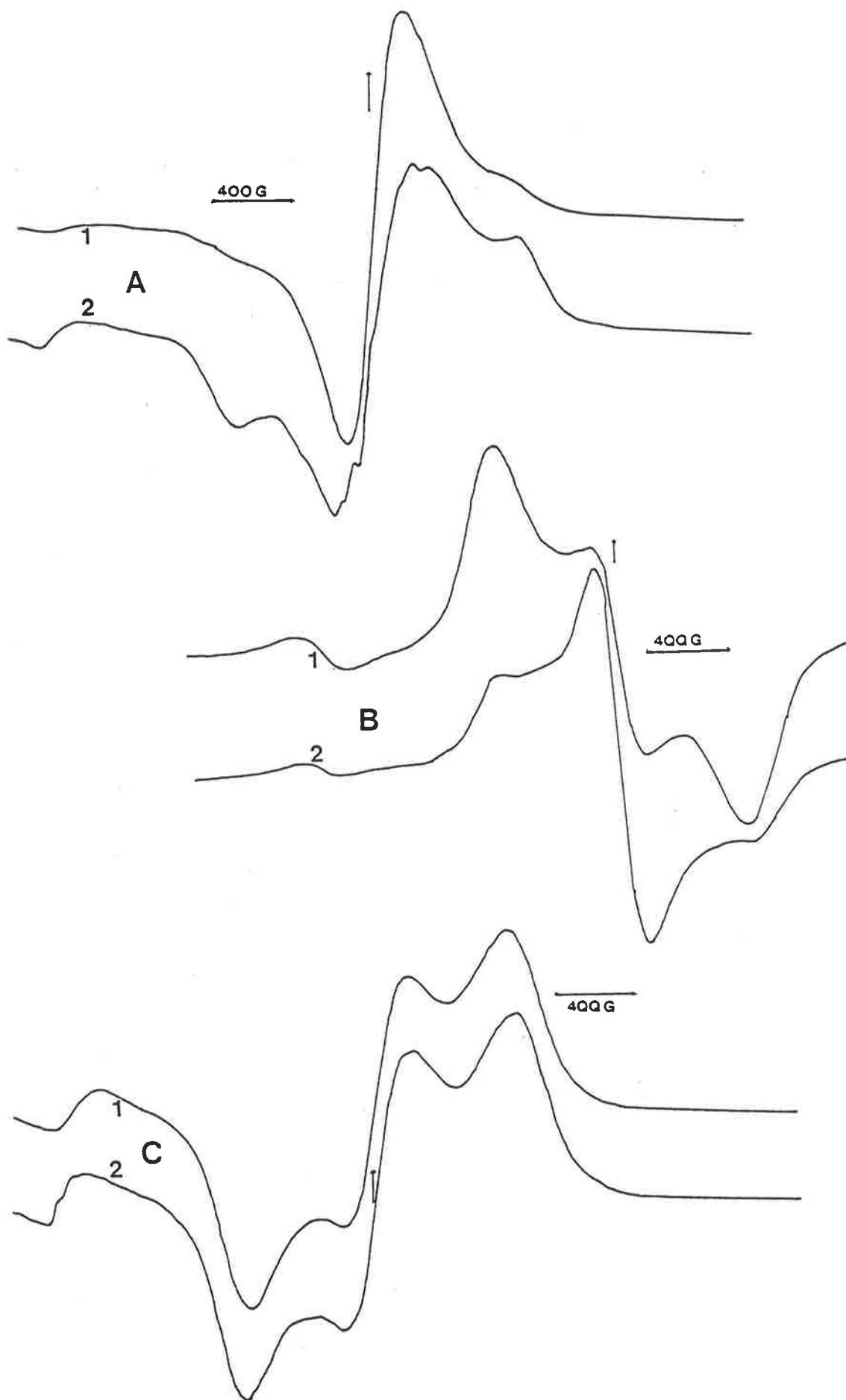
Figure 2.8.1: E.S.R. spectra (1 at room temperature; 2 at -160°C) of
A. [VO(Bzac)(OMe)]$_2$; B. [VO(Bzac)(OEtOMe)]$_2$ and
C. [VO(Bzac)(OBu^2)]$_2$. ($\downarrow$ DPPH).

apparent relative intensity of the two features in the mid-field regions in terms of the ratio of monomer to dimer. Although, no doubt, a small amount of monomer must be present in the solid as a result of hydrolysis, its contribution to the shape of the spectrum must be much higher than its actual concentration in terms of dimer content. Also, because of the different extent of E.S.R. responses of the monomer and the dimer, their relative ratio in the sample can not be deduced merely from the shape of the spectrum.

The low temperature spectra were recorded at -160°C. In these spectra no significant differences were observed from that recorded at room temperature. For $[VO(Bzac)(OEtOMe)]_2$, the low temperature spectrum [Figure 2.8.1 (B)] shows less dimeric and more monomeric feature in the mid-field region. Excluding the effects of relaxation as a function of temperature, one would expect the dimer lines to decrease in intensity as the temperature is lowered due to lower population of the triplet-state and thus the relative intensity of the monomer should increase. However, this may be a fortuitous coincidence because other complexes either showed no significant change in the relative intensities, e.g. $[VO(acac)(OBz)]_2$, $[VO(dbm)(oPr^n)]_2$, $[VO(Bzac)(OBu^2)]_2$ [Figure 2.8.1 (C)] and $[VO(HAP)(OMe)]_2$ or, as in the case of $[VO(Bzac)(OMe)]_2$ [Figure 2.8.1 (A)], the reverse of the expected change was observed. It seems that temperature effects cannot be explained simply in terms of changes in the populations of the singlet and triplet states but that the effect of temperature on the intermolecular spin-spin relaxation must also play a part. Felthouse and Hendrickson[143] also observed similar interesting, unusual temperature dependencies of the E.S.R. spectra of some di-μ-(1,3)-azido copper(II) dimers which, they noted, might be due to the varied degree of contributions from exchange, dipolar, pseudo dipolar and hyperfine interactions.

(b) SPECTRA IN SOLUTION

The E.S.R. spectra of a few of the $[VO(AA)(OR)]_2$ complexes were also recorded in solution at room temperature and at -160°C. At room temperature,

the spectra show a broad absorption with a superimposed 8-line hyperfine structure (Figure 2.8.2). By joining the mid-points of the hyperfine lines (e.g. spectrum F in Figure 2.8.2) it is possible to estimate approximately the half-line widths and the g- values of the dimers. These are given in Table 2.8.1.

Even with extreme precautions to exclude moisture some hydrolysis of the complexes according to

$$[VO(AA)(OR)]_2 \xrightarrow[H_2O]{CH_2Cl_2} VO(AA)_2 + VO(OH)_2$$
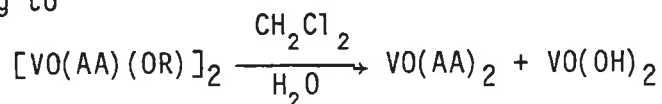
takes place as evident from the formation of $VO(OH)_2$ in E.S.R. tubes filled and sealed on the vacuum line. It is, therefore, not surprising that a monomer spectrum is observed with an A value of 107 G which is in agreement with that for $VO(acac)_2$ or $VO(Bzac)_2$. This does not exclude the possibility of the presence of monomeric species of the type VO(AA)(OH) or VO(acac) (solvent) where, solvent could represent one or more molecules of ROH either as intermediates or in equilibrium with the dimeric form. Because of their sharpness, the monomer signals dominate the spectra. However, by allowing the samples to hydrolyse completely, it was possible to show that good quality specimens contained originally no more than 2-5% of the vanadium in the monomer form. Thus the clearly observed, very broad nature of the signal in the high field region, underneath the 8-line hyperfine splitting, which is caused by the spin-spin relaxation due to the dimer structure of the complex shows the major constituent in the solution to be the principal dimer complex.

The frozen solution E.S.R. spectra of some of the more soluble dimers were recorded in toluene or dichloromethane. In the frozen solution spectra (Figures 2.8.3 and 2.8.4), as in the powder spectra, the broad signal predominates. In all cases, the broad signal has superimposed on it a large number of sharp narrower lines. These spectra show similarities to those of the dimeric vanadyl citrates[147], vanadyl tartrates[146] and vanadyl deuteroporphyrinedimethylester[148] except some satellites.
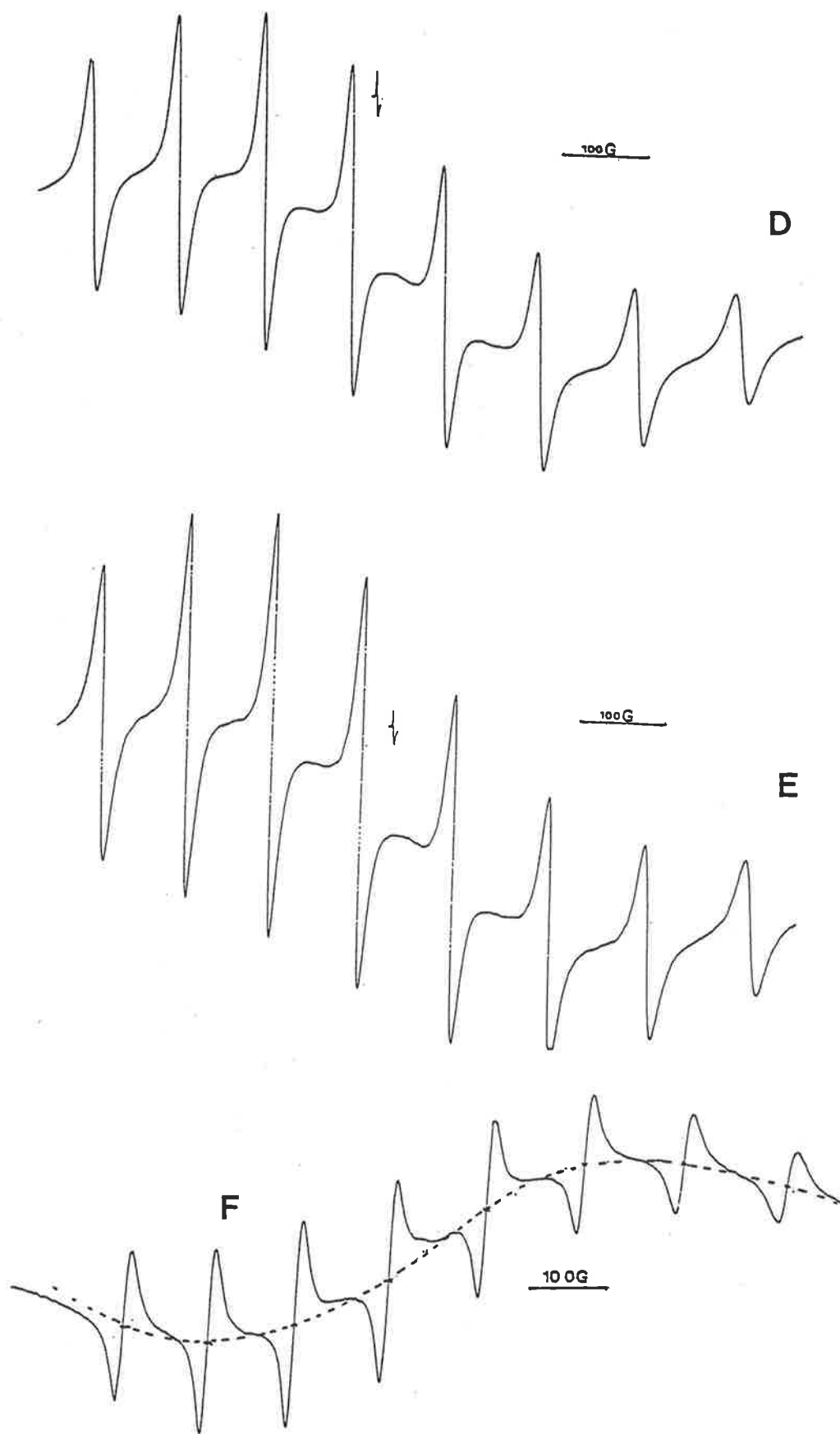
Figure 2.8.2: Room temperature solution E.S.R. spectra (in toluene) of D. $[VO(acac)(OEt)]_2$; E. $[VO(acac)(OPr^n)]_2$ and F. $[VO(acac)(OPr^i)]_2$ (ι DPPH).

TABLE 2.8.1: E.S.R. DATA FOR SOME $[VO(AA)(OR)]_2$ DIMERS

COMPOUND	SOLVENT	TEMP. °C	APPROXIMATE BROADNESS (G) (OF THE MAIN FEATURE)	g VALUES g_2	g_4	A_0 MID-FIELD (G)
$VO(acac)_2$	Solid	26	300	1.98	-	-
$[VO(acac)(OMe)]_2$	Solid	-160	1500	1.96	4.06	-
	CH_2Cl_2	20	470	1.976	-	107
	$C_6H_5CH_3$	20	470	1.973	-	107
	$C_6H_5CH_3$	-160	1700	1.98	3.96	-
$[VO(acac)(OEt)]_2$	Solid	-160	1400	1.94	4.09	-
	CH_2Cl_2	20	470	1.972	-	107
	$C_6H_5CH_3$	20	470	1.974	-	107
	$C_6H_5CH_3$	-160	1700	1.98	-	-
$[VO(acac)(OPr^n)]_2$	$C_6H_5CH_3$	20	470	1.981	-	107
	$C_6H_5CH_3$	-160	1700	1.98	4.00	-
$[VO(acac)(oPr^i)]_2$	$C_6H_5CH_3$	20	470	-	-	-
	$C_6H_5CH_3$	-160	1700	-	-	-
$[VO(Bzac)(OMe)]_2$	Solid	21	1400	1.97	-	-
	Solid	-160	1450	1.96	4.00	-
$[VO(Bzac)(OEt)]_2$	CH_2Cl_2	20	470	1.973	-	107
	Solid	-160	1450	1.96	4.00	-
$[VO(Bzac)(OEtOMe)]_2$	Solid	19	1400	1.98	3.88	-
	Solid	-160	1250	1.98	3.86	-
$[VO(Bzac)(oBu^2)]_2$	Solid	22	1400	1.98	4.00	-
	Solid	-160	1400	1.98	4.00	-
$[VO(HAP)(OMe)]_2$	Solid	20	1400	1.98	-	-
	Solid	-160	1400	1.97	-	-
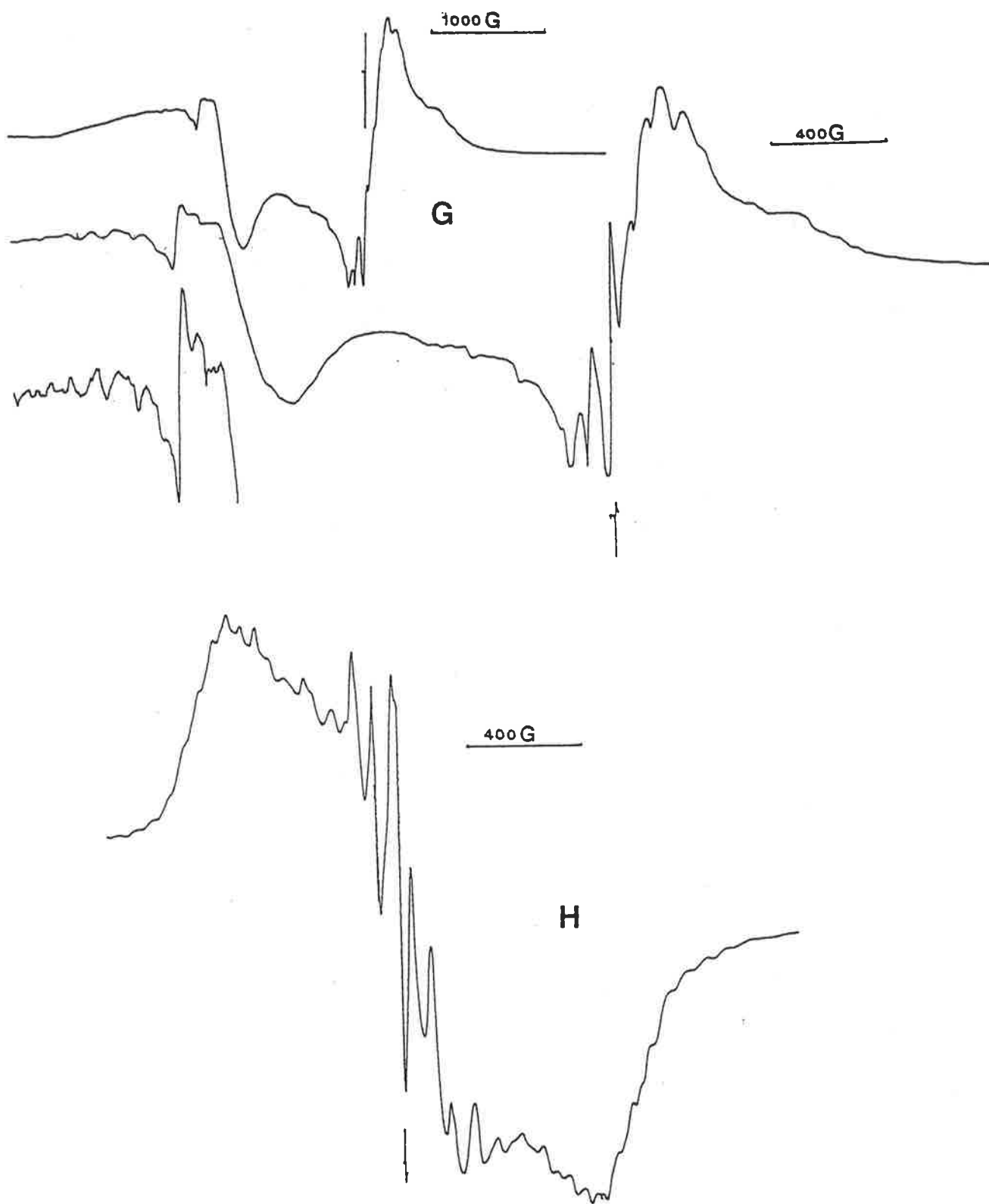
Figure 2.8.3: Low temperature (-160°C) solution (in toluene) E.S.R. spectra of G. [VO(acac)(OMe)]$_2$ and H. [VO(acac)(OEt)]$_2$. (↑ DPPH).
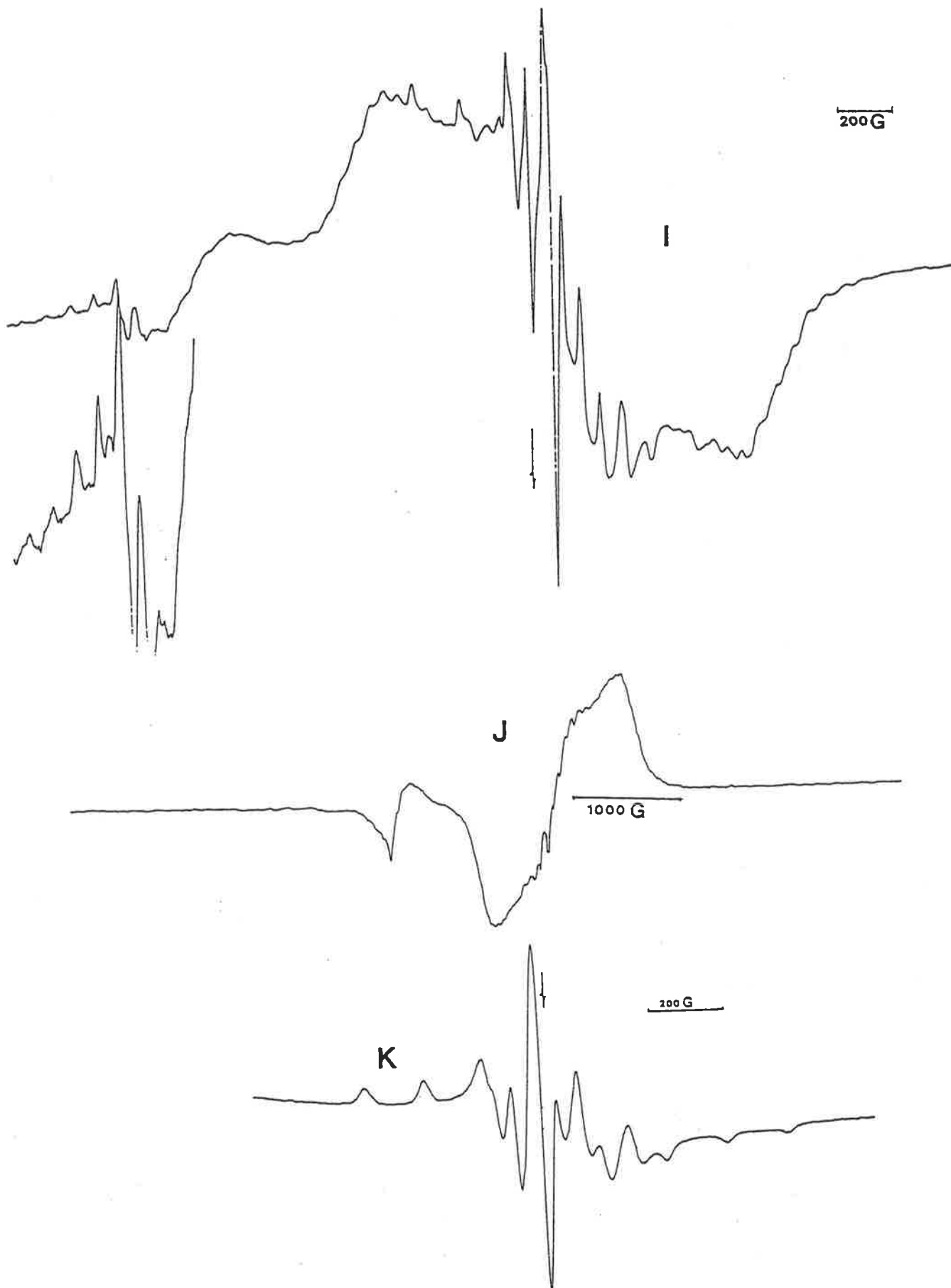
Figure 2.8.4: Low temperature (-160°C) E.S.R. spectra of I. [VO(acac)(OPr^n)]$_2$ in toluene; J. [VO(acac)(OPr^i)]$_2$ in toluene and K. VO(acac)$_2$ in dichloromethane.

The interpretation of these frozen solution spectra is quite straight-forward as has been stated above for powdered solid and room temperature solution spectra. On the central portion of the broad feature there is super-imposed the frozen solution spectrum of $VO(AA)_2$ as can be seen by comparing the $VO(acac)_2$ spectrum K and the dimer spectra G, H and I in Figures 2.8.3 and 2.8.4. The perpendicular features are clearly discernible and have the same hyperfine splitting as for the monomer. Outside the range of the monomer spectrum (about $\pm$ 600 G from the mid-point) the dimer feature shows a complic-ated pattern of hyperfine splitting. The E.S.R. spectra of interacting dimeric metal complexes have been studied extensively by Smith and Pilbrow[149] and such complex hyperfine patterns of the type described are characteristic of dimeric vanadium systems.

In addition, in the half-field region, less intense signal due to the spin-forbidden $\Delta M_s = \pm 2$ transition have been recorded for some complexes. Spectra G and I in Figures 2.8.3 and 2.8.4 show such a signal which shows what appears to be vertical and parallel signals with hyperfine splittings about half of the monomer spectrum as expected from the theory[149,150].

In principle, full analysis of the frozen solution dimer spectra can lead to conclusion about the separation of the magnetic dipoles and hence to conc-lusion about the structure of the dimers. In our case, the interference due to the presence of monomers would make such an analysis difficult.

The value of the E.S.R. studies together with the other spectroscopic studies to the project has been to provide evidence that the complexes which have been prepared are all very closely related and have structures similar to the only one established by X-ray crystallography.

2.9 MAGNETIC PROPERTIES

(i) INTRODUCTION

As has been stated earlier (Section 2.1), the study of the magnetic prop-erties of these complexes is specifically useful in providing an understanding

of the electronic interactions which arise as a consequence of their dimeric structures. Because of the unpaired electron on each of the vanadium centres, the dimeric alkoxo-bridged oxovanadium(IV) complexes are capable of exhibiting magnetic interactions through spin-spin coupling and have a room temperature magnetic moment well below the spin only value of 1.73 B.M., which is a ready diagnostic of their dimeric structure. Determination of the magnetic properties of these complexes over an extensive range of temperature has enabled the evaluation of their coupling constant J, and hence an understanding of the electronic effects in these binuclear complexes.

(ii) THE MAGNETIC INTERACTIONS IN DIMER SYSTEMS

Depending on their magnetic behaviour, the transition metal complexes belong to one of two types, viz. (i) magnetically dilute and (ii) magnetically condensed. In the former case, the metal ion is not involved in magnetic exchange with the neighbouring metal ions. In the magnetically condensed complexes, the metal ion is involved in magnetic exchange with the neighbouring metal ions through exchange forces[100,151-158]. The principal types[159a] of magnetic behaviour give rise to (a) antiferromagnetism, (b) ferromagnetism and (c) ferrimagnetism. Intramolecular antiferromagnetic interactions, confined within discrete molecular structures, are the commonest type of interaction in chemical compounds. Complexes with antiferromagnetic spin-spin coupling, resulting from a binuclear or polynuclear structure, have subnormal room temperature magnetic moments[160-166].

The mechanisms of antiferromagnetic exchange interactions involves the mutual pairing of electronic spins via some form of orbital overlap, analogous to the formation of a chemical bond. Two types of interaction mechanisms are possible: (a) direct interaction and (b) superexchange. The latter[152,155a], involves the interaction of electrons with opposite spins on the two interacting metal ions via an intermediate bridging dimagnetic anion through σ- or π-bonding orbitals. Most complexes with subnormal magnetic moments are

explained using this concept. The mechanism of direct interaction involves direct overlap between the d orbitals containing the unpaired electrons on each metal ion leading to mutual pairing through δ-bonding. The weak δ-bonding overlap which is greatly dependent on the metal to metal distance gives rise to a diamagnetic spin-singlet ground state and an excited paramagnetic spin-triplet state. The observed magnetic behaviour arises from the thermal population of the spin-triplet state. Consequently, paramagnetism will be observed only for weak δ-bonds, in contrast, strong overlaps will lead to a strong metal-metal bond as found in, e.g. many carbonyl and halide cluster compounds[159b] which are diamagnetic.

The singlet state (S = 0) and the triplet state (S = 1), produced by the coupling of two S = $\frac{1}{2}$ spins of an interacting pair of ions, are separated by the exchange coupling constant or the exchange integral, J, an important numerical parameter for studying magnetic interactions. In antiferromagnetic coupling the diamagnetic singlet state is the ground state and magnetic moments of the complexes would decrease as the temperature is lowered, due to the population of the singlet state at the expense of the paramagnetic triplet state. The temperature dependence of the magnetic susceptibility for dimeric systems in which each ion has formally an unpaired electron and therefore S = $\frac{1}{2}$ is well-known[159c,167a] and is adequately described by the Bleaney and Bowers equation[160],

$$\chi_{A'} \, (corr) = \frac{g^2 N \beta^2}{3kT} \left[1 + \frac{1}{3} \exp \, (J/kT)\right]^{-1} + N\alpha \quad \ldots\ldots\ldots (1)$$

where $N\alpha$ is the temperature independent paramagnetism term and the other symbols have their usual significance. J may be evaluated by measuring the susceptibility of a dimer as a function of temperature and fitting the results of the above equation. A negative value of J implies antiferromagnetic coupling (singlet-state lowest) while a positive value indicates ferromagnetism (triplet-state lowest).

(iii) PREVIOUS STUDIES ON RELATED COMPLEXES

The most extensively studied magnetically condensed complexes are the copper(II) complexes and a comprehensive review of subnormal Cu(II) complexes has been published by Kato et al.[153]. D.J. Hodgson[100] also reviewed a number of the magnetic exchange in complexes of various metal ions. A. Syamal[6] reviewed the coordination chemistry of oxovanadium(IV) exhibiting subnormal magnetic moments. Most of the oxovanadium(IV) complexes with subnormal magnetic moments have been prepared from the tridentate dibasic Schiff bases containing O N O or O N S donor atoms[33-43,46,144,168-176]. For most of these complexes, magnetic measurements were confined to room temperatures only, however, a few were studied at six or seven different temperatures starting from about 80K[41-43,144]. The only comprehensive study is that of Ginsberg et al.[36] who determined the magnetic properties of a number of $[VO(O N O)]_2$ dimers over an extensive range of temperatures from 1.4K to 300K and was the first to account for the antiferromagnetic interactions in these dimeric structures. Studies by several authors of such dimeric complexes of oxovanadium(IV) have been mentioned in Section 1.2.1(b). The tridentate dibasic character of the O N O or O N S ligands in such complexes forces the VO^{2+} ion to dimerize in order to achieve the normal penta- coordination. Similar studies on dimeric complexes of various carboxylic acids[6] and of some bidentate O N donor Schiff bases[177,178] have also been reported.

(iv) RESULTS AND DISCUSSION

The magnetic moments and susceptibilities of the dimeric alkoxo-bridged complexes prepared were determined at a single temperature (room) using the Gouy method. For ten complexes, selected on the basis of ligand type, magnetic properties were determined over the extended range of temperature using a Faraday magnetometer. The experimental methods for these measurements are described in the Experimental Section. The room temperature magnetic properties of the complexes other than those subjected to variable temperature

measurements are given in Table 2.9.1. Inspite of the limitations of the Gouy method to give accurate values because of the low specific magnetic suscepti- bilities of the complexes and the magnetic fields used, all the room tempera- ture magnetic moment values obtained are clearly lower than the spin only value of 1.73 B.M. expected for a d^1 oxovanadium(IV) system and suggest that in all the complexes there is antiferromagnetic exchange arising from the dimeric structure. The room temperature magnetic moments, determined by the Gouy method, were comparable within ± 0.04 B.M. to the 300K magnetic moment values obtained in the variable temperature experiment (Table 2.9.2).

As mentioned earlier, the temperature dependence of the magnetic suscept- ibility of the vanadyl dimers is expected to obey the simple Bleaney and Bowers dimer expression (equation 1) where the singlet-triplet separation is equal to 2J. The data obtained from the variable temperature study were fitted to this relationship with the additional correction for the presence of a small amount of monomer by means of the method suggested by Ginsberg[156] and by taking Nα as 50 x 10^{-6} cm^3 mol^{-1} in all cases. Of the ten complexes used in this study only one complex, [VO(acac)(OMe)]$_2$ had its structure determined (Section 2.4). The other dimers, most of which were amorphous or microcryst- alline were assumed to possess the same type of structure on the basis of their various spectroscopic and chemical similarities. In selecting the dimers for the variable temperature magnetic studies, compounds were chosen so that comparisons could be made of the electronic effects of the bidentate ligand and the electronic and/or steric effect of the bridging alkoxo group.

An important characteristic of the presence of an intramolecular (also intermolecular) antiferromagnetic exchange process in a system is the appear- ance of a break in the form of a maximum in the susceptibility versus temper- ature (χ_M - T) plot. The measurements must obviously be carried out over a sufficient temperature range such that the temperature dependence of magnetic susceptibilities as well as a maximum are well observed indicating such

TABLE 2.9.1: ROOM TEMPERATURE MAGNETIC DATA[a] OF SOME

$[VO(AA)(OR)]_2$ COMPLEXES[b]

AA=	R =	TEMPER-ATURE °K	[c] χ_M (Corr) X 10^4 (c.g.s./g-atom V)	μ_{eff}/V B.M.
acac	Pr^n	290.5	10.04	1.53
acac	Pr^i	290.5	9.42	1.48
acac	Bz	290.5	9.80	1.51
Bzac	Pr^n	290.0	9.84	1.52
Bzac	Pr^i	290.0	10.06	1.53
Bzac	Bu^n	298.5	10.44	1.58
Bzac	EtOEt	298.5	10.00	1.55
dbm	Me	290.8	10.05	1.53
dbm	Et	291.0	9.83	1.51
dbm	Pr^n	291.0	9.95	1.52
dbm	Pr^i	291.0	9.91	1.52
dbm	Bz	290.0	10.48	1.56
HNP	Et	290.5	9.50	1.49
HNP	Pr^n	291.0	8.92	1.45
HNP	Pr^i	291.0	9.30	1.47
HNP	Bz	291.0	9.40	1.48
HAP	Et	298.0	8.21	1.40
HAP	Pr^n	298.0	8.40	1.42

a. Determined by Gouy method.

b. Magnetic data for complexes subjected to variable temperature experiments are shown in Table 2.9.2.

c. Corrected for the diamagnetism using Pascal's constants[159a].

TABLE 2.9.2: MAGNETIC PROPERTIES OF THE ALKOXO-BRIDGED

OXOVANADIUM (IV) COMPLEXES[c,d], [VO(AA)(OR)]$_2$

COMPLEX NO.	AA	R	μ_{eff}/V B.M. 300 K	J[a] cm^{-1}	g[a] MONOMER	%[a]
I	HNP	Me	1.48	- 84.5	1.92	6.50
II	HAP	Me	1.38	-125.0[b]	1.94	2.79
III	acac	Et	1.51	- 88.0	1.96	0.64
IV	acac	Me	1.57	- 60.6	1.95	1.10
V	Bzac	Bz	1.60	- 74.0	2.03	2.84
VI	Bzac	Me	1.52	- 73.6	1.92	2.33
VII	Bzac	Et	1.54	- 70.3	1.95	0.65
VIII	Bzac	Bu^2	1.57	- 62.8	1.95	1.07
IX	Bzac	EtOMe	1.59	- 47.2	1.92	0.80
X	Bzac	Ph	1.65	- 45.7	1.98	1.04

(a)   J $\pm$ 0.5 cm^{-1}; g $\pm$ 0.02; % monomer $\pm$ 0.2% unless otherwise stated.

(b)   J $\pm$ 5 cm^{-1}; g $\pm$ 0.05; % monomer $\pm$ 1%.

(c)   T.I.P. (per V) = 50 x 10^{-6} c.g.s.u.

(d)   Diamagnetic corrections were taken from the literature[159a].

exchange behaviour.   The temperature of this maximum, known as the Curie or

Néel temperature (T$_c$ or T$_N$), is related to the value of the coupling constant

increasing monotonically with the value of J.   At temperatures above T$_N$, the

susceptibility obeys the Curie-Weiss law.   In this temperature range the

thermal energy available to the system is sufficient to overcome the anti-

parallel alignment of the spins[159d] thereby increasing the population in the triplet state. Below this critical temperature, the forces aligning the spins in an anti-parallel arrangement predominate thus increasing the population of the singlet state and producing a rapid lowering of the susceptibility with decreasing temperature. At T_N, these effects balance each other and hence result in a maximum in the susceptibility.

The transition from ordered (at low temperature) to the disordered (at higher temperatures than T_N) array may be sharp or gradual depending on the nature of the system. In the present study, all the comlexes I to X (Table 2.9.2) show a broad maximum in the $\chi_M$vs T plot typical of an exchange coupled system. The results from the ten compounds are shown in Figures 2.9.1 to 2.9.5. All the curves are similar in nature showing broad maxima ranging from 85K for $[VO(Bzac)(OPh)]_2$ (X) to 150K for $[VO(HNP)(OMe)]_2$ (I). On the same graphs are plotted the magnetic moments calculated per paramagnetic centre from the χ_M values. These, as expected, show a steady increase with temperature.

The low temperature region of the $\chi_M$vs T plots reveal, in all cases (Figures 2.9.1-2.9.5) a rapid increase in the χ_M value. This is interpreted as being due to varying small amounts of uncoupled vanadium(IV) species. Below about 30K, only the singlet ground state is occupied and the tailing off of the calculated μ_{eff} to a limiting non-zero value results from this paramagnetic monomer impurity. The presence of small amounts of paramagnetic impurities is consistent with the moisture sensitivity of these compounds which, as discussed earlier, results in the formation of monomeric vanadyl complexes. The extent of contamination was relatively high with the unstable $[VO(HNP)(OMe)]_2$ (I) and $[VO(HAP)(OMe)]_2$ (II) dimers as well as with the sterically hindered OBz bridged complex (V). Conversely, it was low with the crystalline OMe and OEt bridged acetylacetonate dimers (III and IV).
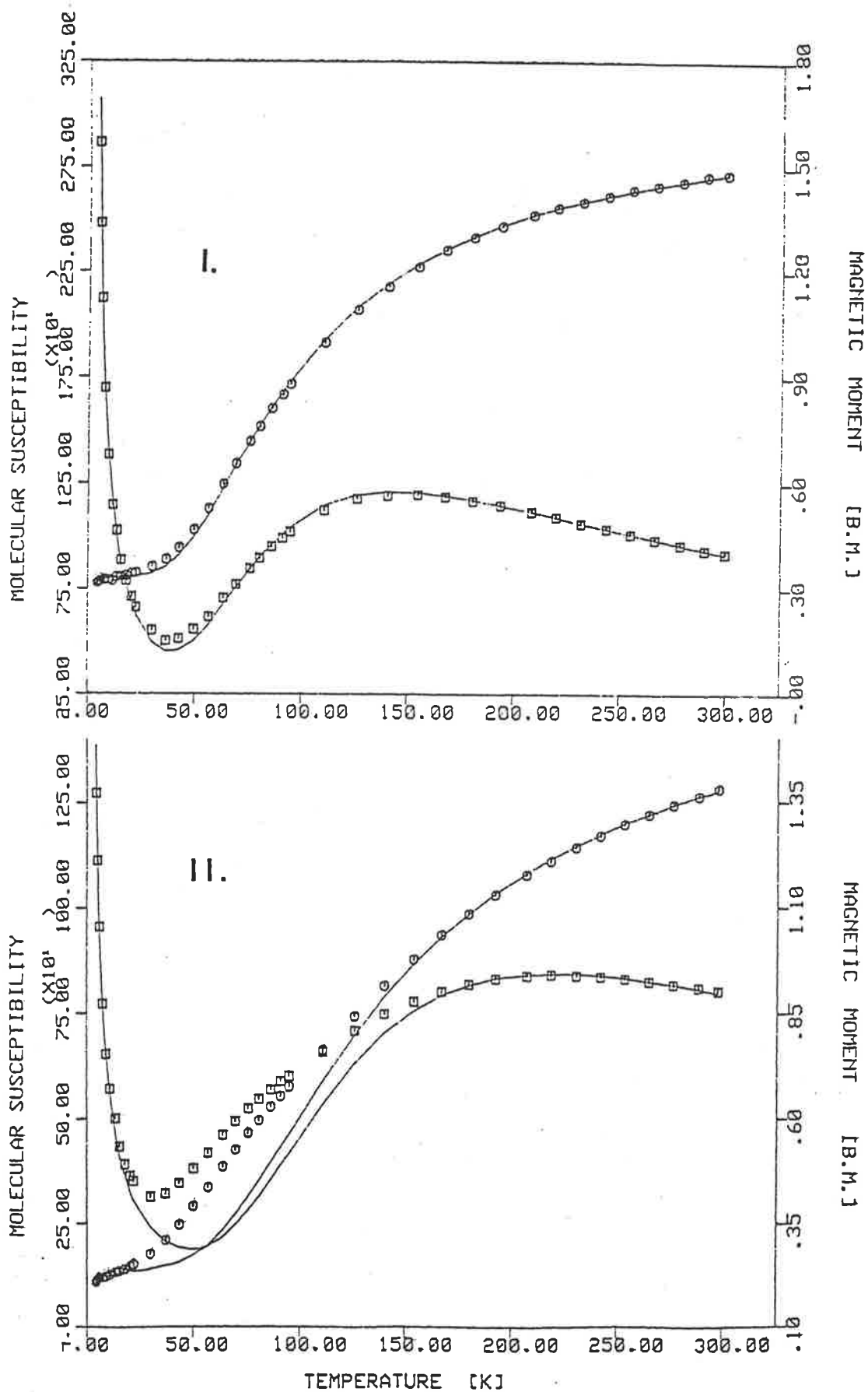
Figure 2.9.1: Temperature-dependent magnetic susceptibility (□) and moment (○) (per V) of compounds I. [VO(HNP)(OMe)]$_2$ and II. [VO(HAP)(OMe)]$_2$. The calculated curve (—) is from parameters in Table 2.9.2.
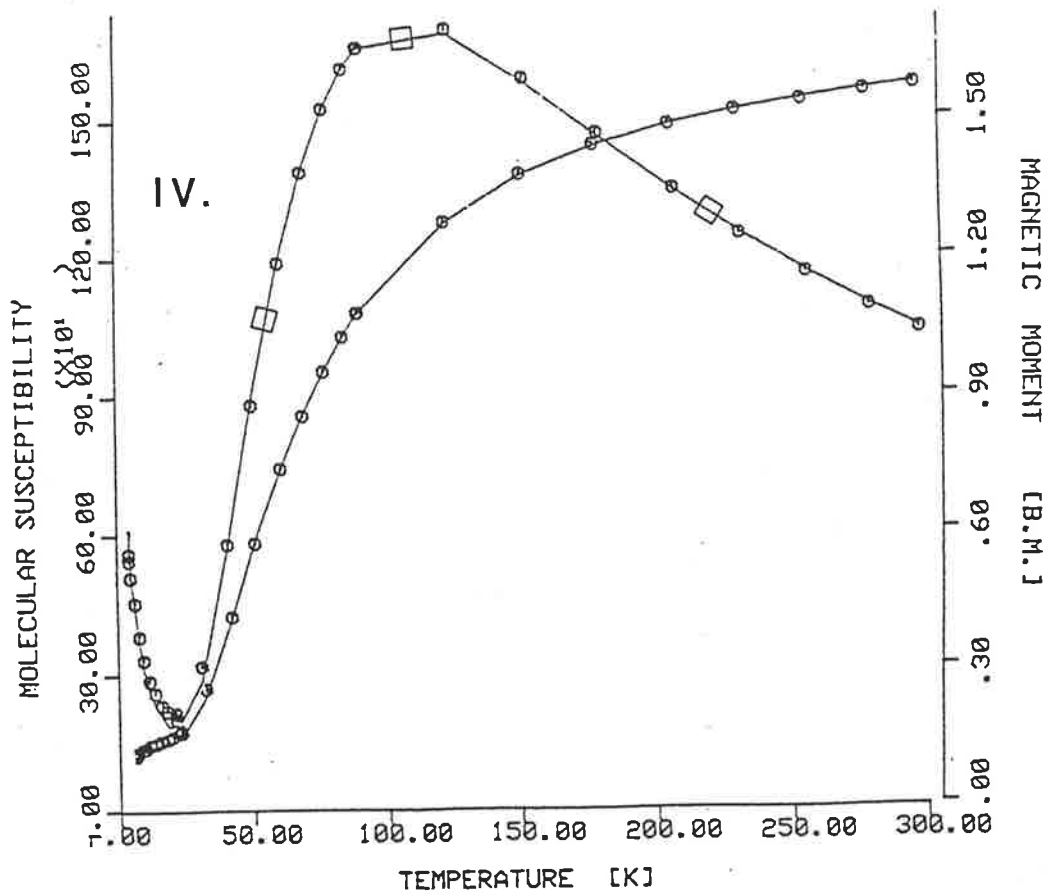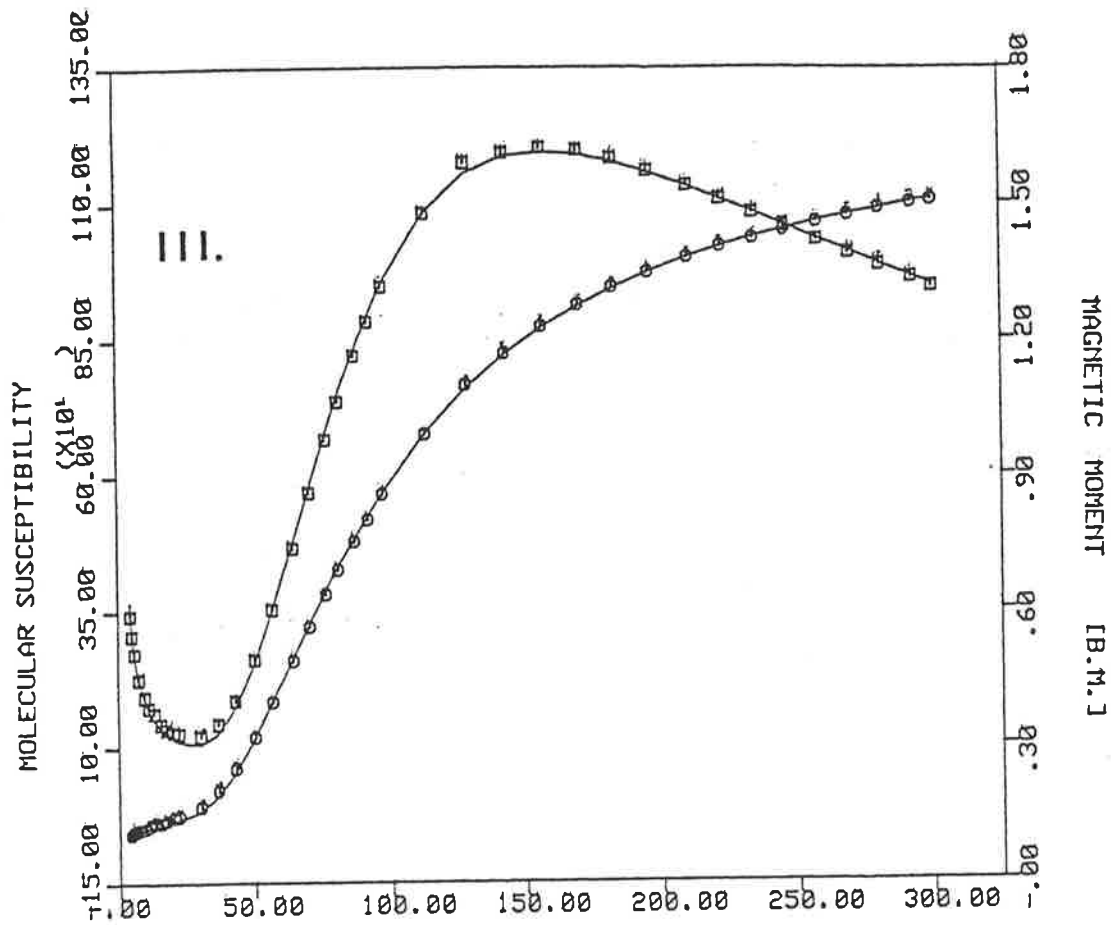
Figure 2.9.2: Temperature-dependent magnetic susceptibility (□) and moment (○) (per V) of compounds III. [VO(acac)(OEt)]$_2$ and IV. [VO(acac)(OMe)]$_2$. The calculated curve (—) is from parameters in Table 2.9.2.
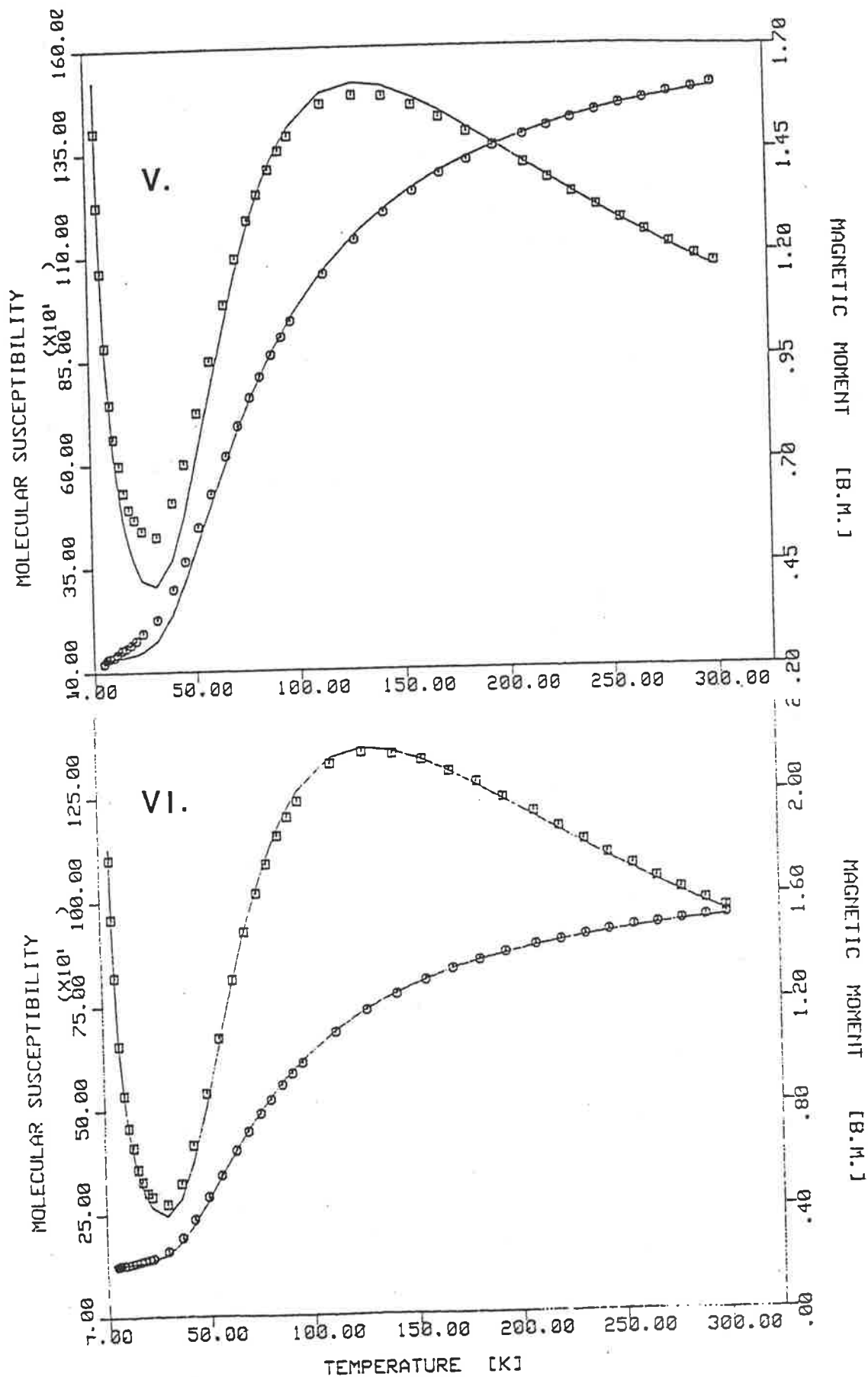
Figure 2.9.3: Temperature-dependent magnetic susceptibility (□) and moment (○) (per V) of compounds V. [VO(Bzac)(OBz)]$_2$ and VI. [VO(Bzac)(OMe)]$_2$. The calculated curve (—) is from parameters in Table 2.9.2.
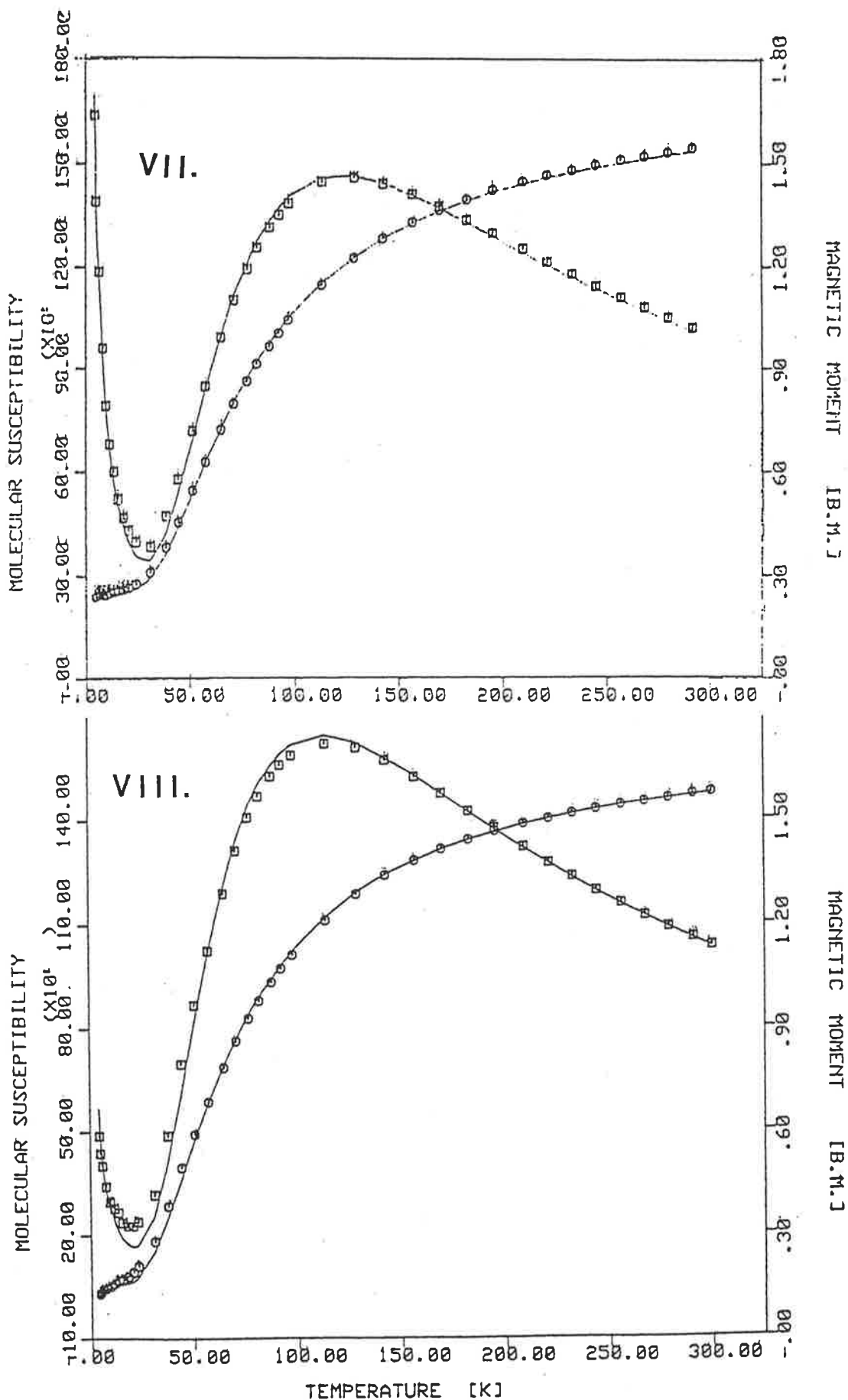
Figure 2.9.4: Temperature-dependent magnetic susceptibility (□) and moment (○) (per V) of compounds VII. [VO(Bzac) (OEt)]$_2$ and VIII. [VO(Bzac)(OBu^2)]$_2$. The calculated curve (—) is from parameters in Table 2.9.2.
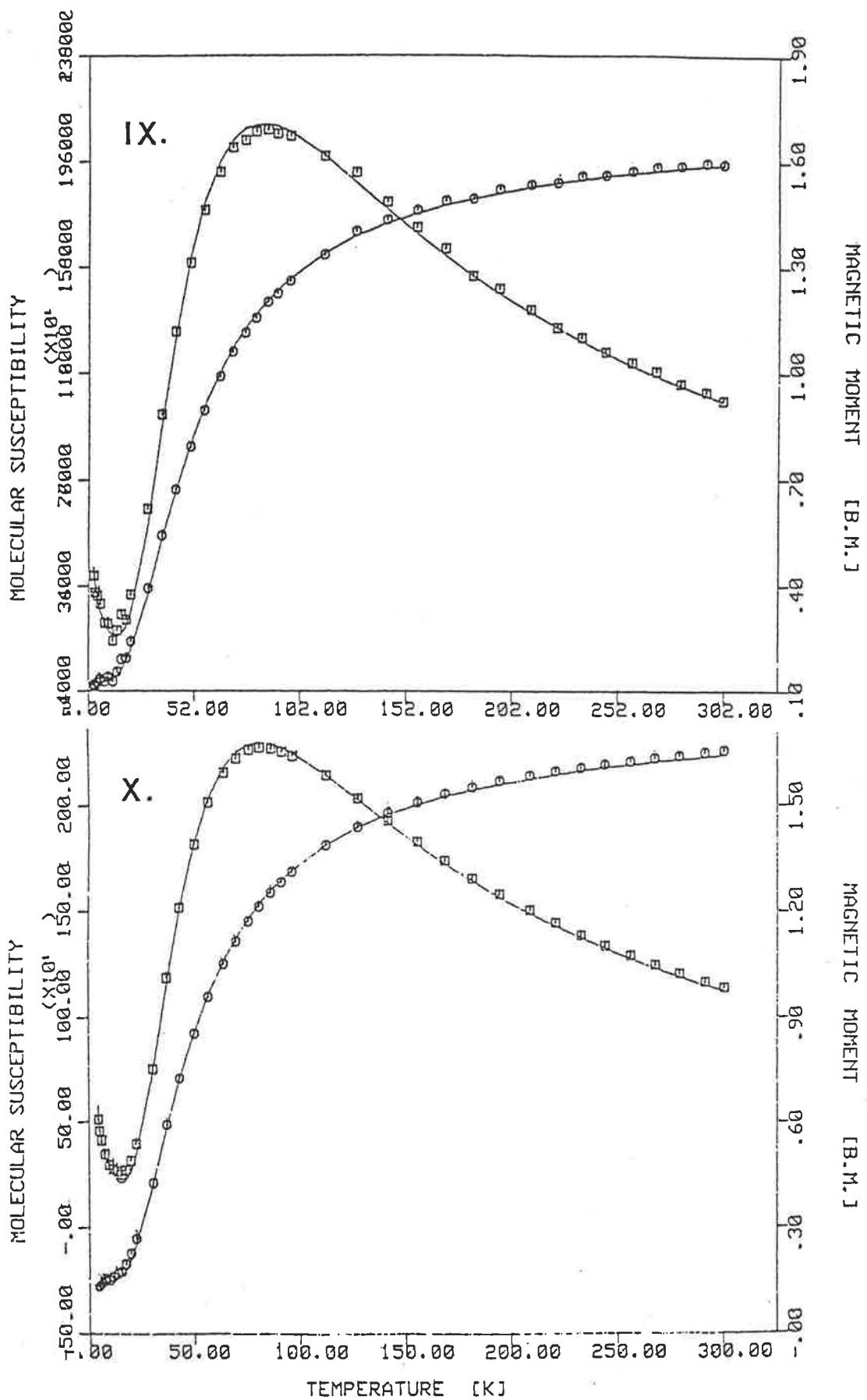
Figure 2.9.5: Temperature-dependent magnetic susceptibility (□) and moment (○) (per V) of compounds IX. [VO(Bzac) (OEtOMe)]₂ and X. [VO(Bzac)(OPh)]₂. The calculated curve (—) is from parameters in Table 2.9.2.

The observed data were fitted by least-squares method to the Bleaney-Bowers equation by programmes R-Oxford and R-Polymer[179] modified to allow the presence of a monomer of S = $\frac{1}{2}$. The fitting procedure enabled the evaluation of J, g and % monomer. The agreement of the experimental and calculated data was expressed in terms of an R value. The parameters obtained by this procedure are listed in Table 2.9.2.

It was possible to obtain good fits of the data over the entire temperature range for all the complexes studied, except for [VO(HAP)(OMe)]$_2$, II. In this case, while it was possible to reproduce the observed susceptibilities above 100K with the parameters listed in the Table, a poor fit was observed at temperatures below this perhaps as a result of weak magnetic interactions with the monomeric impurity. As was mentioned earlier, the HAP-containing dimers were found to be the most air sensitive in the whole series studied. The quality of fits to the simple dimeric expression suggests that all the complexes are discrete dimers, as found in the crystal structure of [VO(acac)(OMe)]$_2$, IV. There is no evidence to suggest a tetrameric arrangement as found[180,181] for the closely related Cu(II) complex, [Cu(acac)(OBz)]$_2$ where the complex exists as pairs of dimers.

As already discussed in Section 2.7, the single 3d electron in the square pyramidal oxovanadium(IV) complexes occupies the d_{xy} orbital[45,182] (t_{2g} set) and the g values deduced from the fitting procedure are symptomatic of such a ground state[36], as are the observed E.S.R. spectra (Section 2.8). In a dimeric structure the d_{xy} orbitals have the correct symmetry for a σ-overlap thus providing a path for the antiferromagnetic exchange between the adjacent vanadyl centres. The strength of the exchange coupling would be primarily determined by the extent of the overlap which amongst other factors depends on the distance between the two vanadium atoms. The geometrical arrangement of the two vanadium centres in the crystal structure of [VO(acac)(OMe)]$_2$ (Section 2.4) is such as to produce a V·······V distance of 3.107Å which

precludes the formation of a V ——— V bond of the type observed for dinuclear V(II) and V(III) compounds[183,184] in which much shorter distances have been observed. Clearly, in our system, although the interaction is weaker, it is nevertheless sufficient to cause the observed exchange which would be sensitive to change in the intermetallic distance. In contrast to the oxovanadium(IV) system, in the copper(II) complexes the unpaired electron is chiefly in the d_{x2-y2} orbitals (e_g set) which are directed in space roughly toward the bridging oxygen atoms and are well oriented for overlap with the oxygen p orbitals and thus the magnetic exchange in many copper(II) complexes occurs via superexchange through the bridging atoms. However, the absence of an electron in the d_{x2-y2} orbitals of the VO-dimers makes a contribution to exchange through this mechanism less significant. Consequently, coupling in the vanadyl system is weaker than in the related Cu(II) dimers which use the more efficient super exchange pathway. This is despite a similar M - M distance in these [M(acac)(OR)]$_2$ systems This work [180,181]. Related arguments have been presented for other Cu-Cu and VO - VO pairs[185,186].

While the room temperature magnetic moments do not vary markedly with AA or R, and hence give little indication about variations in the magnetic interactions, it is evident from Table 2.9.2 and Figures 2.9.1 - 2.9.5 that the magnitude of J and the variation of χ with temperature depend quite markedly on the nature of both these groups. In a discussion of the magnetic behaviour of a range of ligand-bridged vanadyl Schiff base complexes, Ginsberg et al.[36] suggested that for an exchange pathway through a σ-overlap, electron withdrawing substituents on the Schiff base should lead to an increase in the effective charge on the vanadium centre causing the d_{xy} orbitals to contract and so resulting in a weaker exchange. The non-observance of such a dependence was explained as resulting from an increased polarizing effect of each metal on its neighbour causing an increase of the overlap of the d_{xy} orbitals. As a result of these conflicting effects, Ginsberg et al. were unable to determine the exact effect of ligand substituents. The above arguments of course assume

a constant V ··· V distance. In the present systems, the group of four complexes with methoxo bridges (I, II, IV, VI) where the V .... V distance is expected to be similar permits a comparison of the effects due to the terminal AA ligands. The four ligands would be expected to have electron withdrawing ability in the order acac < Bzac < HAP ~ HNP. Table 2.9.3 lists band III (which is influenced by charge transfer) in the $[VO(AA)(OR)]_2$ spectra (Section 2.7) and $V^{IV} - V^{III}$ reduction potential of the complexes VL_2 where L is the dianion of the Schiff base of the above ligands with benzoyl hydrazine (Chapter 5). Table 2.9.4 listing the $E_{1/2}$ values (vs S.C.E.) of some $M(\beta$-diketonato$)_n$ $(= 2,3)$ complexes, combined with the $E_{1/2}$ values of some VL_2 complexes of related ligands (Table 2.9.3) confirms the above order of electron withdrawing ability, on the assumption that band III is a ligand to metal charge transfer. As can be seen from Table 2.9.2, our results also confirm the opposite of the expected correlation between J value and electron withdrawing effects diminishing the σ-overlap of the d_{xy} orbital. Therefore, the second factor suggested by Ginsberg must be more important. In the analogous ethoxo bridged complexes (III and VII) the order of the mangitude of J value is reversed, however, with Bzac > acac. Therefore no specific simple explanation in terms of electronic effects is possible to explain such behaviours.

TABLE 2.9.3: SOME ELECTRONIC PARAMETERS OF THE $[VO(AA)(OR)]_2$ AND RELATED VL_2 COMPLEXES

$[VO(AA)(OR)]_2$ COMPLEX	BAND III (X 10^{-3} cm^{-1})	$-J$ cm^{-1}	VL_2 COMPLEX	$-E_{1/2}$ ($V^{IV} - V^{III}$) (V) [b]
$[VO(acac)(OMe)]_2$	32.7	60.6	V(acac-BH)$_2$	0.42
$[VO(Bzac)(OMe)]_2$	29.8	73.6	V(Bzac-BH)$_2$	0.35
$[VO(HNP)(OPr^n)]_2$	25.0	84.5[a]	V(HNP-BH)$_2$	0.11
$[VO(HAP)(OBz)]_2$	25.9	125.0[a]	V(HAP-BH)$_2$	0.18

a. but with R = Me;   b. See Chapter 5

TABLE 2.9.4: $E_{1/2}$ VALUES OF SOME M(β-DIKETONATO)$_n$ (= 2,3) COMPLEXES

COMPLEX	$-E_{1/2}$ (V) $(M^{+n} - M^{+(n-1)})$	Lit. Ref.	Complex	$-E_{1/2}$ (V) $(M^{III} - M^{II})$	Lit. Ref.
Co(acac)$_2$	1.915	187	Co(acac)$_3$	0.34	188
Co(Bzac)$_2$	1.750	187	Co(Bzac)$_3$	0.21	188
Co(dbm)$_2$	1.570) 1.830)	187	Co(dbm)$_3$	0.13	188
Cr(acac)$_3$	1.73	189	Ru(acac)$_3$	0.728	190
Cr(Bzac)$_3$	1.50	189	Ru(Bzac)$_3$	0.593	190
Cr(dbm)$_3$	1.26	189	Ru(dbm)$_3$	0.501	190

* Data for the analogous complexes of HNP and HAP are not available.

The types of complexes used in this study also permit comparison of the effect of the bridging alkoxo group. The effect could influence the coupling constant by (i) a steric effect changing the V .... V distance or (ii) due to electronic effect. Crystal structure data are only available for one of these complexes and the air sensitivity and micro-crystalline nature of other complexes would make it difficult to obtain crystals suitable for X-ray structure determination. Consequently arguments regarding V .... V distances are conjectural. In the series [VO(Bzac)(OR)]$_2$ dimers, a bulky bridging group, such as OPh (X) or OBu^{sec} (VIII) causes a marked reduction in the value of the coupling compared to a smaller group such as OMe (Table 2.9.2) presumably as a result of an increased V .... V distance. The electronic effect of the OR groups would be difficult to separate from the steric effects. However, if one assumes the same steric effect in the complexes [VO(Bzac)(OCH$_2$X)]$_2$, where X = Ph, H, CH$_3$, CH$_2$OCH$_3$, there does not appear to be any trend and the two compounds V and X with R = PhCH$_2$ and Ph respectively represent almost the extreme ends of the range of J values.

It is worth noting that a recently reported dihydroxy bridged 1,4,7-triazocylononane (= [9] ane N_3) dimer [VO([9] ane N_3)(OH)]$_2$Br$_2$ [191], with V .... V distance of 3.033Å, has a J value of -88.5 cm^{-1} which corresponds in magnitude to the larger J values obtained in the present dialkoxo series. Vanadyl 1,3,5,-triketonate dimers also display J values[186] of ca. -80 cm^{-1} which suggests that J values of this magnitude are rather typical for

> < cycles in which R = H or -C.
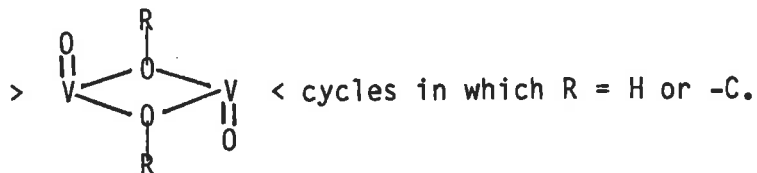
C H A P T E R   3

NON-VANADYL VANADIUM(IV) COMPLEXES WITH TRIDENTATE LIGANDS

GENERAL INTRODUCTION

As has been discussed in Chapter I, the novel aspect of this work is the investigation of the formation of non-vanadyl vanadium(IV) complexes with 0 and N donor ligands. Although a few of such complexes with bidentate ligands are known (Section 1.3), they are unstable tending to form vanadyl complexes. The crystal structure of only one of them, viz. $[Et_3NH]_2[V(cat)_3].CH_3CN$ [71] has been reported. The majority of the stable non-oxovanadium(IV) complexes come from our own work and are bis-tridentate. The ligands which form such complexes are dinegative, tridentate and capable of forming planar five- and six-membered chelate rings of the type $^-O\ N\ O^-$. Ligands containing the azomethine group -RC=N- and the isosteric diazo group -N=N- have been used to prepare the VL_2 complexes. Three types of such ligands that have been developed are (a) Schiff bases of aroylhydrazines (benzoyl and salicyloyl) with β-diketones or ortho-hydroxy aromatic aldehydes or ketones, (b) Schiff bases of o-amino-phenols (also 3-amino-2-napthol) with the same carbonyl compounds and (c) 2,2'-dihydroxyazoarene dyes. A number of VL_2 complexes of each type of ligands have been prepared so that the effects of the ligand type on the formation and properties of the complex as well as substituent effects within each type can be examined. A number of mixed-ligand complexes of the type VLL' have also been prepared.

These novel VL_2 complexes have been characterized by their micro-analysis, infrared, mass, electronic and E.S.R. spectra and by electrochemical studies. The crystal structures of some of these complexes have been determined. The type (a) ligands have the V in the less common trigonal prismatic coordination, the only type (b) complex examined showed an irregular

octahedral coordination. It has not been possible to obtain crystals suitable for an X-ray crystal structure determination of complexes with type (c) ligands.

3.1 BIS-TRIDENTATE VANADIUM(IV) COMPLEXES OF BENZOYLHYDRAZONE SCHIFF BASES

3.1.1. INTRODUCTION

Benzoylhydrazine, because it exhibits keto-enol tautomerism, is capable of forming negatively charged Schiff bases with suitable carbonyl compounds. By itself, it may function as a neutral or as an anionic ligand with metals of the first transition series. The cationic complexes $[M(H_2NHNOCPh)_2]^{2+}$ (M = Co, Cu, Mn, Ni, Zn)[192] are deprotonated by bases to give neutral derivatives, $[M(H_2NNOCPh)_2]$. The former contains benzoylhydrazine (BH) in the keto form and the latter in the enol form. Aroyl hydrazines are also reported to act as tribasic (-3H) mono- and bidentate ligands in some rhenium(V) and molybdenum (VI) complexes[193,194]. The enolization is stabilized by the formation of a Schiff base with a ketone or an aldehyde, e.g. R_1R_2 C = N - NH - OC - Ph[195]. Benzoylhydrazine on condensation with β-diketones or o-hydroxy aromatic carbonyls gives dibasic Schiff bases (LH_2) of the type
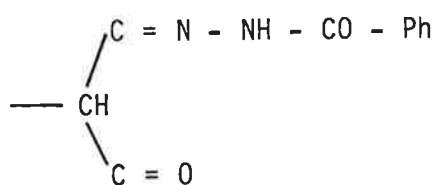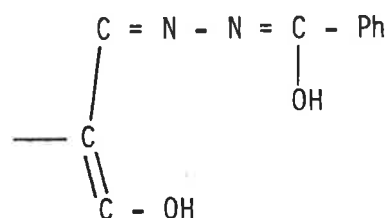
keto-form   enol-form

which, on deprotonation, are capable of acting as a tridentate doubly charged anionic ligand. The ease of formation of the dinegative anion is presumably due to the stabilization of the enol form by the formation of a conjugated system. Thus, with Ni(II), the Bzac-BHH$_2$ gives rise to the neutral complex NiL.NH$_3$ with ammonia coordinated in the fourth position[196]. Although many neutral complexes of various Schiff bases are known, these benzoylhydrazone Schiff bases and related ligands have a special significance in being able to

form bis-tridentate vanadium(IV) complexes. The ligands listed in Table 3.1.1.1 were prepared by literature methods (see Experimental) and used in forming the VL_2 complexes.

TABLE 3.1.1.1: BENZOYLHYDRAZONE SCHIFF BASE LIGANDS

LIGAND	COLOUR	LIGAND	COLOUR
Bzac-BHH$_2$	White	HAP-BHH$_2$	White
Bzac-p^{OMe}-BHH$_2$	White	HAP-p^{Cl}-BHH$_2$	White
Bzac-p^{Cl}-BHH$_2$	White	HPP-BHH$_2$	White
Bzac-p^{NO_2}BHH$_2$	Yellow	DHBP-BHH$_2$	Yellowish White
dbm-BHH$_2$	White	Sal-BHH$_2$	White
HNP-BHH$_2$	Light Yellow		
HNP-p^{Cl}-BHH$_2$	Yellow		

Many of these had been described in the literature and the products obtained were characterized by their melting point and/or infrared and mass spectra. It may be noted that the formation of the dbm-BHH$_2$ Schiff base occurs only when an equimolar mixture of dbmH and BH is heated in an oil bath at a high temperature (155°C). In this case, the removal of H_2O molecule from reacting components to give the Schiff base possibly occurs at a high temperature.

Some tridentate hydrazones can also be formed in situ, during the reaction of some VO(AA)$_2$ (AA = β-diketones or o-hydroxycarbonyls) with benzoylhydrazine in an alcohol under suitable conditions to give the VL_2 complexes. This reaction has been used advantageously to prepare the first VL_2 complex, V(acac-BH)$_2$ [73]. It was subsequently realised that the free ligand, acac-BHH$_2$, could not be prepared because of a cyclization as described below. A series of VL_2 complexes of these Schiff bases have been prepared (Table 3.7.1.1), characterized and their properties studied.

3.1.2. DISCUSSION ON PREPARATIONS AND PROPERTIES OF THE BENZOYLHYDRAZONE

VL_2 COMPLEXES

In forming non-vanadyl VL_2 complexes two general methods were used, viz.

(i) Substitution of LH_2 on VO^{2+} (solvated) where the solvent was a primary alcohol (MeOH or EtOH) and

(ii) Template reaction on $VO(AA)_2$ (where AA = acac, Bzac, HNP and Sal) with benzoylhydrazine.

Although not attempted in this work, substitution on VCl_4 in a non-aqueous solvent is also possible[69].

(i) FORMATION OF VL_2 BY SUBSTITUTION

The reaction of VO^{2+} (solvated) to form the VL_2 complexes proceeds via the removal of the oxo function, presumably in the form of water. Besides our system, substitution of the oxo function, which is very rare, in alcoholic or aqueous solution has been observed only with dithiolene ligands[57-60] and with 1,2-dihydroxy aromatic systems[71]. It seems that the removal of the oxo ligand by substitution takes place only with ligands which are strongly electron donating (σ- as well as π) such as the phenolic and enolic oxygens of the tridentate ligands.

Primary alcohols (methanol or ethanol) were found to be the best solvent for this reaction for a variety of reasons: (i) they facilitate the solution of the ligand and of the base needed to neutralize the displaced H^+ and (ii) also favour the elimination of the H_2O formed by protonation of the oxo ligand. A suitable source for the vanadyl ion was found to be $VOCl_2$, nH_2O, dried to a blue mass over P_2O_5 or $VO(acac)_2$. In the former case, an external base ($LiOAC$ or Et_3N) was added to promote the equilibrium,

$$VOCl_2 + 2\ LH_2 + 2\ LiOAC \rightleftharpoons VL_2 + 2\ LiCl + 2\ HOAC + H_2O \qquad \dots\dots(1)$$
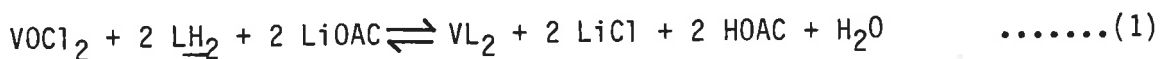
Lithium acetate and triethylamine were commonly used because of their solubility and that of their salts in the alcohol used. $VO(acac)_2$ provided

its own base for the deprotonation of the ligand according to

$$VO(acac)_2 + 2\ \underline{LH_2} \rightleftharpoons VL_2 + 2\ acacH + H_2O \qquad \ldots\ldots(2)$$
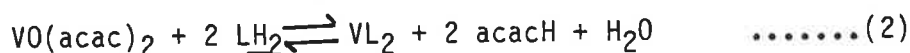
The method had been used before by D.T. Sawyer[197] and Raymond et al.[71] to prepare the tris-catecholates. Evaporation of the solution to dryness followed by addition of fresh solvent help to drive the equilibrium although this was not usually necessary. Although, no doubt, use of MeOH or EtOH as a reaction medium facilitates the formation of the complexes, the stability of the complex is such that they can form in a two phase aqueous system. Thus, VO^{2+}, LH_2 and a base (sodium acetate) in a mixture of $CHCl_3$ and H_2O, on shaking, gave dark purple VL_2 in the $CHCl_3$ layer. The VL_2 was formed in $CHCl_3$ because the reaction was accelerated by the addition of acetylacetone. All VL_2 formation reactions are quite fast and the characteristic dark purple colour of the product appears in about 10 minutes of the reflux with, in most cases, the precipitation of the dark purple/green VL_2 complex.

In the VL_2 complex formation reactions, ligands substitute stepwise. The possibility of forming VOL as an intermediate in the substitution reaction was investigated by performing the substitution reaction (1) using $VOCl_2$ and LH_2 in 1:1 molar ratios. As discussed in Chapter 1.2.1 (b), the expected products would be VOLX, where X = solvent or Cl^- (when L = $\underline{LH}$) or $(VOL)_2$ dimer in order to satisfy the coordination requirements of VO^{2+}. With the present ligand system the possible intermediate products (Chapter 4) have been found to be extremely unstable in the alcohol media and are readily oxidized by the dissolved atmospheric oxygen to give the oxovanadium(V) compounds of the type $V^VOL.OR$ which in the presence of moisture are hydrolysed to $(V^VOL)_2O$ (Chapter 4).

$$VO^{2+} + \underline{LH_2} \xrightarrow{ROH} (VOL)_2,\ VOL\underline{H}^+\ or\ VOL.ROH$$
Intermediate
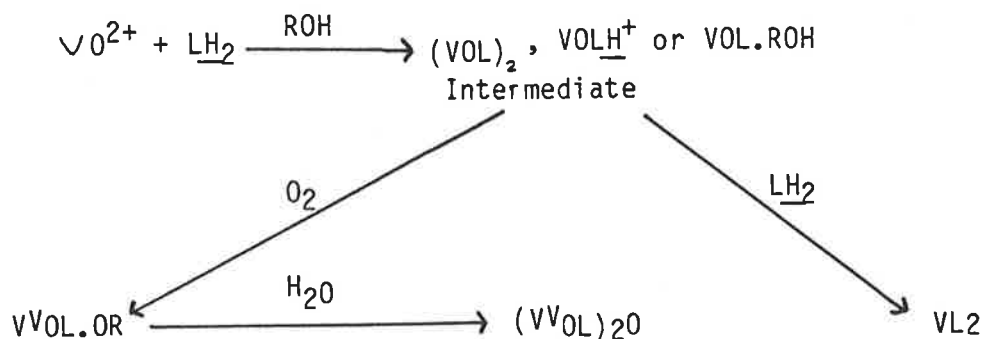
This air sensitivity makes it necessary to carry out preparations in a strictly oxygen-free inert atmosphere (usually nitrogen atmosphere). The above intermediates and their oxidized products can be used as precursors for the synthesis of VL_2 and VLL' complexes (Chapter 4 and Section 3.5). Of all the ligands, the HAP-p^{Cl}-BHH$_2$ forms the exceptionally stable VL_2 complex and a 1:1 mixture of $VOCl_2$ and LH_2 gave VL_2 close to the theoretical yield based on LH_2.

(ii) FORMATION OF VL$_2$ BY TEMPLATE REACTION

VL_2 complexes can also be prepared by reaction of $VO(AA)_2$ with BH in refluxing MeOH.

$$VO(AA)_2 + 2\ BH \longrightarrow VL_2 + H_2O \quad (L = AA-BH) \qquad \ldots\ldots(3)$$
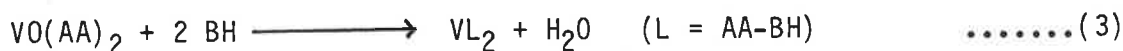
This reaction has been used successfully for AA = acac, Bzac, HNP and Sal. The reaction of $VO(dbm)_2$ with BH in refluxing EtOH did not give the corresponding VL_2 complex but $[VO(dbm)(OEt)]_2$ dimer. The same reaction in chloroform also did not yield any VL_2.

As the template reactions are not likely to produce high concentration of free LH_2 in solution, it is not surprising that oxidation products are isolated as in the 1:1 mixtures in the substitution reactions. The complex $V(acac-BH)_2$, for example, was obtained only in about 10% yield when the reaction was carried out in air, whereas, the yield was much higher under oxygen-free conditions. The oxidized product $[V^VO(acac-BH)]_2O$ can be prepared directly by refluxing $VO(acac)_2$ and BH in ethanol in air and on proper treatments of the product with acetone and water even though that once formed these VL_2 complexes remain very air stable, once formed.

In two reactions, yellow-orange products of compositions $VO(acac-BH).BH$ and $VO(acac-p^{Cl}-BH).p^{Cl}-BH$ were isolated which could be oxidized to V^V complexes or converted to VL_2 by reacting with excess acetylacetone.

Reaction (3) was particularly useful and advantageous for the preparation of $V(acac-BH)_2$ where preparation by substitution was not used as the free

ligand acac-BHH$_2$ could not be prepared due to its cyclization to 3,5-dimethyl-1-benzoylpyrazole (II) through an intermediate product 1-benzoyl-3,5-dimethyl-5-hydroxy-2-pyrazoline (I)[198].

(I)   (II)
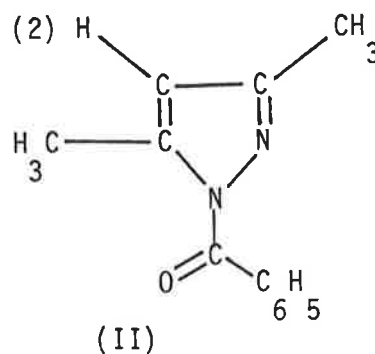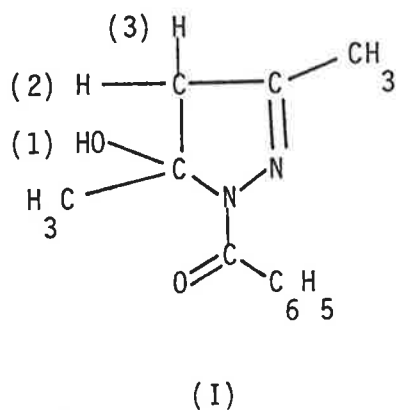
The intermediate compound was also prepared as a solid product as described previously[198]. The compounds were characterized from their N.M.R. data shown in Table 3.1.2.1. The reaction product (liquid) of acacH and BH in ethanol, if not dried properly, gives the N.M.R. signals characteristic of (I). The infrared spectra of this compound showed broad νO-H at 3440 cm^{-1}. This product on drying under high vacuum over P$_2$O$_5$ for a long time gives N.M.R. signals characteristic of (II). Thus, the conversation of the intermediate product (I) to the stable pyrazole (II) proceeds only under extreme dry conditions.

Although the ligands themselves are Schiff bases which are somewhat susceptible to hydrolysis, the VL$_2$ complexes are extremely stable towards hydrolysis. Attempts to try metathesis reaction of the type V(acac-BH)$_2$ + L'H$_2$ → VL'$_2$ in refluxing methanol were unsuccessful. The stability and inertness of the VL$_2$ complexes are consistent with the high oxidation state of vanadium and tridenticity of the ligands. Acids break these complexes down with difficulty. For example, high concentration of methane sulphonic acid in acetone causes slow discharge of the dark purple colour to yellow with oxidation to V^V.

TABLE 3.1.2.1: N.M.R. DATA OF INTERMEDIATE (I) AND PYRAZOLE (II) PRODUCTS

REACTION	δ, ppm		
	I		II
	H(1)	H(2) and H(3)	H(2)
Solid product (I) prepared[198]	5.30 br	2.83 and 3.03 AB quartet J_{AB} = 19 cps	-
acac$\underline{H}$ + BH	5.20 br*	2.76 and 3.11 AB quartet J_{AB} = 19 cps	6.08
Literature[198] value	5.18 br*	2.73 and 3.14 AB quartet J_{AB} = 21 ± 1 cps	6.07
acac$\underline{H}$ + p^{NO_2}-BH	-	-	6.10
acac$\underline{H}$ + p^{Me}-BH	5.17*	2.78 and 3.06 AB quartet	6.04

* Disappeared upon treatment with D_2O

All complexes give clear single deep/dark purple/green T.L.C. spot in chloroform.   These are soluble in dicholoromethane, chloroform, acetone, benzene and DMSO.   Salicylaldehyde-hydrazone complexes are the least soluble (insoluble) and the acetyl-acetone-hydrazone complexes are the most soluble. All these complexes are highly stable and are high melting.

3.2 BIS-TRIDENTATE VANADIUM(IV) COMPLEXES OF SALICYLOYLHYDRAZONE SCHIFF BASES

3.2.1. INTRODUCTION

In searching for new Schiff base ligands we considered compounds of the type,
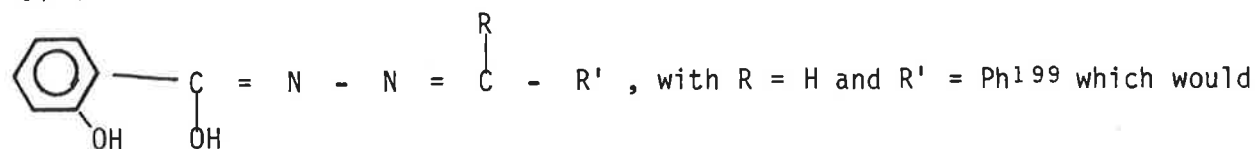
be expected to form neutral VL_2 complexes.   We could not isolate the desired complex from the dark red-purple solution obtained by refluxing this ligand with $VOCl_2$ and Et_3N in MeOH.   However, on repeating the preparation using $VO(acac)_2$ with this ligand in refluxing methanol, we obtained a small amount of VL_2 in which the ligand was found to be acetylacetonesalicyloylhydrazone (acac-SalH) instead of benzaldehyde-salicyloylhydrazone.   Although acac-salHH₂
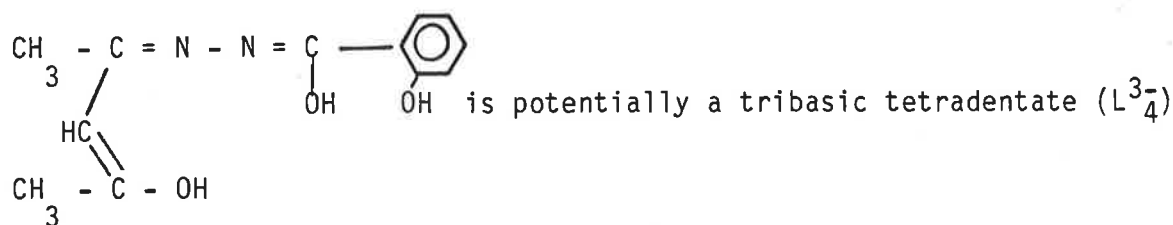
ligand and thus should be capable of forming square pyramidal VOL_4^- type compound analogous to VO(salen), in practice it behaved as a dibasic tridentate ligand like the benzoylhydrazones.   Subsequent experiments using the salicyloylhydrazone Schiff bases of β-diketones or o-hydroxy aromatic aldehydes or ketones gave the neutral VL_2 complexes in good yields.   An X-ray crystal structure determination of $V(acac-SalH)_2$ confirmed this and showed the presence of free <u>ortho</u>-OH group of the salicyloylhydrazide moiety.   The forma-

tion of cationic Cu(II), Ni(II) and Co(II) complexes[200] of neutral SalH further shows that the <u>ortho</u>-OH group does not deprotonate readily and hence does not coordinate. SalH has also been used for the gravimetric determination of palladium, to form the insoluble bis-complex dichloride or sulphate[201].

The VL_2 complexes of the salicyloylhydrazone ligands have been prepared to gain some more information about the modes of coordination of such ligands, the deprotonating and coordinating ability of the three OH groups present as well as the stereochemistry of their VL_2 complexes as compared to that of the corresponding benzoylhydrazone chelates. We note that subsequent to the work of Diamantis[73], Dutta and Paul[202] reported preparation of $V(acac-SalH)_2$.

3.2.2. DISCUSSION ON PREPARATIONS AND PROPERTIES OF THE SALICYLOYLHYDRAZONE VL_2 COMPLEXES

Six ligands of this type as listed in Table 3.2.2.1 were prepared and their VL_2 complexes (Table 3.7.1.1) were obtained by reaction with $VO(acac)_2$ or $VOCl_2$ in methanol. The $V(acac-SalH)_2$ was prepared by a template reaction analogous to that used for $V(acac-BH)_2$ [Section 3.1.2 (ii)]. The complexes are in all respect identical to those of benzoylhydrazone ligands. These

TABLE 3.2.2.1: SALICYLOYLHYDRAZONE SCHIFF BASE LIGANDS

LIGAND	COLOUR	LIGAND	COLOUR
Bzac-Sal<u>HH</u>$_2$	Light Yellow	HAP-Sal<u>HH</u>$_2$	White
dbm-Sal<u>HH</u>$_2$	Creamish White	HPP-Sal<u>HH</u>$_2$	White
HNP-Sal<u>HH</u>$_2$	Yellow	Sal-Sal<u>HH</u>$_2$	White

complexes are also very stable and strongly coloured and give dark purple or green spot on T.L.C. in chloroform. The inertness of the o-OH group of the

SalH part makes these ligands to act as an O‿N‿O donor similar to the benz-oylhydrazones. This o-OH forms a -O-H....N hydrogen bond with the first N of the hydrazine part which would further suppress its hydroxylic characteristics and stabilize the molecule.

3.3 BIS-TRIDENTATE VANADIUM(IV) COMPLEXES OF ORTHO-AMINOPHENOL (AND 3-AMINO-2-NAPTHOL) SCHIFF BASES

3.3.1 INTRODUCTION

Like aroylhydrazines, o-aminophenol (OAP) or its derivatives or 3-amino-2-napthol (3-am-2-nap) also give dibasic tridentate Schiff bases of the type,

$$\begin{array}{c} >C = N - \bigodot \\ -C\diagdown_C - OH \quad\quad OH \end{array}$$
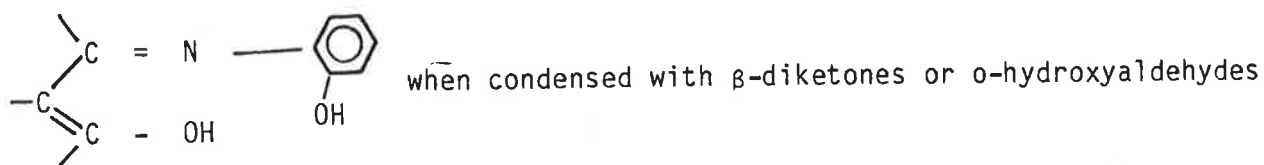
when condensed with β-diketones or o-hydroxyaldehydes or carbonyls. As mentioned in Section 1.2.1(b), several dimeric oxovanad-ium(IV) complexes of the Schiff bases derived from OAP and 2-hydroxy-1-napthaldehyde or salicylaldehyde or their derivatives are known. Instead of the $> C = N - N = C <$ function of the aroylhydrazones, these have the azometh-ine function, $> C = N - C <$ and are capable of forming similar 6- and 5-memb-ered chelate rings with the V^{4+} ion to give the neutral VL_2 complexes. A number of such VL_2 complexes have been prepared to examine the effects of these ligands on VL_2 formations and their structural features.

3.3.2 DISCUSSION ON PREPARATIONS AND PROPERTIES OF o-AMINOPHENOL (AND RELATED) SCHIFF BASE VL_2 COMPLEXES

The tridentate Schiff bases (Table 3.3.2.1) containing O‿N‿O donors obtained by condensation of OAP or its derivatives (or 3-am-2-nap) with β-diketones or o-hydroxy carbonyls have planar configuration and two replace-able hydrogens and are capable of forming neutral bis-tridentade complexes with V^{4+}. The reactions that have been used for the preparations of these VL_2 complexes (Table 3.7.1.1) with these ligands include the reaction of

(a) $VO(acac)_2$ or $VOCl_2$ with the tridentate ligand, (b) $VOL.H_2O$ with $\underline{L}H_2$ and
(c) $VO(AA)_2.H_2O$ with OAP. Only one reaction for each of (b) and (c) was tried
with L = HNP-OAP to demonstrate the validity of such reactions with these

TABLE 3.3.2.1: o-AMINOPHENOL (AND 3-AMINO-2-NAPTHOL) SCHIFF BASE LIGANDS

LIGAND	COLOUR	LIGAND	COLOUR
Bzac-OAP$\underline{H}_2$	Yellowish-White	Sal-OAP$\underline{H}_2$	Orange-Red
dbm-OAP$\underline{H}_2$	Yellow	Sal-p^{Me}-OAP$\underline{H}_2$	(Deep) Red
HNP-OAP$\underline{H}_2$	Orange-Yellow	Sal-p^{Cl}-OAP$\underline{H}_2$	Orange
HNP-p^{Me}-OAP$\underline{H}_2$	Orange-Yellow	HNP-3-am-2-nap$\underline{H}_2$	Orange-Yellow
HNP-p^{Cl}-OAP$\underline{H}_2$	Orange	Sal-3-am-2-nap$\underline{H}_2$	Orange-Red
HAP-OAP$\underline{H}_2$	Yellow		

ligands to give the VL_2 complexes. The enolic and (or) phenolic hydroxyl
groups are readily deprotonated in the presence of VO^{2+} to give the desired
VL_2 complex on scission of the V = O bond. However, the complex $V(acac-OAP)_2$
could not be obtained in the pure form either by method (a) or (c).

These VL_2 complexes give the single dark purple or dark green T.L.C. spot
in chloroform. These complexes are less soluble than the aroylhydrazone-VL_2
complexes in chloroform, benzene and acetone and are high melting.

3.4   BIS-TRIDENTATE VANADIUM(IV) COMPLEXES OF 2,2'-DIHYDROXYAZOARENE DYES

3.4.1 INTRODUCTION

Azo dyes are widely used as coloured organic reagents for special purp-
oses in biology, medicine, chemistry and allied fields. They are character-
ized by the presence of one or more azo groups, -N=N- which form bridges
between organic residues of which one is usually an aromatic nucleus. We are
specifically interested in the 2,2'-dihydroxyazoarene dyes of the type,

$\langle\bigcirc\rangle$ - N = N -$\langle\bigcirc\rangle$ in which the diazo -N=N- group is isosteric with the
 OH   OH
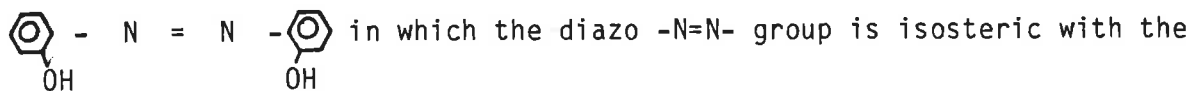
>C=N- azomethine group (Section 3.3) and which have necessary characteristics

to form VL_2 complexes. The presence of a double bond in the -N=N- group gives

rise to the stereoisomerism and it is mostly the trans structure[203] that

exists in metal chelates.

The preparation of these 2,2'-dihydroxyazoarenes is based on the coupling

of an ortho-hydroxy diazonium compound with a suitable phenol or napthol.

However, the presence of the phenolic groups introduces complications and they

usually have to be protected by methoxylation. Bis-complexes of such ligands

with Cr(III), Co(III) and Cu(II) are known[203-208]. Recently, lots of works

are being done on the syntheses and properties of metal chelates of group IV

elements with the azo compounds[209]. Although the VL_2 complexes of 2,2'-dihyd-

roxyazoarenes were formed quite easily, we could not obtain any VL_2X_2 (X = an

anion) type complex with 2-methoxy-2'-hydroxyazoarenes.

3.4.2 DISCUSSION ON PREPARATIONS AND PROPERTIES OF 2,2'-DIHYDROXYAZOARENES

AND THEIR VL_2 COMPLEXES

The 2,2'-dihydroxyazoarene dyes that were prepared are listed in

Table 3.4.2.1. Although, in principle, the preparation of azo dyes by

coupling of the diazonium salt provides a ready access to molecules of this

kind, in practice the presence of substituents, especially OH groups, may lead

to difficulties. The preparation of these particular azo dyes are dependent

on various reaction conditions. Coupling of a diazotized aromatic amine with

a coupling component (phenols, napthols, arylamines, etc.) in aqueous media at

the appropriate pH and temperature gives the azo dyes. Cold conditions (below

10°C) are mostly preferred to prevent the reaction, $ArN_2^+Cl^- + H_2O \rightarrow ArOH + N_2$

+ HCl. The diazonium salts are also sensitive to light. It is necessary to

use an excess of mineral acid to stabilize the diazonium salt by inhibition of

decomposition due to other secondary reactions.

TABLE 3.4.2.1: 2,2'-DIHYDROXYAZOARENE LIGANDS

LIGAND	COLOUR	LIGAND	COLOUR
OAP-β-nap$\underline{H_2}$	Brown-Purple	OAP-p^{OMe}-phenol$\underline{H_2}$	Chocolate-Brown
p^{Me}-OAP-β-nap$\underline{H_2}$	Magenta Red	OAP-p^{Cl}-phenol$\underline{H_2}$	Yellow Brown
p^{Cl}-OAP-β-nap$\underline{H_2}$	Magenta Red	3-am-2-nap-β-nap$\underline{H_2}$	Deep Purple
OAP-p-cresol$\underline{H_2}$	Yellow		

Azocoupling is strongly dependent on pH of the reaction mixture. Figure 3.4.2.1 illustrates the rate of diazo-coupling[210] at various pH values. Steep decrease in rate above pH 9-10 is due to the conversion of the diazonium salt to the undissociated diazo hydroxide and diazotate ion.

$$Ar-\overset{+}{N} \equiv N \underset{H^+}{\overset{OH^-}{\rightleftharpoons}} Ar-N=N-OH \underset{H^+}{\overset{OH^-}{\rightleftharpoons}} Ar-N=N-O^-$$
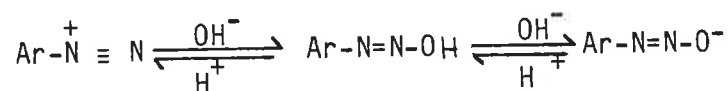
Phenols (pKa ~ 10) are converted to their corresponding anions at high pH values and because it is the anion, and not the phenol, which couples the rate would be maximum at about pH 11.
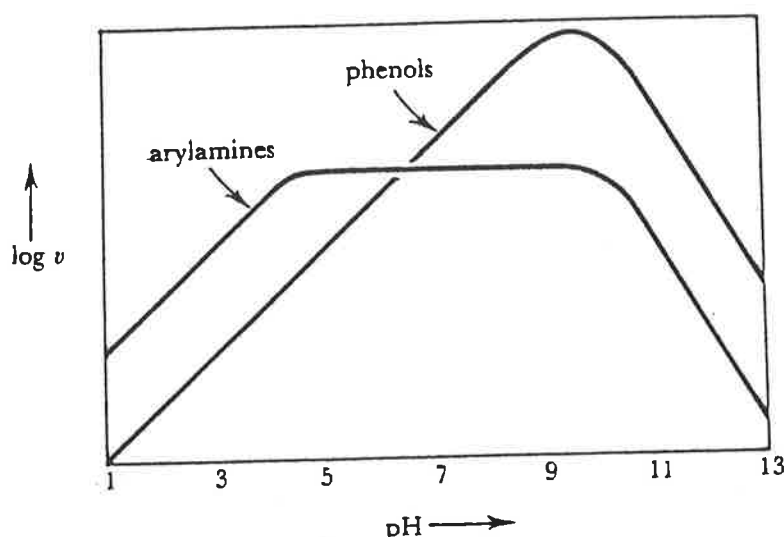
Figure 3.4.2.1: Variation in rates (v) of diazo coupling as a function of pH.

Electron attracting substituents (NO_2, COOH, Cl, SO_3H) in the coupling components[211] decrease their ease of coupling, while electron-repelling substituents (CH_3, OH, NH_2) increase it. In general the weaker the coupling ability of the component, the narrower is the pH range over which coupling takes place. To maintain the proper alkaline reaction condition the coupling component is dissolved in an equivalent amount of NaOH to which an amount of Na_2CO_3 sufficient to convert all the acid in the diazonium salt solution to bicarbonate is added. In alkaline medium, the azo group enters in an _ortho_ or _para_ position with respect to the hydroxyl group. β-Napthols couple exclusively at position 1. Blocking the _p_-position by a suitable group is a convenient way of directing the azo group to the _ortho_ position only.

o-Aminophenols and o-aminonapthols present difficulties in diazotization owing to their tendency to oxidize to quinones[212-214]. Use of trace amounts (0.3%) of $CuSO_4$ as a catalyst helps effect their diazotization by preventing oxidation. Direct coupling of diazonium salt of o-aminophenol with phenol or p^X-phenol (X = CH_3, OCH_3, Cl) produced no product after several attempts, although it gave good yields with β-napthol. Attempts to prepare 2,2'-dihydroxyazobenzene by fusing 2-nitrophenol with KOH[215,216] were unsatisfactory. It was therefore decided to prepare such compounds following a multi-step synthetic procedure involving protection of the -OH group[217]. In doing so, we prepared the diazonium salt of 2-methoxy aniline which on coupling with the phenols gave good yields of 2-methoxy,2'-hydroxydiazophenol. The methoxyl group of this compound was then hydrolysed with anhydrous aluminium chloride in benzene[217,218] to obtain the desired 2,2'-dihydroxyazophenol. As phenol can couple through both o- and p-positions and because we were interested in 2,2'-dihydroxyazo compounds suitable for VL_2 formations, only the p^X-phenols were used as the coupling components.

The 2,2'-dihydroxyazoarene dyes having two protonic hydrogens are capable of acting as dinegative tridentate ligands and of forming a 6- and a 5-membered chelate ring with V^{4+} to give the VL_2 complexes. These complexes

(Table 3.7.1.1) were prepared by refluxing $VO(acac)_2$ and the appropriate dye in the 1:2 molar ratio in methanol. The reaction of $VOCl_2$ with the ligand in the presence of a base also gave the VL_2 product. This VL_2 formation reaction was quite fast and the deep or dark purple (or green) product started separating from the reaction mixture in about ten minutes of refluxing.

Partly because of very low solubility of the VL_2 complexes of the 2,2'-dihydroxyazoarenes in common organic solvents, no suitable crystal for an X-ray crystral structure determination could be obtained by several recrystalization procedures. However, the crystallographic studies of the chromium(III) bis-complexes of o,o'-dihydroxy<u>trans</u>azobenzol have shown the occurrence of the coordination of the metal through a single nitrogen of each azo group and two deprotonated oxygens of the two hydroxy groups, in an approximately octahedral coordination[203].

3.5   MIXED-LIGAND VLL' COMPLEXES OF TRIDENTATE LIGANDS

3.5.1   INTRODUCTION

The mixed-ligand complexes are important in many respects since they occur during transition states of metal-ion catalysed reactions[219], are important in analytical chemistry[220] and can be regarded as models for metalloenzyme-substrate complexes[221]. A number of mixed-ligand VLL' complexes have been prepared using the dinegative tridentate ligands that give the VL_2 complexes. The determination of an X-ray crystal structure of V(Bzac-BH)(HNP-BH) confirmed formation of such mixed-ligand chelates. The formations of these VLL' complexes have been possible only by reactions of $V^{IV}OL\underline{HC}l$ or $V^VOL.OR$ or $(V^VOL)_2O$ with a suitable second ligand $L'H_2$ under appropriate conditions. The chemistry and preparation of these starting materials which contain only one tridentate ligand per vanadium are discussed in Chapter 4.

3.5.2   DISCUSSION ON PREPARATIONS AND PROPERTIES OF VLL' COMPLEXES

The VLL' complexes that were prepared are listed in Table 3.7.1.2.   The

reaction, $VOLHCl + L'H_2 + LiOAC \xrightarrow[\text{Reflux}]{\text{MeOH}} VLL' + H_2O + LiCl + HOAC$ was found to be the most reliable and convenient method for the preparation of VLL' mixed-ligand complexes. They separate as dark purple or green precipitates from the reaction solution which when filtered hot yield the product in the pure form. They can also be prepared by reaction of $V^VOL.OR$ or $(V^VOL)_2O$ with $L'H_2$ in refluxing methanol in the presence of benzoylhydrazine which acts as a reducing agent. It is advantageous to introduce the comparatively weaker ligand second by using as the reacting $L'H_2$. If the reverse procedure is used then the relatively stronger ligand causes rearrangement to form VL_2 and VL'_2. For example, reaction of VO(HNP-BH).OMe with $HAP-BHH_2$ gave all three products VL_2, VL'_2 and VLL' with the major mass spectral peak corresponding to $V(HAP-BH)_2$. Whereas, the reaction of VO(HAP-BHH)Cl with $HNP-BHH_2$ gave only the desired VLL' complex. However, this method was not always successful, e.g. no pure VLL' compound could be obtained from the reaction of VO(HNP-BHH)Cl and $HNP-OAPH_2$. The same ligand on reaction with VO(HAP-BH).OMe in the presence of benzoylhydrazine as a reductant, yielded the product V(HAP-BH)(HNP-BH) instead of the desired V(HAP-BH)(HNP-OAP). All VLL' complexes gave single dark purple or green T.L.C. spot in chloroform.

The existence of VLL' complexes is not unexpected when the two ligands are capable of forming stable VL_2 type complexes on their own. In labile systems, the equilibrium

$$2\ VLL' \rightleftharpoons VL_2 + VL'_2 \qquad \dots\dots\dots(1)$$
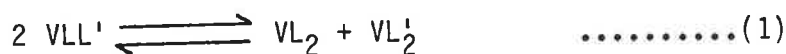
would be established readily and the position of this equilibrium would be determined by relative stability considerations. The fact that such dismutations were not observed in this case, in contrast to attempts to prepare mixed ligand VO(AA)(A'A') complexes from the alkoxo-bridged complexes [Section 2.3 (ii)], is evidence for the inertness of these complexes and consistent with their stability towards ligand exchange and acid decomposition. It is difficult to generalize on the preferred position of the equilibrium in reaction (1). Entropy and steric considerations may form the mixed ligand complex. Studies in other mixed-ligand complexes have shown that

ligand repulsions are generally smaller than in the parent complexes[222] enabling extra stabilization to the mixed-ligand complexes.

3.6 THE CRYSTAL STRUCTURES OF VL_2 COMPLEXES

INTRODUCTION

In the only known structure of a VL_2 complex, which was determined previous to this work, L is a Schiff base of a β-diketone with benzoylhydrazine (see Section 1.3). X-ray crystal structures were determined for four different VL_2 complexes containing various ligand systems viz. (1) HAP-p^{Cl}-BH having the ketonic part as the 2-hydroxyaromatic carbonyl instead of a β-diketone, (2) acac-SalH which although potentially quadridentate, from chemical and spectroscopic evidence, appears to act as a tridentate, (3) HNP-BH and Bzac-BH mixed ligand systems and (4) HAP-OAP in which the amine part is not an aroylhydrazine. Due to the lack of suitable crystals, we were unable to determine the crystal structures of the VL_2 complexes containing 2,2'-dihydroxyazoarene dye or OAP-Schiff base of a β-diketone. Not surprisingly, the first three structures of the hydrazone complexes showed trigonal prismatic coordination and were similar to each other and confirmed the first reported structure of V(acac-BH)$_2$ by Diamantis et al.[73]. The fourth structure of V(HAP-OAP)$_2$ has a geometry in between a trigonal prism (T.P.) and an octahedron.

Depending on the ligand characteristics, the six-coordinate V^{4+} ion may attain a trigonal prismatic or an octahedral configuration or a geometry somewhere in between a T.P. and an octahedron. The twist angle as well as the bond angle, involving the central metal ion and pairs of donor atoms that are farthest apart, are a measure of the extent of distortion of the complex structure from a perfect T.P. or octahedron. The former, defined as the angle with which the trigonal faces are twisted (Figure 3.6.1) with respect to each other[223-226] is 0° for a perfect T.P. and 60° (Figure 3.6.1) for an undistorted octahedron[227]. The latter averages 136 ± 1° in the known trigonal
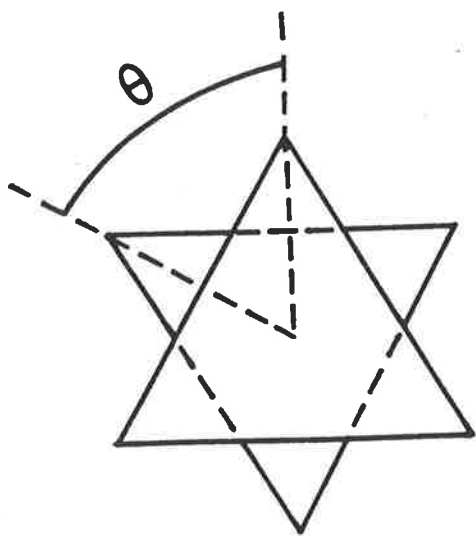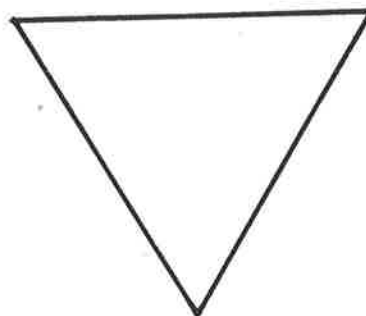
$$\theta = 60^\circ \qquad\qquad \theta = 0^\circ$$
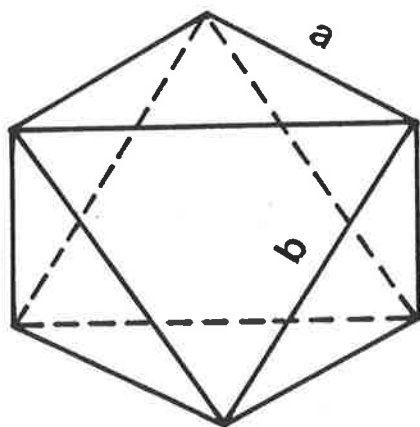
OCTAHEDRON

$$a = b$$
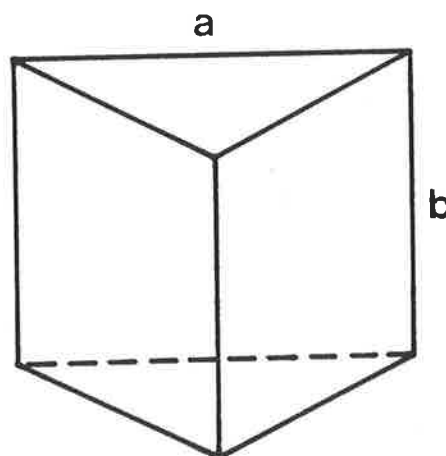
TRIGONAL PRISM

$$a > b$$

Figure 3.6.1:   Octahedral and Trigonal Prismatic Coordination.

prismatic structures[60] and 180° for the perfect octahedron.

These crystal structures also confirmed the presence of six-coordinate V^{4+} and the absence of vanadyl oxygen in the VL_2 complexes.

3.6.1 THE CRYSTAL AND MOLECULAR STRUCTURE OF $V(HAP-p^{Cl}-BH)_2$

The compound $V(HAP-p^{Cl}-BH)_2$ obtained as dark purple crystals from dichloromethane-petroleum spirit, has the crystal structure depicted in Figure 3.6.1.1 which also shows the atomic numbering scheme employed. The bond lengths and bond angles are listed in Tables 3.6.1.1 and 3.6.1.2.

The crystal structure comprises discrete molecules of $V(HAP-p^{Cl}-BH)_2$ as expected. The V^{4+} is surrounded by four O and two N donor atoms of the two tridentate ligands in a trigonal prismatic coordination. The prism is distorted from an ideal T.P. by an average twist angle of 15.3° (20.7, 20.7, 4.6°). The O(2) - V(1) - O(1) angle of 145.9 (1)° [O(2) and O(1) are farthest apart] in this structure is another indication of significant preference for the T.P. coordination.

The two ligands are only approximately planar with some atoms deviating appreciably from the mean plane, e.g. atoms C8 and C8' (of the methyl C). The ligand planes omitting C8 and C8' are at an angle of 93.1° with each other. The O1 and O1' atoms are 0.39Å away from the respective least square ligand planes. Similar deviation of the O1 atom was also found in the V(acac-BH)$_2$ [73]. The angle between the planes defined by O(1), O(2), N(1) and O(1'), O(2'), N(1') is 74.55° and the V atom is situated 0.499Å above and in between these planes. The deviations of various atoms from the O(1), O(2), N(1) plane are given in Table 3.6.1.3.

The V - O bond distances for O(1) and O(2) in the 6- and 5-membered rings are 1.871(3) and 1.900(3)Å respectively and are comparable with those in the V(acac-BH)$_2$ (average 1.943 and 1.919Å)[73] and in other VL_2 and VLL' complexes (Sections 3.6.2, 3.6.3 and 3.6.4). The V - N bond distance of 2.088(4)Å is the largest bond length in the coordination sphere which is also comparable to
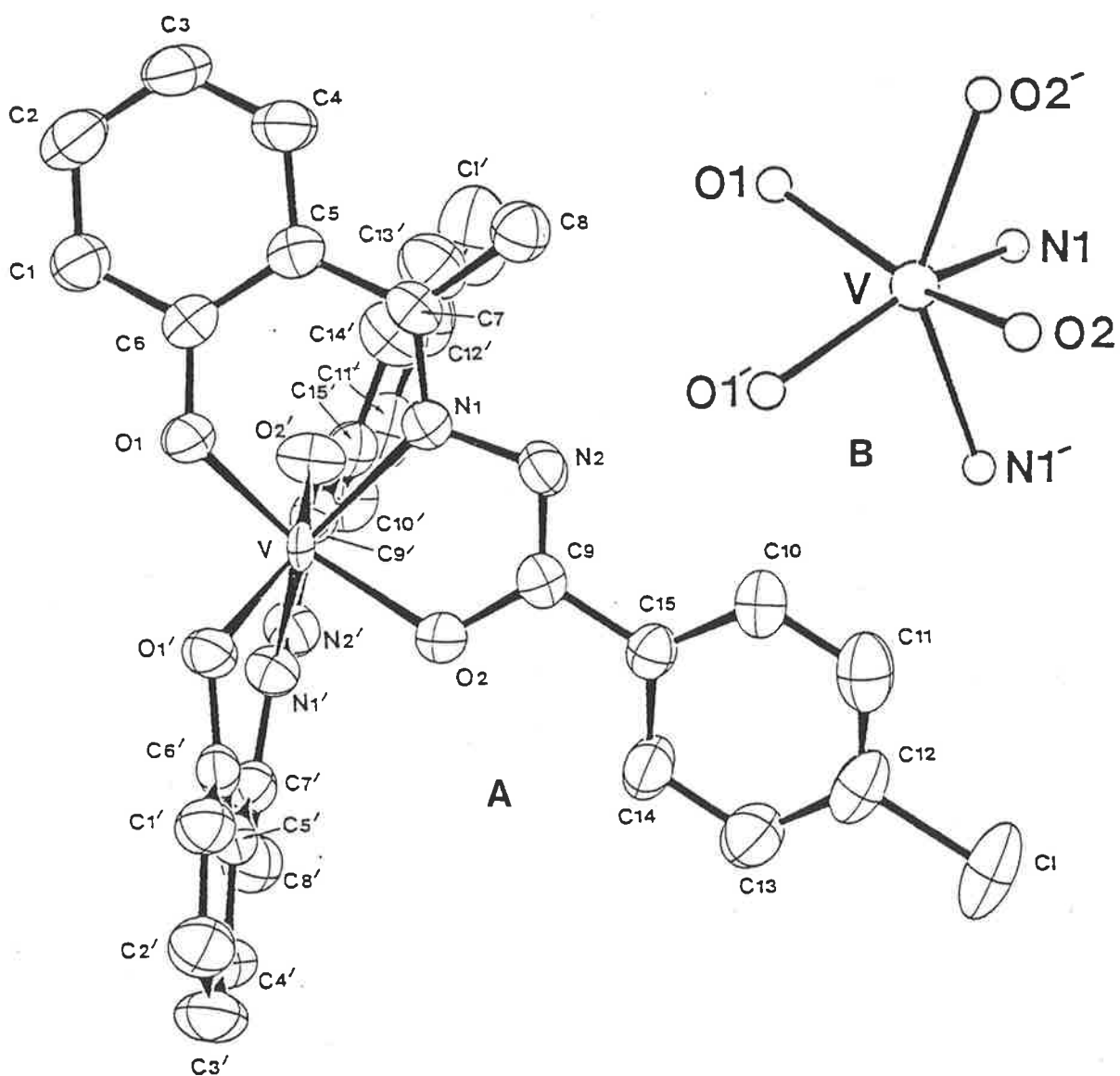
Figure 3.6.1.1: A. A perspective view of the V(HAP-p^{Cl}-BH)$_2$ molecule; B. Coordination sphere.

that in the above complexes. The V - O and V - N bond lengths of 1.950(8)
and 2.059(9)Å respectively in N,N'-ethylenebis(acetylacetoiminato)oxovanad-
ium(IV), VO(acen)[50] are also comparable with those of the present compound.
The V - N distance is also comparable to that of some Salen complexes of
Fe(III) and Cr(III)[228] and V(Sal-N-Bu)$_2$Cl$_2$ [64].

The N(1) - N(2) bond length of 1.401(6)Å indicates slightly greater than
a single bond order. The N - N and the N = N bond distances are 1.46 and

TABLE 3.6.1.1: BOND LENGTHS (Å) FOR V(HAP-p^{Cl}-BH)$_2$

O(1)	---	V(1)	1.871(3)	O(2)	---	V(1)	1.900(3)
N(1)	---	V(1)	2.088(4)	C(6)	---	O(1)	1.324(6)
C(9)	---	O(2)	1.316(5)	N(2)	---	N(1)	1.401(6)
C(7)	---	N(1)	1.323(6)	C(9)	---	N(2)	1.289(6)
C(7)	---	C1(5)	1.464(7)	C(6)	---	C(5)	1.412(7)
C(15)	---	C(9)	1.476(7)	C(8)	---	C(7)	1.498(6)

TABLE 3.6.1.2: BOND ANGLES (°) FOR V(HAP-p^{Cl}-BH)$_2$

O(2)	-	V(1)	-	O(1)	145.9(1)	N(1)	-	V(1)	-	O(1)	83.8(1)
N(1)	-	V(1)	-	O(2)	74.8(1)	C(6)	-	O(1)	-	V(1)	127.7(3)
O(1)	-	V(1)	-	O(1)	82.2(2)	C(9)	-	O(2)	-	V(1)	118.6(3)
O(2)	-	V(1)		O(2)	114.6(2)	N(2)	-	N(1)	-	V(1)	115.5(3)
C(7)	-	N(1)	-	V(1)	128.5(3)	C(7)	-	N(1)	-	N(2)	115.5(4)
C(9)	-	N(2)	-	N(1)	108.1(4)	C(7)	-	C(5)	-	C(6)	121.8(5)
C(1)	-	C(6)	-	O(1)	118.2(5)	C(5)	-	C(6)	-	O(1)	122.7(5)
C(5)	-	C(6)	-	C(1)	118.9(5)	C(5)	-	C(7)	-	N(1)	120.0(4)
C(8)	-	C(7)	-	N(1)	120.4(5)	C(8)	-	C(7)	-	C(5)	119.5(4)
N(2)	-	C(9)	-	O(2)	121.7(5)	C(15)	-	C(9)	-	O(2)	117.1(4)

TABLE 3.6.1.3: DEVIATIONS (Å) OF VARIOUS ATOMS FROM
THE PLANE DEFINED BY O(1), O(2) AND N(1)

N(2) -.226, C(1) .607, C(2) .808, C(3) .726, C(4) .456,

C(5) .280, C(6) .308, C(7) .023, C(8) -.179, C(9) -.173,

C(10) -.548, C(11) -.575, C(12) -.276, C(13) .032, C(14) .046,

C(15) -.236.

1.25Å respectively[229]. The C(7) - N(1) and C(9) - N(2) bond lengths of
1.323(6) and 1.289(6)Å respectively corresponding to double bond character are

comparable to the analogous bond distances [1.298(14) and 1.292(14)Å respectively) in VO(acen)[50].

A comparative discussion of the structural features of various VL_2 and related complexes has been made in Section 3.6.5.

3.6.2 THE CRYSTAL AND MOLECULAR STRUCTURE OF V(acac-SalH)$_2$

The compound V(acac-SalH)$_2$, obtained as dark purple crystals from dichloromethane-petroleum spirit, has the bond lengths and bond angles given in Tables 3.6.2.1 and 3.6.2.2 respectively. Figure 3.6.2.1 shows a perspective view of the molecule as well as the atomic numbering scheme employed.

As the ligand is potentially quadridentate, there are three bonding possibilities through formations of VO(acac-SalH)$^-$ with the O O N O donor tribasic quadridentate acac-SalH or V(acac-SalH)$_2$ where the ligand is dinegative tridentate using either O O N or O N O donors. The structure of the complex clearly indicates the last of these three possible bonding modes with the OH of the salicyloylhydrazine part remaining free. The V atom is six coordinate with no V - O distance less than 1.9Å thus indicating absence of the vanadyl oxygen.

In contrast to somewhat distorted trigonal prismatic geometry of the V(HAP-p^{Cl}-BH)$_2$, this molecule has a structure [Figure 3.6.2.1 (A and B)] in which the V^{4+} has the coordination geometry of an almost ideal trigonal prismatic nature with the average twist angle of only 3.5° (average of 0.95, 4.07, 5.43°). The O(5) - V - O(4) or N(1) - V - N(3) angle of 136.7(1)°, involving the donor pairs that are farthest apart, further confirms its almost ideal trigonal prismatic structure.

The angle between the two ligand planes defined by O(1), C(1), C(3), C(4), N(1), N(2), C(6), O(2) and O(4), C(13), C(15), C(16), N(3), N(4), C(18), O(5) is 77.4°. The angles between the 5- and the 6-membered chelate ring planes of the same ligand are 20.0° between planes O(1), C(1), C(3), C(4), N(1) and O(2), C(6), N(2), N(1) and 15.8° between planes O(4), C(13), C(15),
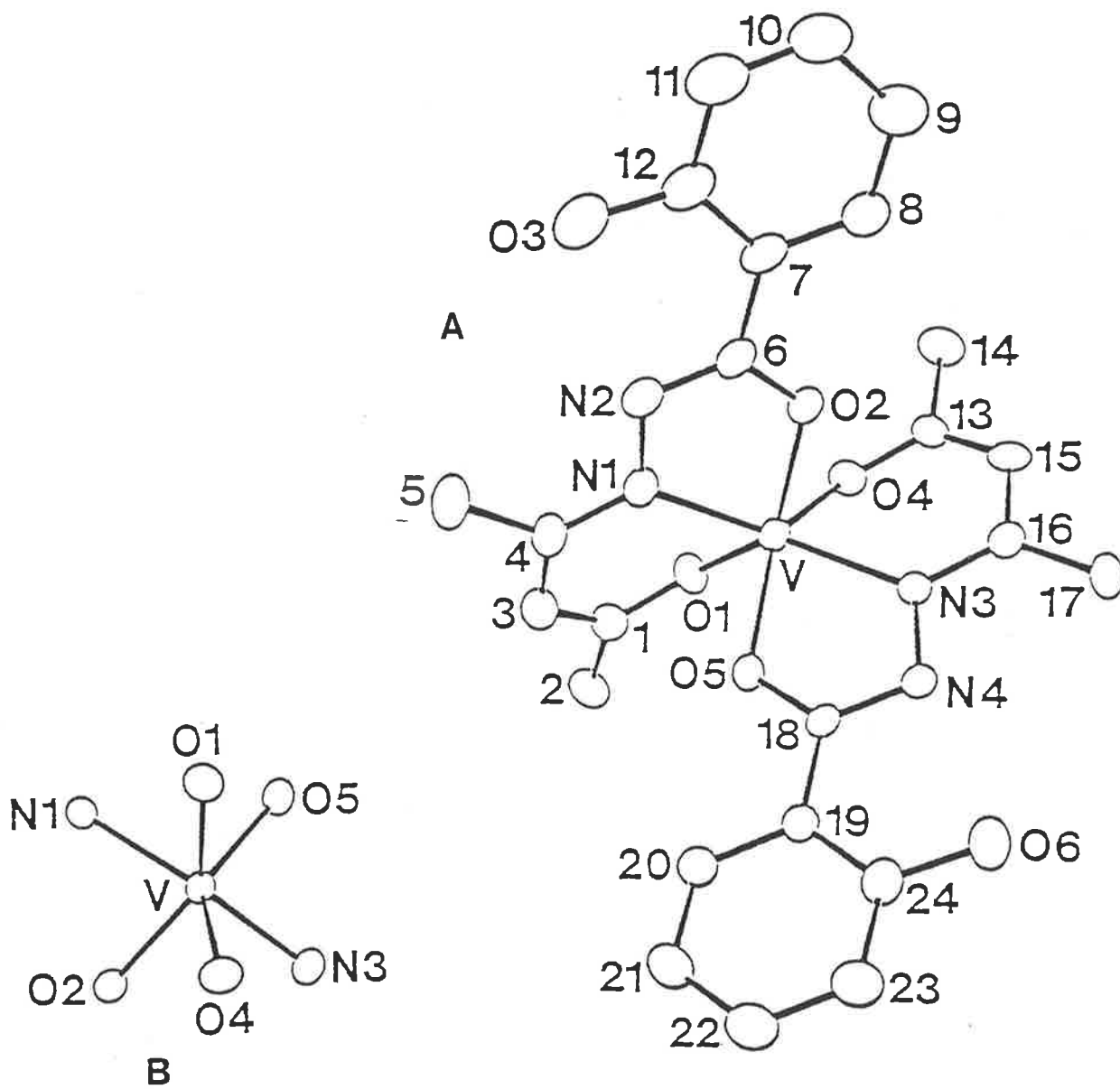
Figure 3.6.2.1: A. A perspective view of the V(acac-SalH)₂ molecule;
B. Coordination sphere.

C(16), N(3) and O(5), C(18), N(4), N(3). If the V is included in these planes, then the angles 20.0° and 15.8° change to respectively 23.5° and 20.4°. Thus the chelate rings are not strictly planar and the deviation from the expected planarity is due to the deviations of some ligand atoms from the mean plane. The atoms O(1) and O(4) are 0.30Å below the 6-membered chelate ring mean planes V, O(1), C(1), C(3), C(4), N(1) and V, O(4), C(13), C(15), C(16), N(3). The V atom is 0.73 and 0.70Å away from but in between the two ligand planes described by respectively O(1), N(1), O(2) and O(4), N(3), O(5) which are inclined at an angle of 67.1°.

The V - O(1) and V - O(4) and V - O(2) and V - O(5) bond distances in the 6- and 5-membered chelate rings [1.922(2), 1.928(2)Å and 1.908(2), 1.926(2)Å respectively] as well as the large V - N bond lengths of 2.045(2)Å for V-N(1) and 2.036(2)Å for V - N(3) are comparable with the analogous distances of the other VL_2/VLL' complexes (Sections 3.6.1, 3.6.3 and 3.6.4) and of VO(acen)[50]. The N(1) - N(2) and N(3) - N(4) bond lengths of 1.383(3) and 1.387(3)Å show slightly greater than single bond character in these pairs. The C(4) - N(1), C(6) - N(2), C(16) - N(3) and C(18) - N(4) bond lengths of respectively 1.337(3), 1.298(4), 1.329(3) and 1.303(3)Å correspond to an effective double bond character in these pairs of atoms.

The H(O3) atom, located in the difference map, is situated at a distance of 0.845 and 1.980Å from O(3) and N(2) respectively. Similarly, the H(O6) atom is located at a distance of 0.776 and 1.954Å from O(6) and N(4) respectively. The above positions of these two hydrogens with respect to O(3), N(2) and O(6), N(4) indicate substantial intramolecular hydrogen bonding. This is further indicated by the O(3) - N(2) and O(6) - N(4) distances of respectively 2.649 and 2.608Å which are well within the range[230] of the intramolecular -O-H....N hydrogen bonds. As a result of this, rotation of the aromatic ring is restricted thus keeping it in the plane of the ligand. In addition, this comparatively strong hydrogen bonding inhibits the OH group from being deprotonated and coordinated to the metal.

TABLE 3.6.2.1: BOND LENGTHS (Å) FOR V(acac-SalH)$_2$

O(1)	---	V	1.922(2)	O(2)	---	V	1.908(2)
N(1)	---	V	2.045(2)	O(4)	---	V	1.928(2)
O(5)	---	V	1.926(2)	N(3)	---	V	2.036(2)
C(1)	---	O(1)	1.298(3)	C(6)	---	O(2)	1.312(3)
N(2)	---	N(1)	1.383(3)	C(4)	---	N(1)	1.337(3)
C(6)	---	N(2)	1.298(4)	C(13)	---	O(4)	1.293(3)
C(18)	---	O(5)	1.307(3)	C(24)	---	O(6)	1.350(3)
C(12)	---	O(3)	1.337(4)	N(4)	---	N(3)	1.387(3)
C(16)	---	N(3)	1.329(3)	C(18)	---	N(4)	1.303(3)
C(4)	---	C(3)	1.397(5)	C(3)	---	C(1)	1.385(5)
C(15)	---	C(13)	1.377(4)	C(16)	---	C(15)	1.403(4)

TABLE 3.6.2.2: BOND ANGLES (°) FOR V(acac-SalH)$_2$

O(2)	-	V	-	O(1)	134.7(1)	N(1)	-	V	-	O(1)	83.5(1)
N(1)	-	V	-	O(2)	74.2(1)	O(4)	-	V	-	O(1)	82.0(1)
O(4)	-	V	-	O(2)	83.9(1)	O(4)	-	V	-	N(1)	131.1(1)
O(5)	-	V	-	O(1)	85.5(1)	O(5)	-	V	-	O(2)	131.2(1)
O(5)	-	V	-	N(1)	87.9(1)	O(5)	-	V	-	O(4)	136.7(1)
N(3)	-	V	-	O(1)	132.5(1)	N(3)	-	V	-	O(2)	87.9(1)
N(3)	-	V	-	N(1)	136.7(1)	N(3)	-	V	-	O(4)	83.9(1)
N(3)	-	V	-	O(5)	74.7(1)	C(1)	-	O(1)	-	V	124.6(2)
N(2)	-	N(1)	-	V	117.6(2)	C(4)	-	N(1)	-	V	126.1(2)
C(4)	-	N(1)	-	N(2)	116.2(2)	C(6)	-	N(2)	-	N(1)	108.1(2)
C(13)	-	O(4)	-	V	123.6(2)	C(18)	-	O(5)	-	V	118.2(1)
C(6)	-	O(2)	-	V	119.6(2)	N(4)	-	N(3)	-	V	117.2(1)
C(16)	-	N(3)	-	V	126.6(2)	C(16)	-	N(3)	-	N(4)	115.9(2)
C(3)	-	C(1)	-	O(1)	122.4(3)	C(18)	-	N(4)	-	N(3)	108.3(3)
C(4)	-	C(3)	-	C(1)	124.9(3)	C(3)	-	C(4)	-	N(1)	119.3(3)
N(2)	-	C(6)	-	O(2)	119.9(3)	C(8)	-	C(7)	-	C(6)	119.6(2)
C(12)	-	C(7)	-	C(6)	121.3(3)	C(12)	-	C(7)	-	C(8)	119.1(3)
C(7)	-	C(12)	-	O(3)	123.2(3)	C(11)	-	C(12)	-	O(3)	118.6(3)
C(15)	-	C(13)	-	O(4)	123.4(2)	C(15)	-	C(16)	-	N(3)	119.3(2)
C(16)	-	C(15)	-	C(13)	124.7(2)	N(4)	-	C(18)	-	O(5)	120.2(2)
C(19)	-	C(24)	-	O(6)	122.8(2)	C(23)	-	C(24)	-	O(6)	117.6(2)

3.6.3 THE CRYSTAL AND MOLECULAR STRUCTURE OF V(Bzac-BH)(HNP-BH)

This mixed ligand complex, also obtained as dark purple crystals from dichloromethane-petroleum spirit, has the crystal structure shown in Figure 3.6.3.1. The interest in this structure is that it confirms the presence of two different ligands Bzac-BH and HNP-BH attached to six coordinate V^{4+}. The bond lengths, bond angles and the calculated least square planes for
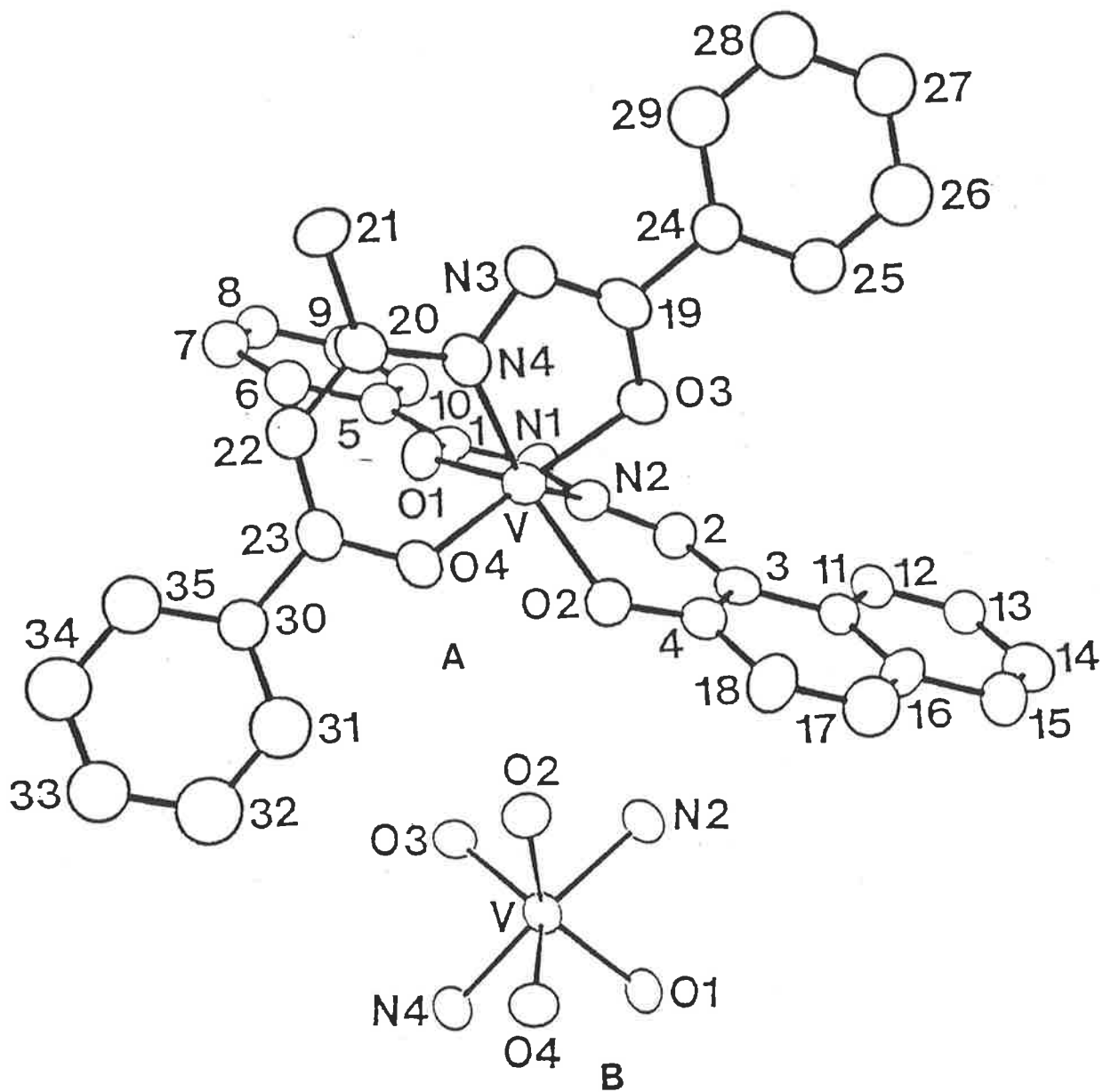
Figure 3.6.3.1:   A.   The molecular structure of V(Bzac-BH)(HNP-BH)$_2$;
                  B.   Coordination sphere.

selected groups of atoms are given in Tables 3.6.3.1 - 3.6.3.3.

The six donor atoms of the two different ligands surround the central V^{4+} in a trigonal prismatic coordination (Figure 3.6.3.1 B) with a twist angle of 4.98° (average of 6.09, 4.16, 4.68°). Also the angles O(4)-V-O(3), O(2)-V-O(1) and N(4)-V-N(2) have the values of 135.6(3), 135.3(3) and 135.2(3)° respectively, as required for a T.P. structure. The dihedral angle between the ligand planes of the atoms constituting the 5- and 6-membered rings in each ligand, i.e. O(1), C(1), N(1), N(2), C(2), C(3), C(4), O(2) and O(3), C(19), N(3), N(4), C(20), C(22), C(23), O(4) is 73.9°. The angle between the 5-membered chelate ring plane V, O(1), C(1), N(1), N(2) and the 6-membered chelate ring plane V, N(2), C(2), C(3), C(4), O(2) of the HNP-BH ligand is 29.1°. The same angle for the Bzac-BH ligand is 28.8° between the planes V, O(3), C(19), N(3), N(4) and V, N(4), C(20), C(22), C(23), O(4). If the vanadium is excluded from the above planes then the angles 29.1 and 28.8° change to 13.9 and 13.3° respectively. In this case also, the oxygen atoms of the 6-membered rings show appreciable deviations. Thus, the O(2) and O(4) atoms are 0.27Å above and 0.31Å below the ring planes V, N(2), C(2), C(3), C(4), O(2) and V, N(4), C(20), C(22), C(23), O(4) respectively. The 5-membered rings are more planar than the 6-membered rings. The angles between the planes defined by O(1), N(2), O(2) and O(3), N(4), O(4) is 65.3° and the V atom is 0.71Å away from but in between these planes.

The average V - O distances in the 6- and 5-membered chelate rings (1.9075 and 1.9095Å respectively) and the V - N distances (average 2.0405Å) are comparable with those in the VL$_2$ complexes (Sections 3.6.1, 3.6.2 and 3.6.4). The N(1) - N(2) and N(3) - N(4) bond lengths of 1.376(10) and 1.374(10)Å are between a single and a double bond[229]. The C(1) - N(1), C(2) - N(2), C(20) - N(4) and C(19) - N(3) distances (Table 3.6.3.1) indicate multiple bond character. A comparative discussion for various structural features has been made in Section 3.6.5.

TABLE 3.6.3.1: BOND LENGTHS (Å) FOR V(Bzac-BH)(HNP-BH)]

O(1)	---	V(1)	1.907(6)	O(2)	---	V(1)	1.906(6)
N(2)	---	V(1)	2.043(8)	O(3)	---	V(1)	1.912(5)
O(4)	---	V(1)	1.909(6)	N(4)	---	V(1)	2.038(8)
C(1)	---	O(1)	1.338(10)	C(4)	---	O(2)	1.290(11)
N(2)	---	N(1)	1.376(10)	C(1)	---	N(1)	1.274(11)
C(2)	---	N(2)	1.339(12)	C(5)	---	C(1)	1.471(11)
C(3)	---	C(2)	1.401(12)	C(4)	---	C(3)	1.424(13)
C(19)	---	O(3)	1.322(11)	C(23)	---	O(4)	1.332(12)
N(4)	---	N(3)	1.374(10)	C(19)	---	N(3)	1.284(13)
C(20)	---	N(4)	1.357(13)	C(22)	---	C(20)	1.389(14)
C(23)	---	C(22)	1.372(14)				

TABLE 3.6.3.2: BOND ANGLES (°) FOR V(Bzac-BH)(HNP-BH)

O(2)	-	V(1)	-	O(1)	135.3(3)	N(2)	-	V(1)	- O(1)	73.8(3)
N(2)	-	V(1)	-	O(2)	83.0(3)	O(3)	-	V(1)	- O(1)	128.9(3)
O(3)	-	V(1)	-	O(2)	86.5(3)	O(3)	-	V(1)	- N(2)	87.8(3)
O(4)	-	V(1)	-	O(1)	86.2(3)	O(4)	-	V(1)	- O(2)	82.3(3)
O(4)	-	V(1)	-	N(2)	132.7(3)	O(4)	-	V(1)	- O(3)	135.6(3)
N(4)	-	V(1)	-	O(1)	86.8(3)	N(4)	-	V(1)	- O(2)	134.1(3)
N(4)	-	V(1)	-	N(2)	135.2(3)	N(4)	-	V(1)	- O(3)	73.6(3)
N(4)	-	V(1)	-	O(4)	83.9(3)	C(1)	-	O(1)	- V(1)	118.5(6)
C(4)	-	O(2)	-	V(1)	128.6(6)	C(1)	-	N(1)	- N(2)	108.4(8)
N(1)	-	N(2)	-	V(1)	117.7(6)	C(2)	-	N(2)	- V(1)	127.0(6)
C(2)	-	N(2)	-	N(1)	115.2(8)	N(1)	-	C(1)	- O(1)	119.6(9)
C(5)	-	C(1)	-	O(1)	117.3(8)	C(5)	-	C(1)	- N(1)	123.1(8)
C(3)	-	C(2)	-	N(2)	123.5(9)	C(4)	-	C(3)	- C(2)	119.8(9)
C(11)	-	C(3)	-	C(2)	119.6(9)	C(11)	-	C(3)	- C(4)	120.4(9)
C(3)	-	C(4)	-	O(2)	123.4(9)	C(18)	-	C(4)	- O(2)	117.9(9)
C(6)	-	C(5)	-	C(1)	119.4(4)	C(10)	-	C(5)	- C(1)	120.6(4)
C(18)	-	C(4)	-	C(3)	118.4(10)	C(19)	-	O(3)	- V(1)	117.4(6)
C(16)	-	C(11)	-	C(3)	118.1(9)	C(19)	-	N(3)	- N(4)	106.0(8)
C(23)	-	O(4)	-	V(1)	125.4(6)	C(20)	-	N(4)	- V(1)	124.9(6)
N(3)	-	N(4)	-	V(1)	119.0(6)	N(3)	-	C(19)	- O(3)	121.8(9)
C(20)	-	N(4)	-	N(3)	116.0(9)	C(22)	-	C(20)	- N(4)	122.2(9)
C(22)	-	C(23)	-	O(4)	121.5(9)	C(23)	-	C(22)	- C(20)	123.8(11)

TABLE 3.6.3.3: THE BEST LEAST-SQUARES PLANES AND THE DISTANCES OF THE

ATOMS FROM THEIR RESPECTIVE PLANES(Å)

PLANE 1:   O(1), C(1), N(1), N(2), C(2), C(3), C(4), O(2)

[O(1) -.09, C(1) .12, N(1) .12, N(2) -.13, C(2) -.01, C(3) -.06, C(4) -.02, O(2) .08, V[a] -.71]

PLANE 2:   O(3), C(19), N(3), N(4), C(20), C(22), C(23), O(4)

[O(3) .09, C(19) -.10, N(3) -.16, N(4) .09, C(20) -.01, C(22) .12, C(23) .07, O(4) -.10, V[a] .70]

PLANE 3:   V, O(1), C(1), N(1), N(2)

[V -.004, O(1) .08, C(1) -.08, N(1) -.08, N(2) .10]

PLANE 4:   V, N(2), C(2), C(3), C(4), O(2)

[V -.017, N(2) .27, C(2) -.01, C(3) -.34, C(4) -.18, O(2) .274]

PLANE 5:   V, O(3), C(19), N(3), N(4)

[V -.004, O(3) .07, C(19) -.12, N(3) -.08, N(4) .11]

PLANE 6:   V, O(4), C(23), C(22), C(20), N(4)

[V .016, O(4) -.31, C(23) .23, C(22) .39, C(20) .01, N(4) -.30]

PLANE 7:   O(1), C(1), N(1), N(2)

[O(1) .001, C(1) -.002, N(1) .002, N(2) -.001, V[a] -.31]

PLANE 8:   N(2), C(2), C(3), C(4), O(2)

[N(2) -.04, C(2) .08, C(3) -.02, C(4) -.06, O(2) .02, V[a] -.71]

PLANE 9:   O(3), C(19), N(3), N(4)

[O(3) -.004, C(19) .02, N(3) -.01, N(4) .005, V[a] .33]

PLANE 10:   O(4), C(23), C(22), C(20), N(4)

[O(4) -.03, C(23), .07, C(22) .03, C(20) -.11, N(4) .05, V[a] .79]

PLANE 11:   O(1), N(2), O(2) [V[a] -.71]

PLANE 12:   O(3), N(4), O(4) [V[a] +.71]

ANGLES BETWEEN THE PLANES

Planes	Angle(°)	Planes	Angle(°)
1 - 2	73.9	7 - 8	13.9
3 - 4	29.1	9 - 10	13.3
5 - 6	28.8	11 - 12	65.3

[a] Atom not defining the plane.

3.6.4 THE CRYSTAL AND MOLECULAR STRUCTURE OF V(HAP-OAP)$_2$

This is the only structure in which the five-membered ring is not due to an aroylhydrazine but an o-aminophenol. As compared to the trigonal prismatic crystal structures of the other VL$_2$/VLL' complexes, this molecule has a coordination geometry lying between T.P. and an octahedron (Figure 3.6.4.1B). The perspective drawing of its crystal structure is shown in Figure 3.6.4.1A. The bond lengths and the bond angles are given in Tables 3.6.4.1 and 3.6.4.2 respectively. As expected, the crystal structure shows absence of the vanadyl oxygen and confirms formation of the VL$_2$ type complexes with Schiff bases of o-aminophenols.

The six donor atoms surround the V^{4+} in a coordination about intermediate between a trigonal prism and a skew trapezoidal bipyramide (see Section 3.6.5) with a twist angle of 32.3° (average of 55.73, 21.68, 19.43°) [Figure 3.6.4.1B]. However, as will be discussed in detail later on, the distorted T.P. coordination in this case places the six-membered ring on the trigonal prismatic edge and the five-membered ring on the triangular face. The reverse order is followed in the other VL$_2$ structures. Also the O(4)-V-N(1) or N(2)-V-O(1) angle of 164.6(2)°, involving the donor pairs that are farthest apart, further indicates a geometry in between a T.P. and an octahedron.

The structure shows considerable differences from the previous structures in the arrangement of the two ligands. The dihedral angle between the planes of the atoms in the 5- and 6-membered rings (except V) in each ligand, O(1), C(1), C(6), N(1), C(7), C(9), C(14), O(2) and O(3), C(15), C(20), C(21), N(2), C(23), C(28), O(4) is only 29.8° as against > 73° in the other VL$_2$/VLL' systems. The angle between the 5-membered and the 6-membered chelate ring planes O(1), C(1), C(6), N(1), V and O(2), C(14), C(9), C(7), N(1), V is 52°. The same angle for the other ligand is 45.2° between the planes O(4), C(28), C(23), N(3), V and O(3), C(15), C(20), C(21), N(2), V. If the vanadium is excluded from the above planes then the angles 52° and 45.2° change to 16.5 and 11.7° respectively. The ligands are not planar as expected due to devia-
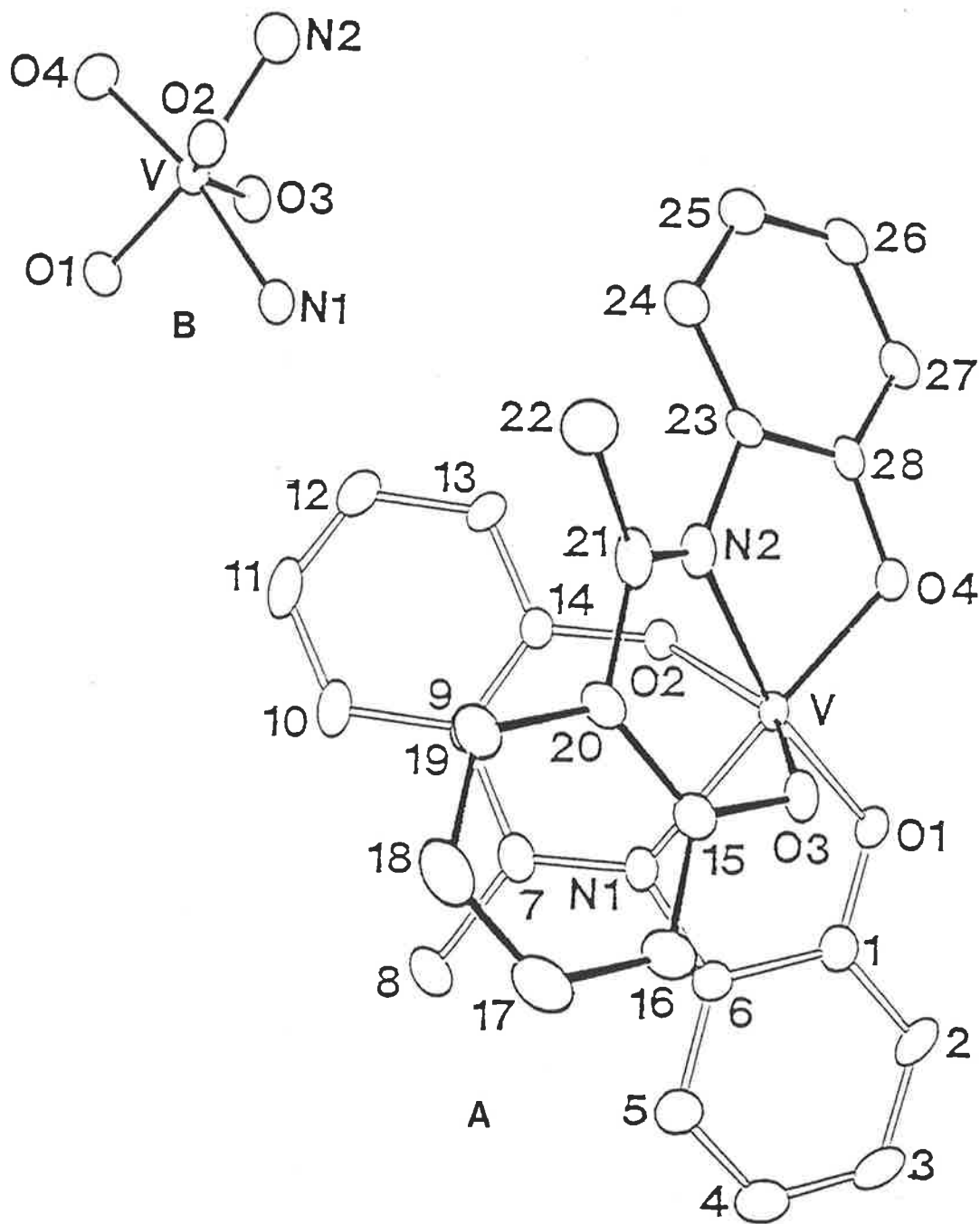
Figure 3.6.4.1: A. The molecular structure of V(HAP-OAP)$_2$ molecule;
B. Coordination sphere.

tions of some atoms from the mean planes. The O(2) and O(3) atoms are .41 and .47Å below the 6-membered chelate ring mean planes V, O(2), C(14), C(9), C(7), N(1) and V, O(3), C(15), C(20), C(21), N(2) respectively. The 5-membered rings are more nearly planar. The angle between the planes defined by O(1), N(1), O(2) and O(3), N(2), O(4) is 26° and the V atom is 1.05° away from but in between these planes.

The average V - O distances in the 6- and 5-membered chelate rings (1.8695 and 1.880Å respectively) are very slightly smaller but the V - N distances (2.176 and 2.141Å) are a bit longer than those in the other VL_2 structures. These V - N distances are comparable with the analogous distances in $([VO(Sal-OAP)]_2O)_2$.dioxane (2.17Å)[92] and octahedral $Ti(acac-BH)_2$ (2.134Å)[99]. The C(21) - N(2) and C(7) - N(1) distances of 1.281(10) and 1.326(10)Å respectively correspond to an effective double bond character[229] in these pairs of atoms.

TABLE 3.6.4.1: BOND LENGTHS (Å) FOR V(HAP-OAP)$_2$

O(1)	---	V	1.862(5)	O(2)	---	V	1.861(5)
N(1)	---	V	2.141(6)	O(4)	---	V	1.898(5)
O(3)	---	V	1.878(5)	C(14)	---	O(2)	1.344(8)
N(2)	---	V	2.176(7)	C(7)	---	N(1)	1.326(10)
C(1)	---	O(1)	1.348(9)	C(6)	---	C(1)	1.421(11)
C(6)	---	N(1)	1.397(9)	C(9)	---	C(7)	1.434(10)
C(15)	---	O(3)	1.337(9)	C(14)	---	C(9)	1.392(11)
C(21)	---	N(2)	1.281(10)	C(28)	---	O(4)	1.318(10)
C(21)	---	C(20)	1.470(12)	C(23)	---	N(2)	1.442(10)
C(20)	---	C(15)	1.393(11)	C(28)	---	C(23)	1.411(12)

TABLE 3.6.4.2: BOND ANGLES (°) FOR V(HAP-OAP)$_2$

O(2)	-	V	-	O(1)	109.6(2)	N(1)	-	V	-	O(1)	79.5(2)
N(1)	-	V	-	O(2)	80.9(2)	O(3)	-	V	-	O(2)	147.3(2)
O(4)	-	V	-	N(1)	164.6(2)	O(4)	-	V	-	O(2)	91.2(2)
O(4)	-	V	-	O(3)	111.5(2)	N(2)	-	V	-	O(1)	164.6(2)
N(2)	-	V	-	O(4)	77.3(3)	N(2)	-	V	-	N(1)	114.0(2)
C(1)	-	O(1)	-	V	115.4(4)	N(2)	-	V	-	O(3)	81.7(3)
C(6)	-	N(1)	-	V	107.8(4)	C(14)	-	O(2)	-	V	120.3(4)
C(7)	-	N(1)	-	C(6)	127.5(6)	C(7)	-	N(1)	-	V	124.6(5)
C(14)	-	C(9)	-	C(7)	121.8(7)	C(6)	-	C(1)	-	O(1)	118.5(6)
C(9)	-	C(14)	-	O(2)	122.2(7)	C(1)	-	C(6)	-	N(1)	111.0(6)
C(28)	-	O(4)	-	V	115.2(4)	C(9)	-	C(7)	-	N(1)	117.8(7)
C(23)	-	N(2)	-	V	108.3(5)	C(15)	-	O(3)	-	V	120.1(4)
C(21)	-	C(20)	-	C(15)	123.4(7)	C(21)	-	N(2)	-	V	126.4(6)
C(20)	-	C(21)	-	N(2)	115.8(8)	C(20)	-	C(15)	-	O(3)	121.2(7)
C(28)	-	C(23)	-	N(2)	108.3(7)	C(23)	-	C(28)	-	O(4)	120.9(6)

3.6.5 GENERAL DISCUSSION OF THE STRUCTURES OF VL$_2$ COMPLEXES

(a) COORDINATION GEOMETRY

In the VL$_2$ complexes, as their structures show, the coordination sphere is occupied by six donor atoms from two tridentate ligands. The geometry around the V^{4+} centre varies from an almost trigonal prism to a severely distorted trigonal prism. Trigonal prismatic geometry is uncommon and in this case the ligand must be an important determining factor because in the few non-vanadyl complexes known, the coordination is octahedral in VCl$_4$(CNH)$_2$ [7] as it is in V(cat)$_3^{2-}$ [71] and V(Sal-NBu)$_2$Cl$_2$ [64], whereas, the tris-dithiolene complexes[57] are trigonal prismatic. Neglecting the donor atom repulsions, the application of crystal field theory and calculations of the crystal field stabilization energies associated with the octahedral and trigonal prismatic coordination geometries show no preference for either trigonal prismatic or octahedral coordination for d$^\circ$, d^1 and low spin d^2 metal ions[231]. A σ-bonding molecular orbital calculation by Jellinek[232], which also considered the bonding orbitals, shows a considerable preference for trigonal prismatic coordination with these d configurations and has been used to account for the trigonal prismatic metal-sulphide structures of the early transition metals. R. Hoffmann et al.[233] on the basis of molecular orbital analysis drew a correlation diagram for octahedral and trigonal prismatic configurations interrelated through a trigonal twist and showed a possible preference for the trigonal prismatic systems with few d electrons (d$^\circ$ - d^2). However, they noted that the geometry of a particular complex is influenced by both the d orbital patterns as well as their energy and other various structural parameters of the coordination sphere, e.g. the size of the metal ion, the bite sizes of the ligands and their mutual steric interferences. Lower d orbital energies favour T.P. configuration. The lowering of the energy of the T.P. is also enhanced in cases where symmetry favours π-bonding. In the case of tris-dithiolene complexes, intraligand bonding, resulting in short ligand bites, was suggested by Eisenberg et al.[60,234] as the reason for the stabilization of

the T.P. coordination.

From our structural observations and taking note of some unpublished work on Ti(IV) complexes [Section (d) below] it seems reasonable to conclude that both the nature of the metal ion as well as the relative bite sizes of the five- and six-membered rings influence stabilization of T.P. coordination.

Kepert in a series of papers[223-225,235-237] and a monograph[224] has considered the stereochemistry of chelate compounds, including the occurrence of T.P. coordination, by energy minimization calculations. The coordination arrangement is determined to a considerable extent by the bite sizes of the chelate rings. To permit comparison between different metals, each case is considered in terms of the 'normalized bite', b which is defined as the distance between the donor atoms of the chelate divided by the metal-donor distance. The predicted and found stereochemistries are very dependent on these normalized bites.

For the tris-bidentate complexes, it has been found that the smaller the bite of the ligand the greater is the distortion towards the T.P. arrangement as the latter reduces the distance between the coordination sites. Kepert examined a large number of complexes with bites ranging from 1.6 to 1.2[223]. At the lower end of the range the twist angles (defined in Figure 3.6.1) are of the order of 30-40°, i.e. half-way between an octahedron and a T.P. However, Kepert observed gross exceptions[224a] to this prediction, especially in $[Mo(O_2C_{14}H_8)_3]$ and $K[Cd(MeCOCHCOMe)_3].H_2O$ which had normalized bites of 1.27 and 1.28 respectively as against θ values of only 0 and 0.4° respectively. The tris-dithiolato complexes also seem to be exceptional in the same way[224b]. Stiefel and Brown[227] also examined a number of tris-bidentate complexes and found the normalized bite to be 1.41 for an octahedron and 1.31 for a T.P.

In the trigonal prismatic structure of V(acac-BH)$_2$ as described by Diamantis et al.[73], the mean normalized bites are calculated to be 1.22 and 1.34 for 5- and 6-membered rings respectively which are in agreement with the

theory presented above and thus the acac-BH ligand type stabilizes the trigonal prismatic stereochemistry with the short bite spanning the edge of the rectangular face. This also applies to the other three VL_2 structures with aroylhydrazone ligands which also have small bites associated with the 5-membered ring (Table 3.6.5.1). The small bite which is also reflected from a very sharp bite angle of 75° (average) in the 5-membered chelate ring (the same angle for the 6-membered chelate ring is ~ 83°) [Table 3.6.5.1] results from a small C - N - N angle compared to the O - C - N angle in the ring (Table 3.6.5.3). The same bite angles are characteristic of the ligand and are observed in the square pyramidal $V^VO(Bzac-BH).OEt$ and $[V^VO(Bzac-BH)]_2O$ (Chapter 4) as well as in two titanium complexes (Table 3.6.5.4).

TABLE 3.6.5.1: THE V-DONOR ATOM DISTANCES AND THE NORMALIZED BITES FOR THE VL_2 COMPLEXES

AVERAGE MOLECULAR DIMENSIONS	$V(acac-BH)_2$	$V(HAP-P^{Cl}-BH)_2$	$V(acac-SalH)_2$	$V(Bzac-BH)$ (HNP-BH)	$V(HAP-OAP)_2$
$V - O_6$ (Å)	1.943	1.871	1.925	1.908	1.870
$V - O_5$ (Å)	1.919	1.900	1.917	1.910	1.880
$V - N$ (Å)	2.052	2.088	2.041	2.041	2.158
$N - O_6$ (Å)	2.686	2.649	2.648	2.630	2.632
$N - O_5$ (Å)	2.423	2.427	2.396	2.373	2.562
BITE ANGLES					
$N - V - O_6$ (°)	83.3	82.2	83.7	83.5	81.3
$N - V - O_5$ (°)	75.1	74.8	74.5	73.7	78.4
NORMALIZED BITE, b					
(i) 5-membered ring	1.22	1.22	1.21	1.20	1.28
(ii) 6-membered ring	1.34	1.34	1.34	1.33	1.31

O_6 and O_5 are the oxygens in the 6- and 5-membered chelate rings respectively.

Favas and Kepert[236] using the same approach also examined the possible stereochemistries in the bis-tridentate complexes. Such complexes depending on the ligand bites may possess meridional, symmetrical-facial and unsymmetrical-facial geometries as shown in Figure 3.6.5.1 (a,b,c) where, ABC and DEF are the two tridentate ligands. One point of interest is the stereochemistry of the unsymmetrical-facial isomer which with unsymmetrical tridentate ligands can attain three possible stable structures as shown in Figure 3.6.5.2 (d,e,f). The first structure 3.6.5.2(d) has a trigonal prismatic geometry with the rings AB and DE having the shorter bites occupying two of the three rectangular edges. The other two structures (e) and (f) in Figure 3.6.5.2 have the short bites on BC and EF and can be described as a distorted T.P. and a skew trapezoidal bipyramid respectively. According to Kepert, this type of distortion makes ABDE into a rectangle, which more accurately is a flattened tetrahedron tending to a rectangle in the limit.

Of the four structures determined for the bis-VL_2 type complexes, the first three have the unsymmetrical tridentate ligands with an aroylhydrazine 5-membered ring with normalized bites of 1.20 - 1.22 and a 6-membered ring with bite in the range 1.33 - 1.34 (Table 3.6.5.1). All these exhibit the predicted T.P. structure (d) in Figure 3.6.5.2 with the 5-membered rings on the rectangular edges. The last structure, for V(HAP-OAP)$_2$, has a 6-membered bite of 1.31 and a 5-membered bite of 1.28 (Table 3.6.5.1). It is remarkable that the apparently irregular coordination, shown in Figure 3.6.4.1(B), resemble closely that predicted by Kepert for the intermediate geometry (Figure 3.6.5.2e). The coordination geometry re-oriented (Figure 3.6.5.3) to the presentation of isomer (e) in Figure 3.6.5.2 shows the similarity. This has the 6-membered rings occyping the rectangular edges. N(2), N(1), O(2), O(3) lie on an approximate plane with deviations from the least square plane of N(2) = .397(6), N(1) = .407(6), O(2) = -.207(5) and O(3) = -.287(5)Å suggesting a flattened tetrahedral arrangement as required by the distortion. Atoms O(1) and O(4) lie respectively -2.103(5) and -2.076(5)Å above this plane
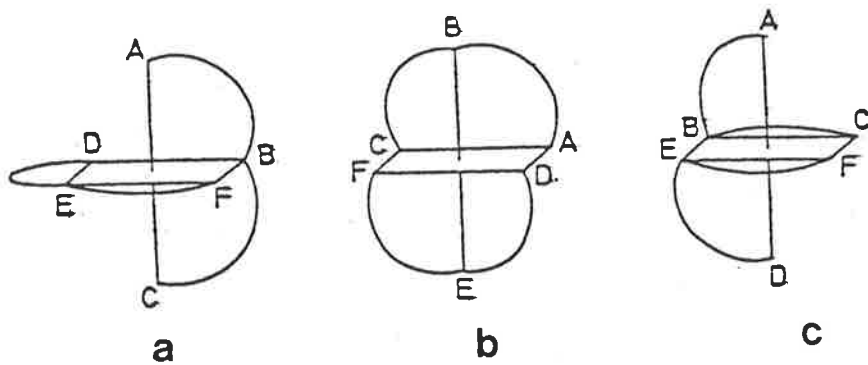
Figure 3.6.5.1: Isomers for M(tridentate)$_2$:
a. mer; b. sym-fac and c. unsym-fac.

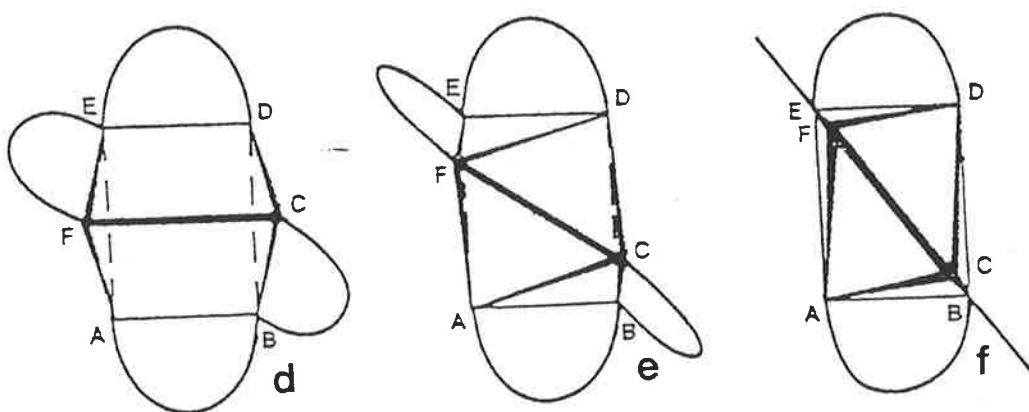Figure 3.6.5.2: Unsym-fac-M(tridentate)$_2$: d. trigonal prism;
e. intermediate; f. skew trapezoidal bipyramid.
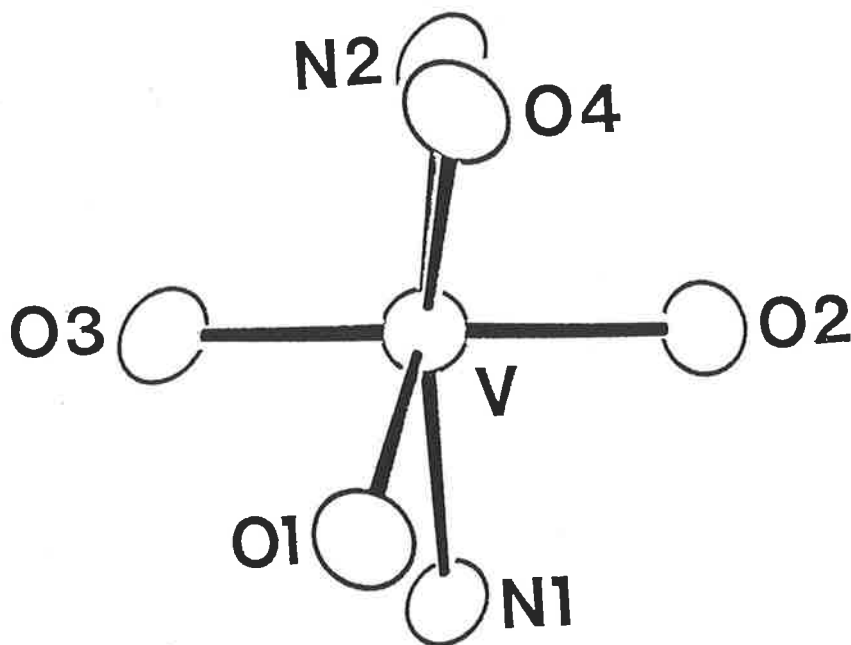

Figure 3.6.5.3: The coordination geometry of V(HAP-OAP)$_2$, reorientated
towards Figure (e) above.

in agreement with the proposed stereochemistry.

The twist angle, θ in the tris-dithiolate complexes generally increases with the increase of the number of d electrons due to reasons not clearly understood[223] and the θ for d^1 should be minimum and hence V^{4+} should show a strong preference for T.P. geometry. Table 3.6.5.2 lists the twist and the donor - V - donor angles of various VL_2 and related structures. An examination of these values clearly shows that the V^{4+} in these complexes possesses generally trigonal prismatic coordination [except $V(HAP-OAP)_2$]. The distor-

TABLE 3.6.5.2: THE TWIST AND THE MAXIMUM DONOR-V-DONOR ANGLES FOR THE VL_2 COMPLEXES

AVERAGE MOLECULAR DIMENSIONS	$V(acac-BH)_2$	$V(HAP-p^{Cl}-BH)_2$	$V(acac-SalH)_2$	$V(Bzac-BH)$ $(HNP-BH)$	$V(HAP-OAP)_2$
Average Twist angle (°)	8.9	15.3	3.5	5.0	-*
Max. donor-V-donor angle (°)	140.8	145.9	136.7	135.6	164.6*

* A twist angle of 32.3° exists between the planes 04, 02, N2 and 03, 01, N1; 164.6° is the angle 04-V-N1. See Figure 3.6.4.1.

tion from T.P. increases in the order $V(acac-SalH)_2$ (3.5, 136.7) < $V(Bzac-BH)(HNP-BH)$ (5.0, 135.6) < $V(acac-BH)_2$ [73] (8.9, 141.6) < $V(HAP-p^{Cl}-BH)_2$ (15.3, 145.9). The figures shown in parentheses are respectively the average twist and the maximum donor - V- donor angles.

It is the shortest bites of the 5-membered chelate rings which are responsible for the T.P. coordination in the aroylhydrazone containing VL_2/VLL' complexes. The comparatively larger bite size of the 5-membered rings in $V(HAP-OAP)_2$ is thought to be responsible for its adopting a different geometry intermediate between a T.P. and a skew trapezoidal bipyramid.

(b) THE LIGAND GEOMETRY

The ligands are generally only approximately planar and the deviation from the mean planarity occurs in most cases due to a few ligand atoms only. Except in V(HAP-OAP)$_2$, the two ligands in VL$_2$ complexes are inclined at near 90° (Table 3.6.5.3) to each other. The V atom lies significantly out of, and

TABLE 3.6.5.3: THE LIGAND GEOMETRY IN THE VL$_2$ COMPLEXES

MOLECULAR DIMENSIONS	V(acac-BH)$_2$	V(HAP-p^{Cl}-BH)$_2$	V(acac-SalH)$_2$	V(Bzac-BH) (HNP-BH)	V(HAP-OAP)$_2$
Mean ligand plane dihedral angle (°)	93.3	93.0	77.4	73.9	29.8
Angle (°) between planes defined by ligand donor atoms only	-	74.6	67.1	65.3	26.0
5-Membered ring Angles					
At C(°)	120.6	121.7	120.0	120.7	119.7
At N2 (°)	107.5	108.1	108.2	107.2	108.0

(5-Membered ring diagram: C — N2 — N1, C — O — V — N1)

O$_6$ and O$_5$ are the oxygens in the 6- and 5-membered chelate rings respectively.

in between the planes determined by the ligands alone. The/planes comprising ~angles between~ the donor atoms only [e.g. O(1), N(1), O(2) and O(1'), N(1'), O(2') in Figure 3.6.1.1] are in the range 65.3-74.6° which is intermediate between the 90° required by the planarity of the ligand (Figure 3.6.5.4) and the 60° required by the T.P. coordination. This approach to T.P. coordination is achieved by significant distortions of the terminal O of the 6-membered ring above the plane of the ligand.

The distortions range from 0.3-0.5Å and are present in the ligands derived from β-diketones where only a rotation around a C-C bond is required
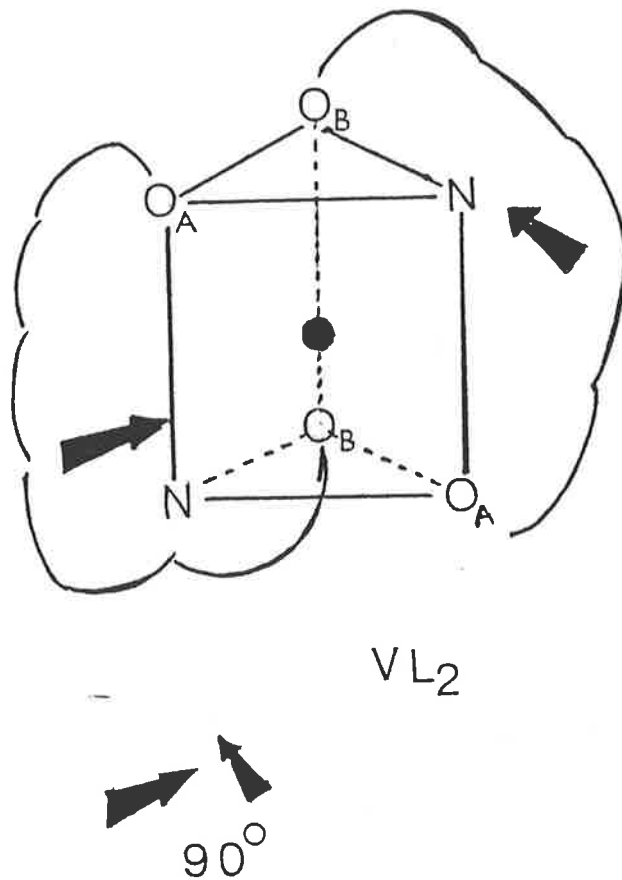
VL$_2$

90°

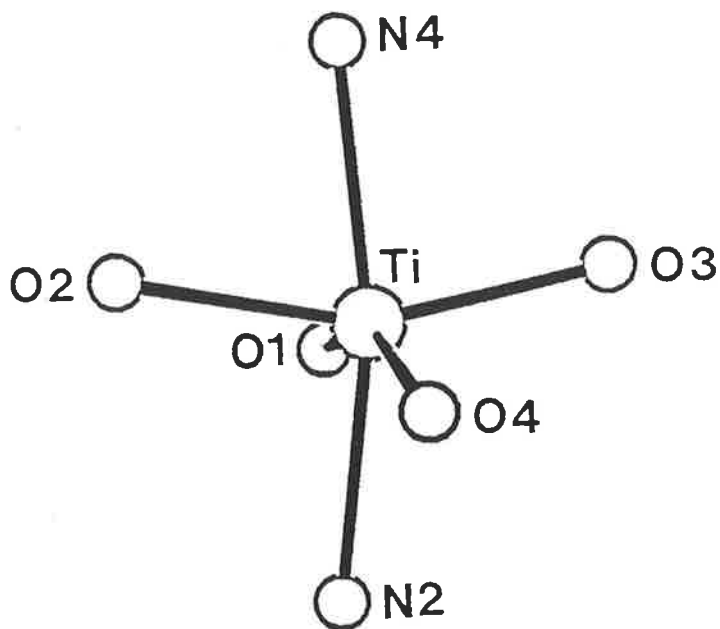Figure 3.6.5.4: Ligand arrangement in trigonal prismatic VL$_2$ complexes.

Figure 3.6.5.5: Coordination sphere of Ti(acac-BH)$_2$.

to achieve this as well as in the ligands derived from o-hydroxyaldehydes or ketones where bending out of the plane of the aromatic ring is required. In the V(HAP-OAP)$_2$ complex, the ligands are approximately planar but with appreciable deviation of some atoms. The dihedral angle between the ligand planes is 29.8° which is only a little bigger than the angle of the ligand donor atom planes of 26°. This is in qualitative agreement with structure 3.6.5.2(e) proposed by Kepert which is intermediate between a T.P. (angle = 60°) and a skew trapezoidal bipyramid (angle = 0°).

(c)   THE V - DONOR ATOM DISTANCES

The V - O and V - N bond distances in the 6- and 5-membered chelate rings in the VL$_2$ structures (Table 3.6.5.1) are generally shorter than those observed in the vanadyl complexes, e.g. VO(acac)$_2$ [21], VO(Bzac)$_2$ [21], Na$_4$[VO-dl-tartrate]$_2$ [238], [VO(acac)(OMe)]$_2$ (Section 2.4) and VO(acen) [50]. The average V - N distances (~ 2.05Å) except for V(HAP-OAP)$_2$ are also shorter than the average of 2.11Å found for the three of the V - N bonds in an oxovanadium(IV) porphyrin complex[239]. The V - O distance in the non-vanadyl V(Sal-NBu)$_2$ Cl$_2$ [64] is 1.807(3)Å. It appears that the removal of the vanadyl oxygen induces significant shortening of the V - O bond lengths. The shorter V - O and V - N bonds in the VL$_2$ complexes indicate substantial vanadium-ligand π bonding interactions through π-electron donation from, particularly the four strongly basic phenolic and/or enolic oxygens situated in a flattened tetrahedral arrangement in these complexes. The molecular orbitals of the ligand which are perpendicular to the principal plane of the ligand and delocalized over the atoms comprising the chelating part can overlap with the metal dπ-orbitals of corresponding symmetry to form stronger and thus shorter V - donor bonds.

The shorter V - O distances involving charge build-up on the central V atom into the V - O bonds from the strong σ- as well as π-donations of the tridentate ligands cause extra electron density near vanadium which in turn help easy expulsion of the vanadyl oxygen through protonation. These

comparatively shorter V - donor distances may also impose constraints on and shorten the inter-donor atom bite distances which might also be a geometric effect of the twisting of an octahedron toward a T.P.

(d)   EFFECT OF METAL ION ON COORDINATION GEOMETRY

The present VL_2 structures are in agreement with Kepert's theory and predictions on trigonal prismatic as well as on distorted intermediate geometry [Figure 3.6.5.2(e)] thus supporting his theory based on donor atom repulsions. The bite sizes and angles in the various aroylhydrazone ligands in the d^1-VL_2 (Table 3.6.5.1) and in the square pyramidal d^o-V^VO(Bzac-BH).OEt and $[V^VO$(Bzac-BH)$]_2O$ complexes (Table 3.6.5.4) have similar values. This indicates that the particular ligand geometries are the determining factors for the trigonal prismatic geometry of the VL_2 complexes. However, two structures of d^o-$Ti^{IV}L_2$ with the same aroylhydrazone ligands[99] produced different results raising doubts as to whether ligand considerations are the only determining factors for the observed stereochemistries. In contrast to the T.P. coordination geometry for the aroylhydrazone containing d^1-VL_2 complexes, the d^o-Ti(acac-BH)$_2$ possesses a meridional structure as shown in Figure 3.6.5.1(a). Because it is yet unpublished, we describe this structure in some detail for comparison: The average Ti-donor atom distances are given in Table 3.6.5.4 and the coordination sphere in Figure 3.6.5.5. The ligand planes including the Ti but excluding the benzene rings are almost planar with the Ti atom deviating from these two planes by only 0.087 and 0.054Å. The angle between these planes is 86.3°. If the benzene rings are included in the planes then this angle becomes 84.5°. The angle between the 6- and the 5- membered chelate rings is 5.9° indicating effective planarity of the ligand. The N(4), Ti, O(3) and O(4), Ti, O(3) are at an angle of 110.5°. The maximum donor(N4)-Ti-donor(N2) angle is 165.1°. Another structure determined[99] for Ti(Bzac-BH)$_2$ is essentially similar in character.

TABLE 3.6.5.4: MOLECULAR DIMENSIONS OF SOME COMPLEXES RELATED TO VL_2

AVERAGE MOLECULAR DIMENSIONS	$Ti(acac-BH)_2$[a]	$Ti(Bzac-BH)_2$[a]	$V^V OL.OEt$[b]	$(V^V OL)_2O$[b]
$M - O_6$ (Å)	1.886	1.888	1.848	1.832
$M - O_5$ (Å)	1.925	1.913	1.907	1.889
$M - N$ (Å)	2.134	2.136	2.070	2.078
$N - O_6$ (Å)	2.636	2.668	2.631	2.619
$N - O_5$ (Å)	2.456	2.403	2.414	2.371
BITE ANGLES				
$N - M - O_6$ (°)	81.7	-	84.2	83.9
$N - M - O_5$ (°)	74.3	-	74.6	73.2
NORMALIZED BITE, b				
(i) 5-membered ring	1.21	1.19	1.22	1.20
(ii) 6-membered ring	1.32	1.33	1.35	1.35

a. Reference - 99   b. Chapter 4; L = Bzac-BH

Thus, in determining the complex geometry, the metal ion must be an important factor. However, it is not clear as to how the metal determines the stereochemistry. Simple crystal field model[231] gives no advantage to T.P. over octahedron for d^o and d^1. However, the method of calculation, specifically what polar angle is used for the T.P. and the value of the parameter ρ, has an effect[240]. So it is not inconceivable that the crystal field stabilization energy in d^1 system may favour T.P. whereas there cannot be such preference in a d^o system.

Another possibility is the effect of π-donation from the ligand to the metal. Because of its position in the first transition series such effects would be stronger in the V^{4+} complex and may tip the balance in favour of the T.P. coordination. In fact, there are significant differences in the M-donor distances in the two complexes although it is not obvious how these can be interpreted. However, both these explanations assume that the octahedron is the preferred stereochemistry which of course contradicts the Kepert's theories. Hoffman's molecular orbital analysis[233] of such systems suggested that for fewer d electrons T.P. may be the preferred stereochemistry. However, he gives no indication that there should be a difference between d^0 and d^1.

3.7 SPECTROSCOPIC STUDIES OF THE VL_2 COMPLEXES

GENERAL INTRODUCTION

The study of the spectral properties of the complexes are extremely important in understanding their formations, formulations and electronic structures which, in turn, can definitively identify the coordination geometry of the complexes. Different spectroscopic measurements are used as analytical tools for characterization of the specific type of complexes. In the present study, a correlation of several spectral features with the six-coordinate trigonal prismatic coordination geometry of the VL_2 complexes has been attempted. The types of spectral measurements that have been made with the VL_2 complexes are (1) mass spectra, (2) infrared spectra, (3) electronic spectra and (4) electron spin resonance spectra.

3.7.1 MASS SPECTRA

As in the $[VO(AA)(OR)]_2$ complexes (Chapter 2.5), the mass spectroscopy is also extremely useful for quick identification of the formation of VL_2 complexes. The mass spectra of all the VL_2 complexes have been examined. They all exhibit the intense spectral peaks at m/e corresponding to the molec-

ular ion along with peaks due to the fragmented products of which VOL and VL are worth-noting. For complexes with odd molecular weights, the observation of the peaks due to m/2e is further evidence for the molecular ion.

The characteristic mass spectral data for the various VL_2 type complexes are given in Tables 3.7.1.1 - 3.7.1.2. The fragmentation peak due to the

TABLE 3.7.1.1: CHARACTERISTIC MASS SPECTRAL PEAKS FOR THE VL_2 COMPLEXES

COMPLEX (1)	MOL. WT. (2)	CHARACTERISTIC PEAKS FOR		
		VL_2 (3)	VOL (4)	VL (5)
$V(acac-BH)_2$	483.48	483	283	-
$V(Bzac-BH)_2$	607.56	607	345	-
$V(Bzac-p^{OCH_3}-BH)_2$	667.62	667	375	-
$V(Bzac-p^{Cl}-BH)_2$	676.45	676, 680	379, 381	363, 365
$V(Bzac-p^{NO_2}-BH)_2$	697.61	697	390	-
$V(dbm-BH)_2$	731.71	731	407	391
$V(HNP-BH)_2$	627.56	627	355	339
$V(HNP-p^{Cl}-BH)_2$	696.44	696, 700	389, 391	-
$V(HAP-BH)_2$	555.49	555	319	303
$V(HAP-p^{Cl}-BH)_2$	624.38	624, 628	353, 355	337, 339
$V(HPP-BH)_2$	583.54	583	333	317
$V(DHBP-BH)_2$	711.63	711	397	381
$V(Sal-BH)_2$	527.43	527	305	289
$V(acac-SalH)_2$	515.42	515	299	283
$V(Bzac-SalH)_2$	639.56	639	361	354
$V(dbm-SalH)_2$	763.71	763	423	407
$V(HNP-SalH)_2$	659.55	659	371	355

COMPLEX (1)	MOL. WT. (2)	VL$_2$ (3)	VOL (4)	VL (5)
V(HAP-SalH)$_2$	587.49	587	335	319
V(HPP-SalH)$_2$	615.54	615	349	333
V(Sal-SalH)$_2$	559.43	559	321	305
V(Bzac-OAP)$_2$	553.51	553	318	302
V(dbm-OAP)$_2$	677.65	677	380	364
V(HNP-OAP)$_2$	573.50	573	328	312
V(HNP-p^{CH_3}-OAP)$_2$	601.56	601	342	326
V(HNP-p^{Cl}-OAP)$_2$	642.39	642, 646	362, 364	-
V(HAP-OAP)$_2$	501.44	501	292	276
V(Sal-OAP)$_2$	473.38	473	278	262
V(Sal-p^{CH_3}-OAP)$_2$	501.44	501	292	276
V(Sal-p^{Cl}-OAP)$_2$	542.27	542, 546	312, 314	296, 298
V(HNP-3-am-2-nap)$_2$	673.62	673	378	362
V(Sal-3-am-2-nap)$_2$	573.50	573	328	312
V(OAP-β-nap)$_2$	575.48	575	329	313
V(p^{CH_3}-OAP-β-nap)$_2$	603.53	603	343	327
V(p^{Cl}-OAP-β-nap)$_2$	644.37	643, 647	363, 365	347, 349
V(OAP-p-cresol)$_2$	503.41	503	293	277
V(OAP-p^{OCH_3}-phenol)$_2$	535.41	535	309	293
V(OAP-p^{Cl}-phenol)$_2$	544.25	544, 548	313, 315	297, 299
V(3-am-2-nap-β-nap)$_2$	675.60	675	379	363
V(Erio T)$_2$	969.68	970	-	-

TABLE 3.7.1.2: CHARACTERIC MASS SPECTRAL PEAKS FOR THE VLL'
MIXED LIGAND COMPLEXES

COMPLEX	MOL. WT.	CHARACTERISTIC PEAKS FOR				
		VLL'	VL_2	VL'_2	VOL	VOL'
V(HNP-BH)(Bzac-BH)	617.56	617	627	607	355	345
V(HAP-BH)(Bzac-BH)	581.53	581	555	607	319	345
V(HAP-BH)(HNP-BH)	591.52	591	555	627	319	355
V(HAP-BH)(Bzac-SalH)	597.53	597	555	-	319	361
V(HNP-BH)(OAP-β-nap)	601.52	601	627	575	355	329

neutral VO(IV) complex, VOL is generally intense and is in agreement with the rupture of the ligand C - O group to leave an oxo group which with the V^{4+} forms the stable VO entity. The variable, generally weak, intensity of the VL fragment must result from a different fragmentation pattern. Such VOL and VL peaks are also observed for the $V^{IV}OL\underline{H}Cl$, $V^VOL.OR$ and $(V^VOL)_2O$ complexes.

For the mixed ligand VLL' complexes, the peaks due to VL_2 and VL'_2 are also observed along with the major VLL' peak. These observations are consistent with a rearrangement due to the pyrolysis of the complex occurring in the mass spectrometer, as the X-ray crystallographic analysis and other spectroscopic and electrochemical techniques revealed only one species. Both VOL and VOL' fragments were observed in all the mixed VLL' complexes. In complexes of the chlorine containing ligands, the observation of the signals due to Cl isotopes is conclusive evidence for VOL and VL fragmentations.

3.7.2 INFRARED SPECTRA

(a) CHARACTERISTIC BAND ASSIGNMENTS: GENERAL

The infrared spectra of the VL_2 complexes have provided information about their formations and structures mainly in respect of (i) absence of the vanadyl oxo function, (ii) conversion of ketonic C = O to enolic C - O on complexation, where appropriate, (iii) absence of N - H and/or OH functions and (iv) on the whole, the presence and coordination of the ligand in the form of L^{2-} in the complexes. The absence of peaks corresponding to V = O and N - H groups (νN-H for hydrazones only) are the most important observations. Comparison of the VL_2 spectra with those obtained for the ligands themselves was most useful in rationalizing the infrared results. All VL_2 complexes were examined between 4000 and 200 cm^{-1} and were found to show absence of the vanadyl oxo ligand, thus indicating them to be the non-oxo vanadium(IV) complexes. Also the VL_2 spectra are comparable to those of the coordinated parent ligands. This information proved the formation of the non-vanadyl complexes incorporating the corresponding ligands. The tentative assignments listed in Tables 3.7.2.1 to 3.7.2.5 of the characteristic infrared peaks of the VL_2 complexes have been made empirically by comparison of the spectra of the corresponding ligand, the VO(AA)$_2$ complexes and by reference to the literature on the spectra of related complexes[241-270].

The ligands formed from β-diketones and amines may be in one of the tautomeric forms I, II and III.
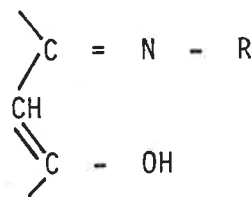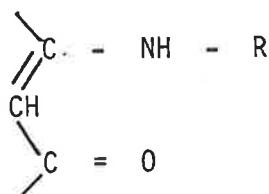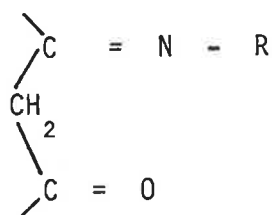
(I) Keto-imine form   (II) Keto-amine form   (III) Enol-imine form

Chromwell et al.[242] and Holtzclaw et al.[243] favoured keto-amine form (II) on the infrared studies of β-amino-substituted-α,β-unsaturated ketones and α,β-

unsaturated-β-keto-amines respectively. Martell et al.[244-246] discussed the infrared spectra of Schiff bases derived from diamines on the basis of an equilibrium between (II) and (III). Dudek and Holm[246a] on the basis of N.M.R. study of bis-(acetylacetone)ethylenediamine and of Schiff bases obtained from monoamines and acetylacetone or 1-hydroxy-2-napthone showed the keto-amine form to be more important in the equilibrium between (II) and (III). However, the bases derived from 2-hydroxy-1-napthaldehyde (or napthone) and salicyl-aldehyde have the obvious phenol-imine form as expected from resonance considerations.

The νOH, νN-H, νC = O, νC = N, νC - O, νC = C, νC - N, νV - O and νV - N stretching modes which are found in the ligands and their complexes in this work have been identified by many authors[247,248]. With few exceptions[249], it is a general observation that the behaviour of the free ligand spectrum changes by chelation[243-245] but the interpretation of the band-shifts depends on the attribution of the observed frequencies to the various bonds C = C, C = O, C = N. The C = N vibration frequency is the most important in Schiff bases with the azomethine group and is generally lowered by chelation by an amount depending on the nature of the metal, especially its electron-attracting properties.

All the Schiff base ligands contain the νC = N modes. The peaks between 1580 and 1670 cm^{-1} have been assigned by Bacon and Lindsay[250] as νC = N. Strattan and Busch[251] also have described the location of C = N band in the same region in several ligands containing C = N groups. ^{15}N and ^{18}O isotope substitution have been used by Percy et al.[241,252,253] to identify the N and O sensitive vibrations in N-alkyl and N-arylsalicylaldimine and salicyledenegly-cinate complexes. On the basis of these studies, the bands in the regions 1575-1634, 1540-1609, 1300-1342 and 1370-1410 cm^{-1} are assigned as due to νC = N, aromatic νC = C, νC - O and νC - N respectively. They also assigned the νC = N - C band at 780-895 cm^{-1}. Also the bands observed in the region 1390-1460 cm-1 have been assigned to variously coupled vibrations involving

δC-H with νC = N, νC - N, νC = O and νC - O. The band which appears in the region 1550-1615 cm^{-1} for the metal complexes is assigned to νC = O. The carbonyl stretching vibration sometimes masks the phenyl vibration normally found near 1600 cm^{-1}. Generally, the C = O frequency lies in the same range as for C = N. Earlier assignments of νC = O and νC = C in β-diketonates by normal coordinate studies[51,52] have been reversed by a further analysis[121] and by ^{18}O-labelling[120] of the carbonyl oxygen atom (cf. Chapter 2.6). The higher frequency peak is sensitive to isotopic substitution of the oxygen atom and is therefore assigned to νC = O. Also Pickard and Polly[254] on the basis of the infrared spectra of a number of ketimines assigned the higher frequency band (1660-1720 cm^{-1}) to νC = O and the lower frequency band (1590-1680 cm^{-1}) to νC = N. Teyssie and Charette[255] from the infrared spectra of a number of salicylidene-alkylamine chelates with various metals (Co, Ni, Cu, Zn, Mn, Pd) reported that the aromatic C = C vibration at 1585 cm^{-1} for the ligand goes down at 1540 cm^{-1} on chelation and remains about independent of the nature of the metal. Dudek and Dudek[256] have assigned a band near 1400 cm^{-1} to νC - N for copper(II)-Schiff base complexes, whereas Bigotto et al.[257] have assigned a band at 1441 cm^{-1} to this vibration for a tetradentate nickel(II)-Schiff base complex.

The normal position of a free OH band is at 3520-3730 cm^{-1} [258] and the broadening and shifting of this band from this normal position indicates involvement of the OH group in hydrogen bonding. The broader bands in the region 3150-3300 cm^{-1} [254] are assigned as due to the N-H stretching mode present in the free ligands. The broad band centred around 3200 cm^{-1} could also be due to overlapping of νN - H and νO - H modes. The absence of these bands in the metal complexes indicates coordination of the phenolic and enolic oxygens on deprotonation.

The above νC = N, νC = C, νC - N, etc. assignments have been considered in making assignments of various infrared bands in the present complexes and are discussed below for the three ligand systems examined in this work.

TABLE 3.7.2.1: SOME CHARACTERISTIC INFRARED FREQUENCIES (CM^{-1}) FOR THE VL_2 COMPLEXES OF BENZOYLHYDRAZONES

VL_2 COMPLEXES OF L =	TENTATIVE ASSIGNMENTS						
	$\nu C = N$	$\nu C = C$	$\nu C - O$	$\nu C - N$[a]	$\delta C - H$[b]	$\nu V - O$	$\nu V - N$
acac-BH	1590 w	1542 s	1325 m	1370 s	1447 s	438 m	495 ms
Bzac-BH	1590 w	1540 s	1332 m	1365 m	1436 msh	457 w	492 w) 560 m)
Bzac-p^{OMe}-BH	1612 s) 1590 m)	1540 s	1336 m	1365 s	1435) m 1420)	470 w	520 w) 557 m)
Bzac-p^{Cl}-BH	1603 w) 1587 m)	1542 s	1328 ms	1370 s	1407 ms	470 w	503 m
Bzac-p^{NO_2}-BH	1600 w) 1586 sh)	1545 s	1325 ms	1345 s	1410 w	467 w	570 m
dbm-BH	1606 w) 1590 w)	1543 s	1335 ms	1370 s	1450 s) 1433 msh)	452 w	548 m
HNP-BH	1616 wsh) 1598 s) 1573 s)	1544 s	1325 s	1357 m	1445 s	452 w	503 ms
HNP-p^{Cl}-BH	1619 msh) 1604 s) 1590 m) 1574 m)	1545 s	1333 s	1354 m	1403 s) 1426 m)	480 w	507 m) 540 m)
HAP-BH	1600 s 1590 msh 1565 s	1543 s	1320 s	1355 s	1445 s) 1418 ms)	439 ms	492 ms
HAP-p^{Cl}-BH	1602 s 1585 s 1568 s	1542 s	1320 s	1365 s	1420 ms	438 s	522 m
HPP-BH	1600 s) 1588 msh) 1562 s)	1536 s	1320 s	1360 s	1422 s	439 m	518 m
DHBP-BH	1605 s) 1590 sh) 1570 w)	1538 ms	1320 w	1365 ms	1447 s) 1418 sh)	460 w	512 w
Sal-BH	1605) 1590) s 1580)	1545 s	1305 m	1340 s	1445 s	455 m	570 m

a. Due to resonance

b. Coupled with $\nu C = N$, $\nu C - O$, $\nu C - N$.

(b) VL$_2$ COMPLEXES OF BENZOYLHYDRAZONE LIGANDS

The broad bands obtained in the range 3150-3365 cm^{-1} for the benzoylhydrazone Schiff bases are attributed to νN - H. In dbm-BHH$_2$ the bands at 3075 and 3464 cm^{-1} were medium sharp. Pickard and Polly[254] reported the N - H frequencies near 3200 cm^{-1} for a number of ketimines. Association of the N - H group with ketonic groups gives absorptions in the range 3240-3320 cm^{-1} and with an adjacent N atom within the range 3150-3300 cm^{-1}[259]. The β-diketone-hydrazone ligands seem to exist in the keto-form and do not show enolic OH bands. In o-hydroxycarbonyl-hydrazones there is no band above 3275 cm^{-1} due to the free OH group thus showing it to be hydrogen bonded with the azomethine nitrogen[258]. The broad band around 3200 cm^{-1} in both cases might be a mixture of νN - H and H-bonded enolic/phenolic OH stretches.

Generally, two bands are obtained between 1600 and 1694 cm^{-1} for the free ligands which are due to νC = O (higher frequency band) and νC = N of the azomethine group (lower frequency band). The νC = N mode is often mixed with νC = C in the range 1600-1630 cm^{-1} and is seen as a strong band. The spectra of the VL$_2$ complexes show no characteristic bands of νN - H and νC = O in agreement with the ligands being coordinated in the enolic form. This mode of coordination is further supported in each case by the appearance of the νC = N band at about 1590 cm^{-1}. The νC = N present in the free ligand shows a downward shift of 10-40 cm^{-1} indicating the involvement of the nitrogen of the azomethine group in the coordination[260]. The band appearing around 1600 cm^{-1} seems to originate from the stretching mode of the conjugate >C=N-N=C< grouping[46] suggesting the participation of the enolic oxygen in coordination. Also, the disappearance of all bands above 3000 cm^{-1} confirms the participation of the enolic/phenolic oxygen in coordination on deprotonation.

(c) VL$_2$ COMPLEXES OF SALICYLOYLHYDRAZONE LIGANDS

In the free salicyloylhydrazone ligands, generally two bands are observed in the region 3030-3300 cm^{-1}. Like in dbm-BHH$_2$, bands in dbm-SalH2 at 3060

and 3847 cm^{-1} are also medium sharp. One of the two bands above 3000 cm^{-1} might be due to the hydrogen bonded (as stated before) OH group, the other being due to νN - H, free or H-bonded. The higher and the lower frequency bands appearing between 1600 and 1665 cm^{-1} are due to νC = 0 and νC = N respectively. The infrared spectra of the SalH Schiff bases are dominated by the C = 0 and N - H absorptions which are absent in their VL$_2$ complexes. As in benzoylhydrazone-complexes, the disappearance of νN - H, νOH, νC = 0 and the shift of νC = N to lower frequency ($\sim$ 1596 cm^{-1}) on complexation indicate that the attached ligands act as dinegative tridentate ones in the enolic form involving coordination through two enolic/phenolic oxygens (on deprotonation) and the azomethine nitrogen. In the VL$_2$ complexes, the bands due to the non-coordinated 2-OH group of the SalH ring are not observed which suggests strong H-bonding of this OH with the non-coordinated N of the ligand as found in the X-ray analysis. The νC = N, νC = C, νC - 0, νC - N, νV - 0, νV - N, etc. band assignments in these complexes (Table 3.7.2.2) have been made similarly as for the benzoylhydrazone-complexes and these bands are exhibited at about the same positions for both these complex types.

(d)   VL$_2$ COMPLEXES OF o-AMINOPHENOL AND RELATED SCHIFF BASE COMPLEXES

o-Aminophenol Schiff bases of benzoylacetone and dibenzoylmethane have single broad absorptions at 3060 and 3160 cm^{-1} respectively. HAP-OAPH$_2$ has a broad absorption at 3350 cm^{-1} and a weak broad absorption at 3055 cm^{-1}. Others show generally weak and broad absorptions at about 3050 cm^{-1}. This seems to be due to a strongly hydrogen bonded N - H stretching mode which originates from the H-bonding between the azomethine N and the OH groups. In most cases, there are also weak broad absorptions at 2630-2735 cm^{-1}. This confirms that the OH is H-bonded to the N atom of the azomethine group. The absence of the above bands in the complexes indicates deprotonation of both the replaceable H atoms and the dibasic character of the Schiff bases leading to the involvement of both the enolic and/or phenolic oxygen atoms in the

TABLE 3.7.2.2: SOME CHARACTERISTIC INFRARED FREQUENCES (CM^{-1}) FOR THE VL$_2$ COMPLEXES OF SALICYLOYLHYDRAZONES

T E N T A T I V E   A S S I G N M E N T S

VL$_2$ COMPEXES OF L=	$\nu C = N$	$\nu C = C$	$\nu C - O$	$\nu C - N$	$\delta C - H$	$\nu V - O$	$\nu V - N$
acac-SalH	1625 s) 1590 s)	1540 s	1330) s 1320)	1370 s	1435) s 1420)	420 w) 486 s)	502 m) 560 w)
Bzac-SalH	1626 m) 1592 m)	1538 s	1333 s	1400 w	1420 msh	425 w) 477 m)	492 m) 560 m)
dbm-SalH	1625 ms) 1600 sh) 1590 ms)	1545 s	1340 s	1368 s	1435 msh	448 w) 476 m)	508 w) 552 m)
HNP-SalH	1623 ms) 1597 s) 1570 ms)	1540 s	1330 s	1360 msh	1420 sh	420 sh) 486 w)	504 w) 562 m)
HAP-SalH	1625 m) 1596 m) 1570 m)	1532 s	1310 s	1365 s	1420 msh	430 w) 465 m)	520 w) 553 w)
HPP-SalH	1625 ms) 1603 ms) 1566 ms)	1535 s	1308 ms	1358 msh	1425 msh	426 w) 465 m)	488 m) 510 w)
Sal-SalH	1625 s 1600) s 1587)	1542 s	1312 m	1347 s	1435 m	445 ms	567 m

coordination.

The strong bands at 1600-1635 cm^{-1} in the ligands are assigned as $\nu C = N$ and aromatic $\nu C = C$ modes which shift downwards to about 1597 and around 1540 cm^{-1} respectively on complexation. The bands at 1616 cm^{-1} for the HNP-p^X-OAP-complexes, 1620 cm^{-1} for the complexes of Schiff bases of 3-amino-2-napthol with 2-hydroxy-1-napthaldehyde and salicylaldehyde as well as absorptions around 1570 cm^{-1} observed for all these VL$_2$ complexes are also assigned as due to the $\nu C = N$ and its coupling or possible conjugation with the neighbouring $C = C$ and $C - N$ modes. The downard shift of the $\nu C = N$ indicates normal coordination of the azomethine nitrogen to the metal atom. The $N \rightarrow V$ σ-bond as well as any possible $V \leftarrow N$ π-electron interaction in the metal chelate rings lower the vibrational frequency of the $C = N$ group. The generally strong bands appearing in the region 780-872 cm^{-1} are assigned to $\nu C = N$ - C[241,252,253]. The bands due to $\delta C - H$, $\nu V - O$ and $\nu V - N$ have been determined empirically by reference to the literatures mentioned in Section (a) and are listed in Table 3.7.2.3.

(e)   VL$_2$ COMPLEXES OF 2,2'-DIHYDROXYAZOARENES

In azodyes and their metal complexes, the $\nu N = N$ lies in the range 1440-1650 cm^{-1} [261]. Appearance of several bands in this region renders the assignment of an $N = N$ stretching vibration difficult. The azomethane complex of Pd shows absorption at 1598 cm^{-1} assigned as $\nu N = N$[262]. Using isotopic labelling with ^{15}N and ^{2}H of some aryldiazo ligands, Hyamore et al.[263] elucidated the origin of the multiple infrared bands of their metal complexes in the 1400-1630 cm^{-1} region which are associated with the $N = N$ stretching modes. For some complexes, they observed and assigned two bands for $\nu N = N$ in the region 1506-1624 cm^{-1}, their exact position being dependent on the resonance interaction of this $\nu N = N$ with other vibrational modes, especially of the phenyl groups.

TABLE 3.7.2.3: SOME CHARACTERISTIC INFRARED FREQUENCIES (CM^{-1}) FOR THE VL_2 COMPLEXES OF o-AMINOPHENOL (AND 3-AMINO-2-NAPTHOL) SCHIFF BASES

TENTATIVE ASSIGNMENTS

VL_2 COMPLEXES OF L=	νC=N	νC=C	νC-O	νC-N	δC-H	δC=N-C	νV-O	νV-N
Bzac-OAP	1600 m) 1577 m)	1552 s	1343 s	1370 m	1416 ms	825 s) 780 s)	458 w 474 m	564) 578)m
dbm-OAP	1605 ssh) 1598 s) 1585 ssh)	1560 s	1325 m	1405 sh	1436 msh	847 w) 810 w)	455 w	565 w
HNP-OAP	1616 m) 1598 s) 1570 ms)	1540) 1534)s	1340 m	1405) 1423)w	1440 s	820 ms) 842 m)	420 msh) 465 w)	500 m) 570 w)
HNP-p^Me-OAP	1616 m) 1597 s) 1570 m)	1533 s	1337 s	1405 w	1450 s	805 s) 830 s)	429 m) 470 w)	506 ms) 571 s)
HNP-p^Cl-OAP	1616 m) 1598 s) 1570 m)	1533 s	1336 s	1405)w 1420)	1450 s	805 m) 825 s) 842 m)	448 w 470 w	505 m) 565 s)
HAP-OAP	1597 s) 1577 m)	1540 m	1330 sh	1405 sh	1438 msh	818 m) 858 m)	430 ms) 467 ms)	510 w) 554 m)
Sal-OAP	1602 s) 1584 ssh) 1565 ms)	1535 s	1325 s) 1300 s)	1410 sh	1436 m	840 s) 872 w)	435 sh) 480 w)	532 m) 552 s)
Sal-p^Me-OAP	1600 s) 1585 ssh) 1565 ms)	1534 s	1305 s	1400 sh	1433 ms	805 s 843 s	440 w) 472 w)	509 w) 552 s)
Sal-p^Cl-OAP	1597 s) 1585 ssh) 1565 ms)	1528 s	1300 s	1410 msh	1425 ms	805 ms) 838 s)	450 w) 470 w)	542 s) 570 m)
HNP-3-am-2-nap	1620 m) 1598 ms) 1574 m)	1535 s	1300 m	1405 w	1425 w	820 ms) 853 s)	454 w) 470 w)	512 m) 582 m)
Sal-3-am-2-nap	1620 ms) 1604 s) 1583 s)	1536 s	1300 m	1390 msh	1430 m	813 m) 852 ms)	464 w	500 w) 563 m)

TABLE 3.7.2.4: SOME CHARACTERISTIC INFRARED FREQUENCIES (CM^{-1}) FOR THE VL_2 COMPLEXES OF 2,2'-DIHYDROXYAZOARENES

TENTATIVE ASSIGNMENTS

VL_2 COMPLEXES OF L =	$\nu N = N$	$\nu C = C$	$\nu C - O$	$\nu C - N$	$\nu V - O$	$\nu V - N$
OAP-β-nap	1617 sh 1597 msh 1584 m	1550 m	1325 s	1405 sh 1355 s	440 w) 465 w)	507 m) 545 w)
p^{Me}-OAP-β-nap	1616 sh) 1596 m/w) ─ 1577 m/w)	1550 m/w	1320 w 1287 s	1420 w 1353 s	435 w) 460 w)	505 ms) 570 ms)
p^{Cl}-OAP-β-nap	1615 w 1597 m 1578 w	1550 m/w	1311 w 1274 s	1420 w 1352 s	436 wsh) 463 w)	508 ms) 563 ms)
OAP-p-cresol	1604 w/m) 1592 m) 1580 sh)	1535 m	1325 m 1288 s	1420 w 1355 sh	435 w) 455 w)	518 sh) 534 m)
OAP-p^{OMe}-phenol	1616) 1603)m 1590)	1540 m	1326 m/w	1360 msh	446 w	502 w 552 m
OAP-p^{Cl}-phenol	1605) 1592)ms	1540 m/w	1325 w	1360 sh	465 w	500 w) 550 w)
3-am-2-nap-β-nap	1620 ms 1597 ms	1550 m	1323 sh	1358 s	455 w 470 w	513 sh) 540 m)
Erio T	1620 m) 1597 m) 1570 w/m)	1552 m	1334) 1340)s	1425 wsh	414 msh) 455 w)	550 w) 580 w)

For both p^{Me}-OAP-β-napthol and Erio T dyes, a very broad as well as a very weak broad band appear at 3450 and 2730 cm^{-1} respectively. For other azo dyes, weak or medium broad bands are observed at 3060-3100 cm^{-1} along with very weak broad absorptions at 2700-2733 cm^{-1}. These bands are assigned respectively to the strong H-bonded N - H and O - H resulting from -O-H....N hydrogen bonding. Infrared spectral data for the VL_2 complexes of 2,2'-

dihydroxyazoarenes are given in Table 2.7.2.4 together with tentative band assignments for the observed fundamental vibrations associated with N = N, C = C, C - O, C - N, V - O and V - N bonds. As expected, the doubly deprotonated ligand complexes do not exhibit any νOH or νN - H vibrations indicating coordination of the phenolic and/or enolic oxygens to the metal.

Generally, two bands appearing in the range 1600-1630 cm^{-1} in the free ligand are assigned to the νN = N which shift to the lower energy region 1597-1620 cm^{-1} on complexation which indicates coordination of one of the diazo nitrogen to vanadium. As in the previous VL$_2$ complexes, the bands in the region 1540-1552 cm^{-1} are assigned to C = C stretching vibration of the phenyl groups. The νC - N bands have been located at 1352-1420 cm^{-1}.

(f)   THE MIXED-LIGAND VLL' COMPLEXES

As for the VL$_2$ complexes, the band assignments as listed in Table 3.7.2.5 for the mixed-ligand VLL' complexes have also been made mainly by reference to

TABLE 3.7.2.5:   SOME CHARACTERISTIC INFRARED FREQUENCIES (CM^{-1}) FOR THE MIXED LIGAND VLL' COMPLEXES

| COMPLEX | T E N T A T I V E   A S S I G N M E N T S |
	νC = N	νC = C	νC - O	νC - N	δC - H	νV - O	νV - N
V(HNP-BH)(Bzac-BH)	1616 wsh) 1598 m) 1590 w) 1575 m)	1543 s	1325) 1333) ms	1353 msh	1420) wsh 1425)	452 wsh) 480 w)	500 w) 528 w) 562 m)
V(HAP-BH)(Bzac-BH)	1602)w/m 1590)	1544 s	1320 w) 1332 m)	1360 ssh	1420 wsh	456 w) 490 w)	515 w) 532 w) 555 w)
V(HAP-BH)(HNP-BH)	1600 ms) 1590 msh) 1570 ms)	1545 s	1324 s	1358 ms	1420 wsh	425 w) 480 w) 501 w)	530 w) 540 w) 563 w)
(HAP-BH))Bzac-SalH)	1625 m) 1603) m 1590) m) 1578 msh)	1535) s 1542)	1305) 1320) w 1335 m	1360 ms	1420 wsh	427 w) 454 w) 475 w) 499 w)	518 w) 556 w)
(HNP-BH)(OAP-β-nap)	1617 wsh) 1598 m) 1590 msh) 1574 m)	1545 s	1322 ms	1352 ms	1410 sh	460 w 480 w	506 m) 570 m)

the literature [Section (a) above] of the related systems. A comparison of the various stretching vibrations of these VLL' complexes with those of the VL_2 and VL'_2 complexes shows that the VLL' complexes exhibit most of the characteristic modes at about the same frequencies as observed in both the individual VL_2 anx VL'_2 complexes. This indicates presence of the component L and L' ligands in these complexes in the deprotonated form as well as the coordinations of the two phenolic and/or enolic oxygens and one azomethine or diazo nitrogen to the vanadium atom.

(g)   V - DONOR ATOM VIBRATIONS

Very little work has been published on the metal-oxygen and metal-nitrogen stretching vibrations for Schiff base complexes in the far infrared region[258]. Some tautomeric assignments have been made on an empirical basis[264] for quadridentate Schiff base complexes. Percy et al.[241,252,253] have made some assignments of $\nu M - O$ and $\nu M - N$ modes in some Schiff base complexes using ^{18}O and/or ^{15}N isotope data. Nakamoto[265] used metal isotope substitution to identify the metal-ligand modes. Bigotto et al.[257] using normal coordinate analysis have assigned $\nu M - O$ and $\nu M - N$ modes for N,N'-ethylenebis(acetylacetoneimine)metal(II) (M = Co, Ni). From these works the regions of $\nu M - N$ and $\nu M - O$ modes may be approximated at 415-580 and 300-530 cm^{-1} respectively. From the infrared studies on various O, N donor Schiff base complexes of oxovanadium(IV)[10,40,46,266-270], the broad regions that may be assumed for the $\nu V - O$ and $\nu V - N$ modes are 420-470 and 470-580 cm^{-1} respectively which seem reasonable on the basis of the above M - O and M - N band regions with other metal complexes of related systems.

The present $\nu V - O$ and $\nu V - N$ assignments (Tables 3.7.2.1-3.7.2.5) are less definitive and tentative. The presence of very few bands in this region was an advantage for attempts of the present assignments. Although the high frequency band is usually taken to be due to M - N and low frequency band due to M - O contributions, the quite larger M - N distances than the M - O distances in the VL_2 complexes suggest the reverse order.

3.7.3. ELECTRONIC SPECTRA

(a)   INTRODUCTION

The d^1-vanadium(IV) complexes, depending on the ligand type as well as their mode of coordination, may show electronic spectra arising from (i) intraligand transitions and (ii) d-d and/or charge transfer transition. The charge transfer bands in the visible and near UV region are characterized by the intense colour of the complexes due to the observed high intensity and position of such bands[271-273]. For the VO^{2+}-complexes, the d-d transitions are associated with the low intensity bands in the 500-800 nm region showing molar absorptivity in the range 10-100 mol dm^{-3} cm^{-1} [4]. Because of their low intensity, the d-d bands in complexes showing intense charge transfer spectra are not identifiable since they are masked by the much stronger absorption bands (^{a}M = 10^3 - 10^4).

Spectra of LMCT (ligand to metal charge transfer) type are mainly found in complexes in which the metal has a high oxidation state, often with few d electrons and the ligands carry a negative charge. Generally the metal is in an oxidizing state.

(b)   LMCT IN RELATED COMPLEXES

Further supporting evidence for the assignment of LMCT bands in the visible and near UV region may be obtained by comparison with the electronic absorptions of some d^o-systems in this region. The analogous Ti(IV) complexes with the identical ligands, e.g. Ti(acac-BH)$_2$ (this is octahedral[99] in contrast to generally trigonal prismatic VL$_2$) show intense absorptions in the visible region although at a shorter λ_{max} because of the lower electron acceptance of Ti^{4+}. Also for various TiX$_4$ Diars, Clark et al.[54,274] reported absorption peaks in the region 510-457 nm with the extinction coefficients ($\sim$ 3000-4100) corresponding to the C.T. transitions. Kyker and Schram[275] reported an empirical correlation between the lowest energy C.T. band and the coordination number (C.N.) of the metal. According to them the position of the C.T. band shifts progressively to lower energy as the C.N. of the metal is

increased. To illustrate this, they cited some Ti(III) and Ti(IV) complexes containing Cl and N ligands where the first C.T. band appears at $\gtrsim$ 35 kK for C.N. 4, ~ 25-34 kK for C.N. 5 and ~ 19-24 kK for C.N. 6. This empirical correlation, however, does not hold good for many vanadium(IV), especially oxovanadium(IV), complexes[4,54,56,276].

In VO^{2+}-complexes the d-d bands are clearly visible and mainly responsible for the colour of these complexes. These also show C.T. absorptions, however, these are in the ultra violet region or the edge of the visible and often mask band III[4] (see Chapter 2.7). The higher energy of these LMCT bands is due to π-donation from the oxo ligand reducing the acceptor ability of the vanadium centre. This is also clearly shown in the spectra of $Tl_2[VO(CH_3.C_6H_3O_2)_2]$[70]. The non-vanadyl vanadium(IV) complexes which were mentioned in Chapter 1.3 are all strongly coloured, obviously due to LMCT. However, the majority of these complexes contain donor atoms from the third period, e.g. $VCl_4.2Diars$[54], $V(S_2CNEt_2)_4$ [276] and VL_4Cl_2 [64]. As the coordinating atoms of the third period are better donors, the spectra of these complexes are not directly comparable to those of the VL_2 complexes containing O and N donors. The various $V(cat)_3^{2-}$ [cat^{2-} = $RC_6H_3O_2$ where R = H, 3-Me, 4-Me, 3-MeO] complexes show C.T. transitions extending through the visible region (11.2-19.0 kK)[70,71] which are worth comparing with the present VL_2 spectra. Like the VL_2 complexes, these catecholato complexes have similar intense colours in the solid and in solution.

Molybdenum, having a diagonal relationship with vanadium, forms many intensely coloured complexes in its +6 oxidation state (d^0) which show very intense LMCT transitions in the visible region with a_M of the order of 10^3-10^4 [277,278]. However, because of the difference in oxidation states of Mo and the presence of oxoligand on the molybdenum as well as the type of donor ligands (mostly S-donors), it is difficult to draw conclusions from comparison of such spectra with the VL_2 spectra.

(c)   SPECTRA OF THE VL$_2$ COMPLEXES

The intensely coloured d^1-VL$_2$ complexes with the vanadium in the high +4 oxidation state and containing dinegative tridentate ligands capable of σ- and π-donations present the right requirements which give rise to LMCT bands. These complexes exhibit three or four intense bands in their electronic spectra, the first of which appearing as a broad band in the visible region, and in some cases associated with a lower energy shoulder (Table 3.7.3.1), is designated as the first charge transfer band C.T. (1). This band shows molar absorptivities between 3500 and 15000 mol dm^{-3} cm^{-1} which are too high to be due to d-d transitions of the metal ion. The different LMCT and the intra-ligand transitions in these complexes have been assigned (see Table 3.7.3.1) by a qualitative comparison with the absorption peaks observed for the free ligand in CHCl$_3$. In these spectra the ligands are in the protonated form and would generally have λ$_{max}$ at longer wavelengths compared to the deprotonated form, especially in β-diketone-Schiff bases because of the delocalization in the diketonato ion. The colour of the azo dyes appears to be associated with an n → π* transition involving the lone pair on the nitrogen atom. Although such transitions are usually weak, the presence of the chromophore in a conjugated system greatly enhances the intensity of the absorption by mixing such transition with the allowed π → π* transition through vibrational borrowing[279,280]. In many of the complexes there is another band appearing above 350 nm which has been designated as the second charge transfer C.T. (2), although in many cases, especially with ligands which themselves show absorptions at longer wavelengths, this may be totally an intraligand band or a C.T. mixed with a π → π* intraligand transition. Such mixed bands have been suggested for other complexes[62]. The bands below 400 nm often resemble the ligand bands and are described as the intraligand transitions I.L.T. (1), I.L.T. (2) and I.L.T. (3). One cannot exclude the possibility that the lower energy I.L.T. (1) may have some C.T. contribution mixed with it. The I.L.T. (2) and occasionally the I.L.T. (3), depending on the ligands and being in the region ～ 325-260 nm, are purely due to π → π* intraligand transitions.

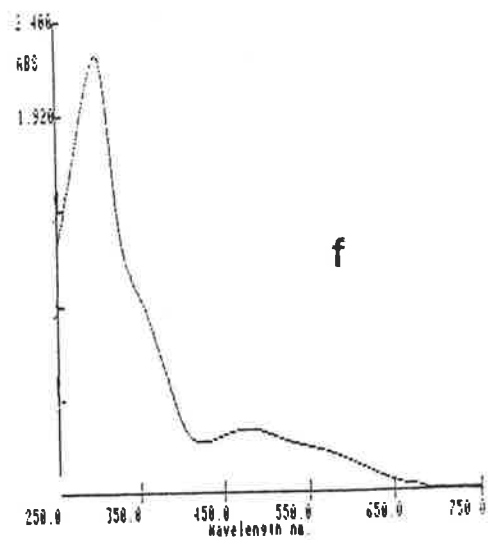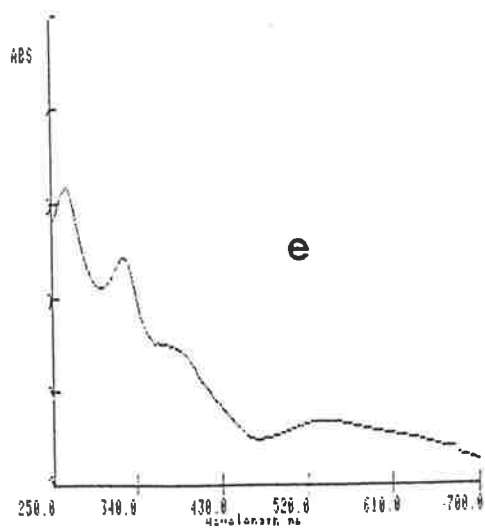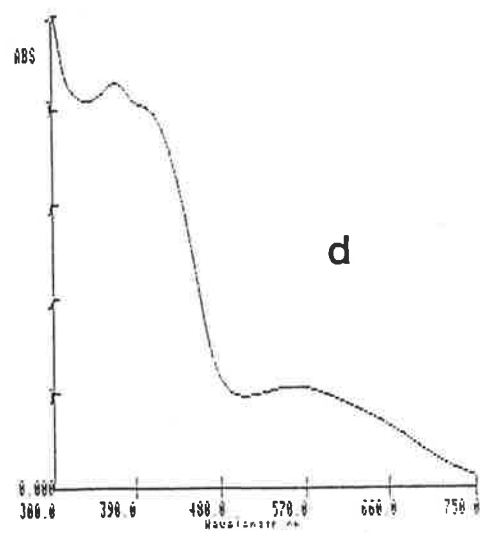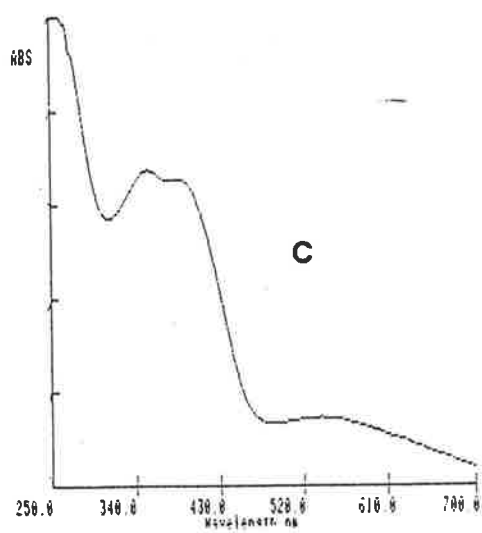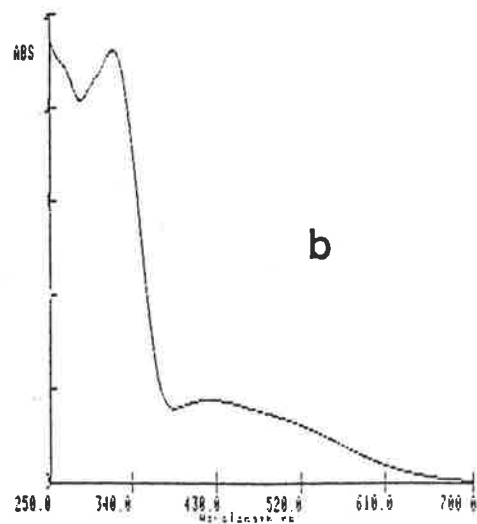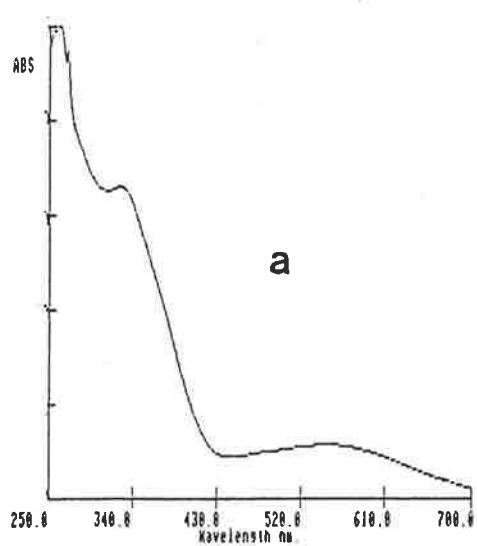**Figure 3.7.3.1:** Electronic spectra of a. V(acac-BH)$_2$; b. Ti(acac-BH)$_2$ for comparison; c. V(Bzac-BH)$_2$; d. V(dbm-BH)$_2$; e. V(HNP-BH)$_2$ and f. V(HAP-p^{Cl}-BH)$_2$ in dichloromethane.
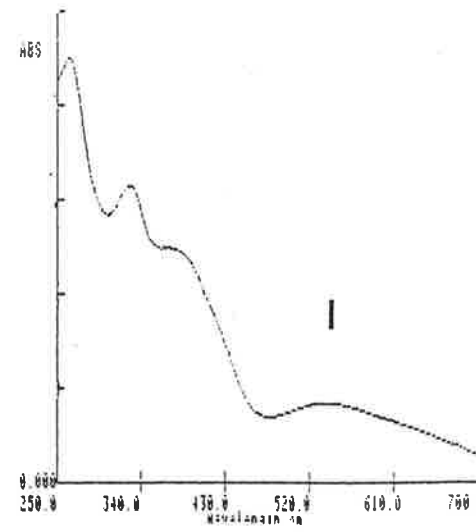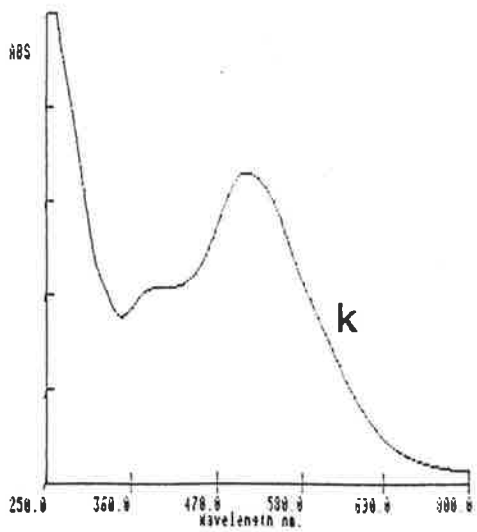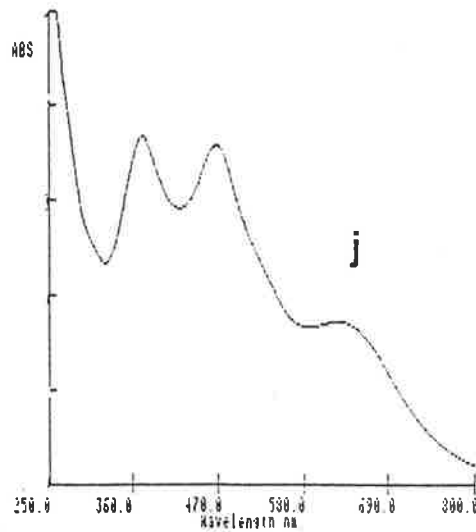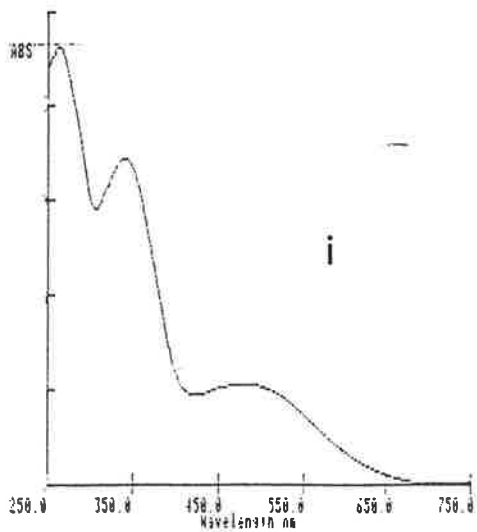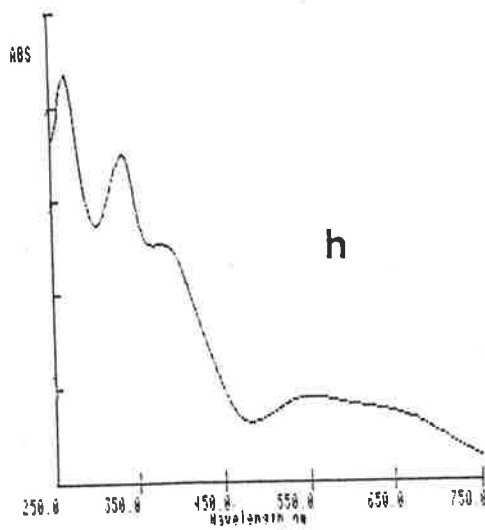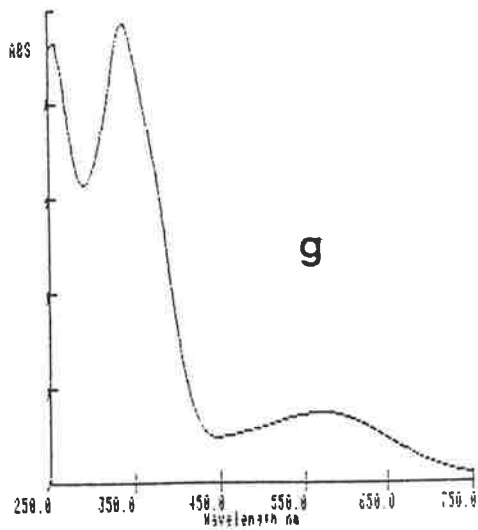
Figure 3.7.3.2: Electronic spectra of g. V(acac-SalH)$_2$; h. V(HNP-SalH)$_2$; i. V(HAP-OAP)$_2$, j. V(OAP-β-nap)$_2$; k. V(3-am-2-nap-β-nap)$_2$ and l. V(Bzac-BH)(HNP-BH) in dichloromethane.

Some of the VL_2 spectra are shown in Figures 3.7.3.1 and 3.7.3.2.

The β-diketone-Schiff base complexes, except that derived from acetylacetone, show two LMCT bands above 380 nm. Bands below 380 nm are assigned to intraligand transitions. As mentioned in Section 3.1.2(ii), the free ligand acac-BHH$_2$ could not be isolated and the band at 325 nm in its VL_2 complex is assigned to an intraligand transition by comparison to the other diketonato Schiff bases. In V(dbm-OAP)$_2$ the band at 382 nm is probably an intraligand transition corresponding to the free ligand absorption at 376 nm and not due to charge transfer. In the spectra of the complexes with HNP-containing Schiff bases only C.T. (1) can be assigned as pure charge transfer with any confidence. The second band often placed under C.T. (2) in Table 3.7.3.1 may be intraligand in character as the ligand itself has absorptions at wavelengths as high as 451 nm. The HAP-Schiff base complexes show only one LMCT band although V(HPP-SalH)$_2$ shows both C.T. (1) and C.T. (2). The Sal-Schiff base complexes also show only one LMCT band. The V(Sal-SalH)$_2$, however, shows a broad shoulder at ~ 380 nm assignable as C.T. (2).

For the p^X-OAP-β-nap dye complexes the first band appearing in the 622-632 nm region is assigned to a pure LMCT. The second band in the region 466-473 nm is comparable to the free ligand λ_{max}. This band, although shown as C.T. (2) in the Table, could be originating mostly from the ligand. In a number of cases, it appears to have shifted to lower wavelengths. This is not inconsistent with the availability of the electron pair on the nitrogen for an n → π* transition being lessened by coordination to the metal. For the OAP-p^X-Phenol dye complexes, only a shoulder is seen at ~ 590 nm and the second C.T. band mostly originates from the intraligand transition.

The spectra of the mixed ligand VLL' complexes are distinguishable from the spectra of VL_2 and VL'_2 and generally show only one LMCT band. The bands below 350 nm are assigned as due to intraligand transitions.

The variety of ligands used in the VL_2 preparations permit the comparison of the effect of the electron withdrawing capabilities of the ligands on the LMCT. Thus, the λmax values for the VL2 complexes with various ligand systems

and their p^X-substituents are observed to fall in the orders:

For the ligands:

(i)   HAP-BH < Sal-BH < Bzac-BH ~ HNP-BH < acac-BH < dbm-BH

(ii)   HAP-SalH ~ Sal-SalH < Bzac-SalH ~ HNP-SalH < dbm-SalH < acac-SalH

(iii) HAP-OAP < Sal-OAP ~ dbm-OAP ~ HNP-OAP < Bzac-OAP

For p^X-substituents:

For Bzac-p^X-BH: NO_2 < Cl ~ OMe ~ H

For HNP-p^X-BH   Cl ~ H

For HNP-p^X-OAP   Cl < H < Me

For OAP-p^X-Phenol   Cl ~ OMe ~ Me

However, the comparisons are difficult because the peak maxima are very flat, i.e. an appreciable range of λ is above log a_M = 3. This flat peak may signify the presence of more than one band, which on occasions are visible as shoulders (e.g. spectrum h in Figure 3.7.3.2). The sequences given above are qualitative and subjective obtained by superimiposing the spectra and estimating the relative position of the bulk of the absorption band. Even with this subjective assessment the results are disappointing in revealing poor correlation between the expected electron withdrawing nature of the ligand and the position of the maximum. However, certain generalizations can be made as follows:

(1)   That the tridentate ligands containing o-hydroxy aromatic carbonyl compounds, especially 2-hydroxyacetophenone produce λ_{max} at a shorter wavelength.

(2)   That the p-substituents in the ligands have a small effect in the expected direction. The more π-attracting groups (e.g. NO_2) should make the transfer of electron from the π-symmetry of the ligand to enable LMCT more difficult.

(3)   That the effect of BH and OAP compared on the same carbonyl compound is about the same.

TABLE 3.7.3.1: ELECTRONIC SPECTRAL DATA FOR THE VL_2

COMPLEXES (SOLVENT = CH_2Cl_2)

COMPLEX	Peak Positions (nm) with Log a_M in Parentheses[a,b]				
	C.T.(1)	C.T.(2)	I.L.T.(1)	I.L.T.(2)	I.L.T.(3)
β-Diketone Schiff Base Complexes:					
$V(acac-BH)_2$	555 (3.59)	-	325 (4.37)	262 (4.55)	-
$V(acac-SalH)_2$	568 (3.63)	-	334 (4.46)	-	-
$V(Bzac-BH)_2$	538 (3.75)	390 (4.40)	352 (4.42) [325]	-	-
$V(Bzac-p^{OMe}-BH)_2$	537 (3.79)	389 (4.50)	357 (4.49)	272 (4.60)	-
$V(Bzac-p^{Cl}-BH)_2$	536 (3.80)	380 fl. sh. (4.49)	354 (4.49) [325]	-	-
$V(Bzac-p^{NO_2}-BH)_2$	~ 517 (3.89)	414 (4.65)	-	258 (4.68)	-
$V(Bzac-SalH)_2$	552 (3.78)	389 (4.52)	356 (4.51) [320]	-	-
$V(Bzac-OAP)_2$	~ 580 fl. sh. (3.54)	382 (4.46)	305 (4.30) [346]	-	-
$V(dbm-BH)_2$	560 (3.83)	400 (4.41)	369 (4.44) [296]	-	-
$V(dbm-SalH)_2$	560 (3.82)	383 (4.47)	375 (4.47) [305]	261 (4.66)	-
$V(dbm-OAP)_2$	~ 500 sh	-	382 (4.45) [376]	262 (4.54) [257]	-
o-Hydroxy Carbonyl Schiff Base Complexes:					
$V(HNP-BH)_2$	540 (3.94)	-	~ 360 sh. [361]	325 (4.51) [324]	-
$V(HNP-pCl-BH)_2$	541 (4.08)	-	~ 374 fl. sh. (4.47)	327 (4.69)	267 (4.76)

COMPLEX	C.T.(1)	C.T.(2)	I.L.T.(1)	I.L.T.(2)	I.L.T.(3)
$V(HNP-SalH)_2$	~ 662 sh; 550 (3.99)	380 (4.45)	334 (4.59)	268 (4.69)	-
			[365 , 328 , 260]		
$V(HNP-OAP)_2$	~ 554 br. sh. (3.89)	395 (4.45)	~ 360 fl. sh. (4.44)	-	
			[445 , 388 , 323]		
$V(HNP-p^{Me}-OAP)_2$	~ 590 br. sh. (3.67)	409 (4.43)	~ 355 sh.	262 (4.50)	-
$V(HNP-p^{Cl}-OAP)_2$	~ 627 sh; ~ 536 sh. (3.89)	410 (4.44)	~ 355 sh.	262 (4.57)	-
$V(HNP-3-am-2-nap)_2$	573 (4.11)	415 (4.64)	~ 353 sh. [451,399,326]	~ 267 sh.	-
$V(HAP-BH)_2$	~ 561 br. sh. 477 (3.88)	-	~ 342 sh. [327]	293 (4.66) [281]	-
$V(HAP-p^{Cl}-BH)_2$	~ 565 br. sh. 477 (3.91)	-	~ 347 sh.	298 (4.75)	-
$V(HAP-SalH)_2$	~ 550 br. sh. 478 (3.90)	-	~ 342 sh. [332]	285 (4.67) [287]	-
$V(HAP-OAP)_2$	482 (3.87)	-	339 (4.38) [329]	262 (4.51) [257]	-
$V(HPP-SalH)_2$	~ 562 (3.73)	473 (3.86)	~ 350 sh. [333]	~ 320 sh. [289]	278 (4.61)
$V(Sal-BH)_2$	497 (3.83)	-	~ 347 sh. [320]	297 (4.69)	-
$V(Sal-SalH)_2$	~ 480 fl. sh. (3.71)	~ 380 sh.	~ 322 sh. [333]	282 (4.61) [289]	-
$V(Sal-OAP)_2$	~ 498 (3.80)	-	370 (4.41) [352]	[267]	-
$V(Sal-p^{Me}-OAP)_2^c$	~ 506 fl. sh. (3.74)	-	376 (4.42)	-	-
$V(Sal-p^{Cl}-OAP)_2$	~ 517 fl. sh. (3.63)	-	374 (4.30)	290 (4.35)	-
$V(Sal-3-am-2-nap)_2^c$	~ 568 fl. sh. (3.94)	395 (4.57)	332 (4.58)	271 (4.81)	-

COMPLEX	C.I.T.(1)	C.T.(2)	I.L.T.(1)	I.L.T.(2)	I.L.T.(3)
2,2'-Dihydroxyazoarene Dye Complexes:					
V(OAP-β-nap)$_2$	622 (4.13)	466 (4.45) [473]	371 (4.66) [309]	- [285]	-
V(p^{Me}-OAP-β-nap)$_2$	630 fl. sh. (4.01)	473 (4.42)	371 (4.36)	-	-
V(p^{Cl}-OAP-β-nap)$_2$	632 (4.10)	473 (4.46) [476]	374 (4.41) [308]	-	-
V(OAP-p-cresol)$_2$	~ 585 br. sh.	400 (4.42) [433]	332 (4.44) [328]	-	-
V(OAP-p^{OMe}-phenol)$_2$	~ 580 br. sh.	~ 440 fl. sh. (4.37) 400 (4.41)	329 (4.44)	-	-
V(OAP-p^{Cl}-phenol)$_2$	~ 595 br. sh.	435 fl. sh. (4.18) [437]	~ 380 sh. [325]	334 (4.27)	-
V(3-am-2-nap-β-nap)$_2$	504 (4.46)	402 fl. sh. (4.26) [487]	-	-	-
V(Erio T)$_2^c$	~ 665 fl. sh. (4.01)	484 (4.68) [503]	332 (4.67) [283]	263 (4.67)	-
Mixed Ligand VLL' Complexes:					
V(HNP-BH)(Bzac-BH)	538 (3.99)	-	~ 326 fl. sh. (4.57)	262 (4.72)	-
V(HAP-BH)(Bzac-BH)	~ 520 fl. sh. (3.85)	-	~ 343 br. (4.46)	264 (4.68)	-
V(HAP-BH)(HNP-BH)	530 (3.99)	~ 377 sh. (4.36)	~ 329 (4.58)	268 (4.72)	-
V(HAP-BH)(Bzac-SalH)	~ 520 fl. (3.83)	-	~ 342 br. sh. (4.45)	265 (4.65)	-
V(HNP-BH)(OAP-β-nap)	~ 580 fl. (4.12)	~ 420 fl. (4.30)	~ 340 fl. br. (4.48)	~ 330 (4.54)	262 sh. (4.71)

C.T.   = Charge transfer
I.L.T. = Intraligand transition
a. a_M in mol dm^{-3}cm^{-1}
b. Figures underlined in third brackets indicate λ_{max} for protonated ligands in CHCl$_3$
c. In DMSO.

(4)   The gross similarity of the electronic spectra of the VL_2 complexes indicates that the electronic structures are quite the same in all these complexes.

(d)   THE MOLECULAR ORBITAL CONSIDERATIONS

The electronic spectra of the VL_2 complexes can be explained in terms of the molecular orbitals arising from the component orbitals of the V^{4+} and the two dinegative tridentate ligands.   On the basis of the crystal structures determined so far and because of the strong similarity exhibited by all these complexes, a trigonal prismatic stereochemistry is assumed in the qualitative discussion of the molecular energy levels.   The spectra of the well studied[59,233,240,281-283] trigonal prismatic tris-dithiolato complexes serve as a useful model for this discussion inspite of the higher energy of the ligand orbitals and the different number and arrangement of the chelate rings.

In discussing the electronic spectra of the second- and third-row trigonal prismatic $M(S_2C_2Ph_2)_3$ complexes, H.B. Gray et al.[281] suggested a molecular orbital model in which the ordering of the energy levels of interest for the assignment of ground and low excited states is $4e' < 2a_2' < 3a_1' < 5e' < 4e''$ where, the symmetry representations in the D_{3h} point group for $a_1' = d_{z^2}$, $e' = d_{x^2-y^2}$, d_{xy} and $e'' = d_{xz}$, d_{yz}. These metal orbitals are considered to form molecular orbitals by overlapping with suitable symmetry adapted combinations of ligand orbitals. The metal e'' orbitals interact most strongly with the six σ-orbitals (sp^2 hybrids on S) adapted to e'' symmetry giving rise to a strongly bonding level $2e''$ localized predominantly on the ligand orbitals and a strongly antibonding level $4e''$ localized primarily on the metal (d_{xz}, d_{yz}) set.   The metal $a_1'(d_{z^2})$ orbital interacts moderately strongly with the six π_h orbitals (sp^2 hybrids on S) which are at 120° to the σ-orbitals adapted to a_1' symmetry giving rise to a bonding $2a_1'$ orbital mainly localized on the π_h ligand orbital and an antibonding $3a_1'$ orbital which is largely metal d_{z^2} in character.   These overlaps have both σ- and π-character.   Of the twelve π_v orbitals arising from four ligand π orbitals

situated perpendicular to the plane of each of the three chelate rings, the $3\pi_V$ is of comparable energy to the d orbitals. The metal e' orbitals interact strongly with e' symmetry orbitals of the $3\pi_V$ set and the 4e' and 5e' orbitals derived from this interaction are thoroughly delocalized over d_{xy}, d_{x2-y2} and $3\pi_V$. The other limiting formulation assigns 5e' as a (d_{xy}, d_{x2-y2}) level and considers 4e' as being derived from $3\pi_V$. The remaining $3\pi_V$ orbital transforming into $2a_2'$ is non-bonding and located at the same energy as the initial $3\pi_V$ orbital level. Similar schemes but with different order in the energy levels were also suggested by others[59,282]. In these schemes a significant factor which accounts for the variable oxidation state and often complex spectra[282] of these compounds is the strong interaction between the d orbitals and the $3\pi_V$ ligand orbitals resutling in the derived orbitals to be thoroughly delocalized over d_{xy}, d_{x2-y2} and $3\pi_V$.

In modifying this scheme for the VL_2 complexes a number of factors must be taken into account.

    (i)   The ligand orbitals are of lower energy and hence the extent of delocalization is much less in the $V(O \frown N \frown O)_2$ complexes.

    (ii)   There are no π_h orbitals on two of the donor N atoms and

    (iii)   The chelate rings are on only two edges of the trigonal prism.

Taking these into account Desideri et al.[283] suggested a modified molecular orbital diagram as depicted in Figure 3.7.3.3 in which the relevant energy levels are shown.

In $V(O \frown N \frown O)_2$ type complexes, the ligand a_1 orbital which is effectively an sp^2 hybrid interacts with the metal d_{z2} and 4s orbitals to give a $3a_1'$ M.O. which is mainly metal-like. They suggested that because of the smaller size of the ligand orbitals, this bond in contrast to the tris-dithiolato complexes is mainly σ and has almost no π-character. The e'' orbitals exhibit much the same behaviour with $O \frown N \frown O$ as with $S \frown S$ since they are effectively sp^2 hybrids pointing towards the metal and forming strong σ-bonds with the metal d_{xz} and d_{yz} orbitals (2e'' not shown in diagram 3.7.3.3). The remaining $2a_2'$ ligand orbital is non-bonding.
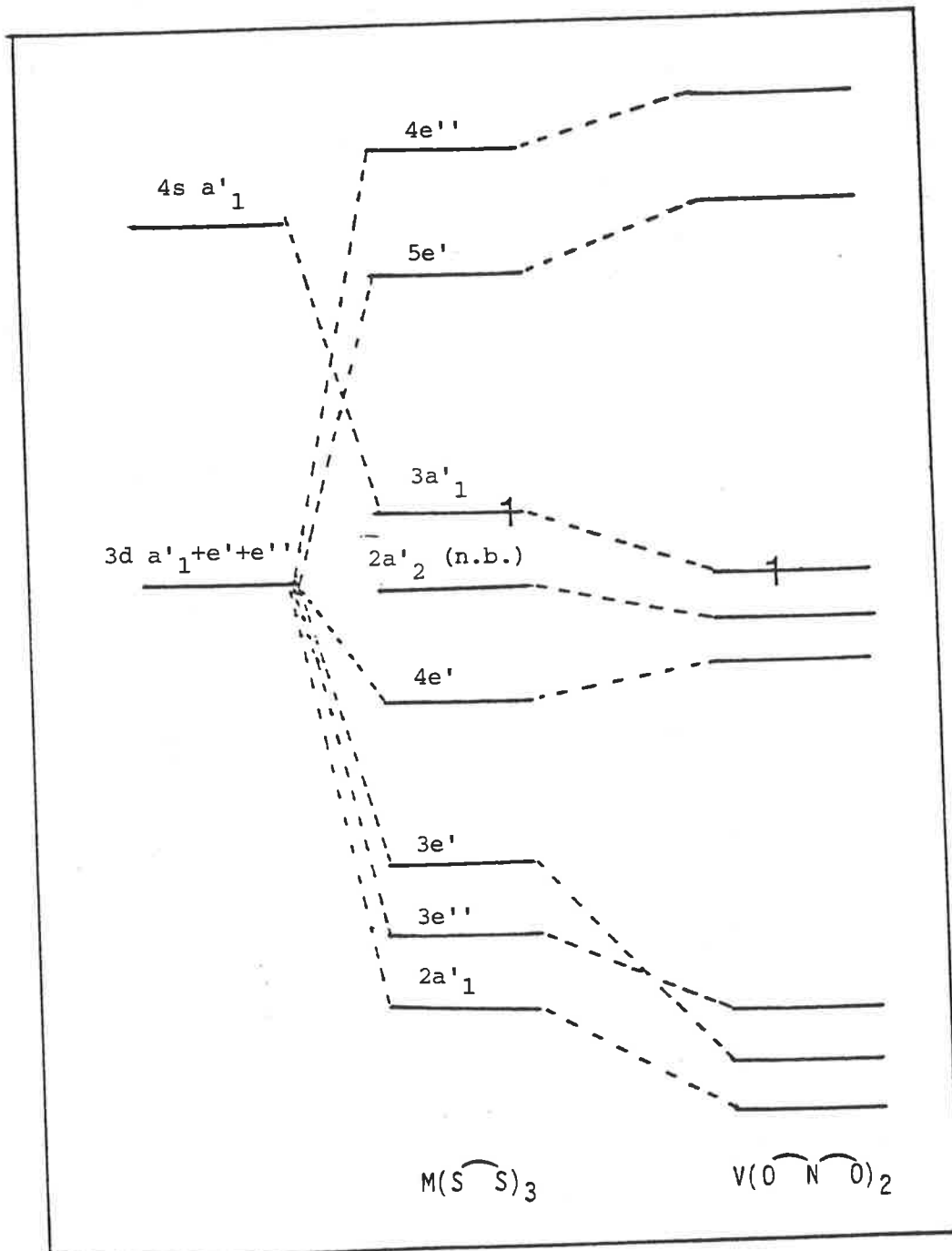
Figure 3.7.3.3: The molecular orbital energy level scheme for the tris-
M($S\frown S$)$_3$ and bis V($O\frown N\frown O$)$_2$ complexes in D$_3$ symmetry.

From above discussions, it is clear that the 2e'', $2a_1$', 4e' as well as the low-lying $1a_2$', $1a_1$'', $2a_2$', $2a_1$'' [281] levels have mostly the ligand character, whereas the levels 4e'', $3a_1$' and 5e' are mainly on the metal d orbitals. Although assignment of the observed electronic transition by means of this diagram is speculative it can be used to indicate qualitatively the possibility of charge transfer bands in the spectra of these complexes. There are a number of filled levels which are essentially ligand orbitals such as 4e', 3e' and 3e'' from which transitions can take place to the essentially metal levels 5e' and 4e''. The transition to 5e' can be identified with the π-symmetry orbital (4e') on the ligand which although not delocalized on to the metal as in the case of the tris dithiolates, could be of sufficiently high energy to give the low energy charge transfer band observed. The transition 4e'-4e'' may also have some possibile contribution to this C.T. band. The shape of the C.T. (1) band suggests that more than one transition may be involved and, in fact, in certain cases shoulders are discernible.

3.7.4. ELECTRON SPIN RESONANCE SPECTRA

(a) INTRODUCTION

The electron spin resonance method can be useful in studying many metal complexes containing unpaired electrons. This is particularly useful for Cu(II) and V(IV) compounds because they contain only one unpaired electron and the absence of inter-electron interaction effects. As a result, the E.S.R. signals for them are obtained conveniently at room or liquid nitrogen temperature without need to go down to liquid helium temperature. The V^{4+} having a nuclear spin of 7/2 gives rise to an easily resolvable characteristic eight-line spectrum. The electron spin resonance properties of the oxovanadium(IV) compounds have been studied quite extensively[5,9,25,284]. The most interesting, in relation to this work, is the E.S.R. behaviour of the non-vanadyl vanadium(IV) complexes which gives information as to the stereochemistry of such complexes and the orbital residence of the unpaired electron.

One class of non-vanadyl vanadium(IV) compounds having V in a tetrahedral

environment are the complexes with chlorides[285], alkoxides[56,286,287] and amino
derivatives[56,287,288] as the ligands, where in each case the unpaired electron
lies essentially in the $3d_{x^2-y^2}$ orbital of the V^{4+} ion. At room temperature
$V(OBu^t)_4$ showed g = 1.964 and A = 64 G[286]. Complexes with two cyclopenta-
dienyl and two alkoxo or chloro ligands can also be considered as having a
pseudo-tetrahedral structure. Stewart and Parte[289] calculated some spin
Hamiltonian parameters for some $(\pi-C_5H_5)_2 V X_2$ complexes (X = Cl, SCN, OCN,
CN) which as well as the A values of 56-71 G showed the unpaired electron to
occupy a molecular orbital which is primarily metal ion d_{z^2} in character with
some contribution from the metal ion $d_{x^2-y^2}$ orbital. Also a recent E.S.R.
study of bis(chloroalkoxyl)bis(η-cylcopentadienyl) vanadium(IV) in CH_2Cl_2
showed it to have g and A values of respectively 1.990 and 74 G[290].

Dimeric $V_2(OEt)_8$, where V is five coordinated, gave broad signals with
partial resolutions of the eight-line hyperfine interaction in benzene,
methylcyclohexane or carbon disulphide solution and showed the g and A values
in the regions 1.951-1.953 and 78.0 - 79.1 G[287] respectively. The benzene
solution of the eight coordinated $V(S_2CNEt_2)_4$ at room temperature gave a
resolved eight-line spectrum[287] with g = 1.975 and A = 72.5 G.

Of more relevance are the six-coordinate V^{4+} complexes investigated by
Jezierski and Raynor[66]. They determined the E.S.R. spectra of a range of
twenty compounds of the type $VX_2(L_4)$ [X = Cl or Br, L_4 = quadridentate or two
bidentate ligands] prepared from reactions of $SOCl_2$ or $SOBr_2$ with $VO(L_4)$ [64]
and obtained g and A values in the ranges 1.950-1.963 and 71-80 G respect-
ively. The $VO(L_4)$ compounds showed larger A values. For a few complexes with
the possible trigonal prismatic geometry, they located the unpaired electron
in the d_{z^2} orbital.

Because of their coordination geometry, the trigonal prismatic tris-
dithiolato complexes are also of particular interest for the present study.
Davison et al.[291] determined the g and A values of some $[V(S_6C_6R_6)]^z$ complexes
(R = C_2H_5, CN, etc.), the magnitude of which were respectively in the ranges
1.980-1.990 and 61.5-65.5 G. Schrauzer and Mayweg[282] for some V(1,2-dithio-

lato)$_3$ complexes reported the g value of the order of 1.99 and A values lying in the range 61.5-67.8 G. Atherton and Winscom[292] as well as Kwik and Steifel[293] studied the single crystal E.S.R. spectrum of V(mnt)$_3^{2-}$ and identified the orbital bearing the unpaired electron. Also the six-coordinate V^{4+} complexes with O and N donors are important in relation to this work. An isotropic eight-line E.S.R. signal with A = 75G was obtained for (Et$_3$NH)$_2$ [V(cat)$_3$].CH$_3$CN [71] in acetonitrile. Also E.S.R. studies of some other triethylammonium-tris-catecholato (-2) vanadium(IV) in this laboratory[72] gave A values in the range 82-83G. The same study but on (Et$_3$NH)$_2$[V(BHA)$_3$] and (Et$_3$NH)$_2$[V(4-NO$_2$-BHA)$_3$] (BHA = benzohydroxamato (-2)) in CH$_2$Cl$_2$ gave A values of respectively 75.6 and 77.0G.

Although the VL$_2$ complexes are new and mostly reported in this work, Diamantis et al.[283,294] reported the detailed analyses of the E.S.R. spectra of V(acac-BH)$_2$.

(b) RESULTS AND DISCUSSION
(i) ROOM TEMPERATURE E.S.R. SPECTRA

In the present work, the room temperature isotropic E.S.R. spectra for the VL$_2$ complexes, in dichloromethane or 1:1 dichloromethane-toluene, consist of the usual eight hyperfine lines (Figures 3.7.4.1-3.7.4.2) resulting from the coupling of the unpaired electron with the 7/2 spin of the ^{51}V nucleus. The spectra were analysed to the second order correction[284] to give the isotropic g and A values listed in Table 3.7.4.1. The hyperfine coupling constant (A) values of the VL$_2$ complexes of different ligand types are in the range 65-72G. These values are comparable to those observed in various non-vanadyl vanadium(IV) complexes as mentioned in Section (a) above. The vanadyl complexes are found to have broader spectra and thus larger hyperfine coupling constants[25].

As expected, the g values for the present complexes are lower than the free electron value g$_e$ (2.00232)[295]. This lowering of g values is generally observed with all V^{4+} complexes. The spread in the observed g values (1.960-

1.975) is relatively small compared to the variation in the isotropic hyperfine constant values.

The most striking characteristic of the E.S.R. spectra of VL_2 complexes is the low value of the isotropic hyperfine coupling. Davison et al.[296] explained the hyperfine interaction in terms of (a) direct admixture of the $(n + 1)s$ wave function into the nd^m configuration and (b) the admixture of the excited states. According to their calculations, the observed A_{iso} value of 63.3G for $[V(S_6C_6(CN)_6]^{2-}$ should be consistent with a maximum of 3% admixture of 4s into the ground state. It is significant that in the present generally trigonal prismatic VL_2 complexes the A_{iso} values generally comparable to those for the trigonal prismatic tris-dithiolato complexes are observed. By contrast, for complexes with octahedral or pseudo-octahedral environment[64,66,71,72] the A_{iso} values, although less than for the vanadyl complexes, are appreciably higher than those for the present VL_2 complexes.

TABLE 3.7.4.1: ISOTROPIC g AND A VALUES OF SOME VL_2 COMPLEXES

(SOLVENT - CH_2Cl_2)

COMPLEX	g-VALUE[a]	A-VALUE (G)[b]
V(acac-BH)$_2$	1.973	70.74
V(Bzac-BH)$_2$	1.973	70.40
V(dbm-BH)$_2$	1.975	70.85
V(HNP-BH)$_2$	1.973	67.49
V(HAP-BH)$_2$	1.972	65.89
V(HAP-p^{Cl}-BH)$_2$	1.972	65.38
V(acac-SalH)$_2$	1.973	70.55
V(HAP-SalH)$_2$	1.971	68.09
V(HAP-OAP)$_2$	1.966	71.08
V(OAP-β-nap)$_2$	1.970	65.52
V(OAP-p-cresol)$_2$	1.960	65.43
V(Bzac-BH)(HNP-BH)	1.971	71.54

a. ± 0.01 ; b. ± 0.1
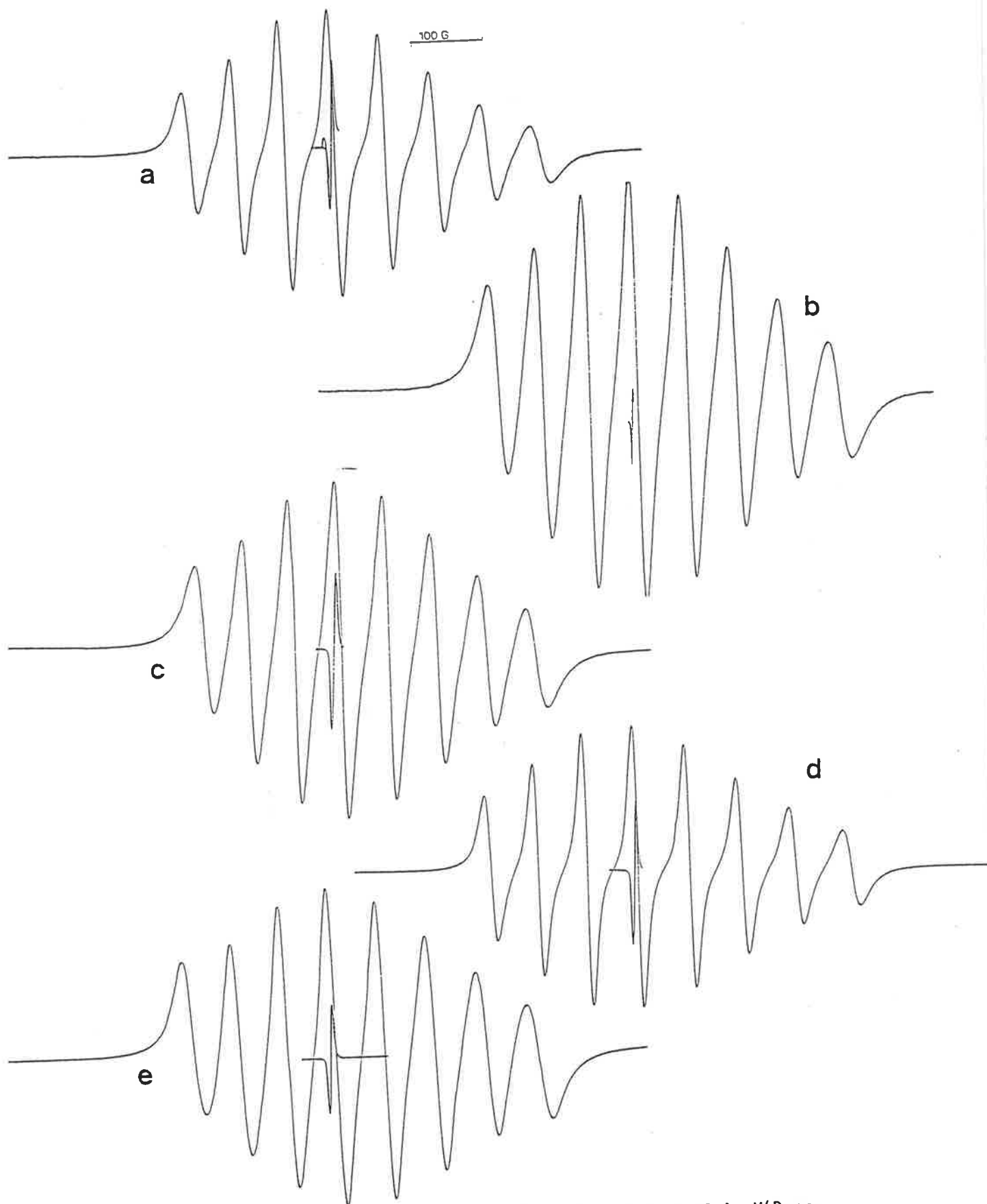
Figure 3.7.4.1: Room temperature X-band E.S.R. spectra of A. V(Bzac-BH)$_2$; b. V(HNP-BH)$_2$; c. V(HAP-p^{Cl}-BH)$_2$; d. V(acac-SalH)$_2$ and e. V(HAP-SalH)$_2$ in dichloromethane/toluene (↓ DPPH).
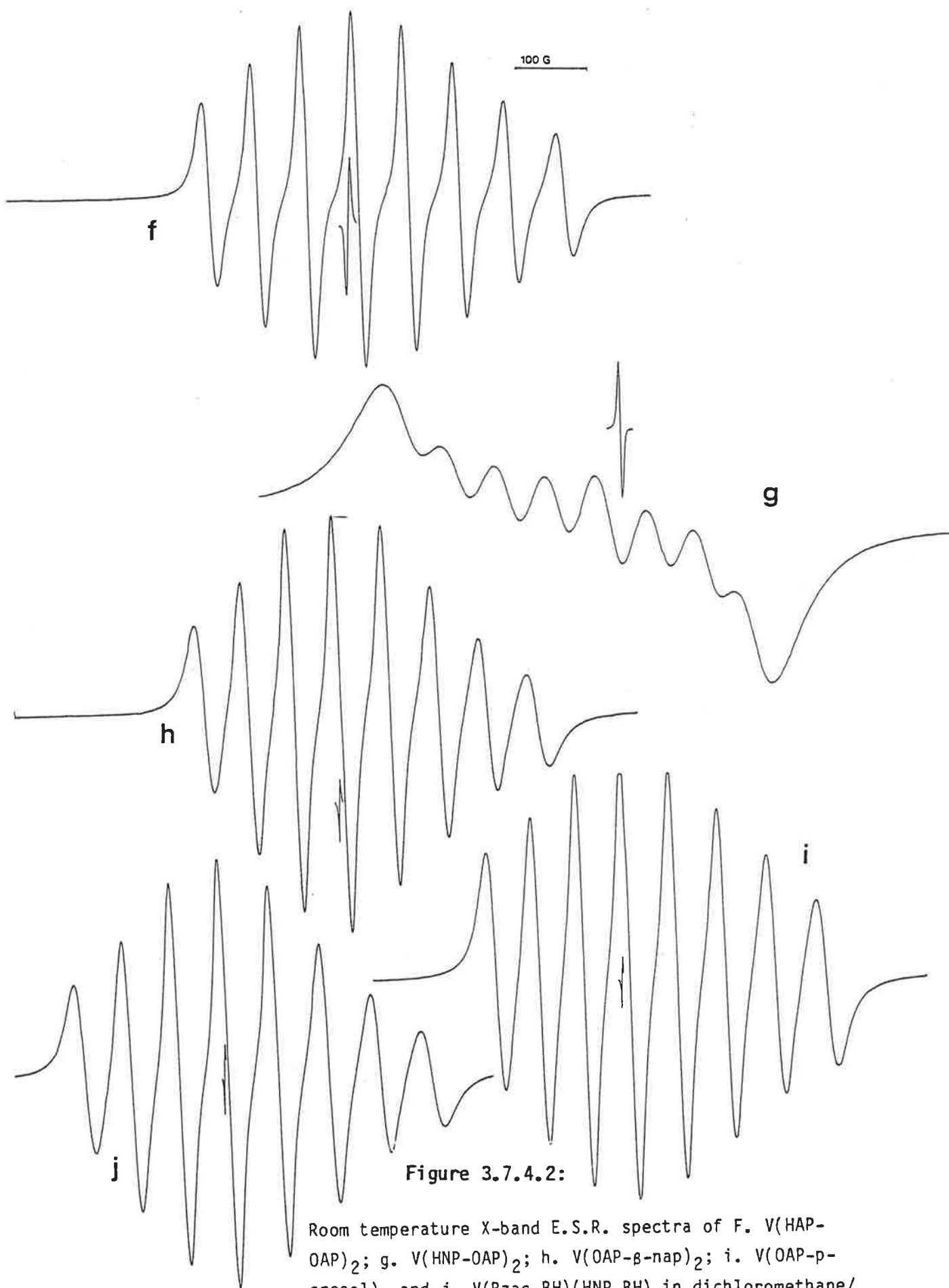
Figure 3.7.4.2:

Room temperature X-band E.S.R. spectra of F. V(HAP-OAP)$_2$; g. V(HNP-OAP)$_2$; h. V(OAP-β-nap)$_2$; i. V(OAP-p-cresol)$_2$ and j. V(Bzac-BH)(HNP-BH) in dichloromethane/toluene. (ı DPPH).
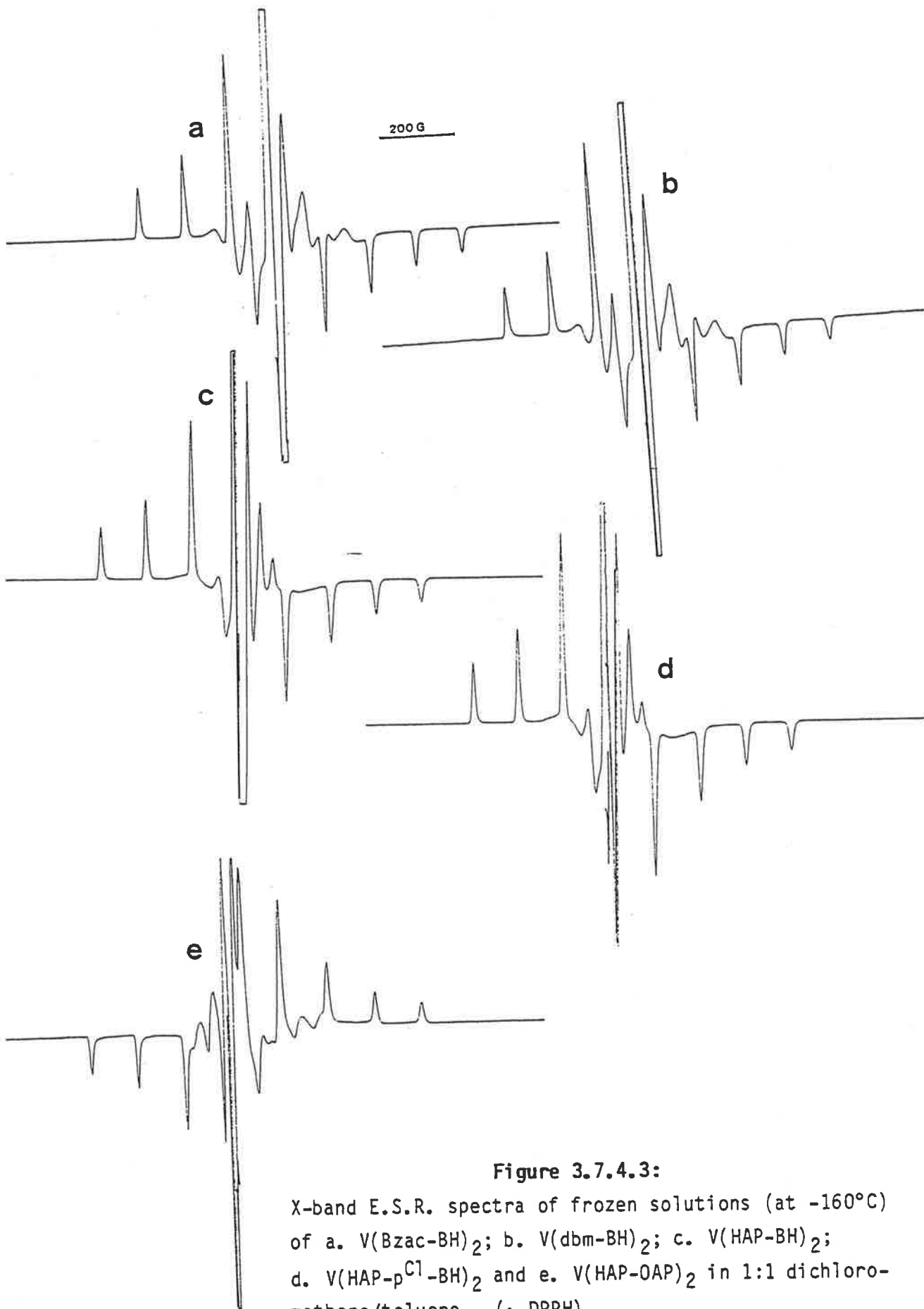
Figure 3.7.4.3:

X-band E.S.R. spectra of frozen solutions (at -160°C) of a. $V(Bzac-BH)_2$; b. $V(dbm-BH)_2$; c. $V(HAP-BH)_2$; d. $V(HAP-p^{Cl}-BH)_2$ and e. $V(HAP-OAP)_2$ in 1:1 dichloromethane/toluene. ($\downarrow$ DPPH).

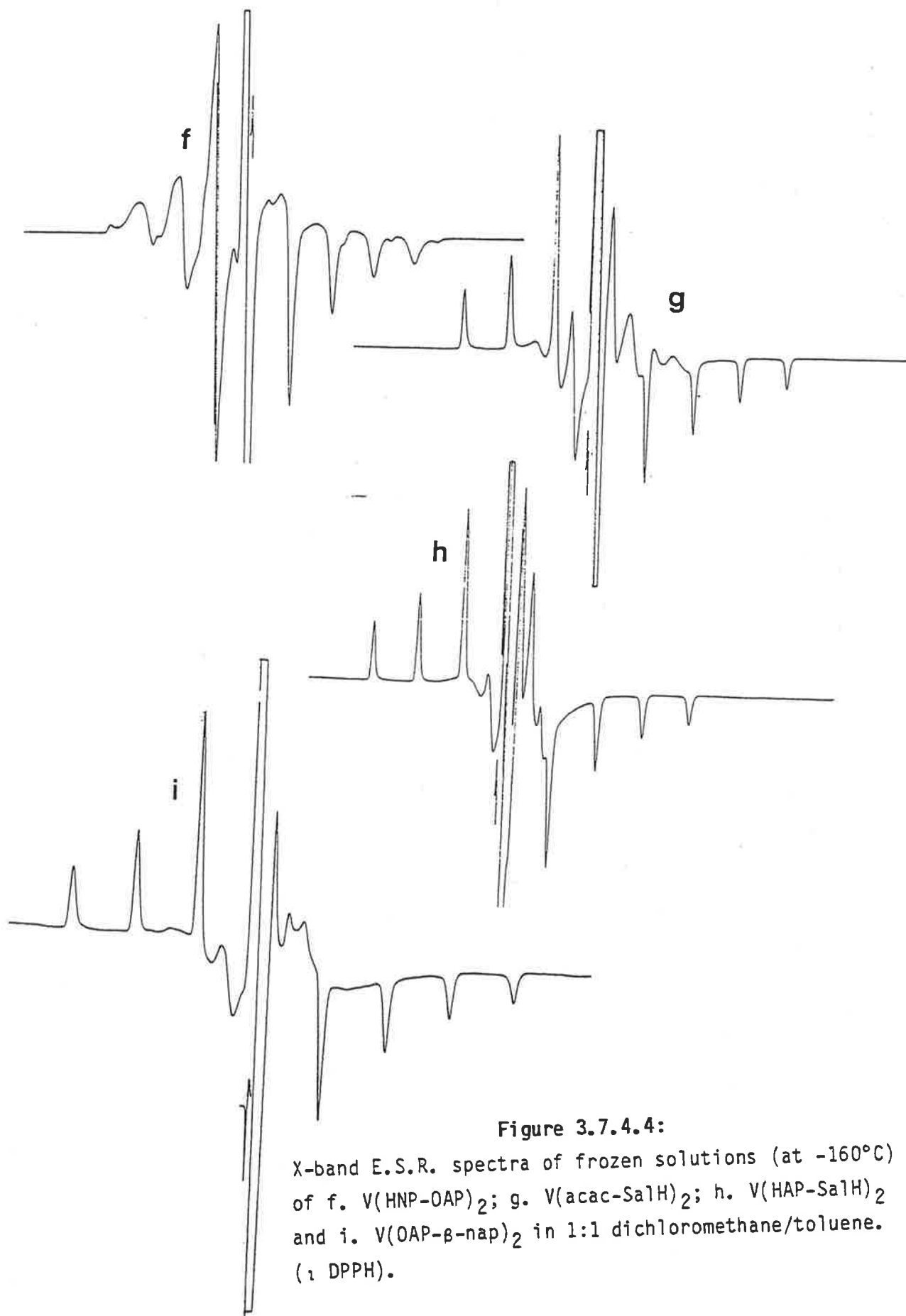**Figure 3.7.4.4:**

X-band E.S.R. spectra of frozen solutions (at -160°C) of f. V(HNP-OAP)$_2$; g. V(acac-SalH)$_2$; h. V(HAP-SalH)$_2$ and i. V(OAP-β-nap)$_2$ in 1:1 dichloromethane/toluene. (↓ DPPH).

A comparison of the E.S.R. spectra of oxovanadium(IV) and non-vanadyl VL_2 type complexes shows that the E.S.R. method can be used as a very convenient and quick tool to identify the formation of and distinguish the trigonal prismatic or octahedral non-vanadyl vanadium(IV) complexes from the square-pyramidal vanadyl complexes.

(ii) THE FROZEN SOLUTION SPECTRA

Diamantis et al.[283,294] determined and analysed the low temperature E.S.R. spectrum of V(acac-BH)$_2$ and found the simulated spectrum to compare well with the observed spectrum. The averaged and isotropic g and A values (averaged from g_1, g_2, g_3 and A_1, A_2, A_3 respectively) for the system were in good agreement.

We examined the E.S.R. spectra routinely for all the main types of VL_2 complexes measured in frozen solution. The spectra in most cases show a remarkable similarity to that for the V(acac-BH)$_2$[283,294]. For this reason no detailed analysis of the spectra was undertaken as no significant correlation were anticipated. However, the room as well as the low temperature E.S.R. spectra for V(HNP-OAP)$_2$ [Figures 3.7.4 (g) and 3.7.4.4 (f)] are different from the other spectral type which could be due to some stereochemical difference in this case. We could not obtain any good crystal of this compound suitable for X-ray analysis.

(iii) THE LOCATION OF THE d^1-ELECTRON

The most significant E.S.R. examination of trigonal prismatic complexes were that of V(mnt)$_3^{2-}$ doped in single crystals of [As(C$_6$H$_5$)$_4$]$_2$[Mo(mnt)$_3$] [293] or (PPh$_4$)$_2$Mo(mnt)$_3$ [292] which showed the unpaired electron to occupy an orbital which is largely d_{z^2} in nature but with significant admixture of other 3d-orbitals. Jezierski and Raynor[66] showed this electron to be in a d_{z^2} orbital for a few VX_2L_4 type complexes which were thought to have trigonal prismatic structures. Diamantis, Raynor and Rieger[294] on the basis of the

magnitude of the E.S.R. hyperfine tensor components as well as of the g tensors calculated from the V(acac-BH)$_2$ spectrum suggested that the unpaired electron occupies an orbital which is largely vanadium 3d in character (78% d_{z^2}, 10% $d_{x^2-y^2}$, 2% 4s) and the large d_{z^2} nature of this orbital is consistent with the expected ordering of the d-orbitals in a trigonal prismatic configuration.

CHAPTER 4

OXOVANADIUM(IV) AND -(V) COMPLEXES WITH TRIDENTATE LIGANDS

4.1 INTRODUCTION

In this chapter, a number of VO^{2+} and VO^{3+} complexes with benzoylhydrazone tridentate ligands are described. The VO^{2+} complexes were considered as the possible intermediates in the formation of VL_2 complexes. Such intermediates would have the formula VOL as a result of stepwise formation of the bis complexes. With tridentate ligands there are two likely structures (i) VOLX where X is usually a monodentate ligand in a monomeric complex[297] or (ii) dimeric $(VOL)_2$ as discussed in detail in Section 1.2(b). Attempts to isolate such intermediates have shown them to be extremely air-sensitive and no crystalline derivative could be isolated. The only stable product that could be isolated was the monomeric VOLHCl type complexes in which only one protonic hydrogen was removed from the reacting LH_2. These intermediate complexes were found to be readily converted to the VL_2 complexes and easily oxidized to give the vanadium(V) complexes of the type VOL.OR and $(VOL)_2O$.

The air-sensitive nature of the reaction mixture used for the preparation of VL_2 either from $VO^{2+} + 2L^{2-}$ or from $VO(\beta-diketonato)_2 + 2$ benzoyl-hydrazine have been noted[73] (Chapter 3) and vanadium(V) complexes of the type mentioned above can be isolated from such systems unless oxygen is excluded. The formation and existence of the VOL.OR and $(VOL)_2O$ type complexes were confirmed by N.M.R. studies (Section 4.8) and by determining the X-ray crystal structures of VO(Bzac-BH).OEt and $[VO(Bzac-BH)]_2O$ (Section 4.3).

Although we could not isolate the $(V^{IV}OL)_2$ or $V^{IV}OL.ROH$ type complexes using the tridentate benzoylhydrazine Schiff bases, the existence and extremely unstable nature of such complexes were discernible from their solution spectroscopic studies.

4.2   DISCUSSION ON PREPARATIONS AND PROPERTIES

(a)   FORMATION OF (VOL)$_2$ OR VOL.ROH IN SOLUTION

Attempts to prepare VOL complexes by the addition of VOCl$_2$ to an alcoholic solution containing an equimolar amount of LH$_2$, in the presence of lithium acetate, produced dark green solutions from which, even under the most rigorous exclusion of atmospheric oxygen, no vanadyl(IV) complexes could be isolated. It seems that with such dinegative tridentate ligands, vanadyl(IV) complexes are stable only if they can be obtained in an insoluble form. For example, with L = o-aminophenol Schiff bases of salicylaldehyde and 2-hydroxy-1-napthaldehyde, the insoluble (VOL)$_2$ and VOL.H$_2$O complexes, respectively, were isolated. Similar behaviour has been noted by other workers[36,37,92]. The green solutions react with a second molar equivalent of LH$_2$ to give the VL$_2$ complex. Also, in contact with air they are easily oxidized to yield the vanadium(V) complexes. Thus, the green colour of the solution, the lack of any precipitation from it and the quantitative formation of VL$_2$ and VOL.OR indicate that the latter are formed via a (VOL)$_2$ or VOL.ROH intermediate.

The electronic spectra of the green solution prepared by mixing Bzac-BHH$_2$, LiOAC and VOCl$_2$ in the molar ratio of 1:2:1.2 in methanol were examined under strict oxygen-free conditions using vacuum-line techniques. The initial spectrum (A in Figure 4.2.1) showed a distinct and intense peak at 411 nm ($a_M \sim 1 \times 10^4$ mol dm^{-3}cm^{-1}). On allowing the solution to oxidize, this peak decreased and a new peak at 363 nm appeared. Finally, the spectrum of the resultant brown solution became identical to that of VO(Bzac-BH).OMe (spectrum B in Figure 4.2.1) with a λ_{max} at 363 nm [cf. Table 4.6.2 for VO(Bzac-BH).OEt]. The high extinction of the absorption at 411 nm suggests that it is due to a LMCT transition. It seems that the tridentate ligand is responsible for this intense C.T. band at the edge of the visible region which together with the d-d transition (not observed in our case due to dilution) gives rise to the green colour of such complexes. It is interesting to note that (VOL)$_2$
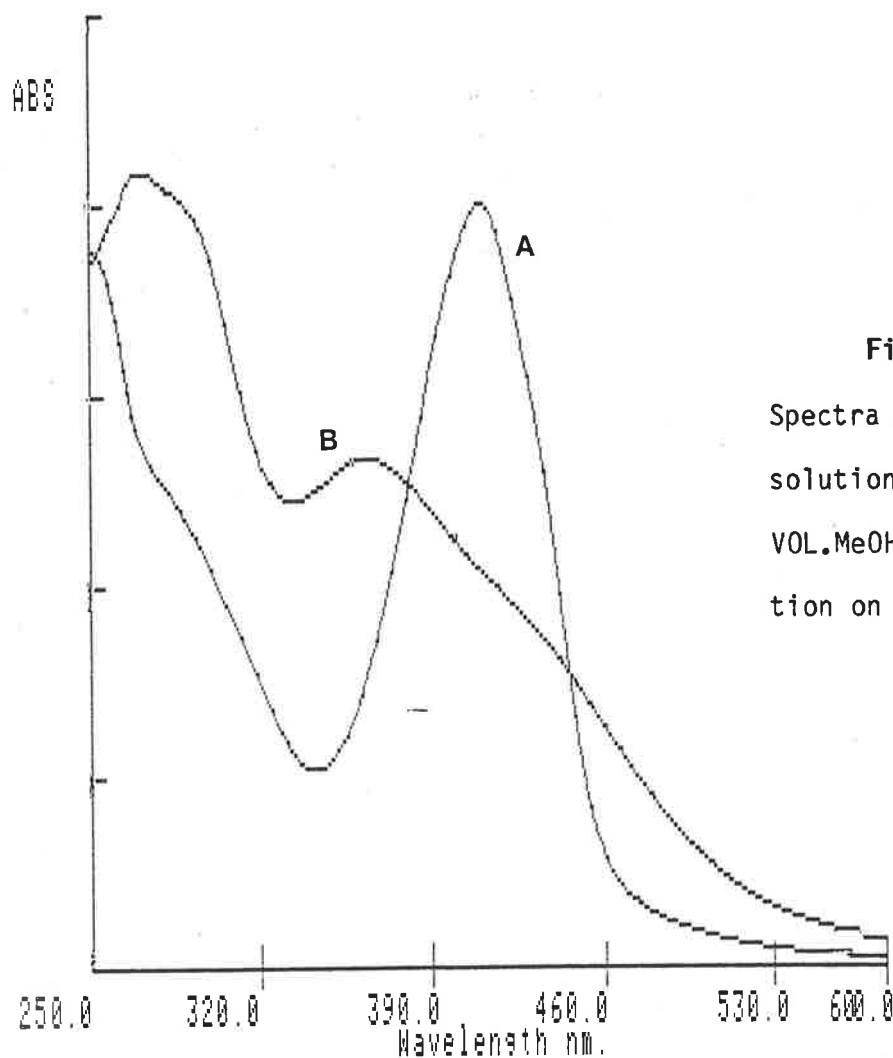
ABS

Figure 4.2.1:

Spectra of A. The green solution of $(VOL)_2$ or VOL.MeOH; B. The brown solution on oxidation of A.

with L = Sal-OAP[92] is also green-brown and $K_2[VO(cat)_2]$.EtOH.H_2O and $(Et_3NH)_2$ $[VO(3,5-di-\underline{tert}-butylcat)_2].2CH_3OH$ are green[71], likewise, $[VO(CHO.C_6H_3O_2)_2]_2^{2-}$ has a strong C.T. at 385 nm[70]. It appears that ligands which favour the formation of six-coordinated non-vanadyl vanadium(IV) complexes also give rise to C.T. bands at the edge of the visible region on a VO^{2+} centre. These shift to ~ 540 nm on the substitution of the oxo ligand to give the VL_2 complexes.

(b) MONOMERIC VOLHCl COMPLEXES

By using concentrated solutions at room temperature and in the absence of base it was possible to isolate a monomeric intermediate containing the tridentate ligand. Thus, with a slight molar excess of $VOCl_2$, in the minimum volume of methanol (or ethanol), and a saturated solution of $\underline{LH2}$ in acetone, a

green precipitate of VOLHCl was obtained. Under these conditions, formation of VL_2 was prevented and the rapid precipitation of the solid protected it from oxidation. In the absence of base, and in acetone as the solvent, the hydrazone part of the tridentate ligand coordinates in the keto-form (see Section 4.5 for infrared evidence) and thus the ligand in these complexes is present as singly deprotonated LH⁻. The Cl⁻ appears to be in the coordination sphere as there is no immediate AgCl precipitation on adding acidified $AgNO_3$ solution to the compound in diluted HNO_3. The complexes that were prepared by the above method are listed in Table 4.2.1.

Although the green VOLHCl complexes have low solubility in alcohol, addition of an alcohol in the presence of air to the solid causes the latter to dissolve rapidly producing brown to chocolate brown solution from which the oxidation product VOL.OR can be isolated. The VOLHCl complexes can be used as intermediates in the preparation of VL_2, i.e. their reaction with LH_2 in the presence of LiOAC in methanol (or ethanol) under oxygen-free conditions yields a quantitative amount of VL_2. It is possible to utilize this reaction for the convenient preparation of the mixed ligand VLL'complexes by adding a different ligand $L'H_2$.

TABLE 4.2.1: THE PREPARED VOLHCl COMPLEXES

| COMPLEX	COLOUR	COMPLEX	COLOUR
VO(Bzac-p^{Cl}-BHH)Cl	Green	VO(HAP-BHH)Cl	Green
VO(HNP-BHH)Cl	Green (Yellowish)	VO(Sal-BHH)Cl	Green

(ε) VO^{3+} COMPLEXES

The ease of oxidation of the intermediate described in Sections (a) and (b) above serves as an easy method for the preparation of a range of oxovanad-

ium(V) complexes. This explains the need to avoid any oxygen in the preparation of VL_2 complexes. A convenient method of preparation of the VO^{3+} complexes is by bubbling of air through a stoichiometric mixture of $VOCl_2$ present in a small excess to suppress formation of VL_2, lithium acetate and $\underline{LH_2}$ in an alcohol (ROH), and thus enabling rapid oxidation of V^{IV} to V^V. The refluxing of this solution, and then cooling it, result in precipitation of the VOL.OR type complexes in good yield. In some cases, the reaction proceeds readily at room temperature and refluxing is unnecessary.

Alkoxo groups are easily hydrolysable. In these compounds, evidence was found of the hydrolysis reaction with a trace of water in nujol, and $CDCl_3$, used to determine the infrared and N.M.R. spectra. Because alcohols stabilize the alkoxo groups, a preparative procedure for the μ-oxo dimers of the type $(VOL)_2O$ was developed using a two-phase system consisting of water, and the chloroform solution of the alkoxo compound. This method was used to hydrolyse the alkoxo compounds in $CHCl_3$ to obtain the oxo-bridged $(VOL)_2O$ compounds in good yield. Such VOL.OR and $(VOL)_2O$ complexes that were prepared are listed in Table 4.2.2.

From infrared and N.M.R. studies it was found that the addition of alcohol to the $CHCl_3$ solution of $(VOL)_2O$ complexes converts them to the alkoxo compounds. The reversal of the hydrolytic reaction, which is analogous to the esterification of an acid anhydride, was utilized to convert the oxo-bridged dimers to the alkoxo monomers. Thus, refluxing of $(VOL)_2O$ (L = Bzac-BH, dbm-BH, HNP-BH, HAP-BH and Sal-BH) in methanol gave the VOL.OMe complexes in good yield which were identified by their characteristic infrared spectra.

The above reactions clearly show the VOL.OR and $(VOL)_2O$ type complexes to be completely interconvertible as,

$$2 \text{ VOL.OR} \underset{+\ 2\ \text{ROH}}{\overset{+\ H_2O}{\rightleftharpoons}} (VOL)_2O.$$
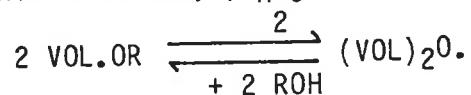
A recent kinetic and equilibrium study on the esterification of $[VO(AA)_2]_2O$ (AA = 8-quinolinato) by butyl alcohol[94] confirms the above equilibrium.

The VOL.OR when refluxed in R'OH gives the metathesis reaction product VOL.OR' and this can be used as a preparative scheme analogous to that described in Chapter 2.

The molecular weight determination of the VOL.OR complexes (Table 4.2.3) indicates that some kind of association takes place in solution. The association can be explained in terms of dimerization to give dialkoxo-bridged complexes of the type described in Chapter 2. Another possibility is the reaction,

$$2 \text{ VOL.OR} + H_2O \rightarrow (VOL)_2O + 2 \text{ ROH}$$
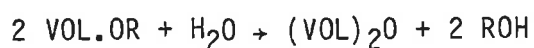
which, in principle, should not affect the osmometry as the number of particles does not change. —

At first, these complexes were thought to be the sought V^{4+} intermediate $(VOL)_2$ type dimers, because on reaction with $\underline{LH_2}$ under oxygen-free condition they gave VL_2 complexes, although in low yields (~ 30%). The same reaction, when repeated in the presence of a small amount of benzoylhydrazine, gave a quantitative yield of the VL_2 complex. Thus, addition of the second ligand to give the VL_2 requires benzoylhydrazine, or in its absence, $\underline{LH_2}$ itself, to reduce V^V to V^{IV}. By this reaction, VL_2 or mixed ligand VLL' complexes can also be obtained from both VOL.OR and $(VOL)_2O$ compounds.

TABLE 4.2.2: THE PREPARED $V^VOL.OR$ AND $(V^VOL)_2O$ COMPLEXES

COMPLEX	COLOUR	COMPLEX	COLOUR
VO(Bzac-BH).OEt	(Dark) Brown	[VO(Bzac-BH)]$_2$O	Brown-Red
VO(Bzac-p^{Cl}-BH).OMe	(Dark) Brown	[VO(Bzac-p^{Cl}-BH)]$_2$O	(Magenta) Red
VO(dbm-BH).OMe	(Dark) Brown	[VO(dbm-BH)]$_2$O	Brown-Red
VO(HNP-BH).OMe	(Dark) Brown	[VO(HNP-BH)]$_2$O	Yellow-Brown
VO(HNP-p^{Cl}-BH).OMe	Red-Brown	[VO(HNP-p^{Cl}-BH)]$_2$O	Magenta-Brown
VO(HAP-BH).OMe	(Dark) Brown	[VO(HAP-BH)]$_2$O	Chocolate Brown
VO(Sal-BH).OMe	(Dark) Brown	[VO(Sal-BH)]$_2$O	Brown
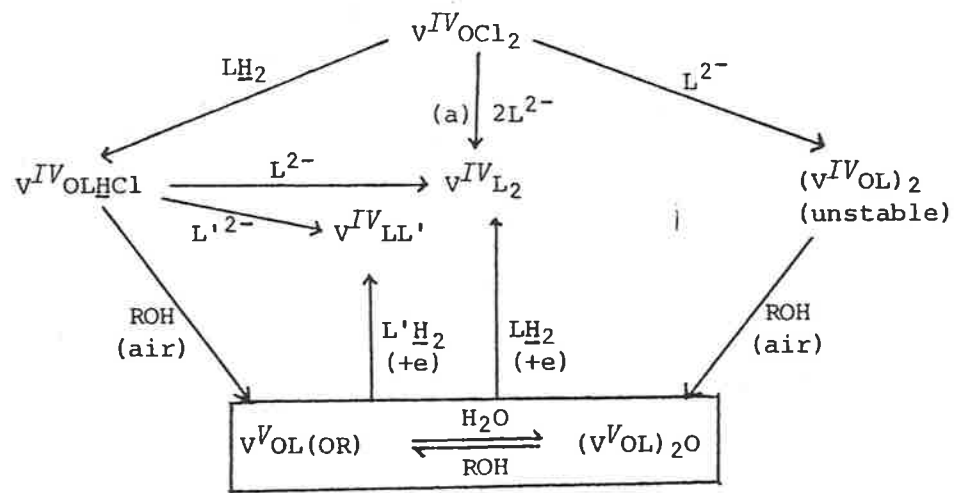
Figure 4.2.2:   Formations and reactions scheme of the VOL$\underline{\text{H}}$Cl, VOL.OR and (VOL)$_2$O complexes.

(+e) reducer, usually benzoylhydrazine   (a) also from VO(acac)$_2$ and LH$_2$

TABLE 4.2.3: MOLECULAR WEIGHT OF VOL.OR COMPLEXES AS DETERMINED

BY V.P.O. METHOD

COMPLEX	F. WT.	MOL. WTS. FOUND
VO(Bzac-BH).OEt	390	659, 670, 692, 715
VO(dbm-BH).OMe	438	607, 621, 691, 706
VO(HNP-BH).OMe	386	581, 604, 637, 714
VO(HAP-BH).OMe	350	475, 517, 558, 617
VO(Sal-BH).OMe	336	565, 573, 604, 650

V.P.O. = Vapour Pressure Osmometry; Values underlined - more probable.

(d) THE FORMATION AND REACTION SCHEME

The interrelation of various VOLHCl, VOL.OR and $(VOL)_2O$ complexes as described above are shown schematically in Figure 4.2.2 which illustrates (i) the formation of VOLHCl and its ready reaction to formation of VL_2, VLL', VOL.OR and $(VOL)_2O$ complexes, (ii) the need for an oxygen-free condition in preparing VL_2 complexes to avoid oxidation of the intermediate product to vanadium(V) compounds and (iii) interconversion of VOL.OR and $(VOL)_2O$ and their ability to form VL_2 and VLL' complexes in the presence of a reducer, usually benzoylhydrazine.

4.3 THE CRYSTAL AND MOLECULAR STRUCTURES OF VO(Bzac-BH).OCH$_2$CH$_3$ AND (VO(Bzac-BH)$_2$O

The two vanadium(V) complexes VO(Bzac-BH).OCH$_2$CH$_3$ (I) and [VO(Bzac-BH)]$_2$O (II), recrystallized from dichloromethane-petroleum spirit and chloroform-petroleum spirit, respectively, have the crystal structures shown in Figures 4.3.1 and 4.3.2. In both structures the coordination environment of
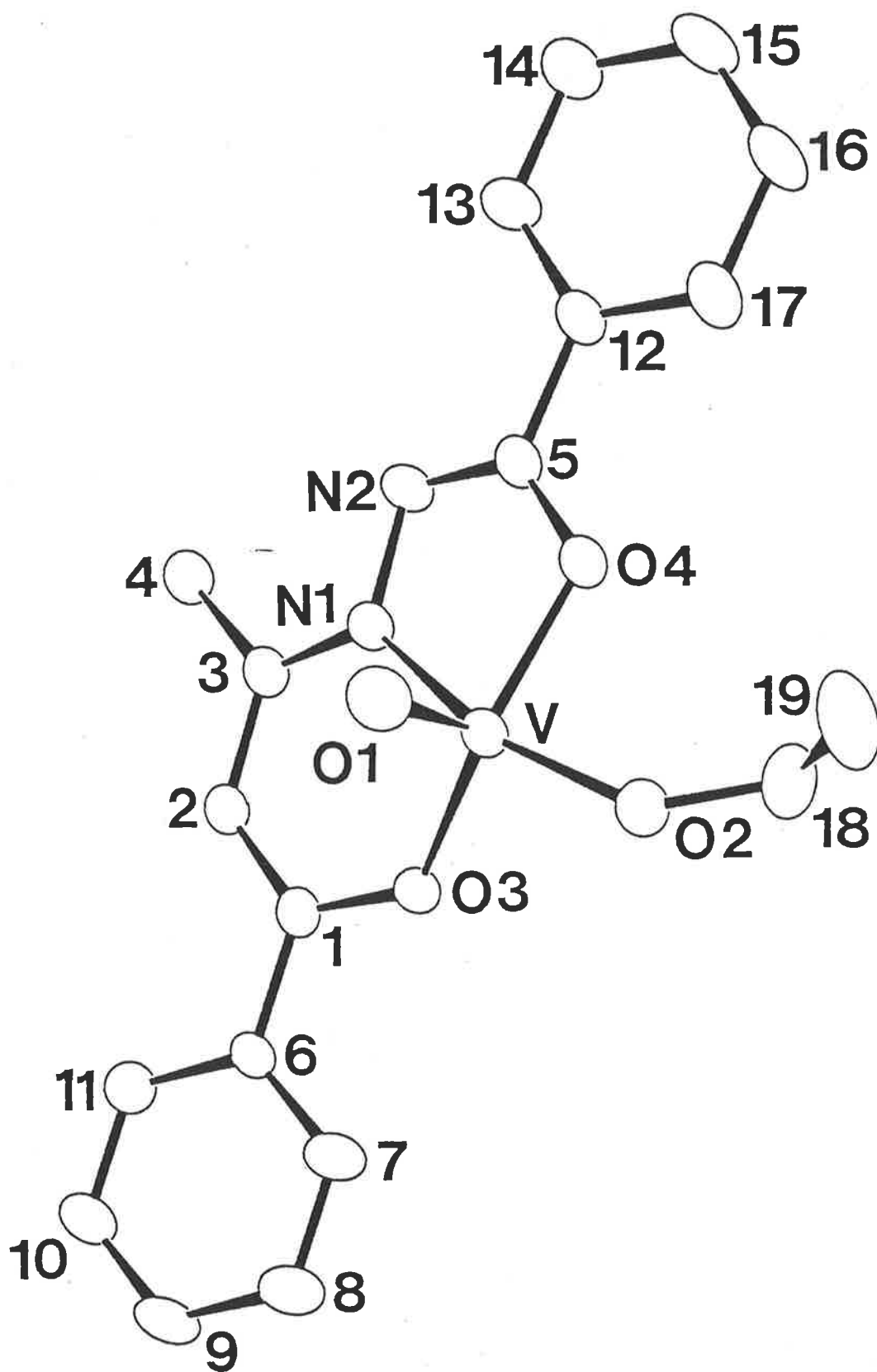
Figure 4.3.1:   Molecular structure and numbering scheme for
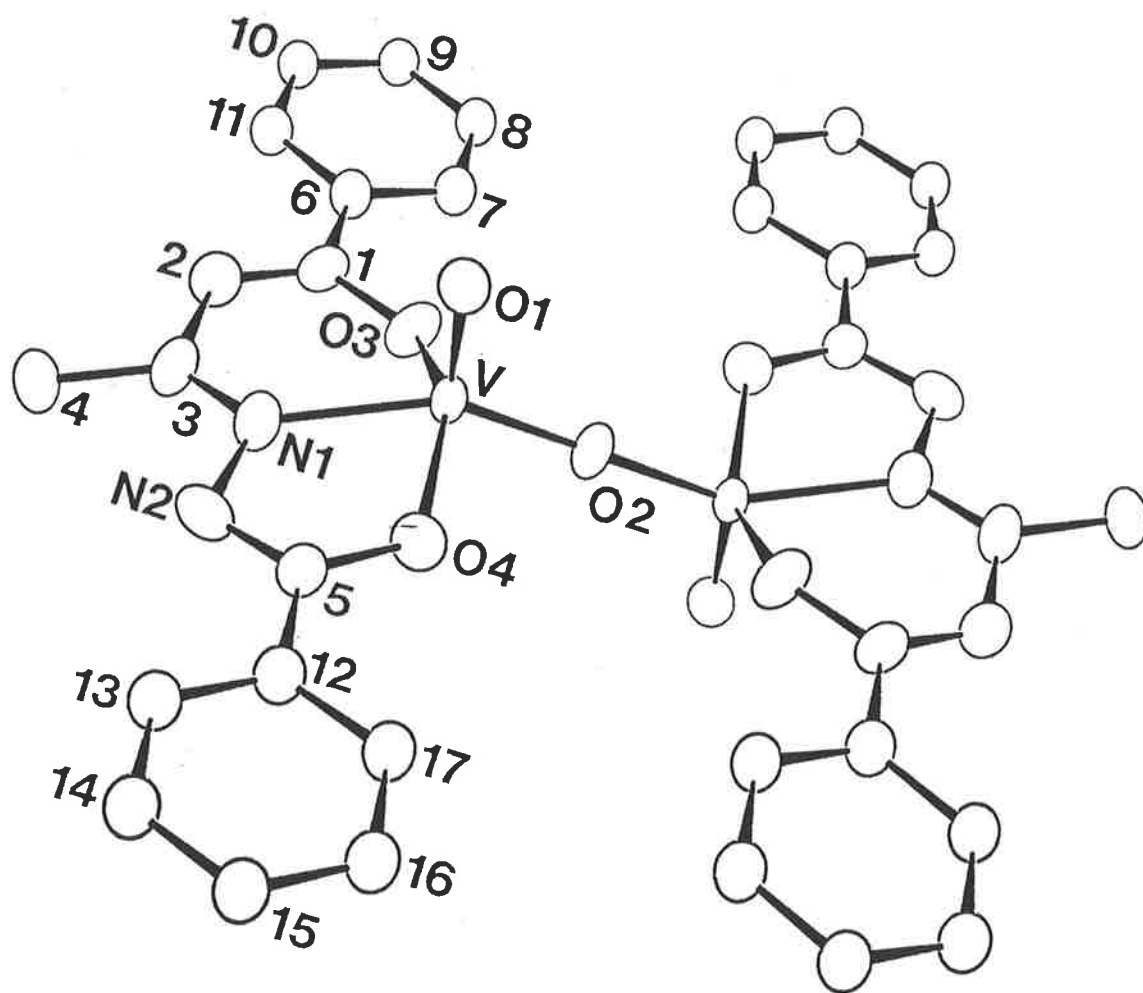VO(Bzac-BH).OCH_2CH_3, (I).

Figure 4.3.2: Molecular structure and numbering scheme for [VO(Bzac-BH)]$_2$O, (II).

the vanadium atom approximates a square pyramid with the oxo ligand occupying

$$C(18) - O(2) \overset{\displaystyle \overset{O}{\|} }{\underset{\displaystyle \underset{O(3)}{}}{V}} \overset{O(4)}{\underset{N(1)}{}}$$

I

$$V' - O(2) \overset{\displaystyle \overset{O}{\|} }{\underset{\displaystyle \underset{O(3)}{}}{V}} \overset{O(4)}{\underset{N(1)}{}}$$

II

the apical position and the donor atoms of the tridentate ligand occupying

three of the positions in the basal plane. The fourth position, O(2), as

shown in the Figures above, in compound (I) is linked to the ethyl group and

in compound (II) forms the bridge to an identical unit which is related to the

first by a centre of inversion at the site of O(2).

The important bond distances and the bond angles for the two coordina-

tion environments are given in Tables 4.3.1 and 4.3.2. From Table 4.3.1 it is

obvious that the two coordination environments are almost identical. The

terminal oxo groups in (I) and (II) show the short bond distances character-

istic of a V = O double bond and are in agreement with the vanadyl group in

other vanadium(V) complexes[86,90-92] as well as vanadium(IV) complexes[21]. The

shortest V - O distance is to the ethoxo oxygen atom in agreement with the V -

O distance to the terminal -OCH_3 group in $[VO(OCH_3)_3]_2$ [85]. The V - O

(bridging) distances are also similar to those found in other oxo-bridged

vanadium(V) complexes[86,90,92]. The V - N distances are appreciably longer

than the V - O distances, a fact which seems to be characteristic of several

chelating ligands containing O and N donors[79,86,90-92]. This suggests that

some π-donation, leading to a partial multiple bond, is a feature of oxygen

coordination in vanadium(V) complexes. Least square calculations show the

vanadium atom to be 0.492 and 0.468Å above the basal planes of structures (I)

and (II), respectively. The square pyramid is significantly distorted so as

to raise the N atom above the plane formed by the three donor atoms of the

tridentate ligand. This is also evident from the apical oxygen-vanadium-

nitrogen angles which are significantly less than the apical angles involving

the oxygen atoms in the basal plane. This effect has also been observed in the [VO(Sal-OAP)]$_2$O [92] unit and attributed to a greater repulsion between the non-bonding electrons on the oxygen donors. One major difference, however, between structure (II) and [VO(Sal-OAP)]$_2$O lies in the disposition of the two tridentate units with respect to the bridging oxgyen. In structure (II), the V - O - V bond is linear with the two vanadyl group trans to each other and in the same plane. The planes of the ligands are almost parallel. In [VO(Sal-OAP)]$_2$O, the planes of the two tridentate ligands are almost at right angles to each other and the bridging oxygen atom forms an angle of 156° with the two vanadium atoms. Comparison of the angles in four μ-oxo complexes shows them to range from 154 to 180° [86,90,92]. Such a variation in structures of metal complexes in the same oxidation state and similar coordination environments suggests that packing considerations and non-bonding interactions are more important in determining this angle than the bonding between the oxygen and the two vanadium centres. The angle subtended by the oxygen of the coordinated ethoxo group is appreciably higher than the tetrahedral angle, a fact which is consistent with the relatively short V - O bond implying some π-donation and partial multiple bond character.

The angles at N(2) and C(5) in the 5-membered chelate ring as well as the bite angles N(1) - V(1) - O(4) and the bite sizes in both the structures are comparable to those for the VL$_2$ structures (Chapter 3.6). In the same way the similar parameters for the 6-membered chelate ring are also comparable. The angles at N(1) in the 6-membered ring are, as expected, larger than in the 5-membered ring. The C(3) - N(1) and C(5) - N(2) bond lengths (1.251 - 1.309Å) are characteristic of double bonds whereas N(1) - N(2) seems to be essentially a single bond in nature. The C(1) - O(3) and C(5) - O(4) distances (1.320 - 1.327Å) compare well with partial double bond character.

TABLE 4.3.1: BOND DISTANCES (Å) FOR STRUCTURES (I) AND (II)

	STRUCTURE - I	STRUCTURE - II
V(1) - O(1)	1.595(3)	1.573(6)
V(1) - O(2)	1.750(3)	1.776(1)
V(1) - O(3)	1.848(2)	1.832(6)
V(1) - O(4)	1.907(2)	1.889(6)
V(1) - N(1)	2.070(3)	2.078(8)
C(3) - N(1)	1.309(4)	1.251(11)
C(5) - N(2)	1.296(4)	1.276(11)
N(1) - N(2)	1.401(4)	1.448(10)
C(1) - O(3)	1.327(4)	1.327(10)
C(5) - O(4)	1.320(4)	1.320(10)

TABLE 4.3.2: BOND ANGLES (°) FOR STRUCTURES (I) AND (II)

	STRUCTURE - I	STRUCTURE - II
O(1) - V(1) - O(2)	107.1(2)	109.2(2)
O(1) - V(1) - O(3)	105.4(1)	104.0(3)
O(1) - V(1) - O(4)	106.8(1)	105.2(3)
O(1) - V(1) - N(1)	97.7(1)	98.3(3)
O(3) - V(1) - O(2)	99.1(1)	95.4(2)
N(1) - V(1) - O(3)	84.2(1)	83.9(3)
O(4) - V(1) - O(3)	143.3(1)	145.0(3)
N(1) - V(1) - O(2)	153.0(1)	151.7(2)
N(1) - V(1) - O(4)	74.6(1)	73.2(3)
V(1) - O(2) - V(2)	-	180.0
V(1) - O(2) - C(18)	139.8(3)	-
V(1) - N(1) - C(3)	127.6(2)	131.8(8)
V(1) - N(1) - N(2)	116.0(3)	116.8(6)
C(5) - N(2) - N(1)	107.8(3)	105.7(8)
N(2) - C(5) - O(4)	121.1(3)	121.4(9)

4.4 MASS SPECTRA

As for the other complexes (Chapters 2 and 3), the mass spectra of the VOLHCl, VOL.OR and $(VOL)_2O$ complexes were used as a quick means to identify their formation. The mass spectra of all the complexes prepared were examined and their characteristic peaks are given in Tables 4.4.1 - 4.4.3. In all cases, the intense molecular ion peaks at m/e were observed. The most interesting feature of the spectra was the presence of the $V^{IV}OL$ as well as dimeric $(V^{IV}OL)_2$, formed on fragmentation of both the vanadium(IV) and vanadium(V) complexes. The dimeric $(VOL)_2$ peaks observed from fragmentation of VOLHCl were especially very intense. It is not difficult to understand the loss of HCl from VOLHCl, OR from VOL.OR and OVOL from $(VOL)_2O$ necessary to produce the apparently stable VOL unit. It is a characteristic feature of the VOL unit that under the conditions of determining the mass spectra these units dimerize to form $(VOL)_2$. They cannot be taken as evidence for the existence of such a structural unit in a dimeric parent complex, because they are observed in complexes which are known to be monomeric (e.g. the crystal structures of VO(Bzac-BH).OEt and $[VO(Bzac-BH)]_2O)$. Analogous dimeric species $[VO(AA)]_2$ where AA is a bidentate ligand, were also observed in the alkoxo-bridged oxovanadium(IV) complexes (Chapter 2.5) which are known not to contain such a structural unit. Peaks of a VL fragment of variable, generally weak, intensity were also observed. In the chlorine containing complexes, the signals due to Cl-isotopes were observed in the molecular ion as well as in the VOL, $(VOL)_2$ and VL fragmentations.

TABLE 4.4.1: CHARACTERISTIC MASS SPECTRAL PEAKS FOR THE VOLHCl COMPLEXES

COMPLEX	MOL. WT.	CHARACTERISTIC PEAKS FOR		
		VOLHCl	VOL	$(VOL)_2$
VO(Bzac-p^{Cl}-BHH)Cl	416.16	416, 420	379, 381	758, 762
VO(HNP-BHH)Cl	391.71	391, 393	355	710
VO(HAP-BHH)Cl	355.68	355, 357	319	638
VO(Sal-BHH)Cl	341.65	341, 343	305	610

TABLE 4.4.2: CHARACTERISTIC MASS SPECTRAL PEAKS FOR THE V^VOL.OR COMPLEXES

COMPLEX	MOL. WT.	CHARACTERISTIC PEAKS FOR			
		VOL.OR	VOL	$(VOL)_2$	$(VOL)_2O$
VO(Bzac-BH).OEt	390.31	390	345	690	706
VO(Bzac-p^{Cl}-BH).OMe	410.73	410, 412	379, 381	-	
VO(dbm-BH).OMe	438.36	438	407	-	
VO(HNP-BH).OMe	386.28	386	355	-	
VO(HNP-p^{Cl}-BH).OMe	420.73	420, 422	389, 391	-	
VO(HAP-BH).OMe	350.25	350	319	638	654
VO(Sal-BH).OMe	336.22	336	305	610	626

TABLE 4.4.3: CHARACTERISTIC MASS SPECTRAL PEAKS FOR THE $(V^V OL)_2O$ COMPLEXES

COMPLEX	MOL. WT.	CHARACTERISTIC PEAKS FOR		
		$(VOL)_2O$	VOL	$(VOL)_2$
[VO(Bzac-BH)]$_2$O	706.50	706	345	690
[VO(Bzac-p^{Cl}-BH)]$_2$O	775.39	775, 779	379, 381	758, 762
[VO(dbm-BH)]$_2$O	830.65	830	407	814
[VO(HNP-BH)]$_2$O	726.50	726	355	710
[VO(HNP-p^{Cl}-BH)]$_2$O	795.39	795, 799	389, 391	778, 782
[VO(HAP-BH)]$_2$O	654.43	654	319	638
[VO(Sal-BH)]$_2$O	626.38	626	305	610

4.5   INFRARED SPECTRA

(a)   GENERAL ASSIGNMENTS

As for the VL_2 complexes, the infrared spectra of the VOLHCl, VOL.OR and $(VOL)_2O$ complexes gave indications about their structure in respect of (i) the presence of the vanadyl oxo function, (ii) the absence of any O - H mode and thus the coordination of enolic and/or phenolic oxygens and (iii) retention of the N - H bond in the singly charged $\underline{LH}^-$ in VOLHCl type complexes.

Knowledge about the positions of $\nu C = N$, $\nu C = C$ (aromatic), $\nu C = O$, $\nu C - O$ (enolic/phenolic) in the spectra for the related systems [Chapter 3.7.2(a)] as well as for the prepared benzoylhydrazone VL_2 complexes [Chapter 3.7.2(b)] and a qualitative comparison with the corresponding free ligand band positions were the basis for the present empirical assignments. The tentative assignments of some principal infrared absorptions for the VOLHCL, VOL.OR and $(VOL)_2O$ complexes are given in Tables 4.5.1 - 4.5.3. As discussed previously (Chapter 3.7.2), the band in the regions 1570-1630, 1535-1555, 1300-1348 and 1355-1395 cm^{-1} are assigned as due to $\nu C = N$, aromatic $\nu C = C$, $\nu C - O$ and $\nu C - N$ respectively. Generally, the C = O stretching frequency lies in the same region as for $\nu C = N$. The decrease in the frequency of $\nu C = N$ upon coordination indicates the coordination of the imine nitrogen in the V - N bond formation[247]. Also the absence of $\nu O - H$ indicates coordination of the deprotonated C - O (enolic/phenolic) function of the ligand through oxygen. The $\nu V = O$, as usual, is characteristic of all the oxovanadium complexes.

(b)   VOLHCl COMPLEXES

For the prepared VOLHCl complexes the bands in the region 975-1000 cm^{-1} (Table 4.5.1) are strong and sharp and are well within the range expected for the V = O stretching frequencies[5]. The infrared spectra of each of the VOLHCl complexes also show broad bands at ~ 3200 cm^{-1} characteristic of $\nu N - H$ stretching[254]. Accordingly, the hydrazone ligand in these

complexes acts as a singly negative tridentate one and is coordinated to the metal ion via the azomethine nitrogen, carbonyl oxygen of the hydrazine part of the Schiff base and the enolic/phenolic oxygen of the ketone part. The νC = N and νC = 0 for these complexes are exhibited in the region 1570-1626 cm^{-1}.

TABLE 4.5.1: SOME CHARACTERISTIC INFRARED FREQUENCES (CM^{-1}) FOR THE VOLHCl COMPLEXES

COMPLEX	$\nu N - H$	TENTATIVE ASSIGNMENTS						
		$\nu C = N$ & $\nu C = 0$	$\nu C = C$	$\nu C - 0$	$\nu C - N^a$	$\nu V = 0$	$\nu V - Cl$
VO(Bzac-p^{Cl}-BHH)Cl	3220 mbr	1600 s 1590 s	1535 s	1325 m	1363 s	998 s	410 ms
VO(HNP-BHH)Cl	3190 mbr	1626 s 1610 s 1588 s 1576 s	1545 s	1301 ms	1345 m	1000 s	420 s
VO(HAP-BHH)Cl	3220 mbr	1605 s 1575 w	1548 s	1315 s	1350 ms	975 s	395 m
VO(Sal-BHH)Cl	3190 mbr	1610 s 1600 sh 1570 ms	1546 s	1325 m	1390 s 1347 w	1000 s	413 ms

a. Due to resonance

(c)   VOL.OR AND (VOL)$_2$O COMPLEXES

All the prepared complexes (Tables 4.5.2 and 4.5.3) exhibit strong bands characteristic of νV = 0 in the region 972-1005 cm^{-1} typical of vanadyl complexes[298]. With respect to the νC = N, νC = C, νC - 0 and νC - N band regions, the spectra of these complexes are very similar to that of the VL$_2$ complexes [Chapter 3.7.2.(b)] containing the same ligands. As expected, the νC = N

present in the free ligand is decreased in each case by about 10-40 cm^{-1} on coordination through N of the azomethine group. Also the absence of any band above 3000 cm^{-1} characteristic of $\nu O - H$ and $\nu N - H$ confirms the ligands being coordinated in the deprotonated L^{2-} form through involvement of the enolic and phenolic oxygens.

In the VOL.OR complexes, the $\nu C- O$ of the coordinated alkoxo group have been assigned (Table 4.5.2) by taking into consideration the C - O stretching band typically found near 1050 cm^{-1} in the free primary alcohols[248] as well as literature values for various metal alkoxides[126,127] and the assignment of $\nu C - O$ (alkoxo) in the prepared $[VO(AA)(OR)]_2$ complexes (Chapter 2.6). Butcher et al.[127] assigned the vibrational frequencies for the symmetric C - O stretches of the $Me_2Sn(OR)_2$ complexes at 1036 cm^{-1} for R = Me and 1045 cm^{-1} for R = Et. The assignment of the $\nu C - O$ (alkoxo) in the range 1015-1047 cm^{-1} is in agreement with the above values. In the $(VOL)_2O$ complexes the apperance of intense bands in the region 725-790 cm^{-1} (which are absent in the VOL<u>H</u>Cl and VOL.OR complexes) may be associated with the group OV - O - VO in agreement with the similar observations in the $[VO(Sal-OAP)]_2O$ [92]. Partially hydrolysed VOL.OR complexes due to the moisture in the nujol also exhibit weak bands in this region due to the formation of small amounts of the μ-oxo-complexes.

(d)   V-DONOR VIBRATIONS

Following the $\nu V - O$ and $\nu V - N$ assignments for the same coordinated L^{2-} in the VL_2 complexes and the literature values of some related systems [Chapter 3.7.2(g)], the relatively strong absorptions in the regions 420-470 and 470-580 cm^{-1} for the VOL<u>H</u>Cl, VOL.OR and $(VOL)_2O$ complexes may tentatively be attributed to the $\nu V - O$ and $\nu V - N$, respectively. This, however, on the basis of the larger V - N distances than the V - O distances found in the crystal structures of VO(Bzac-BH).OEt and $[VO(Bzac-BH)]_2O$ (Section 4.3) might be in the reverse order.

TABLE 4.5.2: SOME CHARACTERISTIC INFRARED FREQUENCIES (CM^{-1})
FOR THE VOL.OR COMPLEXES

COMPLEX \ TENTATIVE ASSIGNMENTS	$\nu C = N$	$\nu C = C$	$\nu C - O$ (enolic/ phenolic)	$\nu C - N$[a]	$\nu C - O$ (alkoxo)	$\nu V = O$	$\nu V - OR$
VO(Bzac-BH).OEt	1600 ms 1591 s 1568 ms	1550 s	1336 ms	1370 s	1029 m 1037 m	986 s	612 m
VO(Bzac-p^{Cl}-BH).OMe	1598 s 1584 s 1575 m	1551 s	1340 m	1370 m	1015 m	1000 s	620 ssh
VO(dbm-BH).OMe	1604 m 1594 ms 1589 ms 1564 s	1544 s	1348 s	1392 ms	1025 m	1003 m 935 vs	622s
VO(HNP-BH).OMe	1620 ms 1608)s 1600)	1550 s	1335 ms	1393 m	1032 s	975 vs	633 s
VO(HNP-p^{Cl}-BH).OMe	1625 ms 1608 s 1598 ssh 1590 sh	1550 s	1330 s	1365 m	1033 s	982 s	627 s
VO(HAP-BH).OMe	1601 s 1590 s 1580 s	1550 s	1340 m 1312 s	1355 s	1047 s 1015 sh	997 s	610 ms
VO(Sal-BH).OMe	1610 s 1577 sh	1555 s	1343 s	1355 s	1026 s	972 s	626 mssh

ET = C_2H_5; Me = CH_3; [a] due to resonance

TABLE 4.5.3: SOME CHARACTERISTIC INFRARED FREQUENCIES (CM^{-1})
FOR THE (VOL)$_2$0 COMPLEXES

(VOL)$_2$0 COMPLEX OF L =	TENTATIVE ASSIGNMENTS					
	νC = N	ν C = C	νC - O	νC - N[a]	νV = 0	νV - 0 - V
Bzac-BH	1604 msh 1594 ms 1579 w	1557 s	1337 m	1376 s	989 s	790 s
Bzac-p^{Cl}-BH	1599 s 1588 ssh 1580 msh	1553 s	1338 ms	1370 ms	990 s	726 s
dbm-BH	1604 ms 1594 s 1570 s	1550 s	1343 ms	1377 s	1000 s	725 s
HNP-BH	1620 m 1608 s 1598 s	1552 s	1334 ms	1390 s	999s	740 s
HNP-p^{Cl}-BH	1622 ms 1608 s 1597 ssh	1553 s	1330 s	1390 m	1002 vs	760 s
HAP-BH	1604 s 1594 s 1570 s	1555 s	1340 m	1365 s	1005 vs	755 s
Sal-BH	1610 s 1598 ssh	1555 s	1345 s	1370 sh	999s	770 m

[a]. Due to resonance

The bands in the region 610-633 cm^{-1} for the VOL.OR complexes have been assigned tentatively as due to the νV - O(R) stretching modes in comparison to such modes in the VOCl$_2$.OR[298] and other related compounds[299,300].

For the VOL$\underline{H}$Cl complexes, the fairly strong and sharp band appearing in the region 395-420 cm^{-1}, which are absent in the VOL.OR and (VOL)$_2$O complexes, may be assigned to the V - Cl stretching modes. This is in agreement with the νV - Cl observed by other workers[80,300,301], in several vanadium comp- lexes, such as VCl$_4$, VCl$_4$(L)$_2$ (L = S donor ligands) and VOCl$_3$.B (B = a bidentate ligand). In the related TiCl$_4$, the νTi-Cl was reported to be at 386-495 cm^{-1} [302]. In these compounds, containing more than one coordinated chloro groups, two V - Cl stretching modes are reported, but in the present VOL$\underline{H}$Cl complexes containing a single coordinated chloro group, only one mode is obtained. The presence of this νV - Cl confirms that the Cl$^-$ is coordinated to the vanadium and not present in the singly deprotonated ligand L$\underline{H}^-$ in the form of a hydrochloride (-$\overset{|}{N}$- HCl).

4.6   ELECTRONIC SPECTRA

The electronic spectra of d^1-VOL$\underline{H}$Cl and d^o VOL.OR and (VOL)$_2$O complexes, as expected, are quite different and attributed to different types of electronic transitions in them.

(a)   VOL$\underline{H}$Cl COMPLEXES

Because of the insolubility, the electronic spectra of the VOL$\underline{H}$Cl comp- lexes were examined in nujol mulls. The spectra show a broad shoulder which possibly contains two bands extending from ~ 750-550 nm. Besides this broad shoulder, the spectra also show a sharp band in the region 487-416 nm. The four complexes of this type have similar spectra with two bands, I and II, appearing as very broad shoulders. The general appearance of the spectra are similar to those observed by many others[5,37,41,43,140] for several related vanadyl complexes. The spectra can be interpreted in terms of the energy

level scheme given by Ballhausen and Gray (Chapter 2.7) and accordingly band I in the region $\sim$ 736-710, band II in the region $\sim$ 600-585 and band III in the region 487-416 nm may be assigned to the $d_{xy} \rightarrow d_{yz}, d_{xz}, d_{xy} \rightarrow d_{x^2-y^2}$ and $d_{xy} \rightarrow d_{z^2}$ transitions respectively. The fourth band below 360 nm appears to parallel quite closely the intraligand $\pi^* \leftarrow \pi$ transition found in the spectra of the free ligands and of the same ligands in the VL_2 complexes. The electronic spectral data and band assignments for the VOLHCl complexes are given in Table 4.6.1. However, such assignments are based on the unresolved d-d bands in the region 750-550 nm in the solid state, and although reasonable, can only be considered as tentative.

TABLE 4.6.1: ELECTRONIC SPECTRAL DATA FOR VOLHCl COMPLEXES (NUJOL MULL)

COMPLEX	BAND I $^2E(1) \leftarrow {}^2B_2$ $e\pi^* \leftarrow b_2$ $xz, yz \leftarrow xy$	BAND II $^2B_1 \leftarrow {}^2B_2$ $b_1^* \leftarrow b_2$ $x^2-y^2 \leftarrow xy$	BAND III $^2A_1 \leftarrow {}^2B_2$ $^1a_1^* \leftarrow b_2$ $z^2 \leftarrow xy$	BAND IV a Intra- b ligand c transi- d tion
VO(Bzac-p^{Cl}-BHH)Cl	$\sim$ 710 br	$\sim$ 585 br	416	266
VO(HNP-BHH)Cl	$\sim$ 740 br	$\sim$ 600 br	487	354
VO(HAP-BHH)Cl	$\sim$ 732 br	$\sim$ 585 br	427	336
VO(Sal-BHH)Cl	$\sim$ 736 br	$\sim$ 593 br	446	350

a. Band number

b. Ballhausen-Gray (B-G) M.O. assignments

c. Transition in C_{4v} symmetry

d. Transition in d-orbitals.

(b) VOL.OR AND (VOL)$_2$O COMPLEXES

Being a d^0 system the vanadium(V) complexes show no d-d transition in

the visible region and are coloured only through their intense charge transfer absorptions tailing in from the ultraviolet. The spectra of VOL.OR and $(VOL)_2O$ complexes in dichloromethane are very similar in shape which indicates that the electronic structures are the same in all these complexes. From this gross spectral similarity, it can be suggested that these complexes in solution also have the same square pyramidal structures observed in the crystal structures of VO(Bzac-BH).OEt and $[VO(Bzac-BH)]_2O$ (Section 4.3). Both types of complexes generally exhibit three intense bands in their electronic spectra.

As expected for the charge transfer bands, the molar absorptivity, a_M was found to be very high in each of the VOL.OR and $(VOL)_2O$ complexes being of the order of 10^4 mol $dm^{-3}cm^{-1}$. Like in the VL_2 complexes (Chapter 3.7.3), the first band observed in the present oxidizing vanadium(V) complexes of the same negatively charged ligands is assigned to the LMCT. The other two bands designated as I.L.T.(1) and I.L.T.(2) have been assigned to $\pi - \pi^*$ intraligand transitions by a qualitative comparison with the free ligand absorptions. It is possible for the low-energy I.L.T.(1) to possess some contribution from the charge transfer transition. The electronic spectral data of these complexes, including the band assignments, are given in Table 4.6.2. The spectra of some of these complexes are shown in Figure 4.6.1. It can be noted that several vanadium(V) complexes, such as $VOCl_2.L$, $VOCl.L_2$ (L = a monobasic Schiff base), $VO(OH)(oxinate)_2$ and $VOCl_3.X^{82,303-4}$ are reported to have shown absorption maxima at as longer wavelength as 550 nm presumably arising from the LMCT.

Compared to that for the related VL_2 complexes (see Table 4.6.2), the higher energy of the LMCT bands in the present vanadium(V) complexes is due to a π-donation from the oxo ligand, thus reducing the acceptor ability of the vanadium centre. Thus, surprisingly, although in the formal +5 oxidation state, the π-donation from the oxo function makes it less accepting than V^{4+}.
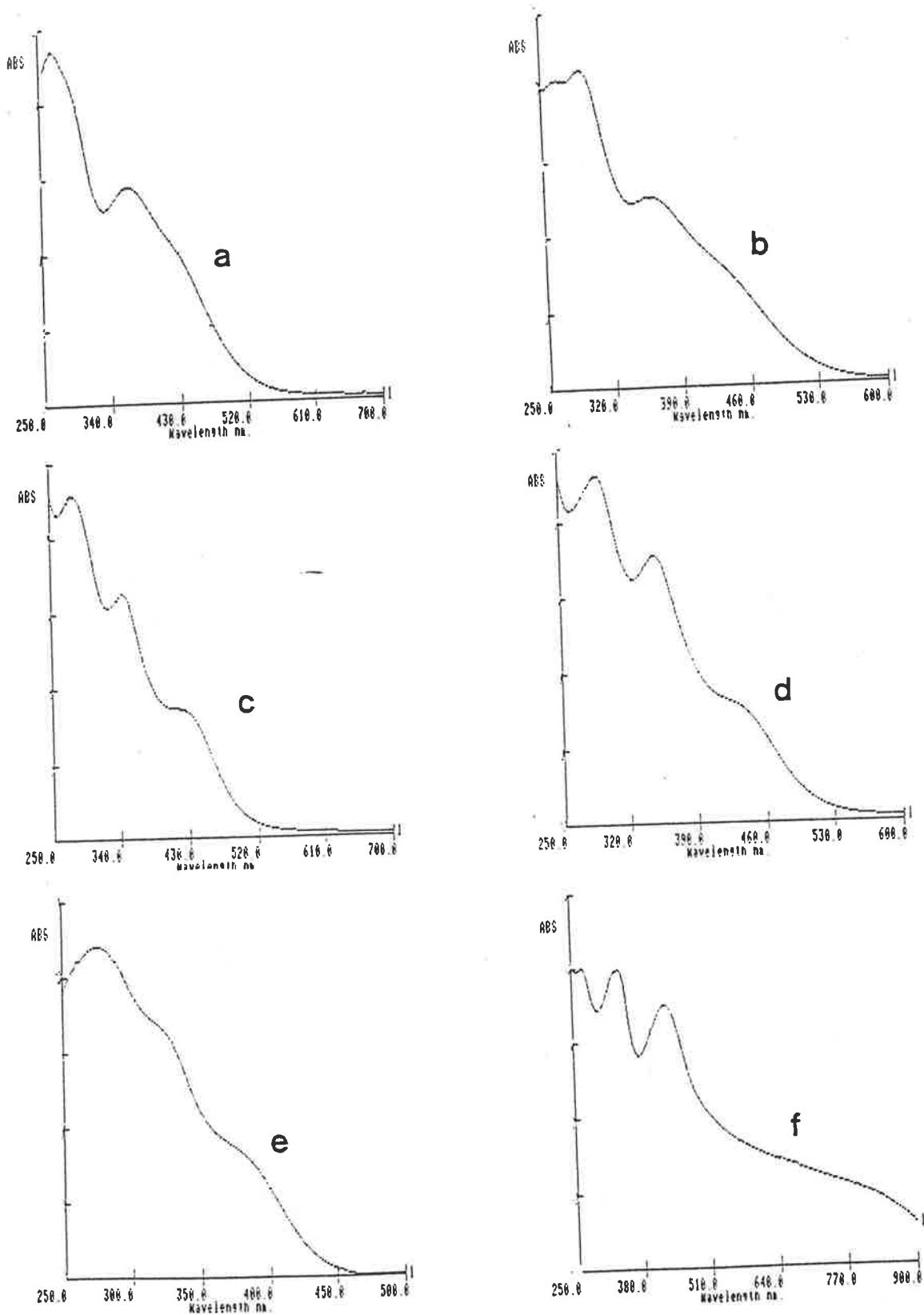
Figure 4.6.1: Electronic spectra of a. VO(Bzac-BH).OEt; b. [VO(Bzac-BH)]$_2$O; c. VO(HNP-BH).OMe; d. [VO(HNP-BH)]$_2$O and e. VO(HAP-BH).OMe in dichloromethane. f. VO(HAP-BHH)Cl in nujol mull.

TABLE 4.6.2: ELECTRONIC SPECTRAL DATA FOR THE VOL.OR AND
(VOL)$_2$0 COMPLEXES (SOLVENT = CH$_2$Cl$_2$)

LIGAND (L)	COMPLEX	BAND POSITIONS (nm) WITH LOG a$_M$ IN PARENTHESES[a]		
		C.T.	I.L.T.(1)	I.L.T.(2)
Bzac-BH	VOL.OEt	~ 430[b] (~ 3.92)	363 (4.08)	265 (4.30)
	(VOL)$_2$0	~ 430[b]	360 (4.42)	292 (4.65)
	VL$_2$[c]	538, 390	352	-
Bzac-p^{Cl}-BH	VOL.OMe	~ 440[b] (~ 3.96)	364 (4.17)	283 (4.39)
	(VOL)$_2$0	~ 440[b]	363 (4.48)	289 (4.71)
dbm-BH	VOL.OMe	~ 410 fl. (4.11)	~ 330[b]	270 (4.46)
	(VOL)$_2$0	~ 415[b] (~ 4.25)	~ 370[b]	284 (4.72)
	VL$_2$[c]	560, 400	369	-
HNP-BH	VOL.OMe	~ 413 sh (~ 4.00)	343 (4.27)	282 (4.42)
	(VOL)$_2$0	~ 415 sh (~ 4.21)	349 (4.55)	288 (4.67)
	VL$_2$[c]	540	~ 360 sh	325
HNP-p^{Cl}-BH	VOL.OMe	~ 420 sh (~ 4.04)	347 (4.35)	288 (4.48)
	(VOL)$_2$0	421 (4.38)	339 (4.61)	277 (4.78)
HAP-BH	VOL.OMe	~ 380[b] (~ 3.97)	~ 320 sh (~ 4.26)	275 (4.37)
	(VOL)$_2$0	~ 386[b]	~ 322[b]	283 (4.71)
	VL$_2$[c]	~ 561[b]	~ 342 sh	293
Sal-BH	VOL.OMe	~ 385 sh (~ 3.93)	~ 320 sh (~ 4.25)	271 (4.37)
	(VOL)$_2$0	~ 390[b]	327 sh (~ 4.62)	285 (4.74)

a. a$_M$ in mol. dm^{-3}cm^{-1}

b. Broad shoulder

c. For comparison

C.T. Charge transfer

I.L.T. Intraligand transition

4.7   ELECTRON SPIN RESONANCE AND MAGNETIC STUDIES

Although the mass spectra and the insolubility of the VOLHCl complexes in common organic solvents, except when assisted by oxidation, raises the possibility of polymerization, the room and low temperature E.S.R. spectra (Figures 4.7.1 and 4.7.2) of the undiluted powders are characteristic of monomeric entities.   Unlike very broad E.S.R. signals for the dimeric [VO(AA)(OR)]$_2$ complexes (Chapter 2.8), these VOLHCl spectra are sharp and comparable to the spectra for the monomeric complexes, e.g. VO(acac)$_2$ under the same conditions.   The coordination of Cl$^-$ to the vanadium centre satisfies the normal coordination requirements for vanadium to attain a generally occurring square pyramidal configuration.

These complexes were also subjected to the magnetic measurements using a Gouy balance.   Although the magnetic moment values (Table 4.7.1) appear to be below the normal value, they are within our experimental error of the spin-only moment of 1.73 B.M. for V^{4+}.   This also indicates that there is no dipolar interaction, at least at room temperature, and thus a monomeric structure with five coordinate arrangement around V^{4+} is most likely.   The crystal structure of an analogous compound VO(N-salicylidene-L-alaninato)(H$_2$O) showed the molecule to be monomeric[297].

TABLE 4.7.1: MAGNETIC MOMENT AND 'g' VALUES FOR THE VOLHCl COMPLEXES

COMPLEX	MAGNETIC DATA			'g' VALUES
	TEMPERATURE (K)	$x_M \times 10^6$ (c.g.s.u.)	μ (B.M.)	
VO(Bzac-p^{Cl}-BHH)Cl	300.2	1163.4	1.68	1.985
VO(HNP-BHH)Cl	298.2	1176.6	1.68	1.983
VO(HAP-BHH)Cl	297.0	1199.6	1.70	1.982
VO(Sal-BHH)Cl	303.3	1146.0	1.67	1.987
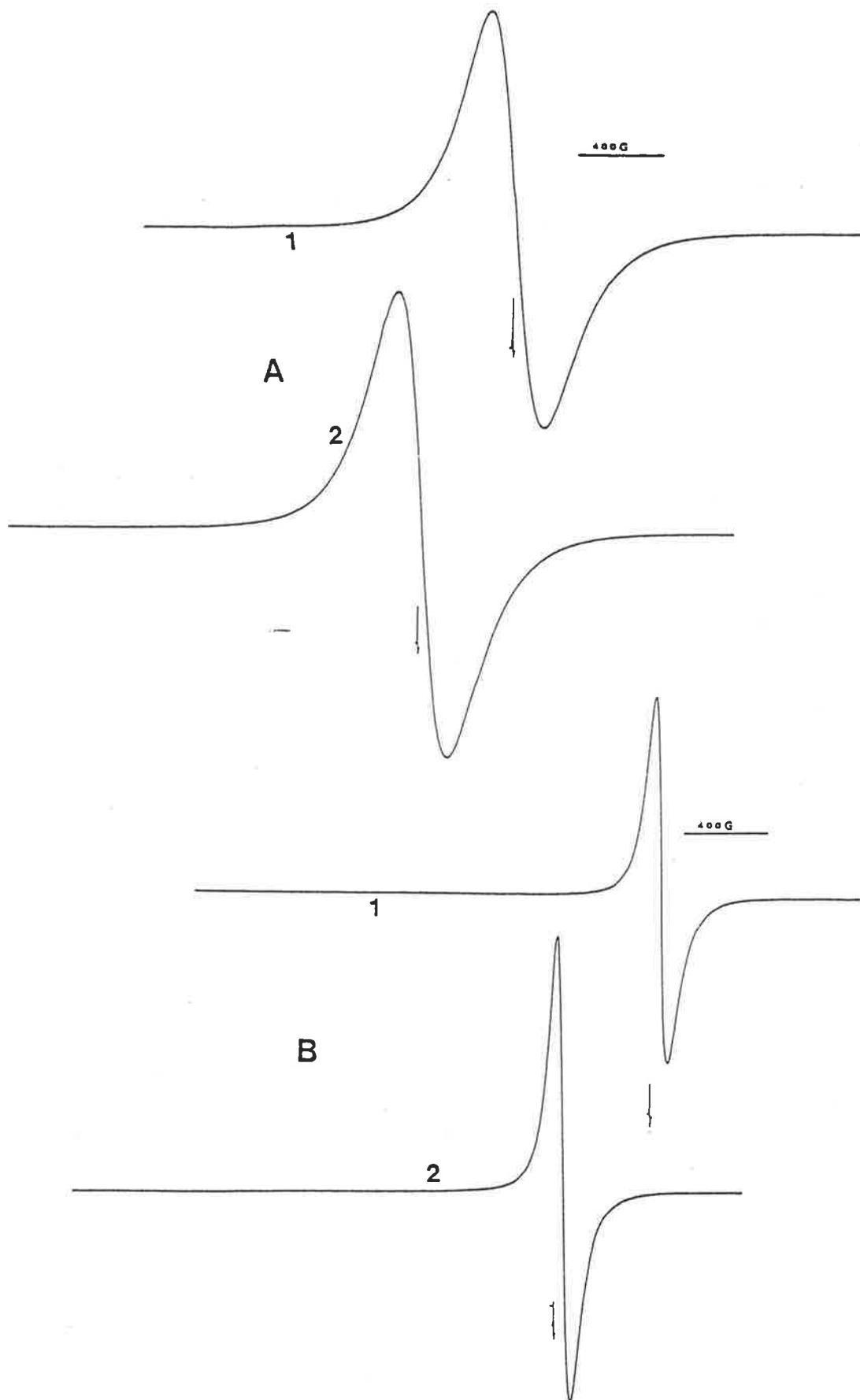
Figure 4.7.1: X-band E.S.R. spectra of A. VO(Bzac-p^{Cl}-BH$\underline{H}$)Cl and B. VO(HNP-BH$\underline{H}$)Cl (powdered solid). [1. at room temperature; 2. at -160°C]. ($\imath$ DPPH).
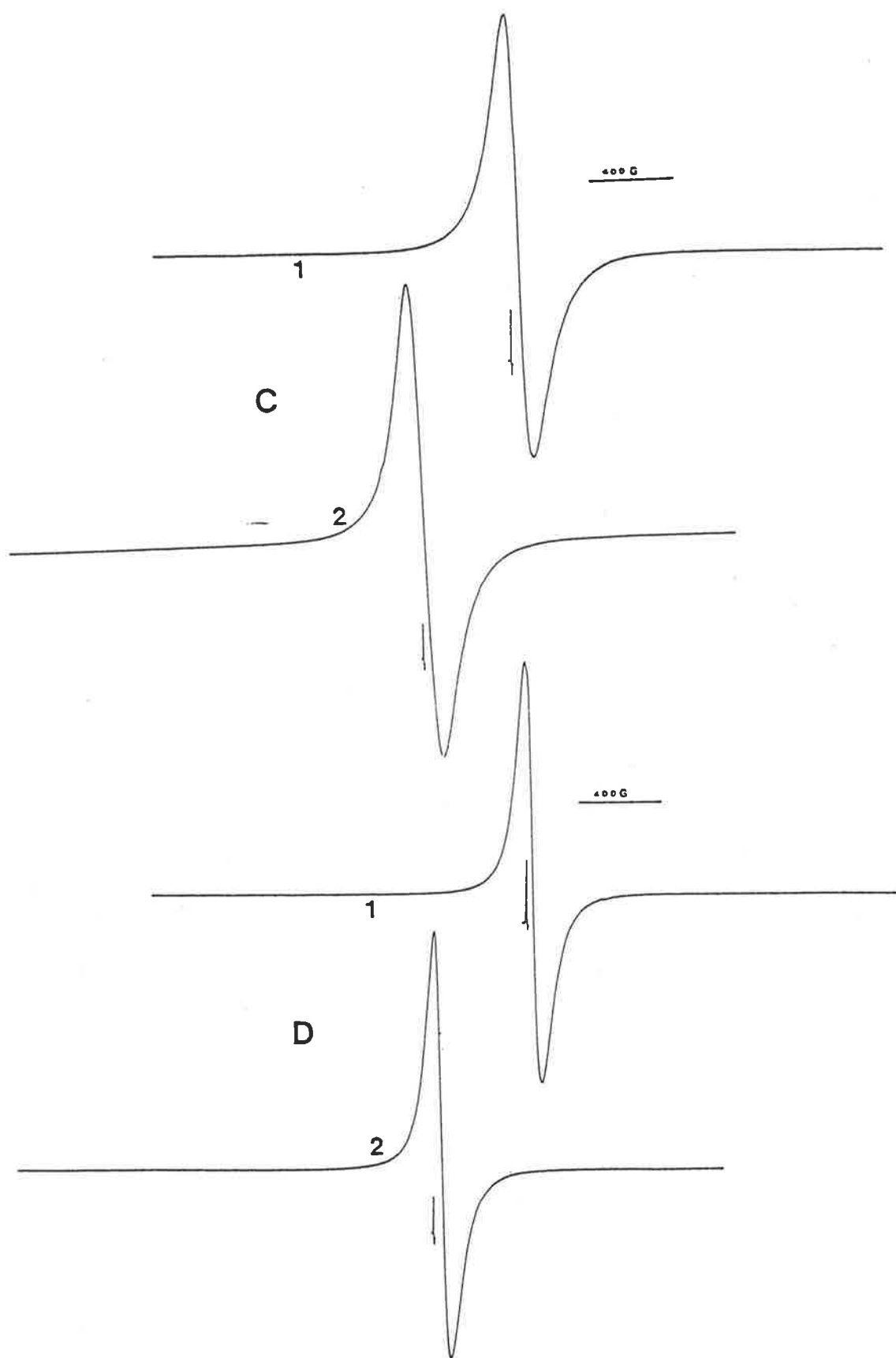
Figure 4.7.2: X-band E.S.R. spectra of C. VO(HAP-BHH)Cl and D. VO(Sal-BHH)Cl (powdered solid). [1. at room temperature; 2. at -160°C]. (↓ DPPH).

4.8 NUCLEAR MAGNETIC RESONANCE SPECTRA

As has been stated earlier [Section 4.2(b)], the alkoxo (tridentate Schiff base) oxovanadium(IV) complexes, in the presence of a trace amount of water, hydrolyse readily to the dimeric oxo-bridged $(VOL)_2O$ complexes. The reaction is reversible and the $(VOL)_2O$ dimers, in the presence of an alcohol, easily undergo alcoholysis reactions to give the parent VOL.OR monomers. The reaction equilibrium,

$$2 \text{ VOL.OR } + H_2O \xrightarrow[]{CDCl_3} (VOL)_2O + 2 \text{ ROH } \dots\dots(1)$$
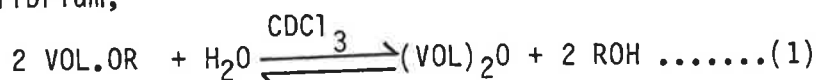
as well as the characterization of the molecules, have been studied by means of N.M.R spectra. In solutions in which the alkoxide is partially hydrolysed, the $\underline{CH}_3$ and/or $\underline{CH}$ protons of the tridentate ligand are present in two different environments. These are designated as (a) for the alkoxo monomer and (o) for the oxo-bridged dimer and are sufficiently resolved to enable study of the equilibrium by the N.M.R spectra. The assignment of the observed resonance signals was verified by determining the N.M.R. spectra in $CDCl_3$ solution and in the presence of alcohol, deuterated alcohol, water or deuterated water. In addition, all the [1]H-N.M.R. spectra of the VOL.OR and $(VOL)_2O$ complexes showed aromatic resonances. Integrations of peak areas were consistent with the proposed formulations.

The VOL.OR complexes also show N.M.R. peaks characteristic of the protons of the alkoxo group and of the free alcohol, which also indicate the presence of the above equilibrium (1). The relative intensities of these peaks depend on the extent of this equilibrium. The peaks obtained from the spectra of $VO(Bzac-BH).OCH_2CH_3$ in $CDCl_3$, and in $CDCl_3$, to which a trace amount of dry ethanol was added are listed in Table 4.8.1. As can be seen from this Table, in $CDCl_3$ there is a quartet at 5.53 p.p.m. characteristic of methylene $(\alpha-)$ protons of the $CH_3\underline{CH}_2O$ group in agreement with the proposed structure. In addition, there are resonances due to $\underline{CH}_3$ (a) and $\underline{CH}$ (a) as well as minor peaks due to $\underline{CH}_3$ (o) and $\underline{CH}$ (o). Addition of a trace amount of dry ethanol to the $CDCl_3$ solution intensifies the peaks due to $\underline{CH}_3$ (a) and $\underline{CH}$ (a) protons as

well as the peak due to OCH_2CH_3, whilst the peaks due to CH_3 (o) and CH (o) are weakened indicating shifting of the equilibrium (1) towards the ethoxo monomer. The increase in the intensity ratio (a)/(o) of the peaks due to CH_3 and CH protons indicates the conversion of $(VOL)_2O$ to VOL.OEt in the presence of ethanol. The relative intensity of the peak due to α-protons of the ethoxo group, CH_3CH_2O, with respect to CH_3 (o), is also increased as expected because of adding ethanol. The peaks, due to free CH_3CH_2OH and CH_3CH_2OH protons which were present in the $CDCl_3$ spectrum, as a result of slight hydrolysis, are strongly intensified due to the presence of excess added ethanol and this helps in confirming identification of these peaks. Figure 4.8.1 shows the spectra of $VO(Bzac-BH).OCH_2CH_3$ in $CDCl_3$ and in $CDCl_3$ + trace dry CH_3CH_2OH and of $[VO(Bzac-BH)]_2O$ in $CDCl_3$.

When the $CDCl_3$ solution of $VO(Bzac-BH).OCH_2CH_3$ is shaken with a drop of water, the peaks, due to CH_3 (o) and CH (o) protons are enhanced while that due to CH_3 (a), CH (a) and OCH_2CH_3 protons disappear. This indicates complete conversion of the alkoxo compound to the oxo-bridged dimer. All peaks in the spectra assigned to various protons bound to the oxo-bridged dimer are confirmed by comparison with the spectrum of the oxo-compound.

Similar behaviour was observed with the other $VOL.OCH_3$ methoxo complexes. The data for the ^1H-N.M.R. of some $VOL.OCH_3$ and $(VOL)_2O$ are given in Table 4.8.2. Like $VO(Bzac-BH).OCH_2CH_3$, the $VO(dbm-BH).OCH_3$ and $VO(HAP-BH).OCH_3$ in $CDCl_3$ show the presence of CH (o) and CH_3 (o) signals, respectively, which disappear or diminish on addition of a trace of free CH_3OH to the experimental $CDCl_3$ solution. The appearance of CH (o) and CH_3 (o), respectively, at the same δ-values for the corresponding $[VO(dbm-BH)]_2O$ and $[VO(HAP-BH)]_2O$ complexes confirms identification of such signals. In some cases, the CH (o) signal was not observed or seemed to be superimposed with the aromatic peaks. The resonances due to the coordinated OCH_3 group in various complexes appeared at about 5.3 p.p.m., the intensity of which increases, as expected, on adding a trace of CH_3OH to the solution.

The lability of the alkoxo group can be demonstrated by adding an excess of CD_3OD to the experimental solution. For example, in the spectrum of VO(Sal-BH).OCH_3 in the presence of excess CD_3OD, the OCH_3 signal disappears and the CH_3OH signal, which in $CDCl_3$ is at 1.11 p.p.m., shifts to 4.28 p.p.m. (Figure 4.8.2) and is increased in intensity, presumably due to alcoholysis of the oxo-compound. The change in the chemical shift is probably due to the different hydrogen bonding environment in the presence of an excess of CD_3OD.

TABLE 4.8.1: ^{1}H-N.M.R. OF VO(Bzac-BH).OCH_2CH_3 AND [VO(Bzac-BH)]$_2$O

PROTONS	VOL(OCH_2CH_3)				$(VOL)_2O$
	In $CDCl_3$		In $CDCl_3$ + ethanol		In $CDCl_3$
	δ (ppm)	Ratio (a)/(o)	δ (ppm)	Ratio (a)/(o)	δ (ppm)
CH_3 (a)	2.69		2.69		-
		4.0		9.6	
CH_3 (o)	2.23		2.17		2.15
CH (a)	6.45		6.45		-
		4.0		14.8	
CH (o)	6.34		6.34		6.36
CH_3CH_2O	5.53(q)	~ 3.0	5.51(q)	~ 5.0	-
CH_3CH_2OH	3.73(q)	trace	3.73(q)	excess	-

(a) : Proton signals from VOL.OCH_2CH_3

(o) : Proton signals from $(VOL)_2O$

+   . Relative intensity with respect to CH_3 (o)

TABLE 4.8.2: ¹H-N.M.R. OF VOL.OCH₃ AND (VOL)₂O COMPLEXES

PROTONS	VOL.OMe					(VOL)₂O
	CDCl₃		CDCl₃ + (trace) MeOH		CDCl₃ + trace MeOH + excess CD₃OD	CDCl₃
	δ (ppm)	Relative Intensity (1,2)	δ (ppm)	Relative Intensity (1,2)	δ (ppm)	δ (ppm)
[1]	[2]	[3]	[4]	[5]	[6]	[7]
FOR L = dbm-BH:						
C$\underline{H}$ (a)	6.69	1.8*	6.69	∝*		
C$\underline{H}$ (o)	6.59	-			6.59	6.59
OC$\underline{H_3}$	5.31	1.7[1]	5.31	2.1[1]	-	-
C$\underline{H_3}$OH	3.50	1.9[1]	3.50	21.3[1] (excess)	3.40 (shifted)	-
CH₃O$\underline{H}$	1.25	0.2[1]	1.25	2.3[1] (excess)	4.50 (shifted)	
FOR L = HNP-BH:						
C$\underline{H}$ (a)	9.93					9.86[b]
OC$\underline{H_3}$ (a)	5.31					-
C$\underline{H_3}$OH	3.49					3.41[b]
CH₃O$\underline{H}$	1.27					4.41[b] (shifted)

	[1]	[2]	[3]	[4]	[5]	[6]	[7]

FOR L = HAP-BH:

	[1]	[2]	[3]	[4]	[5]	[6]	[7]
CH$_3$ (a)	3.02			3.02			
			6.6*		35.0*		
CH$_3$ (o)	2.28			2.28			2.28
OCH$_3$	5.23	2.4^2		5.2	12.0^2		
CH$_3$OH	3.48	1.2^2		3.48	64.3^2 (excess)		
CH$_3$OH	1.06	0.15^2		1.42	8.7^2 (excess)		

FOR L = Sal-BH:

	[1]	[2]	[3]	[4]	[5]	[6]	[7]
CH (a)	9.08			9.08		8.94	
CH (o)	c			c		c	c
OCH$_3$	5.32	3.6^1		5.32	4.2^1	-	
CH$_3$OH	3.49	10.6^1		3.49	22.5^1 (excess)	3.44	
CH$_3$OH	1.11	1.1^1		1.12	1.9^1 (excess)	4.28 (shifted)	

(a) Proton signals from VOL.OR

(o) Proton signals from (VOL)$_2$O

*   Intensity ratio (a)/(o)

1. Relative intensity w.r.t. CH (a) [CH (o) absent or not distinct]

2. Relative intensity w.r.t. CH$_3$ (o)

b. Solvent in this case is CDCl$_3$ + CD$_3$OD

c. CH (o) seems to be superimposed with aromatic peaks.
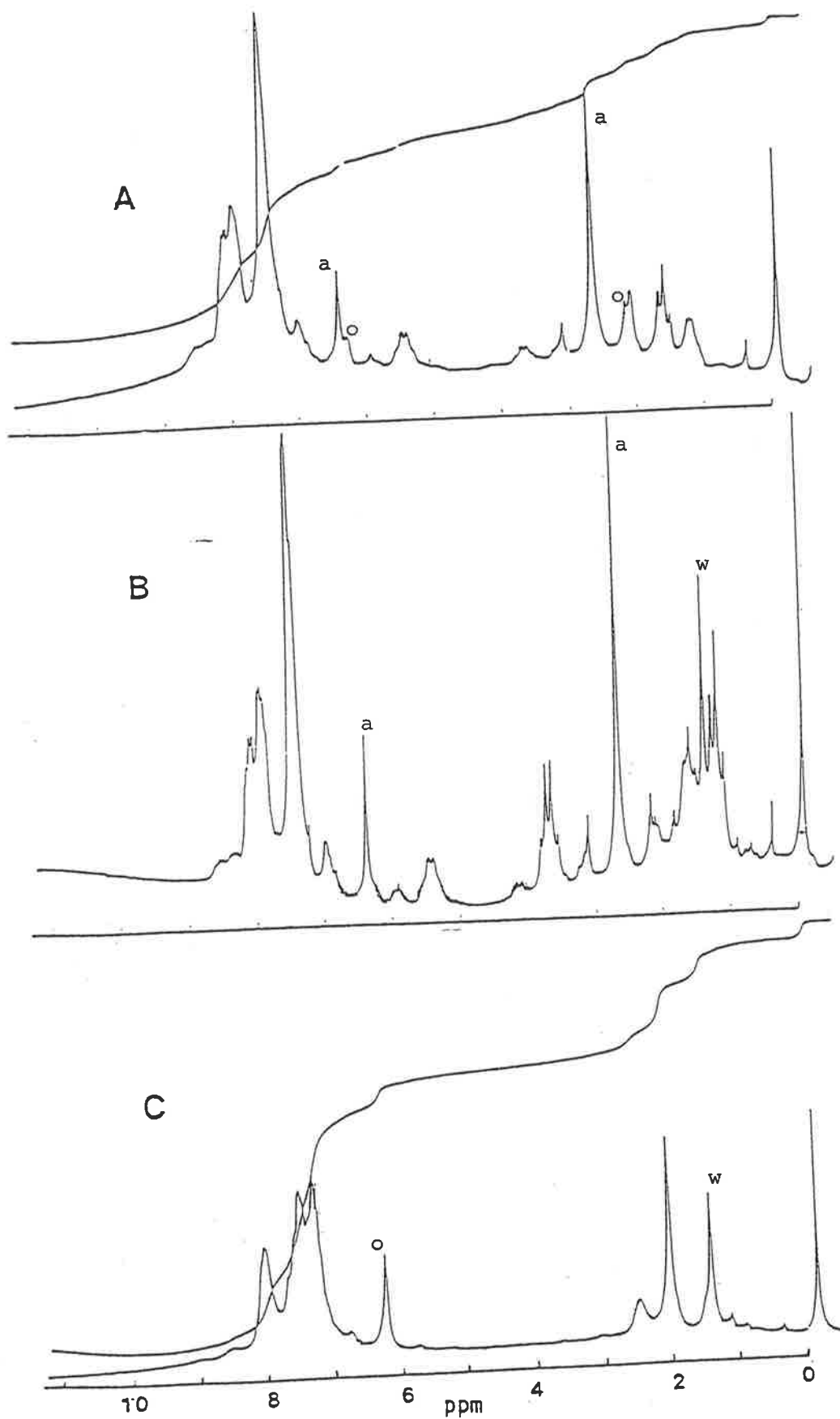
Figure 4.8.1: ^{1}H-N.M.R. spectra of A. VO(Bzac-BH).OCH$_2$CH$_3$ in CDCl$_3$; B. on adding trace of C$_2$H$_5$OH to A and C. [VO(Bzac-BH)]$_2$O in CDCl$_3$. [w. due to H$_2$O in CDCl$_3$; a. and o. protons from respectively alkoxo-and oxo-complexes].
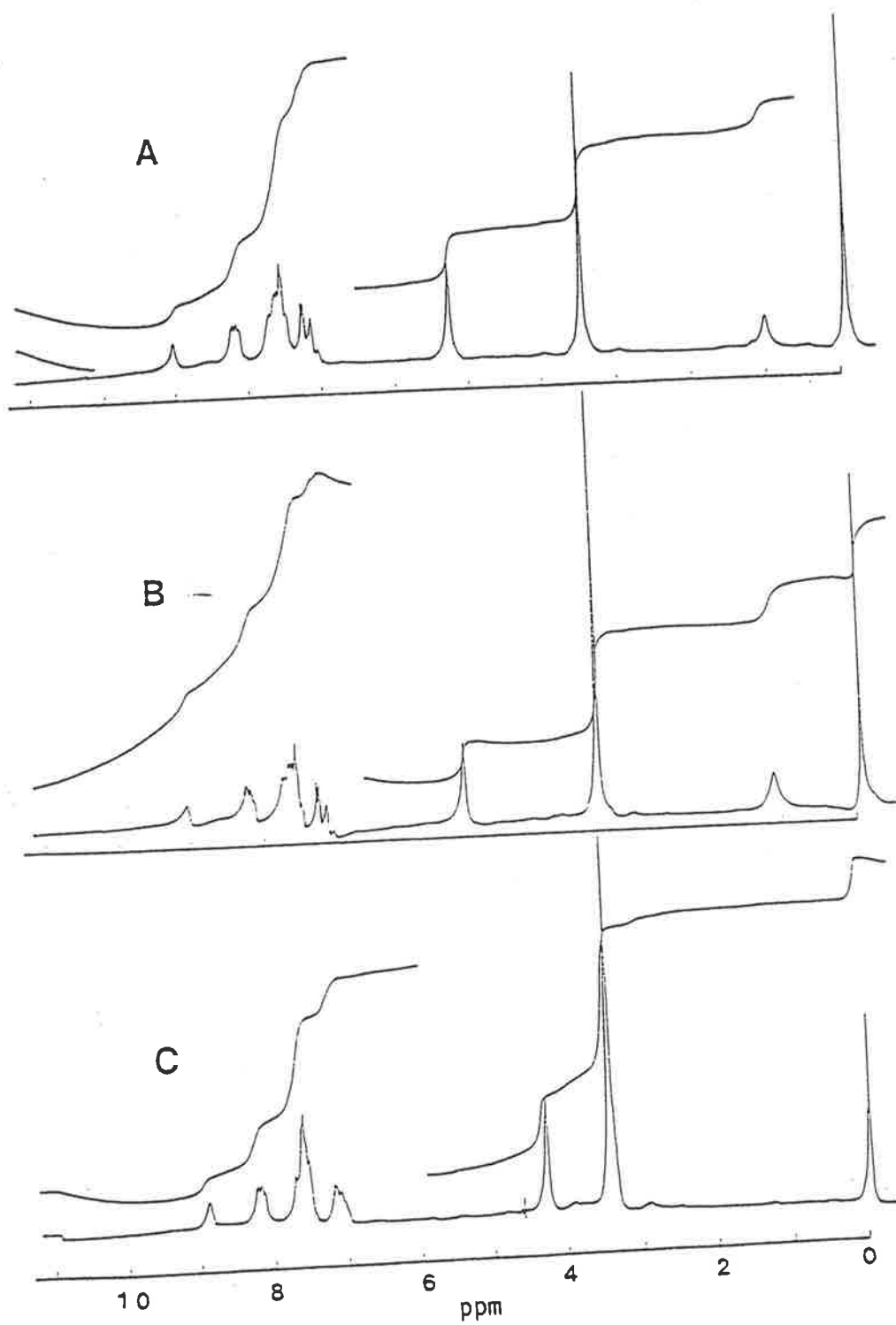
Figure 4.8.2: ^{1}H-N.M.R. spectra of VO(Sal-BH).OCH$_3$ in A. CDCl$_3$; B. CDCl$_3$ + trace CH$_3$OH and C. CDCl$_3$ + trace CH$_3$OH + excess CD$_3$OD.

CHAPTER 5

ELECTROCHEMISTRY

5.1 INTRODUCTION

Many transition metal complexes undergo electron-transfer (oxidation-reduction) reactions between various stable oxidation states. Such reactions can be reversible, quasi-reversible or irreversible. The electrochemistry of several of the vanadium(IV) and -(V) complexes prepared in the present work were studied in order to investigate the electron transfer characteristics of these complexes. It can be mentioned that little information is available about the electron-transfer properties of the non-vanadyl vanadium(IV) complexes.

The cyclic voltammograms of all the VL_2 complexes in DMSO (or CH_3CN) show reversible or quasi-reversible behaviour in the (-)0.050 - (-)0.400V vs. S.C.E. potential range. The oxovanadium(IV) and -(V) complexes do not show such waves in this region. The vanadium(V) complexes are reduced at more positive potentials, whereas oxovanadium(IV) complexes are reduced, usually irreversibly at potentials more negative than -0.4V[27,305-307]. Thus, the electrochemical techniques can be used both to characterize as well as quantitatively estimate the non-vanadyl vanadium(IV) complexes.

5.2 THE ELECTROCHEMICAL TECHNIQUES

The technique of voltammetry utilizes a three-electrode system consisting of a polarized electrode (the working electrode; in this work a circular platinum or rarely glassy carbon electrodes were used as the working electrode) on to which a potential is applied, a counter electrode (platinum wire) and a reference electrode (usually a saturated calomel electrode). This method investigates the oxidation or reduction of a chemical species at the working electrode as the potential is varied.

Cyclic voltammetry (C.V.) is capable of generating a new species during forward scan and then examining its behaviour on the reverse and subsequent scans. Figure 5.2.1A shows a typical response signal for a cyclic voltammogram which also defines the anodic and cathodic peak potentials (E_{pa}, E_{pc}) and currents (i_{pa}, i_{pc}). Electrochemical reactions may generate an intermediate which undergoes further chemical reactions. One of the most useful aspect of cyclic voltammetry is the ability to diagnose such reactions and study the products and reaction kinetics. The formal reduction potential ($E^{\circ'}$) or the half-wave potential ($E_{1/2}$) for a reversible couple is centred between the anodic and cathodic potentials. Thus,

$$E_{1/2} \text{ (or } E^{\circ'}) = (E_{pa} + E_{pc})/2 \ldots\ldots\ldots\ldots(1).$$

A redox couple in which both species are stable and rapidly exchange electrons with the working electrode is termed an electrochemically reversible couple. The number of electrons transferred (n) during the electrode reaction for a reversible couple can be determined from the separation between the anodic and cathodic peak potentials from,

$$\Delta E_p = E_{pa} - E_{pc} = \frac{0.058}{n} \ldots\ldots\ldots\ldots\ldots(2).$$

Frequently, slow electron transfer causes equation (2) not to be obeyed strictly and in such cases, n cannot be determined by this method, however $E^{\circ'}$ or $E_{1/2}$ can still be estimated from equation (1). Controlled potential electrolysis, however, can be used to estimate the value of n by determining the charge transferred. In the controlled potential electrolysis (C.P.E.) technique the analyte is completely electrolysed by applying a fixed potential to an electrode, usually having a large surface area (in this work a platinum gauze was used) to minimize electrolysis time. This is an excellent technique for determining the amount of material, N (no. of moles), and the number of electrons, n, transferred per molecule or ion by means of Faraday's law:

$$N = \frac{Q}{nF} \ldots\ldots\ldots\ldots\ldots\ldots\ldots\ldots\ldots\ldots(3)$$

where Q is the total charge obtainable from the charge-time curve (Figure 5.2.1B) on 100% completion of electrolysis and F the Faraday number, 96, 485 coulombs/equivalent.
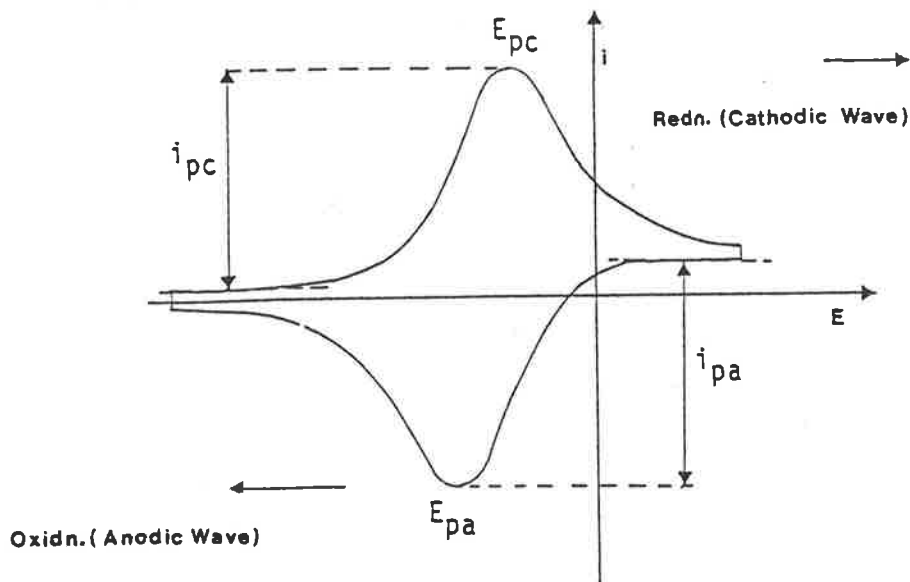
Figure 5.2.1A: Reversible cyclic voltammogram.
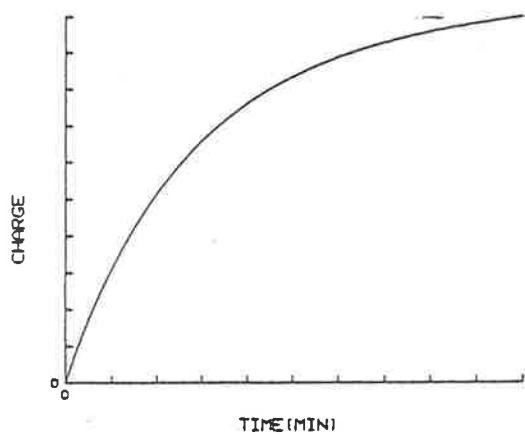

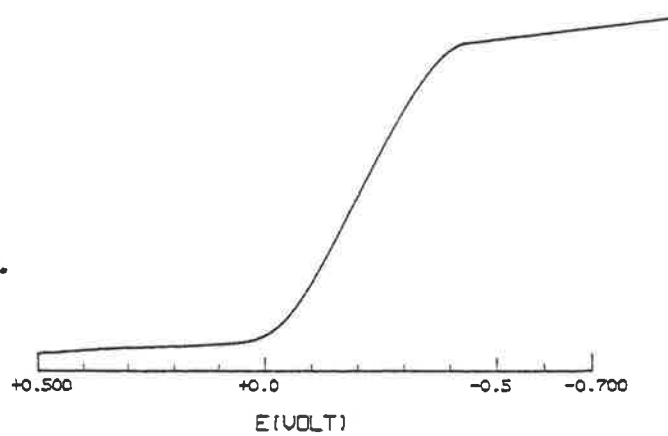Figure 5.2.1B: Charge-time curve.
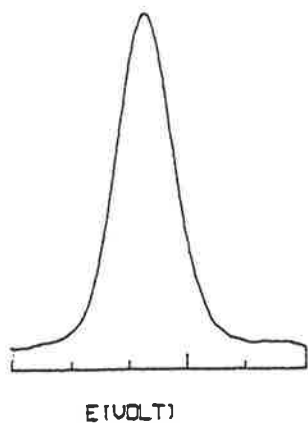

Figure 5.2.1C: Normal pulse voltammogram.

Figure 5.2.1D: Differential pulse voltammogram.

The normal pulse voltammetry (N.P.V.) combines a pulse excitation waveform with current sampling at the end of each pulse. The output is a plot of sampled current vs. pulse potential as shown in Figure 5.2.1C from which $E_{1/2}$ value can be estimated. Much like sampled D.C. polarography, N.P.V. is primarily a quantitative tool with detection limits of 10^{-6} to 10^{-7} M for many heavy metal compounds.

The differential pulse voltammetry (D.P.V.) produces a peak shaped output with the current difference plotted vs. the base potential (Figure 5.2.1D). The peak potential E_p is a function of the polarographic $E_{1/2}$ and the pulse amplitude, P.A.

$$E_p = E_{1/2} - \frac{P.A.}{2} \dotfill (4).$$

Thus, lower pulse amplitudes (but must be greater than the product of the pulse period and scan rate) will help better comparison of E_p and $E_{1/2}$.

5.3 PREVIOUS RELATED WORK

Although there have been many electrochemical studies of vanadium complexes, these usually involved aqueous solution and consequently the oxo species. Of relevance to this work there are a few current studies with some non-vanadyl systems.

The electrochemistry of various catecholato complexes of vanadium(V), -(IV) and -(III) have been described by Sawyer and, independently by Cooper and their co-workers[71,308,309]. $(Et_3NH)_2[V(cat)_3].CH_3CN$ in acetonitrile at a platinum disk electrode showed an oxidation wave at -0.035V[71]. $Na_2VCl_2(DTBC)_2$ showed the first peak ($V^{IV} \rightarrow V^{III}$) at +0.08V vs. S.C.E. coupled to an oxidation at +0.13V. Kapturkiewicz[310] studied the comparative electrochemical behaviour of VO(Salen) and V(Salen)X_2 (X = Cl, ClO$_4$), the latter showing $E_{1/2}$ of reduction waves at the same -0.450V vs. S.C.E. Bond et al.[311,312] studied the polarographic behaviour of bis(π-cyclopentadienyl)-N,N-dialkyldithiocarbamato vanadium(IV) complexes and reported that these non-oxo vanadium complexes exhibit two one-electron polarographic reduction waves in the potential range

+0.75 to -2.2V relative to a Ag-AgCl (acetone) reference electrode. The first reduction at ~ (-)0.4V has been reported to be fully reversible.

The electrochemistry of the diethyldithiocarbamate complexes of V(III), -(IV) and -(V)[313,314] has been studied by cyclic voltammetry and controlled potential coulometry in acetonitrile at a platinum electrode and a comparison of the redox properties of these complexes with those of the analogous 8-quin-olinol complexes has been made to evaluate ligand effects. Hepler and Riechel[13,315] reported on the electrochemical synthesis of a bi-nuclear mixed-valence vanadium(IV,V) and its principle oxidation product V(V,V), (VOQ_2)-O-(VOQ_2) [Q = 8-quinolinato anion).

5.4   ELECTROCHEMISTRY OF VL$_2$ COMPLEXES

5.4.1   THE REDOX PROPERTIES

A good number of the prepared VL$_2$ complexes were subjected to different voltammetric studies under argon in DMSO with Et$_4$NBF$_4$ as the supporting elect-rolyte at a circular platinum electrode. The cyclic voltammetry data for the VL$_2$/VLL' complexes of various ligand systems are summarized in Table 5.4.1. The cyclic voltammograms for some complexes are shown in Figures 5.4.1 - 5.4.4. An examination of these data and Figures indicates that the voltammo-grams obtained are qualitatively similar and that the VL$_2$ complexes generally show two C.V. waves, one appearing in the potential range (-)0.050 - (-)0.400V vs. S.C.E., and the other in the region (-)1.500 - (-)1.800V. These C.V. waves are respectively related to the V^{4+}/V^{3+} and V^{3+}/V^{2+} redox couples. Although the second C.V. wave was not observed for some of the complexes in the above potential range under the experimental condition, all the complexes exhibited the well defined reversible first wave. We suggest that the observ-ance of this first C.V. wave for the V^{4+}/V^{3+} redox couple can be taken as evidence for the formation of the non-oxo vanadium(IV) complexes. Similar C.V. behaviour for the V^{4+}/V^{3+} couple was observed for the non-oxo $V(cat)_3^{2-}$
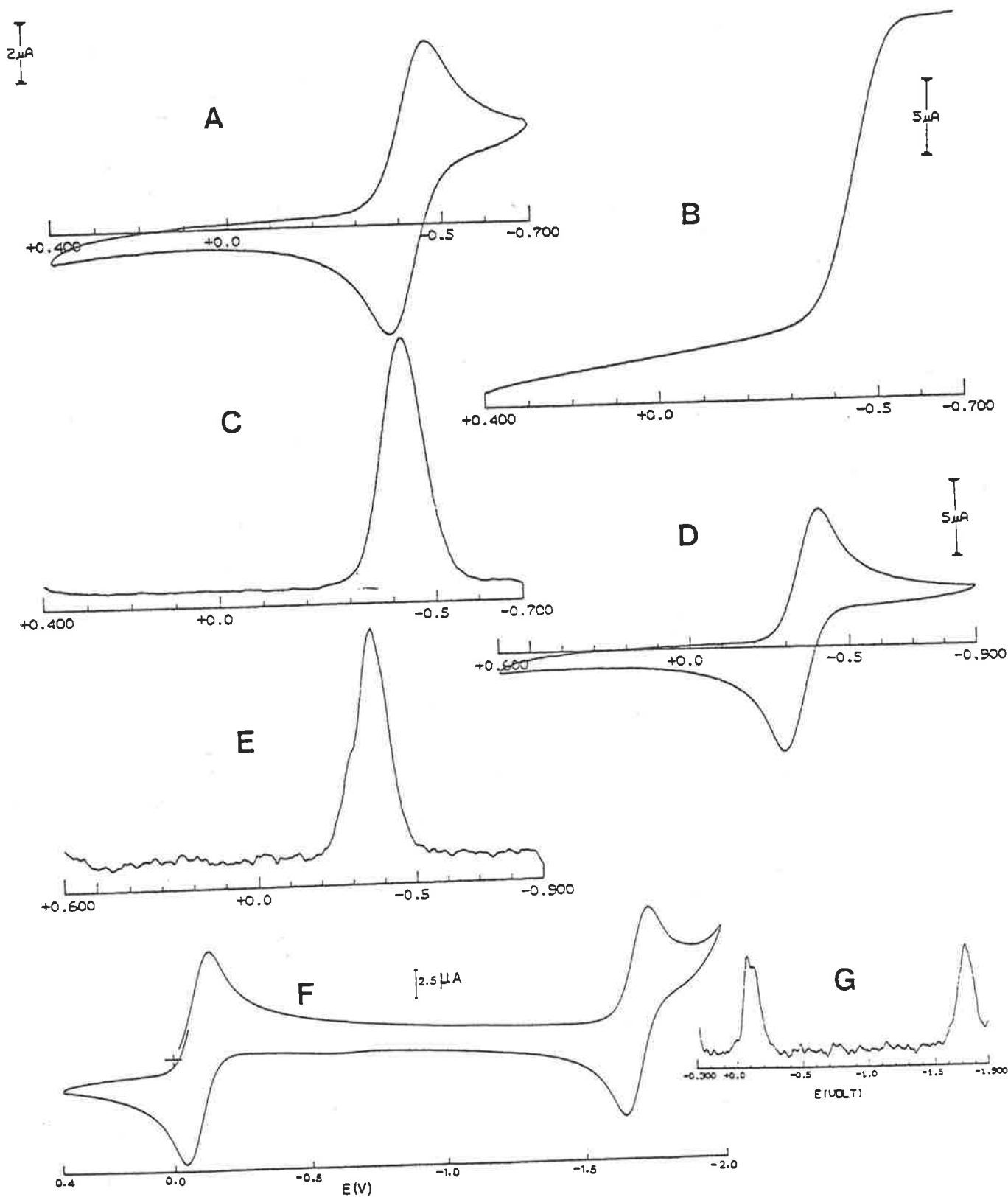
Figure 5.4.1:   Cyclic voltammograms (in DMSO/0.1M Et$_4$NBF$_4$/Pt) of
A. V(acac-BH)$_2$, [B. Normal pulse voltammogram (N.P.V.)
of A; C. Differential pulse voltammogram (D.P.V.)
of A]; D. V(Bzac-BH)$_2$, [E. D.P.V. of B]; F. V(HNP-
BH)$_2$, [G. D.P.V. of F].   Scan rate for C.V. 100 mV/
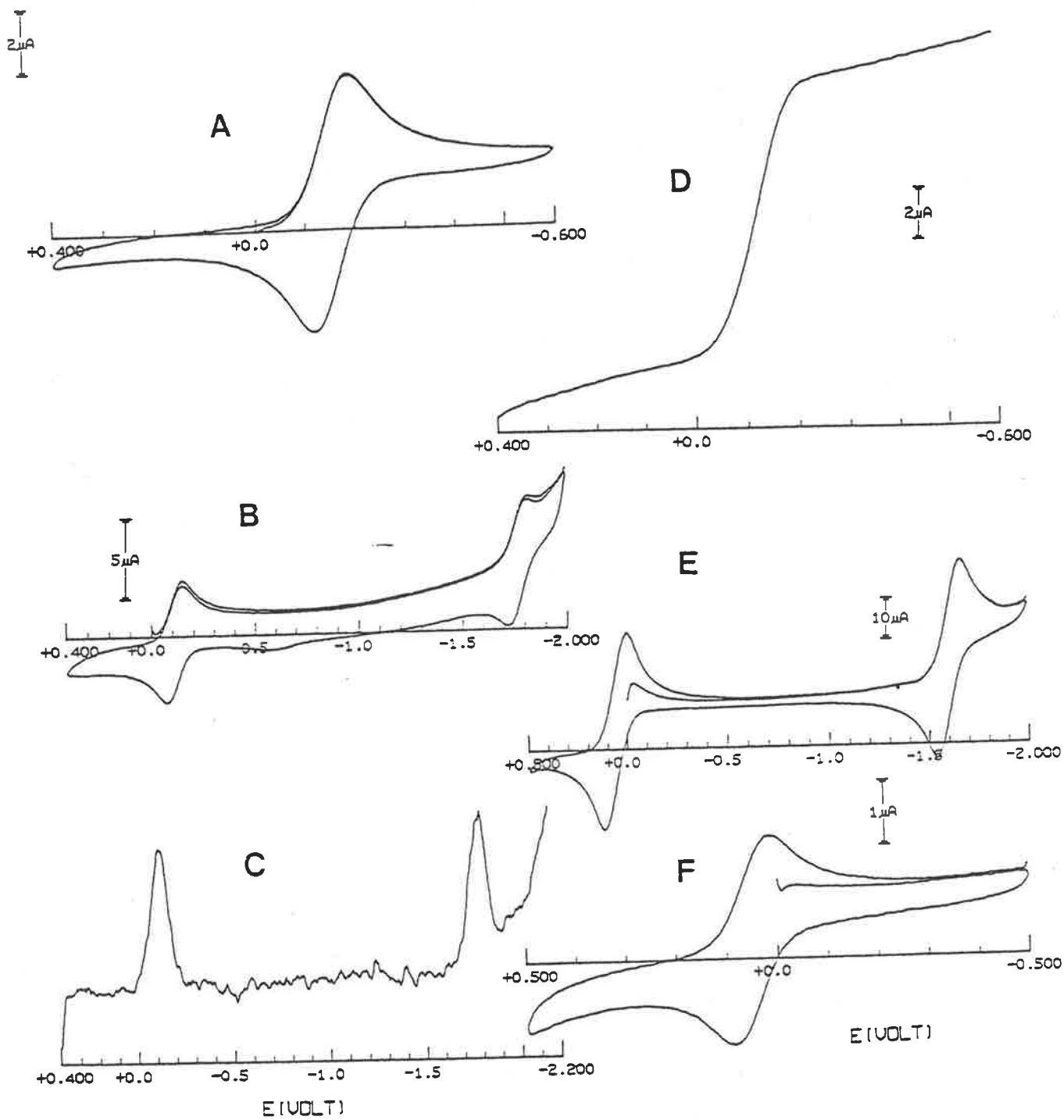sec.; for N.P.V. and D.P.V. 4 mV/sec.

Figure 5.4.2: Cyclic voltammograms (in DMSO/0.1M Et$_4$NBF$_4$/Pt) of
A. V(acac-SalH)$_2$; B. V(Bzac-SalH)$_2$, [C. D.P.V. of B;
D. N.P.V. of B]; E. V(HNP-SalH)$_2$ and F. V(HAP-SalH)$_2$.
Scan rate for C.V. 100 mV/sec.; for normal pulse and
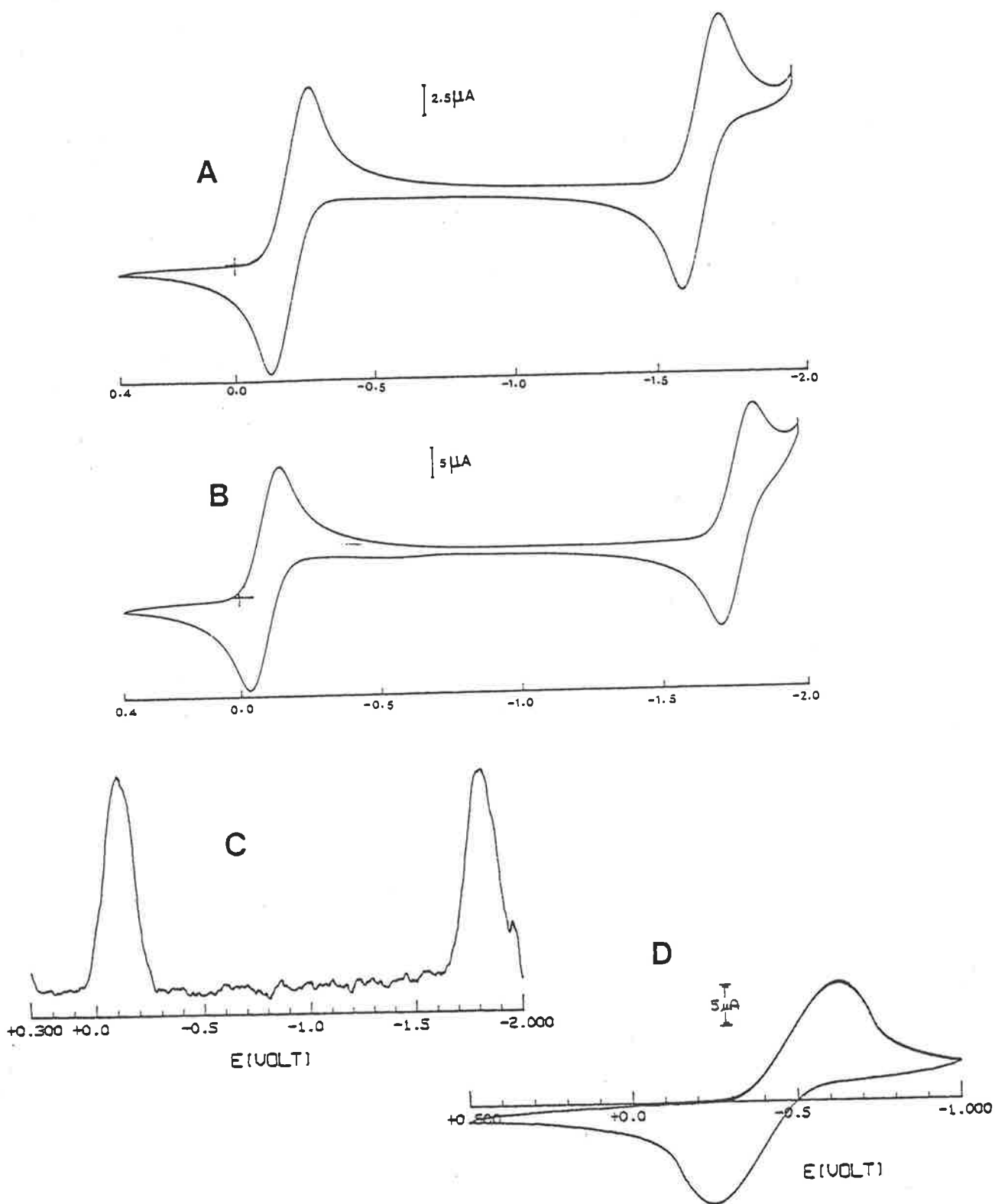differential pulse voltammograms 4 mV/sec.

Figure 5.4.3: Cyclic voltammograms (in DMSO/0.1M Et$_4$NBF$_4$/Pt) of A. V(HNP-OAP)$_2$; B. V(Sal-OAP)$_2$, [C. D.P.V. of B] and D. V(HAP-OAP)$_2$. Scan rate for C.V. 100 mV/sec.; for differential pulse voltammogram 4 mV/sec.
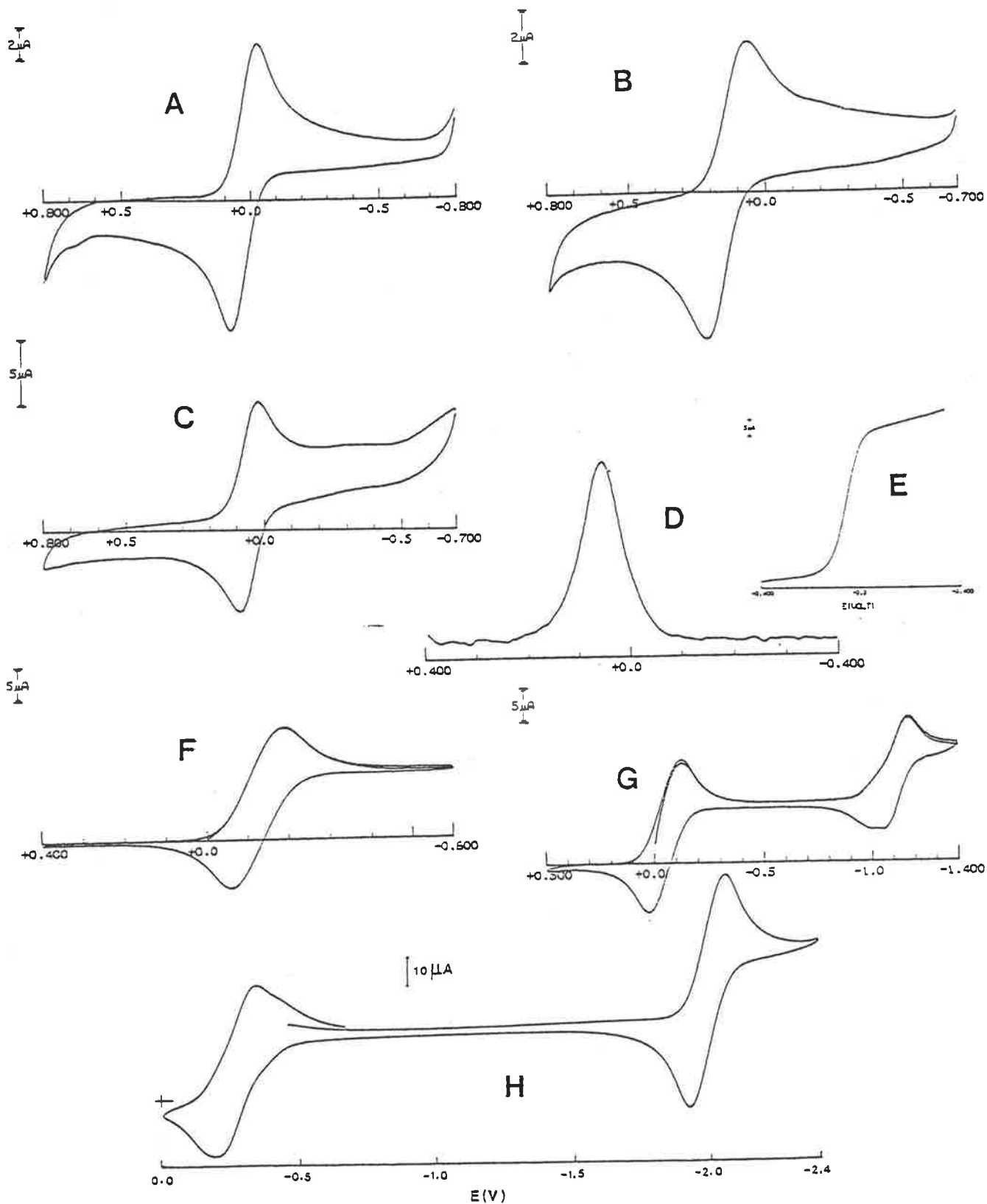
Figure 5.4.4: Cyclic voltammograms (in DMSO/0.1M Et$_4$NBF$_4$/Pt) of
A. V(OAP-β-nap)$_2$; B. V(ErioT)$_2$; C. V(OAP-p-cresol)$_2$,
[D. D.P.V. of C; E. N.P.V. of C]; F. V(HAP-BH)(HNP-BH);
G. V(HNP-BH)(OAP-β-nap) and H.* V(HAP-BH)(Bzac-BH).
Scan rate for C.V. 100 mV/sec.; for differential pulse
and normal pulse voltammograms 4 mV/sec. (* Used
glassy carbon as the working electrode).

TABLE 5.4.1: CYCLIC VOLTAMMETRIC DATA FOR THE VL_2 COMPLEXES IN DMSO WITH 0.1M Et_4NBF_4 AND AT 100 mV/SEC SCAN RATE (WORKING ELECTRODE - PLATINUM)

VL_2 COMPLEXES L=	E_{pa} (V)	E_{pc} (V)	$E_{1/2}$ (V)	ΔE_p (mV)	i_{pa}/i_{pc}
(1)	(2)	(3)	(4)	(5)	(6)
ß-Diketone Schiff Base Complexes					
acac-BH	-0.37	-0.46	-0.42	90	0.94
acac-SalH	-0.12	-0.19	-0.16	70	1.00
Bzac-BH	-0.29	-0.41	-0.35	120	1.01
Bzac-p^{OMe}-BH	-0.25	-0.50	-0.38	250	1.00
Bzac-p^{Cl}-BH	-0.20	-0.37	-0.29	170	0.99
Bzac-p^{NO_2}-BH	-0.13	-0.26	-0.20	130	1.03
	-0.97	-1.14	-1.06	170	-
Bzac-SalH	-0.07	-0.15	-0.11	80	1.00
	-1.72	-1.80	-1.76	80	-
dbm-BH	-0.27	-0.36	-0.32	90	0.98
	-1.74	-1.84	-1.79	100	-
o-Hydroxycarbonyl Schiff Base Complexes					
HNP-BH	-0.07	-0.15	-0.16	80	0.99
	-1.66	-1.75	-1.71	90	-
HNP-SalH	+0.12	0.00	+0.06	120	1.02
	-1.54	-1.67	-1.61	130	-
HNP-OAP	-0.11	-0.30	-0.21	190	0.97
	-1.60	-1.76	-1.68	160	-
HNP-p^{Me}-OAP	-0.22	-0.30	-0.26	80	0.98
	-1.63	-1.73	-1.68	100	-
HNP-p^{Cl}-OAP	-0.09	-0.19	-0.14	100	1.00
	-1.51	-1.62	-1.57	110	-

(1)	(2)	(3)	(4)	(5)	(6)
HNP-3-am-2-nap	-0.10	-0.22	-0.16	120	0.98
	-1.49	-1.61	-1.55	120	-
HAP-BH	-0.15	-0.21	-0.18	60	0.98
HAP-p^{Cl}-BH	-0.10	-0.16	-0.13	60	1.00
HAP-SalH	+0.09	+0.01	+0.05	80	1.00
HAP-OAP	-0.24	-0.60	-0.42	360	-
Sal-BH	+0.03	-0.05	-0.01	80	1.00
	-1.75	-1.83	-1.79	80	-
Sal-SalH	+0.21	+0.14	+0.18	70	1.06
	-1.60	-1.69	-1.65	90	-
Sal-OAP	-0.03	-0.17	-0.10	140	1.00
	-1.70	-1.84	-1.77	140	-
Sal-3-am-2-nap	-0.02	-0.11	-0.07	90	1.01
	-1.58	-1.68	-1.63	100	-

2,2'Dihydroxyazoarene Complexes

(1)	(2)	(3)	(4)	(5)	(6)
OAP-β-nap	+0.06	0.00	+0.03	60	1.17
p^{Me}-OAP-β-nap	+0.01	-0.11	-0.05	120	1.05
p^{Cl}-OAP-β-nap	+0.15	+0.09	+0.12	60	1.04
OAP-p-cresol	+0.09	+0.02	+0.06	70	0.88
3-am-2-nap-β-nap	+0.11	+0.01	+0.06	100	1.01
Erio T	+0.22	+0.06	+0.14	160	1.09

Mixed Ligand VLL' Complexes

(1)	(2)	(3)	(4)	(5)	(6)
V(HNP-BH)(Bzac-BH)	-0.15	-0.23	-0.19	80	0.90
V(HAP-BH)(Bzac-BH)	-0.17	-0.27	-0.22	100	0.94
V(HAP-BH)(HNP-BH)	-0.06	-0.19	-0.13	130	1.00
V(HAP-BH)(Bzac-SalH)	-0.05	-0.15	-0.10	100	1.00
V(HAP-BH)(OAP-β-nap)	+0.02	-0.13	-0.06	150	1.04

All potentials vs S.C.E.

and V(Salen)X$_2$ complexes[71,310] also. The appearance and positions of these two C.V. waves were confirmed by recording the differential pulse voltammograms for a few systems (see in Figures 5.4.1 - 5.4.4) which clearly showed two distinct peaks at the E $\frac{1}{2}$ values corresponding to those obtained from C.V., within experimental error. In a few cases, comparable E $\frac{1}{2}$ (V^{4+}/V^{3+}) values were also obtained by recording the normal pulse voltammograms from the same solution used to determine the cyclic voltammograms.

In no case were we able to obtain any well-defined C.V. wave for the V^{4+}/V^{5+} couple before the anodic limit of the medium which indicates lack of stabilization of the vanadium(V) state in the presence of two coordinated dinegative tridentate ligands. As seen before [Chapter 4.2, Sections (c) and (d)] reaction of VOL.OR with excess L$\underline{H}_2$ produces the V^{4+} complex and not VL$_2^+$. The same reaction with the potential trinegative tridentate ligand (L'$\underline{H}_3$) formed by the hydrogenation of o-(o'-hydroxyphenyl)iminomethylphenol (Sal-OAPH$_2$) also gave non-vanadyl vanadium(IV) complex instead of the expected neutral V^{V}LL'. Thus, it appears that ligands of this type do not stabilize vanadium(V) in the absence of oxo function.

For the mixed-ligand VLL' complexes, it can easily be seen in Table 5.4.1 that these complexes showing well defined C.V. waves (F.G.H. in Figure 5.4.4) reduce at a different potential than either the VL$_2$ or VL'$_2$ complexes which is a clear indication for their existence as a single entity.

5.4.2 REVERSIBILITY OF THE REDOX PROCESSES

The most common tests of reversibility are[316-318]: (i) the constancy of $i_{pc}/v^{\frac{1}{2}}$ over a wide range of scan rates (v); (ii) the constancy of ΔE_p [60/n (mV)] as a function of scan rate; (iii) the ratio of peak currents, i_{pa}/i_{pc} being equal to 1.00 and (iv) the ability to exactly reproduce the wave on successive scans both forward and in reverse. This last criterion is important for systems in which the oxidized (or reduced) form is unstable or reacts with the solvent. In such a case, slow scans will show the absence of the

TABLE 5.4.2: CYCLIC VOLTAMMETRIC DATA AS A FUNCTION OF SCAN

RATE FOR SOME VL$_2$ COMPLEXES[a]

COMPLEX	SCAN RATE v, [(mV)s^{-1}]	$-E_{1/2}$ [V]	ΔE_p [mV]	i_{pa}/i_{pc}	$i_{pc}/v^{1/2}$ [μA/(mV)s^{-1}]
V(acac-BH)$_2$	10	0.427	72	1.00	0.41
	50	0.421	84	0.94	0.40
	100	0.417	89	0.94	0.40
	200	0.412	126	0.93	0.41
	500	0.422	232	0.89	0.28
V(HNP-BH)$_2$	10	0.112	77	1.03	1.68
		1.724	95	0.58	1.84
	100	0.106	100	1.00	1.48
		1.716	122	0.76	1.52
	500	0.102	170	1.00	1.32
		1.707	1.76	0.81	1.36
	1000	0.100	197	1.01	1.34
		1.720	197	0.78	1.37
	5000	0.100	320	1.01	0.47
		1.729	317	0.80	0.41
V(HNP-OAP)$_2$	100	0.207	200	1.01	0.83
		1.681	200	0.70	0.79
	200	0.194	309	1.04	0.35
		1.697	317	0.81	0.31
	500	0.203	305	1.04	0.61
		1.685	323	0.83	0.59

a. DMSO/0.1 M Et$_4$NBF$_4$/Pt.

All potentials vs. S.C.E.
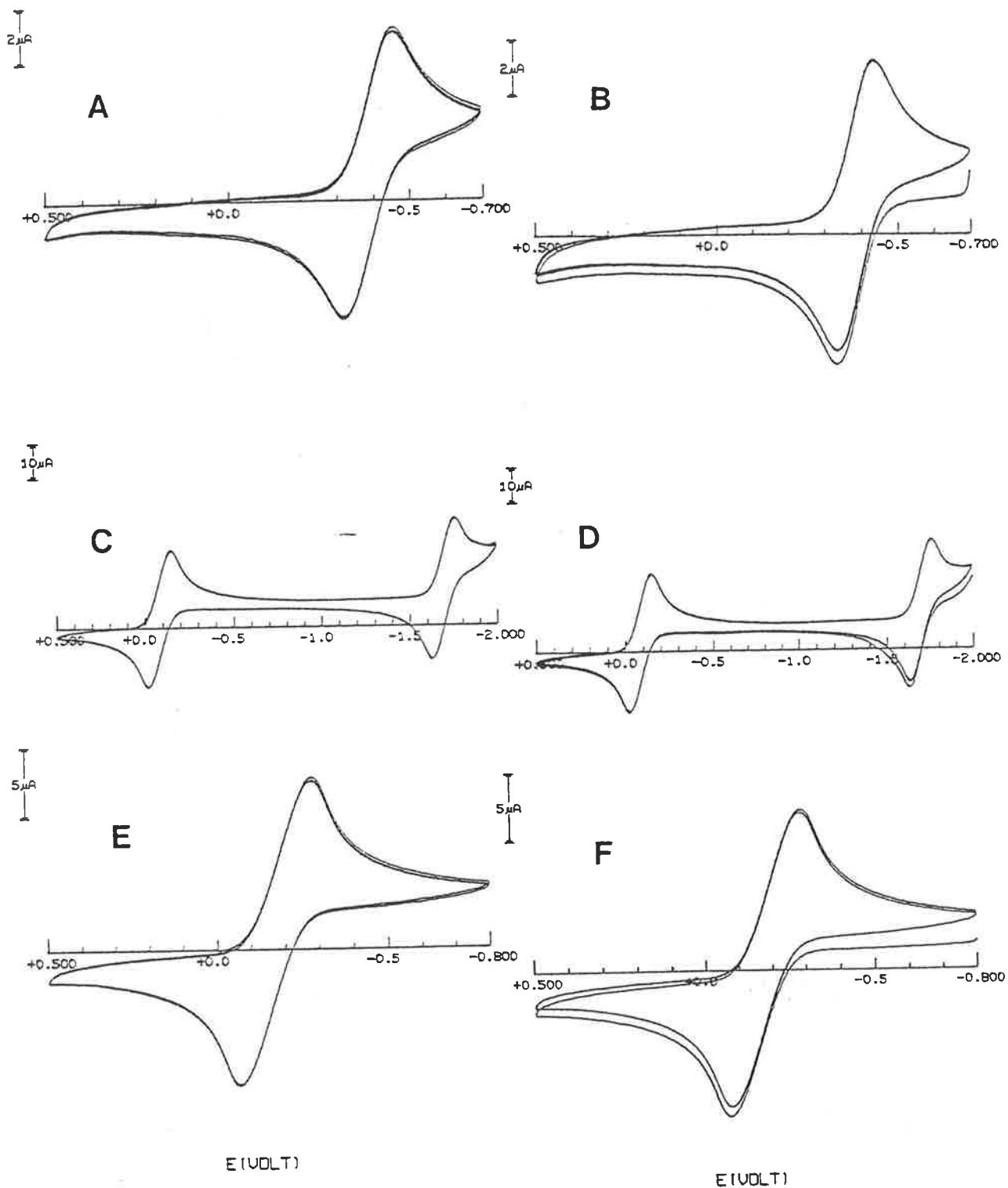
Figure 5.4.5: Reproducibility of C.V. waves on successive scans both forward and in reverse. A. V(acac-BH)$_2$; B. A after sitting at -0.7V for 1 min.; C. V(HNP-BH)$_2$; D. C after sitting at -2.0V for 1 min.; E. V(HNP-OAP)$_2$ and F. E after sitting at -0.8V for 1 min. Scan rate 200 mV/sec.; media DMSO/0.1M Et$_4$NBF$_4$/Pt.

anodic (or cathodic) wave. For the VL_2 complexes, as has been observed for a few such systems (Table 5.4.2), the faster scan rates generally result in a larger peak separation (ΔE_p). In general, the anodic and cathodic peak currents for the V^{4+}/V^{3+} couple were found to be equal. For the V^{3+}/V^{2+} couple, the $^i pa/^i pc$ was below unity because of the significant increase of the cathodic peak current at such potentials. On the basis of the effect of scan rates on the ΔE_p and $^i pc/v^{1/2}$ (Table 5.4.2) and the generally larger ΔE_p values than the expected 60/n (mV)[318] it appears that the C.V. waves of these systems are more correctly described as quasi-reversible.

Cyclic voltammograms A to F in Figure 5.4.5 shows that the C.V. waves are reproduced exactly on successive scans in both forward (-ve) and reverse (+ve) directions. To test further the stability of the reduced species, the cyclic voltammograms of three complexes (B, D and F in the same Figure) were recorded after the systems were allowed to remain at potentials sufficiently negative to form the reduced species.

5.4.3 CONTROLLED-POTENTIAL ELECTROLYSIS

To identify the number of electrons (n) involved in the electrochemical reduction controlled-potential electrolyses (C.P.E.) were carried out for a few of the complexes. A platinum gauze electrode and stirred solutions under argon were used. The solvents used are indicated in Table 5.4.3. The coulome tric data obtained from the controlled potential reductions (Table 5.4.3) at -0.500V for $V(acac-BH)_2$ and $V(Bzac-BH)_2$ and at -0.200V for $V(HNP-BH)_2$ confirm that the first C.V. wave corresponds to a one-electron process. The C.V. waves of these reduced solutions (Figure 5.4.6) are essentially identical with the initial ones confirming the stability of the +3 species. $V(HNP-OAP)_2$ was subjected to C.P.E. at -1.700V to investigate the second reduction wave. In this case, a total of two electrons per molecule was transferred corresponding to V^{4+}/V^{3+} and V^{3+}/V^{2+} reductions. In the C.V. of this reduced species, two minor new redox processes were observed in addition to the V^{4+}/V^{3+} and V^{3+}/V^{2+}

TABLE 5.4.3: CONTROLLED-POTENTIAL COULOMETRIC DATA FOR SOME VL_2 COMPLEXES

COMPLEX	C.P.E. AT (V)	MEDIA	FOR ONE ELECTRON REDN.	
			CALC. Q Ceq	OBS. Q Ceq
V(acac-BH)$_2$	-0.500	a	1.624	1.581
V(Bzac-BH)$_2$	-0.500	b	2.226	2.153
V(HNP-BH)$_2$	-0.200	a	1.013	0.893
V(HNP-OAP)$_2$	-1.700	c	4.010	4.182
Ti(acac-BH)$_2$	-1.100	d	3.454	3.070

a. Propylene carbonate/Et_4NBF_4/Pt   c. DMSO/Et_4NClO_4/Pt

b. CH_2Cl_2/Et_4NCl d. CH_3CN/Et_4NBF_4/Pt

couples. The first process is associated with the waves at -1.098 (anodic) and -1.162V (cathodic) and the second with +0.033 (anodic) and a small wave at (~) 0.030V (cathodic). From the relative intensities of the two waves, these two processes appear to be related and due to the formtion of a new species which is not the free ligand.

The electronic spectra of these reduced solutions were different from the initial spectra (see Figure 5.4.7), the main difference being the absence of the low energy charge transfer band with the rest of the spectrum remaining approximately the same. The disappearance of the following LMCT bands were observed on reduction:

For V(acac-BH)$_2$ in propylene carbonate LMCT at 545 nm.

For V(Bzac-BH)$_2$ in dichloromethane LMCT at 538 nm.

These observations confirm our assignment (see Section 3.7.3) of these bands as LMCT.

V(HNP-OAP)$_2$ which was reduced at -1.700V to the +2 state gave a spectrum with a number of shoulders suggesting the presence of more than one species.
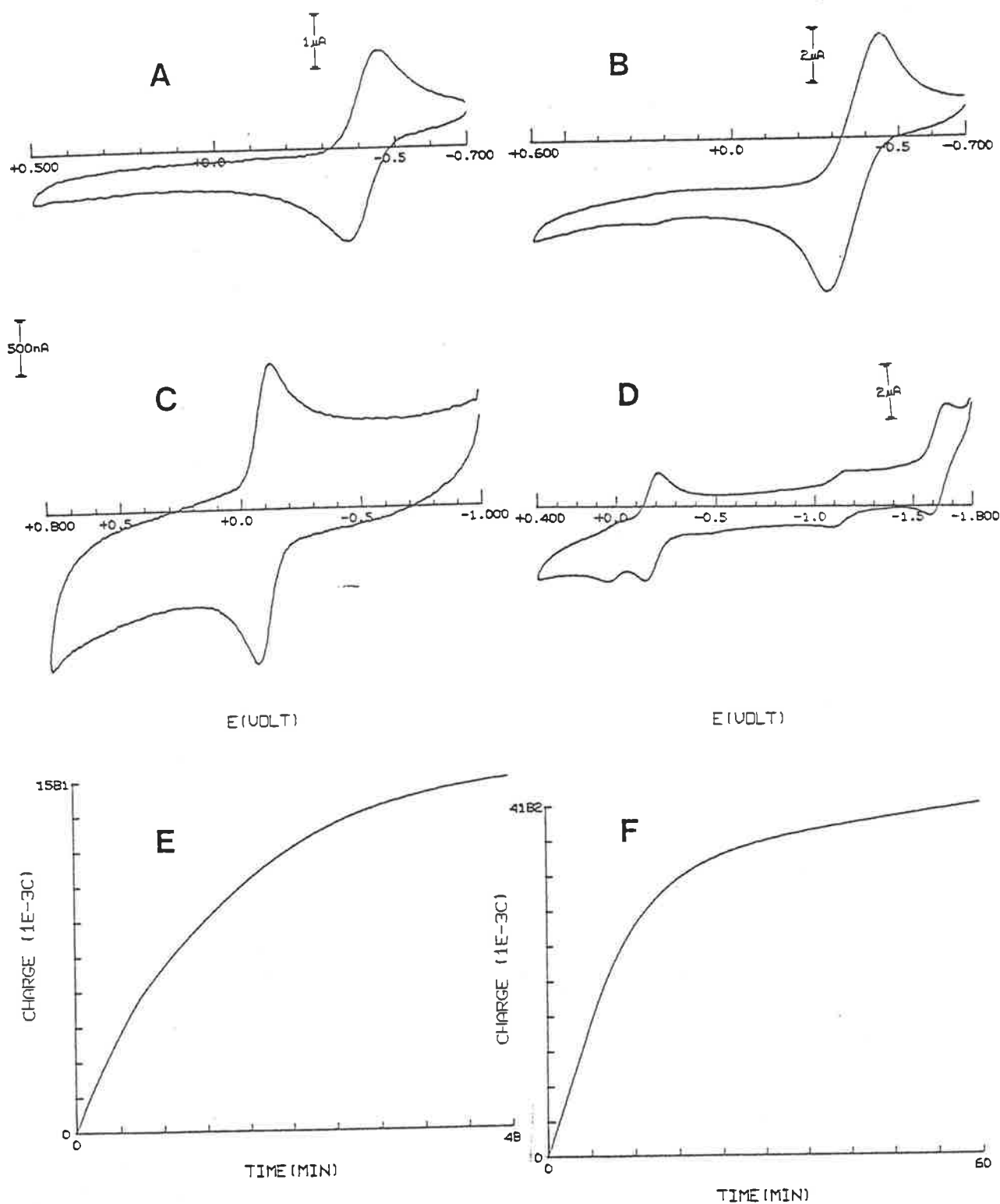
Figure 5.4.6: Cyclic voltammograms obtained after controlled-potent-
ial electrolysis (C.P.E.) of
A. V(acac-BH)$_2$ at -0.5V in PC/Et$_4$NBF$_4$/Pt;
B. V(Bzac-BH)$_2$ at -0.5V in CH$_2$Cl$_2$/Et$_4$NCl/Pt;
C. V(HNP-BH)$_2$ at - 0.2V in PC/Et$_4$NBF$_4$/Pt and
D. V(HNP-OAP)$_2$ at -1.7V in DMSO/Et$_4$NClO$_4$/Pt.
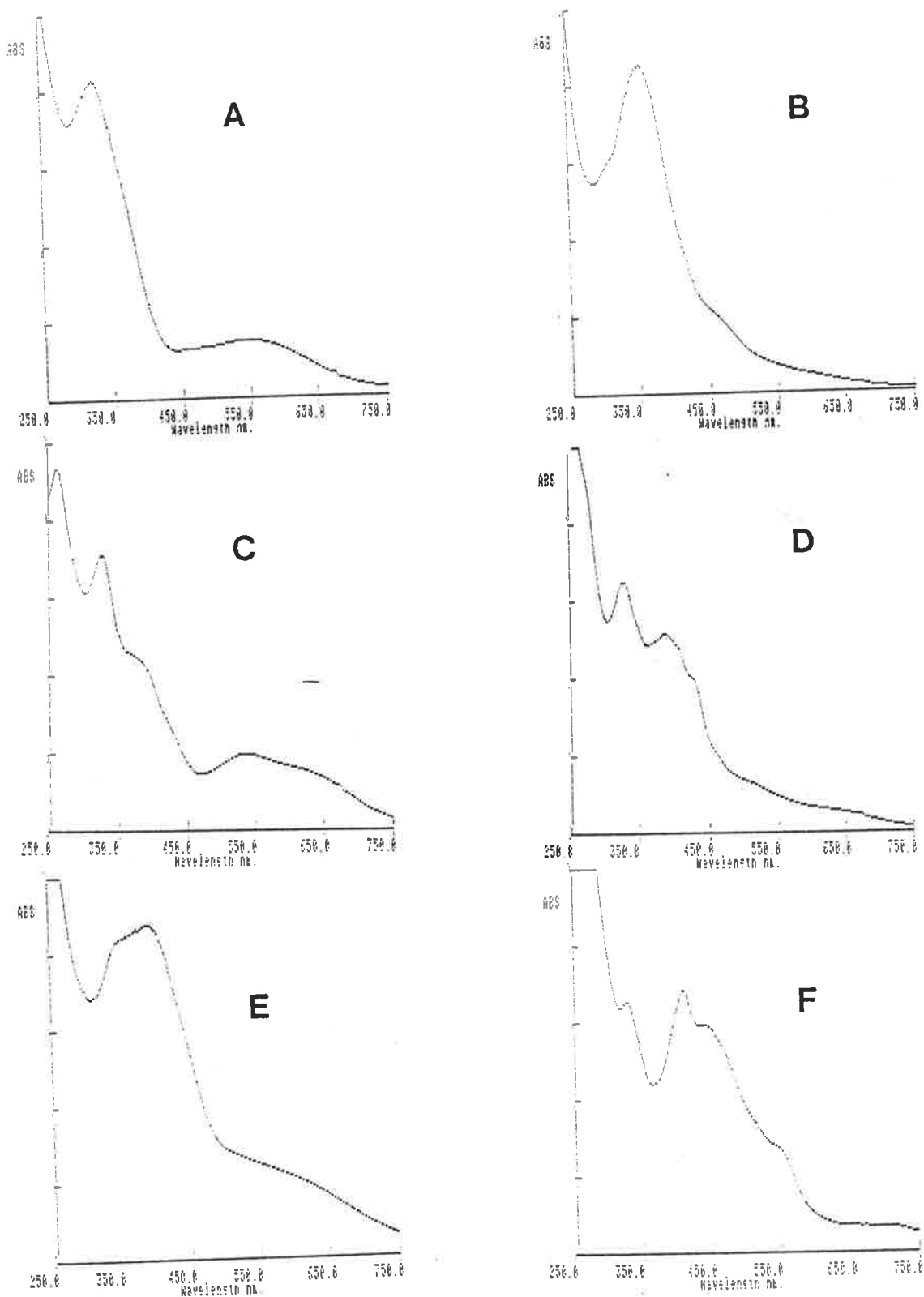Typical charge-time curves E. for A and F. for D.
(P.C. - Propylene carbonate).

Figure 5.4.7:   Electronic spectra of A. $V(acac-BH)_2$ in PC/Et_4NBF_4
before controlled-potential electrolysis (C.P.E.); B. A
after C.P.E.; C. $V(HNP-BH)_2$ in PC/Et_4NBF_4 before
C.P.E.; D. C after C.P.E.; E. $V(HNP-OAP)_2$ in DMSO/
Et_4NClO_4 before C.P.E. and F. E after C.P.E.
(PC - Propylene carbonate).

5.4.4 THE REDOX MECHANISM

It is likely that the electron involved in the electrochemical reduction is accommodated in the empty d orbital of the vanadium atom. The V(III) species formed on reduction appears to be stable under the experimental conditions, over appreciable periods of time. The electronic spectra of the reduced yellow to brown solutions, showing absence of the strong LMCT absorption maxima at ~ 540 nm, are consistent with the species to be of vanadium(III). Well-defined C.V. waves for the V^{3+}/V^{2+} redox couple also indicate the stability of the V(II) species formed, although there is evidence of some decomposition. The above observations suggest the following equilibrium reactions:

$$V(IV)L_2 + e \rightleftharpoons V(III)L_2^-$$

$$V(III)L_2^- + e \rightleftharpoons V(II)L_2^{2-}$$
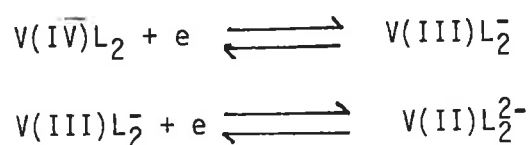
5.4.5 FACTORS GOVERNING REDOX POTENTIALS

In order to observe the electrochemical reduction of an oxovanadium(IV) complex, it is necessary to replace the oxo function by a ligand system compatible with the coordination requirements of the vanadium(III) oxidation state. For example, the reversible electro-reduction of $VO(acac)_2$ gives $V(acac)_3$ in the presence of excess acetylacetone[27,305]. It is not surprising, therefore, that easy reversible reduction is observed in the VL_2 complexes as it only requires the addition of one electron which may be associated with an intramolecular rearrangement of the coordination geometry.

The availability of VL_2 complexes in which the ligand can be varied systematically permits study of the effect of the ligand on the redox potential. Acceptance of an electron in the d orbital will be facilitated by an increased electron-withdrawing effect in the ligand with a consequent increase in the $E_{1/2}$ value.

The $-E_{1/2}$ values obtained for different VL_2 complexes (Table 5.4.1) with Schiff bases of varying amino- and constant ketonic groups fall in the order:

K-OAP > K-BH > K-SalH (K = Ketonic part).

Thus, the $E_{1/2}$ values are most negative for the OAP-Schiff base complexes and the most positive for the salicyloylhydrazone VL_2 complexes. In the benzoyl-hydrazone complexes, the electron density from the $-N-C-$/$O-$ conjugated system is drawn into the phenyl ring thereby making vanadium susceptible to easy reduction. In the salicyloylhydrazone complexes, the -OH is hydrogen-bonded to the first N of the hydrazine part. As a result, the electron donation from this N to the $O^-\left(\substack{N-C-\\ -O}\right)$ as well as from oxygen of the -OH group will be restricted. This will lower electron density on the O^- bonded to vanadium thus making vanadium more susceptible to electro-reduction. It appears that OAP is less electron-withdrawing than BH. Compared to the OAP-Schiff base compounds, the azo-complexes reduce at lower (by ~ 0.2V) $-E_{1/2}$ values which shows them to be much more electron withdrawing. This is attributed to the replacement of -CH= of the OAP-Schiff bases by the -N= in the diazo ligands which can attract electron more easily through an inductive effect.

A similar but less pronounced effect is observed when electron-withdrawing substituents are introduced in the aromatic ring of the ligands. Thus, the following order is observed for the $-E_{1/2}$ values of V^{4+}/V^{3+} couples in various p^X-substituted ligand complexes:

For Bzac-p^X-BH: NO_2 < Cl < OMe

For HNP-p^X-OAP: Cl < H < Me

For p^X-OAP-β-nap: Cl < H < Me
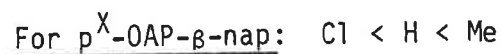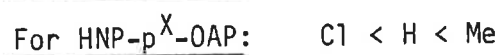
Similar order has also been observed for the V^{3+}/V^{2+} couples when they can be observed, e.g. in the HNP-p^X-OAP complexes. Thus, the preference of more electron-withdrawing group in the ligand causes the complex to reduce at a more positive potential. The electron-donating methyl substituent on the ligand produces the opposite effect.

Keeping the amine part constant, the $-E_{1/2}$ values for the V^{4+}/V^{3+} couples

fall in the order:

$$acac-A > Bzac-A > dbm-A > HAP-A$$

$$> HNP-A > Sal-A$$
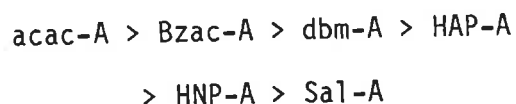
for all the A = BH, SalH and OAP Schiff base complexes. The $-E\frac{1}{2}$ values for the V^{3+}/V^{2+} couples also fall in the above order but with the HNP-A and Sal-A positions being interchanged. The same sequence in $E\frac{1}{2}$ is observed in the TiL_2 complexes so far investigated. The electronic effect of the diketonato moieties in Schiff bases is parallel to that seen in the bidentate diketonato complexes. Thus, for various $M(AA)_n$ complexes [M = Co(II), Co(III), Cr(III), Ru(III); AA = acac, Bzac, dbm; n = 2,3] the $-E\frac{1}{2}$ values also fall in the order acac > Bzac > dbm (see Table 2.9.4 and references therein). These electronic effects are readily attributed to the electron-withdrawing effect of the phenyl and napthyl aromatic rings.

The $E\frac{1}{2}$ values for the V^{4+}/V^{3+} and V^{3+}/V^{2+} couples and the $\Delta E\frac{1}{2}$ $(V^{3+}/V^{2+} - V^{4+}/V^{3+})$ values indicate that the $E\frac{1}{2}$ (V^{3+}/V^{2+}) is not linear with $E\frac{1}{2}$ (V^{4+}/V^{3+}) and that the differences in the reduction potentials of V^{4+}/V^{3+} and V^{3+}/V^{2+} couples range from 1.4-1.8V. These differences must be related to the differing extents to which the oxidation states are stabilized by the various ligands.

Titanium(IV) forms similar bis-tridentate neutral TiL_2 complexes[99] [see Section 3.6.5(d)] with the ligands forming VL_2 chelates. The electro-chemistry of some of these TiL_2 complexes was studied in the same media (DMSO/ Et_4NBF_4/Pt) in order to make comparisons with the VL_2 complexes and to examine the effect of the metal on the redox properties. All TiL_2 complexes examined showed well defined C.V. waves for the Ti^{4+}/Ti^{3+} redox couple. In some of them the second wave for the Ti^{3+}/Ti^{2+} couple occurred at a potential which could be seen before the cathodic reduction limit of the medium. A controlled potential electrolysis of $Ti(acac-BH)_2$ (see Table 5.4.3) at -1.10V confirmed the reduction at this potential to be a one-electron process. These observations confirm similar behaviour of the bis-VL_2 and $TiL2$ complexes.

An examination of the $E\frac{1}{2}$ values of TiL_2 and VL_2 complexes (Table 5.4.4) as well as the $\Delta E\frac{1}{2}$ (TiL_2-VL_2) values which range from 0.4 to 0.8V indicate that in addition to the metal ion characteristics, factors relating the metal-ligand interactions are also responsible for the observed $E\frac{1}{2}$ values. As against the first electron-transfer reduction at 0- (-)0.4V for the VL_2 complexes, the TiL_2 complexes reduce at a more negative $E\frac{1}{2}$ value ranging from (-)0.45 - (-)0.90V which is consistent with the position of the metals in the first transition series. It is, however, interesting that although Ti^{4+}/Ti^{3+} reductions occur at more negative potentials with respect to the V^{4+}/V^{3+} couple, the Ti^{3+}/Ti^{2+} redox potentials are at about the same values as that of the V^{3+}/V^{2+} couple. It reflects greater stabilization of the reduced Ti(II) species than V(II). Accommodation of the accepted electron in a molecular orbital which is more like ligand orbital might be an explanation for the observed effect.

TABLE 5.4.4: THE $E\frac{1}{2}$ AND $\Delta E\frac{1}{2}$ VALUES FOR THE TiL_2 AND VL_2 COMPLEXES IN DMSO WITH 0.1M Et_4NBF_4 AND AT 100 mV/SEC SCAN RATE (WORKING ELECTRODE - PLATINUM)

LIGAND	$-E\frac{1}{2}$ OF TiL_2^* (V)	$-E\frac{1}{2}$ OF VL_2 (V)	$\Delta E\frac{1}{2}$ (TiL_2-VL_2) (V)
acac-BH	0.98	0.42	0.56
Bzac-BH	0.89	0.35	0.54
	1.79	-	-
HNP-BH	0.75	0.11	0.64
	1.63	1.71	0.08
Sal-BH	0.79	0.01	0.78
OPA-p-cresol	0.47	-0.06	0.53

All potentials vs S.C.E. * The last two TiL_2 compounds were supplied by M. Manikas (Summer Vacation Research Student).

5.5. ELECTROCHEMISTRY OF VOL.OR AND (VOL)$_2$O COMPLEXES

The electron transfer characteristics of a number of alkoxo-(tridentate) oxovanadium(V) and oxo-bridged-(tridentate)oxovanadium(V) complexes were studied at a platinum electrode in DMSO using Et_4NClO_4 as the supporting electrolyte.

Although monomeric and dimeric vanadium(V) complexes are capable of showing C.V. waves corresponding to V^{5+}/V^{4+}, V^{4+}/V^{3+} and V^{3+}/V^{2+} redox couples, dimeric vanadium(V,V) complexes can also show the intermediate stages $V(V,V) \rightarrow$ mixed-valence $V(V,IV) \rightarrow V(IV,IV)$. Coulometric experiments can demonstrate the production of the mixed-oxidation V(V,IV) species.

The cyclic voltammetric data are summarized in Table 5.5.1 and voltammograms for some complexes are shown in Figure 5.5.1. These waves are reproducible on reversing the scan and have large ΔEp values indicating that electron transfer in these systems is quasi-reversible. This is particularly so for the wave at the most positive potentials. In general, the main waves are in the regions around +0.3 and -1.0V and, in some cases, -1.65V. These waves, from the knowledge with other systems, correspond to V^{5+}/V^{4+}, V^{4+}/V^{3+} and V^{3+}/V^{2+} couples respectively. In addition, there are some weaker cathodic peaks in most of the systems.

To identify the number of electrons (n) associated with the reduction in the +0.3V region, controlled-potential electrolysis (C.P.E.) for a few systems were carried out. The coulometric data presented in Table 5.5.2 show that approximately 0.5 electron per vanadium was transferred. This suggests that the [VO(Bzac-BH)]$_2$O dimer is reduced to the mixed-valence vanadium(V,IV) dimer species. Mixed-oxidation vanadium(V,IV) complexes, including $(NH_4)_3[V_2O_3(nit$-roacetate)$_2]\cdot 3H_2O$ the crystal structure of which has been determined, are known[13,319,320].

The red-brown solutions of VO(Bzac-BH).OEt and (VO(Bzac-BH)]$_2$O in DMSO before C.P.E. had identical electronic spectra. The yellow solutions obtained after C.P.E. again had identical spectra but differing from the initial ones

TABLE 5.5.1: CYCLIC VOLTAMMETRIC DATA FOR THE VOL.OR AND $(VOL)_2O$ COMPLEXES IN DMSO WITH Et_4NClO_4 AT 100 mV/SEC SCAN RATE (WORKING ELECTRODE - PLATINUM)

LIGAND L=	COMPLEX	E_{pa} (V)	E_{pc} (V)	$E_{1/2}$ (V)	ΔE_p (mV)
Bzac-BH	VOL.OEt	+0.45	+0.21	+0.33	240
		-0.90	-1.10	-1.00	200
		-1.58	-1.75	-1.67	170
	$(VOL)_2O$	+0.43	+0.20	+0.32	230
		-0.94	-1.13	-1.04	190
		-1.66	-1.90	-1.78	240
dbm-BH	VOL.OMe	+0.42	+0.27	+0.35	150
		-0.89	-1.06	-0.98	170
	$(VOL)_2O$	+0.56	+0.17	+0.37	390
		-0.90	-1.10	-1.00	200
HNP-BH	VOL.OMe	+0.45	+0.21	+0.33	240
		-0.87	-1.09	-0.98	220
		-1.55	-1.70	-1.63	150
	$(VOL)_2O$	+0.50	+0.20	+0.36	300
		-0.93	-1.06	-1.00	130
		-1.51	-1.76	-1.64	250
HAP-BH	VOL.OMe	+0.37	+0.13	+0.25	240
		-0.94	-1.15	-1.05	210
	$(VOL)_2O$	+0.37	+0.20	+0.29	170
		-0.100	-1.14	-1.07	140
Sal-BH	VOL.OMe	+0.42	+0.19	+0.31	230
		-0.86	-1.08	-0.97	220
	$(VOL)_2O$	+0.41	+0.16	+0.29	250
		-0.96	-1.14	-1.05	180

All potentials vs S.C.E.
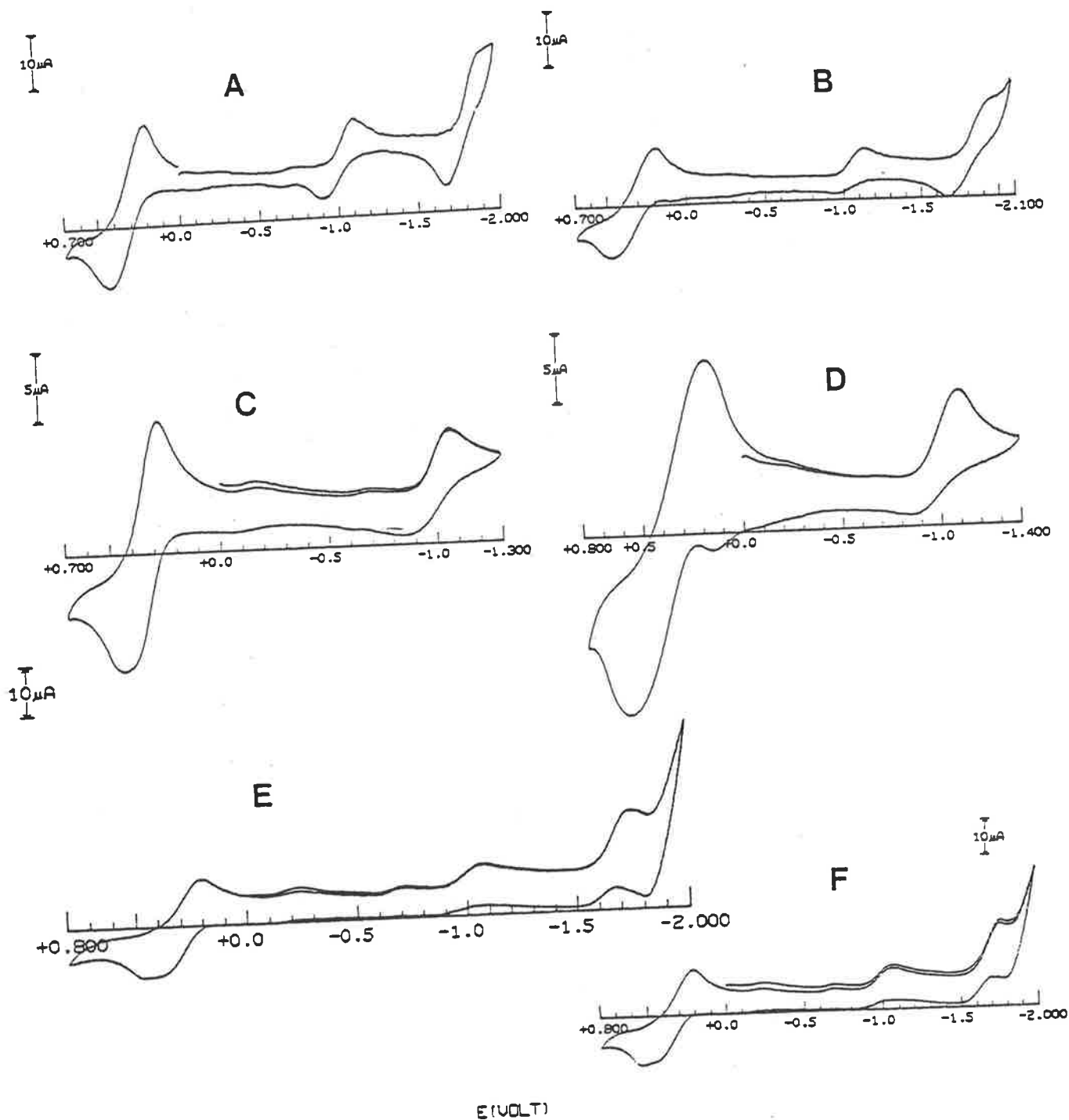
Figure 5.5.1: Cyclic voltammograms (in DMSO/0.1M Et$_4$NClO$_4$/Pt) of A. VO(Bzac-BH).OEt; B. [VO(Bzac-BH)]$_2$O; C. VO(dbm-BH).OMe; D. [VO(dbm-BH)]$_2$O; E. VO(HNP-BH).OMe and F. VO(HNP-BH)]$_2$O. Scan rate 100 mV/sec.
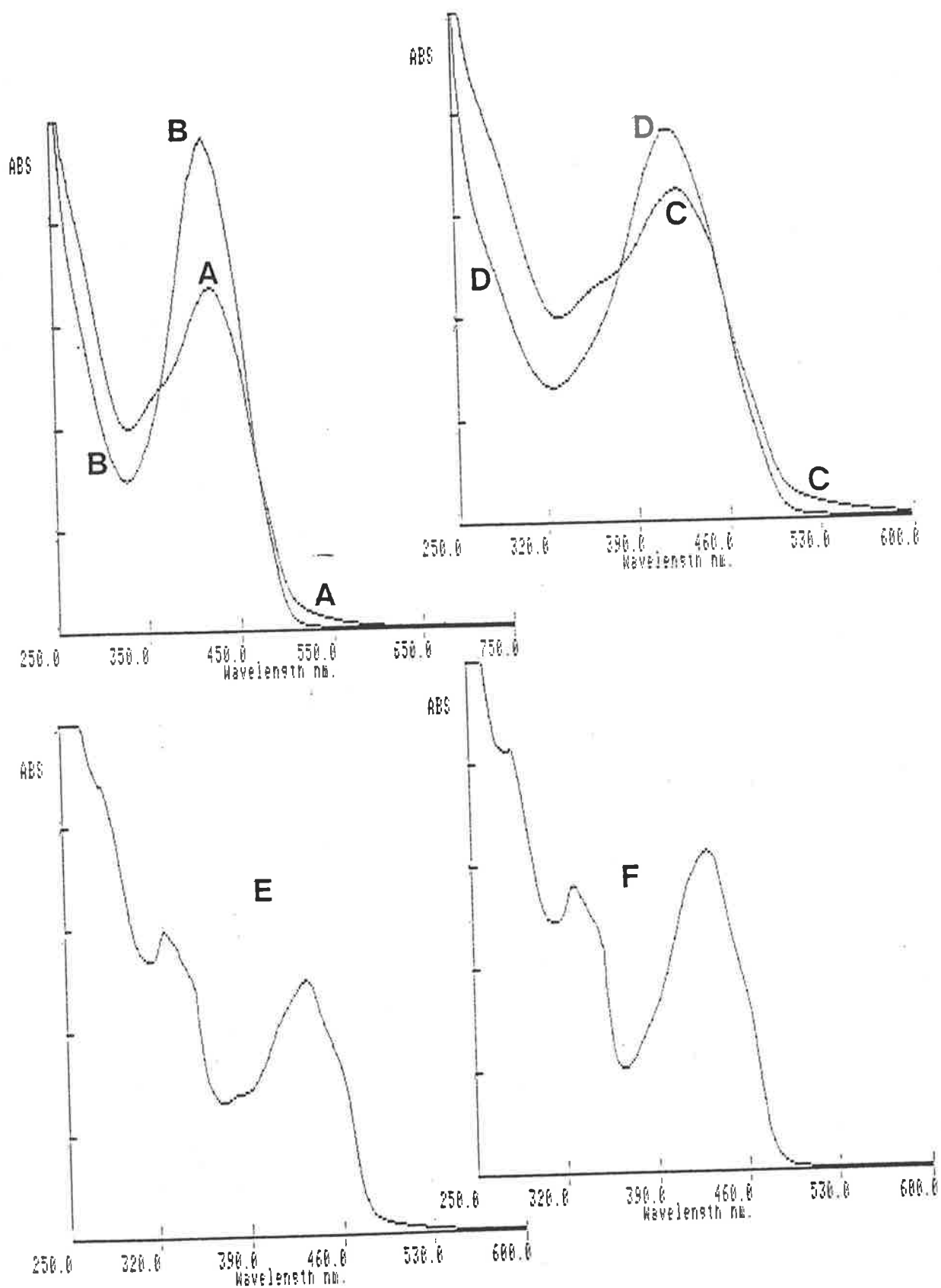
Figure 5.5.2: Electronic spectra of A. VO(Bzac-BH).OEt in DMSO/
Et$_4$NClO$_4$ before controlled-potential electrolysis
(C.P.E.); B. A after C.P.E.; C. [VO(Bzac-BH)]$_2$O before
C.P.E., D. C after C.P.E., E. VO(HNP-BH).OMe before
C.P.E. and F. E after C.P.E.

(see Figure 5.5.2). Also, both complexes showed identical C.V. waves (A and B in Figure 5.5.1) with comparable $E_{1/2}$ values. These observations, especially the n value of about 0.5 electron/vanadium, confirm that the VOL.OR complexes in DMSO rearranges into a dimeric configuration, probably by reaction with traces of moisture [see Section 4.2(c)], and that the first reduction species of V(V,V) dimer is a mixed-valence V(V,IV) compound. In the voltammetric study of the $(VOQ_2)-O-(VOQ_2)$ (Q = 8-quinolinato), Hepler and Riechel[3][15] reported its reduction to the vanadium(V,IV) species $(VOQ_2)-O-(VOQ_2)^-$ at -0.05V.

The shape of the electronic spectra of the species obtained by the reduction of VOL.OEt and $(VOL)_2O$ (L = Bzac-BH) at +0.2V is identical to the spectrum of the assumed $(VOL)_2/VOL.MeOH$ [see spectrum A in Figure 4.2.1 and Section 4.2(a)]. This was obtained from $VOCl_2$, LiOAC and $\underline{LH_2}$ (L = Bzac-BH) under oxygen free condition. From the above evidence it is now clear that some oxidation must have taken place inspite of the rigorous oxygen free procedures followed. This is further supported by the fact that the molar absorptivity at the λ_{max} of 415 nm was significantly lower in the spectrum of '$(VOL)_2$' which now must be considered to be that of a mixture.

With some of the other ligands (e.g. HAP-BH) the $E_{1/2}$ obtained from VOL.OR were significantly different from those of $(VOL)_2O$. This may be due to incomplete hydrolysis of the alkoxo complexes in solution.

TABLE 5.5.2: COULOMETRIC DATA FOR SOME VOL.OR AND $(VOL)_2O$ COMPLEXES

COMPLEX	C.P.E. AT (V)	FOR ONE ELECTRON REDN.	
		CALC. Q Ceq	OBS. Q Ceq
VO(Bzac-BH).OEt	+0.200	5.216	2.603
[VO(Bzac-BH)]$_2$O	+0.200	2.387	1.846
VO(HNP-BH).OMe	-0.100	4.825	2.102

a. In DMSO/Et$_4$NClO$_4$/Pt medium.

5.6   ALKOXO-BRIDGED OXOVANADIUM(IV) COMPLEXES

A number of the alkoxo-bridged $[VO(AA)(OR)]_2$ complexes described in Chapter 2 were subjected to voltammetric studies in order to examine the possibility of using electrochemical methods for their characterization and investigation of solution properties. However, comparison of their cyclic voltammograms, including differential pulse in some cases, with those of the bis-$VO(AA)_2$ complexes (Figures 5.6.1 and 5.6.2) show that (i) the oxidation waves above +0.7V are comparable to those of the corresponding $VO(AA)_2$ complexes and (ii) the oxidation waves between +0.2 and +0.5V which are observed in all $[VO(AA)(OR)]_2$ dimers irrespective of the alkyl group are relatively weak and seem to be due to some other species formed by the decomposition of these dimers. It has been observed (Section 2.3) that these alkoxo-bridged complexes readily decompose in the presence of a trace of moisture to $VO(AA)_2$ and $VO(OH)_2$. In DMSO, we speculate that the second species produced is most probably a solvated vanadyl species which oxidizes at potentials in the region +0.2-(+)0.5V. Inspite of all precautions to exclude moisture, the possibility of sufficient traces to hydrolyse the alkoxo group cannot be ignored. In most cases, the peak position and intensity were found to differ with time as well as for initial positive or negative scans. It is interesting to note that on standing in DMSO solution or better on repeated scans the $VO(AA)_2$ complexes also developed weak-additional peaks in this region. To draw any definite conclusions on the species formed and these wave characteristics, it is appropriate to further study these complexes in a rigorous air and moisture-free condition and most suitably using spectro-electrochemical techniques enabling monitoring of the decomposition of the experimental solutions.
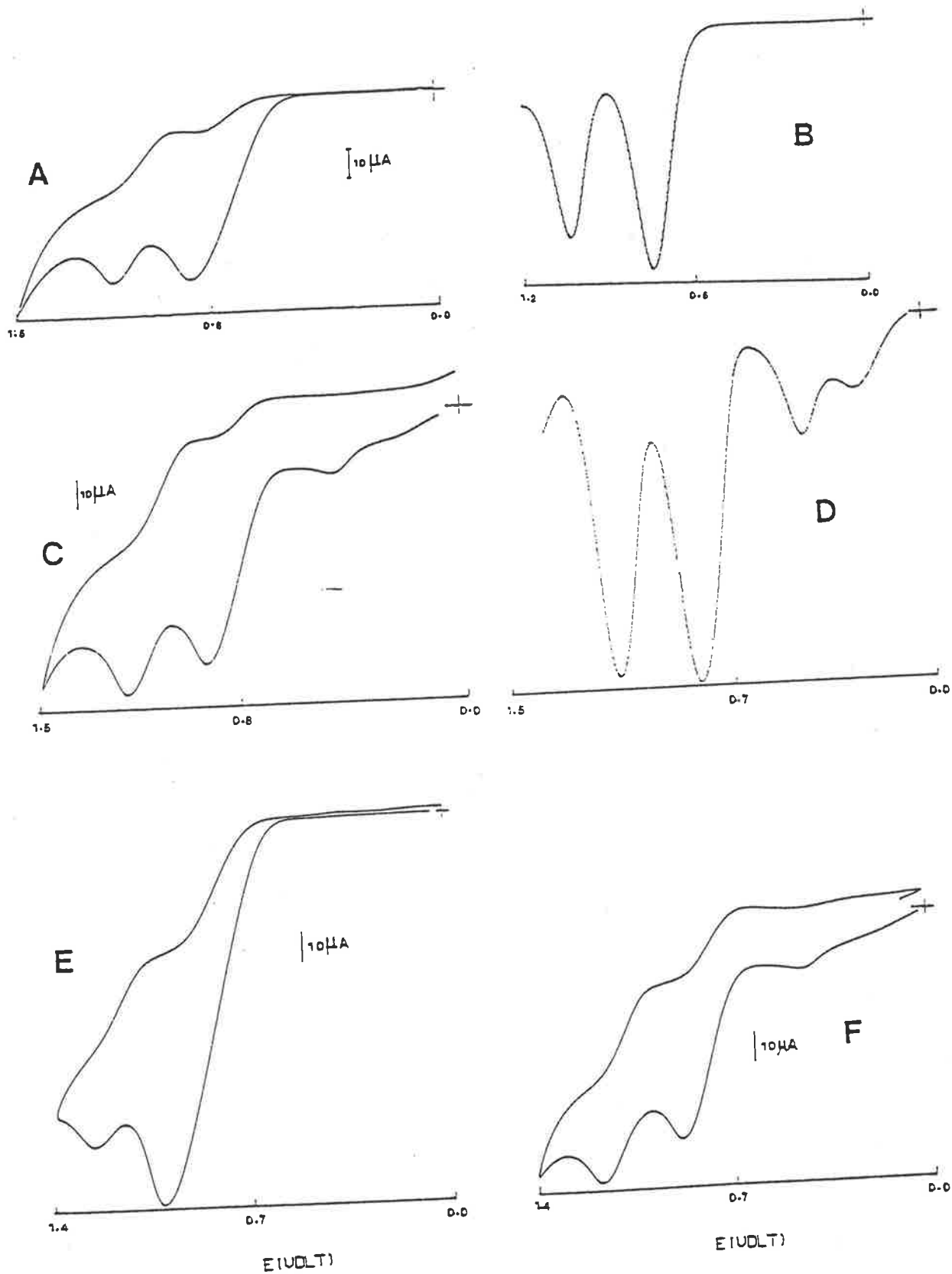
Figure 5.6.1: Cyclic voltammograms (in DMSO/0.1M Et$_4$NBF$_4$/Pt) of A. VO(acac)$_2$, [B. Differential pulse voltammogram (D.P.V.) of A]; C. [VO(acac)(OEt)]$_2$, [D. D.P.V. of C]; E. VO(Bzac)$_2$ and F. [VO(Bzac)(OBu^2)]$_2$. Scan rate for C.V. 100 mV/sec.; for D.P.V. 5 mV/sec.
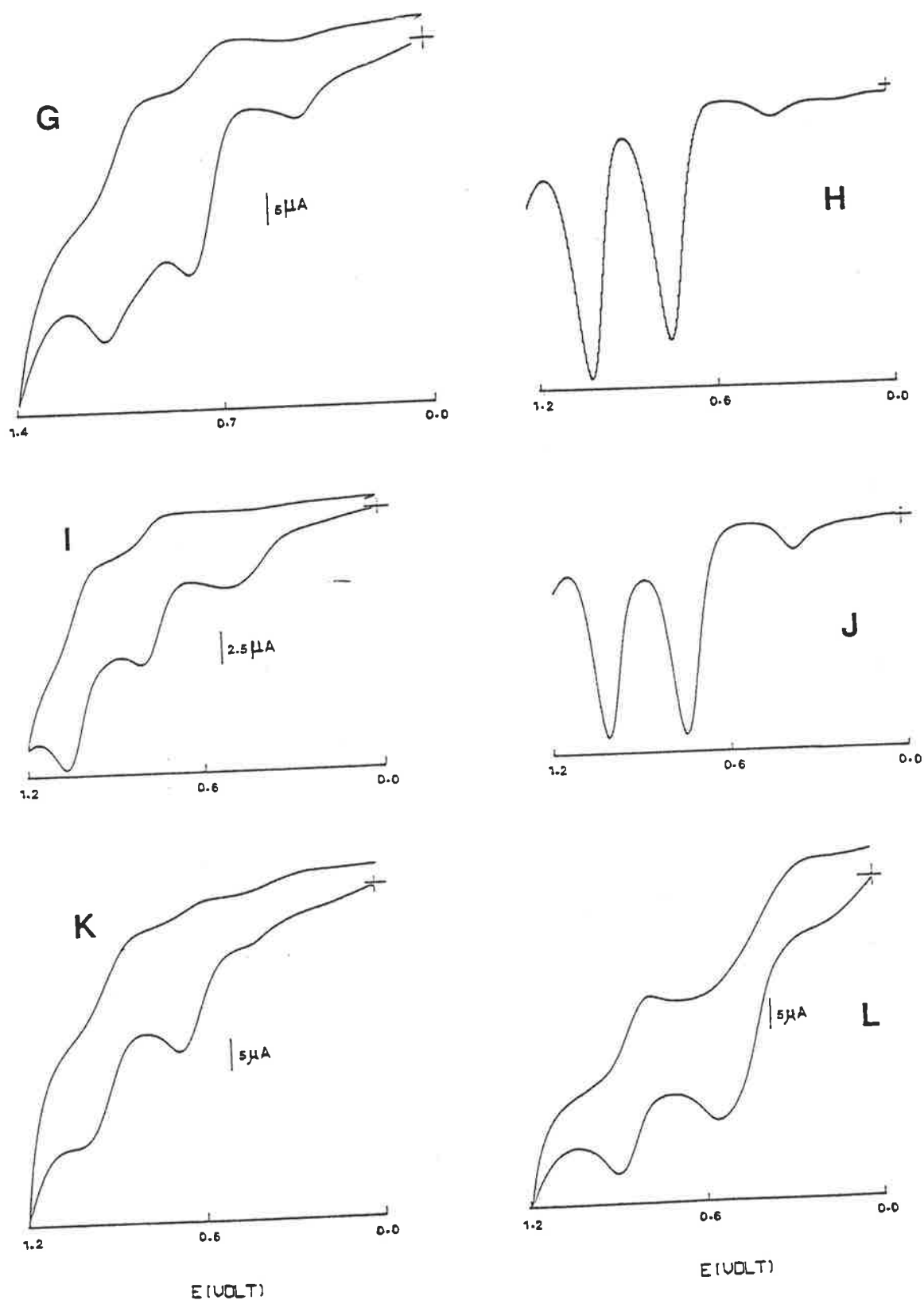
Figure 5.6.2: Cyclic voltammograms (in DMSO/0.1M Et$_4$NBF$_4$/Pt) of G. [VO(Bzac)(OMe)]$_2$, [H. D.P.V. of G], I. [VO(dbm) (OMe)]$_2$, [J. D.P.V. of I]; K. [VO(HNP)(OMe)]$_2$ and L. [VO(HAP)(OMe)]$_2$. Scan rate for C.V. 100 mV/sec.; for D.P.V. 5 mV/sec.

CHAPTER   6

E X P E R I M E N T A L

6.1   STARTING MATERIALS

Acetylacetone, benzoylacetone, dibenzoylmethane, 2-hydroxy-1-napthalde-hyde, 2-hydroxyacetophenone, 2-hydroxypropiophenone, 2,4-dihydroxybenzophen-one, salicylaldehyde, o-aminophenol, p-methyl-o-aminophenol, p-chloro-o-amino-phenol, 3-amino-2-napthol, p-methoxyphenol, p-cresol, p-chlorophenol, phenyl-hydrazine, ethylbenzoate and ethyl salicylate were obtained from Aldrich Chem-ical Company Inc.   Phenol and β-napthol were obtained from BDH Chemicals. Most of the solid compounds were of sufficient purity to use directly.   The liquid materials were distilled before use.

6.1.1   Vanadyl Chloride - $VOCl_2$

$VOCl_2 \cdot nH_2O$, obtained as a 50% solution from BDH Chemicals, was dried over P_2O_5 under vacuum until a blue solid mass was obtained.   This was then dissolved in the appropriate dry alcohol and the vanadium content of the solu-tion was determined from the spectrum in 1 M H_2SO_4 solution [a_M of $VO(OH_2)_n^{2+}$ = 17.8 M^{-1} cm^{-1}].

BIS-BIDENTATE OXOVANADIUM(IV) COMPLEXES

6.1.2   Bis(acetylacetonato)oxovanadium(IV) - $VO(acac)_2$

This was prepared by the method of Rowe and Jones[321].   A dark blue solu-tion of vanadyl sulphate was obtained by reducing V_2O_5 (100 mmol) on heating in water (50 ml) containing H_2SO_4 (35 ml) and ethanol (100 ml) for about 30 minutes.   Freshly distilled acetylacetone (45 ml) was added to this and the

solution was neutralized slowly by Na_2CO_3 solution (16%) on continuous stirring when blue precipitate appeared. This was filtered and recrystallized from chloroform solution and identified from its vanadium and ligand contents determined by methods as described in Section 6.3 (ii).

6.1.3 Bis(benzoylacetonato)oxovanadium(IV) - VO(Bzac)$_2$

This compound was prepared by the published procedure[21]. A mixture of an aqueous solution of $VOSO_4$ and an ethanol solution of benzoylacetone was neutralized with dilute ammonium hydroxide with constant stirring. The green precipitate formed was filtered, washed with water, then ether, dried and recrystallized from chloroform solution. This was identified by its V and ligand contents.

6.1.4 Bis(dibenzoylmethano)oxovanadium(IV) - VO(dbm)$_2$

The above procedure 6.1.3 gave this apple-green compound which was identified similarly.

6.1.5 Monoaquo-bis(salicylaldehydo)oxovanadium(IV) - VO(Sal)$_2$.H_2O

This was prepared by following a published procedure[322]. A solution of salicylaldehyde (22 mmol) in ethanol (50 ml) was added, under nitrogen atmosphere, to $VOCl_2$ (10 mmol) solution in water (50 ml). This, after stirring for 5 minutes, was neutralized with excess of sodium acetate solution. The olive-green precipitate was filtered, washed with water and then diethyl ether, dried and characterized by its vanadium content and infrared spectrum.

6.1.6 Monoaquo-bis(2-oxo-1-napthaldehydo)oxovanadium(IV) - VO(HNP)$_2$.H_2O

This olive-green compound was prepared following the literature method[266] similar to the above (6.1.5) preparation and characterized by its vanadium and ligand contents.

AROYLHYDRAZINES

6.1.7 Benzoylhydrazine - $C_6H_5CONHNH_2$

This was prepared by refluxing ethylbenzoate with hydrazine hydrate for 21 hours and then recrystallizing twice from ethanol. m.p. 112°C (lit.[323] 112.5°C).

6.1.8 p-Chlorobenzoylhydrazine - $p-Cl-C_6H_4CONHNH_2$

A mixture of ethyl-p^{Cl}-benzoate (prepared by literature method[324]; b.p. 238°C) and hydrazine hydrate was refluxed for 3 $\frac{1}{2}$ hours and the white solid mass recrystallized twice from hot water. m.p. 163°C (lit.[325] 163°C).

6.1.9 p-Nitrobenzoylhydrazine - $p-NO_2-C_6H_4CONHNH_2$

A mixture of p-nitrobenzoyl chloride and hydrazine hydrate was refluxed for 14 hours and the white solid mass recrystallized twice from ethanol. m.p. 210°C (lit.[326] 210-2°C).

6.1.10 Salicyloylhydrazine - $2-HO-C_6H_4CONHNH_2$

Ethylsalicylate was refluxed with hydrazine hydrate for 5 hours and the white solid mass obtained was recrystallized twice from hot water. m.p. 146°C (lit.[327] 146.5°C).

6.2 REAGENTS, SOLVENTS AND GASES

REAGENTS

The 0.5 M sodium tungstate solution, used in the vanadium analysis of the prepared complexes, was prepared by dissolving Na_2WO_4, $2H_2O$ (16.5 g, A.R., BDH) in water (100 ml). Tetraethylammonium perchlorate and tetraethylammonium tetrafluoroborate, used as supporting electrolytes in the electrochemical experiments, were prepared following literature methods[328]. The former was

prepared by treating Et_4NBr (25 mmol) in water (~ 8 ml) with aqueous 70% $HClO_4$ (26 mmol) and recrystallized twice from water. m.p. 350-352°C with decomposition. Et_4NBF_4 was similarly prepared by reacting Et_4NBr (25 mmol) in water (~ 8 ml) with HBF_4, concentrating and then diluting with diethyl ether and recrystallizing the product twice from a methanol-petroleum ether (40-60°C) mixture. m.p. 376-8°C with decomposition.

SOLVENTS

All solvents were dried by standard methods[324,329] and distilled under dinitrogen atmosphere before use.

GASES

High purity dinitrogen and argon obained from C.I.G. Australia Ltd. were used as received.

6.3   EXPERIMENTAL TECHNIQUES

(i)   HANDLING OF AIR-SENSITIVE COMPOUNDS

These compounds were manipulated under an inert atmosphere using schlenk glassware. Such glassware was fitted with one or more taps allowing evacuation of the apparatus followed by the introduction of the inert gas.

(ii)   ANALYSES

Microanalyses were performed by the Canadian Microanalytical Service Ltd., Vancouver, B.C.

The vanadium contents were determined by the phosphotungstate method[330]. The organic content of the complex was destroyed and the vanadium converted to the +5 state by treating an accurately weighed (~ 5 mg) sample of the complex, first with concentrated H_2SO_4 (0.2 ml), and evaporating to dryness with 2-3 ml portions of concentrated HNO_3, and finally with $HClO_4$ (70%) (2-3 ml portions). Absorption at 410 nm was used to determine the V-content. A calibration curve

was prepared with NH_4VO_3 (ANALAR).

For vanadyl complexes, including some alkoxo-bridged dimers, the % of the chelate ligand was determined from the UV spectrum of a solution of the freshly prepared complex in 0.5 M H_2SO_4 in 50% aqueous-ethanol. The spectrum was compared with that of the bidentate ligand in the same solvent after allowing for the absorptions by VO^{2+} and the relevant alcohol in the same solvent.

6.4 PREPARATION OF ALKOXO-BRIDGED OXOVANADIUM(IV) COMPLEXES-[VO(AA)(OR)]$_2$

The following three general methods were employed to obtain the dimeric complexes.

METHOD A: From bis(β-diketonato)oxovanadium(IV), VO(AA)$_2$

VO(AA)$_2$ and phenylhydrazine in the ratio of 1:1 in degassed ROH (R = Me, Et, ^nPr) were refluxed under dinitrogen for about 45 minutes. The dimer product was collected on cooling in a refrigerator at $\sim$ 6°C.

METHOD B: Direct Synthesis from VOCl$_2$

VOCl$_2$ solution in dry ROH (R = Me, Et, ^nPr) was degassed and added to it appropriate amounts of the bidentate ligand AA$\underline{H}$ and a base (LiOAC or Et$_3$N). This was refluxed under dinitrogen for about 45 minutes and the product collected on cooling.

METHOD C: Metathesis Reaction

The methoxo (or ethoxo)-bridged dimer in the appropriate deoxygenated alcohol, ROH (R = Pr^n, Pr^i, Bu^n, Bu^2, EtOMe, EtOEt, Ph, Bz, p^{X}Bz) was refluxed under dinitrogen for about 45 minutes. In almost all cases, the higher alkoxo-bridged dimers, [VO(AA)(OR)]$_2$ were formed readily by metathesis.

Below are the methods employed to prepare the individual dimer complexes.

6.4.1 Di-μ-methoxo-bis[(acetylacetonato)oxovanadium(IV)] - [VO(acac)(OMe)]$_2$

(a)   To VO(acac)$_2$ (25 mmol) in dry and rigorously oxygen-free MeOH (150 ml) was added, PhNHNH$_2$ (25 mmol) and the mixture on further degassing with dinitrogen was refluxed for 45 minutes. The blue crystals that separated slowly on cooling were filtered, washed with degassed methanol and petroleum spirit (40-60°C) and dried over fused granular CaCl$_2$ under high vacuum. Yield 74%, m.p. 182-5°C (decomposition); Analysis, found: C, 36.55; H, 5.08; V, 25.11. (VC$_6$H$_{10}$O$_4$)$_2$ requires C, 36.57; H, 5.11; V, 25.85%.

(b)   To VOCl$_2$ (12 mmol) in dry and degassed MeOH (30 ml) were added acetylacetone (11.5 mmol) and Et$_3$N (23 mmol) and refluxed the solution for 40 minutes. The blue product formed slowly on cooling was collected and identified from its infrared spectrum. Yield 75%.

6.4.2 Di-μ-ethoxo-bis[(acetylacetonato)oxovanadium(IV)] - [VO(acac)(OEt)]$_2$

(a)   PhNHNH$_2$ (25 mmol) was added to VO(acac)$_2$ (25 mmol) in dry and degassed ethanol under dinitrogen and the mixture was refluxed for 40 minutes. The beautiful sky-blue crystals that formed slowly on cooling were filtered, washed with degassed ethanol and petroleum spirit (40-60°C) and dried. Yield 75%, m.p. 180-5°C (decomposition); Analysis, found: C, 39.20; H, 5.41; V, 24.32. (VC$_7$H$_{12}$O$_4$)$_2$ requires C, 39.82; H, 5.73; V, 24.13%.

(b)   Following procedure for 6.4.1 (b), this compound was also prpeared by refluxing degassed solution of VOCl$_2$, acac<u>H</u> and Et$_3$N and identified from its infrared spectrum. Yield 75%.
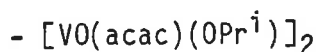
6.4.3 Di-μ-n-propoxo-bis[(acetylacetonato)oxovanadium(IV)]
- [VO(acac)(OPr^n)]$_2$

(a)   The same procedure as for 6.4.1 (a) using n-propanol as the solvent

gave a blue product. Yield 40%, m.p. 182-6°C (decomposition), Analysis, found: C, 42.48; H, 5.97; V, 22.95. $(VC_8H_{12}O_4)_2$ requires C, 42.68; H, 6.27; V, 22.63%.

(b) $[VO(acac)(OMe)]_2$ (5 mmol) in dry and degassed n-propanol (40 ml) was refluxed for 40 minutes and the blue crystals separated on cooling were collected and identified from the infrared spectrum. Yield 90%.

## 6.4.4 Di-μ-isopropoxo-bis[(acetylacteonato)oxovanadium(IV)]

- $[VO(acac)(OPr^i)]_2$

The same metathesis method and quantities as for 6.4.3 (b) were used to obtain a blue crystalline product. Yield 84%, m.p. 160-3°C, Analysis, found: C, 42.57; H, 6.27; V 23.16. $(VC_8H_{12}O_4)_2$ requires C, 42.68; H, 6.27; V, 22.63%.

6.4.5 Di-μ-benzyloxo-bis[(acetylacetonato)oxovanadium(IV)] - $[VO(acac)(OBz)]_2$

$[VO(acac)OEt)]_2$ (3 mmol) in dry and degassed benzyl alcohol (35 ml) was refluxed for 40 minutes and the blue precipitate formed on cooling was filtered, washed with excess ether (to remove benzyl alcohol) and dried. Yield 95%, m.p. 200-1°C, Analysis, found: C, 53.35; H, 5.05; V, 18.65. $(VC_{12}H_{14}O_4)_2$ requires C, 52.76; H, 5.16; V, 18.65%.

6.4.6 Di-μ-p-methoxybenzyloxo-bis[(acetylacetonato)oxovanadium(IV)]

- $[VO(acac)(OBz-p^{OMe})]_2$
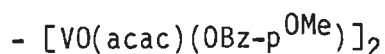
$[VO(acac)(OMe)]_2$ (1 mmol) in dry and degassed toluene (60 ml) containing a high excess (4.0 g) of p-methoxybenzyl alcohol was refluxed for 40 minutes. The blue precipitate that formed after standing at room temperature was filtered and washed with excess ether (degassed) to remove any adhering alcohol and toluene and dried. Yield 90%, m.p. 155-160°C (decomposition), Analysis, found: C, 50.64; H, 5.41; V, 17.13. $(VC_{13}H_{16}O_5)_2$ requires C, 51.50; H, 5.32; V, 16.80%.

6.4.7 Di-μ-methoxo-bis[(benzoylacetonato)oxovanadioum(IV)] - [VO(Bzac)(OMe)]$_2$

(a) PhNHNH$_2$ (10 mmol) was added to dry and degassed MeOH (120 ml) containing VO(Bzac)$_2$ (10 mmol) and the degassed mixture was refluxed for 45 minutes when an olive-green precipitate was formed. This was filtered on cooling, washed with degassed MeOH and petroleum spirit (40-60°C) and dried under vacuum. Yield 94%, m.p. 215-8°C, Analysis, found: C, 51.06; H, 4.71; V, 19.39. (VC$_{11}$H$_{12}$O$_4$)$_2$ requires C, 50.98; H, 4.67; V, 19.66%.

(b) To VOCl$_2$ (3.2 mmol) solution in dry and degassed MeOH (35 ml) were added BzacH (3 mmol) and Et$_3$N (6 mmol) and stirred the solution for a few minutes when a green precipitate was observed to form. Refluxed the mixture for 30 minutes and the precipitate was collected on cooling and characterized by its infrared spectrum. Yield 90%.

6.4.8 Di-μ-ethoxo-bis[(benzolyacetonato)oxovanadium(IV)] - [VO(Bzac)(OEt)]$_2$

(a) The same procedure as for 6.4.7 (a) gave an olive-green product. Yield 92%, m.p. 213-5°C, Analysis, found: C, 52.46; H, 4.92; V, 18.85. (VC$_{12}$H$_{14}$O$_4$)$_2$ requires C, 52.76; H, 5.17; V, 18.65%.

(b) The direct method as detailed for 6.4.7 (b) gave the same compound characterized by its infrared spectrum. Yield 90%.

6.4.9 Di-μ-n-propoxo-bis[(benzoylacetonato)oxovanadium(IV)]
   - [VO(Bzac)(OPr^n)]$_2$
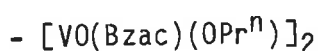
(a) A (bluish) green product was obtained by following the same procedure as for 6.4.7 (a) which was characterized by its V-content and characteristic infrared spectrum. Yield 85%.

(b) [VO(Bzac)(OMe)]$_2$ (4 mmol) in dry and degassed n-propanol (80 ml) was refluxed for 35 minutes. The green mostly insoluble starting methoxo-bridged dimer was converted into the n-propoxo-bridged dimer. A green (slightly bluish) precipitate was collected on cooling, washed with degassed petroleum spirit (40-60°C) and dried. Yield 95%, m.p. 230-2°C, Analysis,

found: C, 54.46; H, 5.52; V, 17.93. $(VC_{13}H_{16}O_4)_2$ requires C, 54.37; H, 5.61; V, 17.74%.

6.4.10 Di-μ-isopropoxo-bis[(benzoylacetonato)oxovanadium(IV)]

- $[VO(Bzac)(OPr^i)]_2$
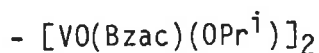
The same metathesis method as for 6.4.9 (b), but using isopropanol as the solvent, gave an olive-green compound. Yield 96%, m.p. 207-10°C (decomposition); Analysis, found: C, 54.40; H, 5.54; V, 18.06. $V(C_{13}H_{16}O_4)_2$ requires C, 54.37; H, 5.61; V, 17.74%.

6.4.11 Di-μ-n-butoxo-bis[(benzoylacetonato)oxovanadium(IV)]

- $[VO(Bzac)(OBu^n)]_2$
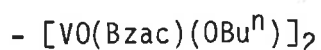
The same metathesis method as for 6.4.9 (b) gave a light bluish green product. Yield 80%, m.p. 166-70°C (decomposition), Analysis, found: [Bzac], 52.97; V, 17.12. $V(C_{14}H_{18}O_4)_2$ requires [Bzac], 53.52; V, 16.91%.

6.4.12 Di-μ-sec-butoxo-bis[(benzoylacetonato)oxovanadium(IV)]

- $[VO(Bzac)(OBu^2)]_2$
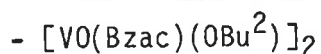
The same metathesis reaction as for 6.4.9 (b), but using sec-butanol as the solvent, gave a light bluish green product. Yield 85%, m.p. 228-30°C, Analysis, found: C, 55.43; H, 6.23; V, 16.97. $(VC_{14}H_{18}O_4)_2$ requires C, 55.82; H, 6.02; V, 16.91%.

6.4.13 Di-μ-2-methoxyethoxo-bis[(benzoylacetonato)oxovanadium(IV)]

- $[VO(Bzac)(OEtOMe)]_2$
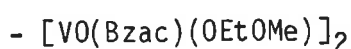
(a) Following the same procedure as for 6.4.9 (b) a green compound was obtained by metathesis reaction of $[VO(Bzac)(OMe)]_2$ (4 mmol) in 2-methoxyethanol (40 ml). Yield 80%, m.p. 191-2°C, Analysis, found: C, 51.57; H, 5.53; V, 16.80. $(VC_{13}H_{16}O_5)_2$ requires C, 51.50; H, 5.32; V, 16.80%.

(b) This compound was also prepared by refluxing equimolar amounts of $VO(Bzac)_2$ and $PhNHNH_2$ in dry and degassed 2-methoxyethanol and characterized by its infrared spectrum and V- and [Bzac] contents.

6.4.14 Di-μ-2-ethoxyethoxo-bis[(benzoylacetonato)oxovanadium(IV)]
### - [VO(Bzac)(OEtOEt)]₂
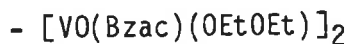
A green product was obtained by the metathesis reaction as described for 6.4.9 (b). m.p. 170-5°C (decomposition), Analysis, found: [Bzac], 50.53; V, 16.54. $(VC_{14}H_{18}O_5)_2$ requires [Bzac), 50.81; V, 16.06%.

6.4.15 Di-μ-phenoxo-bis[(benzoylacetonato)oxovanadium(IV)] - [VO(Bzac)(OPh)]₂

$[VO(Bzac)(OMe)]_2$ (4 mmol) in a degassed solution of an excess (5.0 g) of phenol in dry and degassed toluene (40 ml) was refluxed for 45 minutes. A light bluish-green precipitate formed was filtered hot, washed with excess ether to remove phenol and toluene, if any, and dried under high vacuum over fused $CaCl_2$. Yield 90%, m.p. 265-80°C (decomposition), Analysis, found: C, 59.70; H, 4.59; V, 15.95. $V(C_{16}H_{14}O_4)_2$ requires C, 59.83; H, 4.39; V, 15.86%.

6.4.16 Di-μ-benzyloxo-bis[(benzoylacetonato)oxovanadium(IV)]
- [VO(Bzac)(OBz)]₂
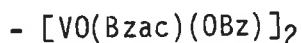
The metathesis method 6.4.9 (b) gave a green product which was washed with excess ether to remove any adhering benzyl alcohol. Yield 91%, m.p. 206-8°C (decomposition), Analysis, found: C, 60.67; H, 4.84; V, 15.56. $(VC_{17}H_{16}O_4)_2$ requires C, 60.90; H, 4.81; V, 15.20%.

## 6.4.17 Di-μ-p-methoxybenzyloxo-bis[(benzoylacetonato)oxovanadium(IV)]
- [VO(Bzac)(OBz-p^{OMe})]₂
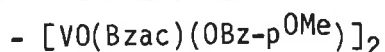
A green compound was prepared following the same procedure as for 6.4.15, but using p-methoxobenzylalcohol as the reacting alcohol. m.p. 186-9°C

(decomposition), Analysis, found: [Bzac], 44.76; V, 14.20. $V(C_{18}H_{18}O_5)_2$
requires [Bzac], 44.13; V, 13.95%.

6.4.18 Di-μ-p-nitro-benzyloxo-bis[(benzoylacetonato)oxovanadium(IV)]

　　　- [VO(Bzac)(OBz-p^{NO_2})]$_2$
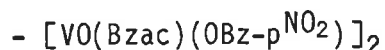
A green product was obtained by the same procedure as for 6.4.15.
m.p. 191-2°C, Analysis, found: [Bzac], 41.97; V, 13.67. $V(C_{17}H_{15}NO_6)_2$
requires [Bzac], 42.39; V, 13.40%.

6.4.19 Di-μ-methoxo-bis[(dibenzoylmethano)oxovanadium(IV)] - [VO(dbm)(OMe)]$_2$

A light yellow solution of dibenzoylmethane (10 mmol) and Et_3N (20 mmol)
in dry methanol (50 ml) was degassed with dinitrogen and slowly added to a
degassed solution of $VOCl_2$ (11 mmol) in MeOH (30 ml). During stirring at room
temperature an apple-green precipitate appeared. The mixture was refluxed for
35 minutes and the precipitate collected on cooling was washed with degassed
methanol and petroleum spirit and dried under vacuum. Yield 86%, m.p. 251-4°C
(decomposition), Analysis, found: C, 59.55; H, 4.42; V, 16.13. $(VC_{16}H_{14}O_4)_2$
requires C, 59.82; H, 4.39; V, 15.86%.

6.4.20 Di-μ-ethoxo-bis[(dibenzoylmethano)oxovanadium(IV)] - [VO(dbm)(OEt)]$_2$

A green product was obtained by the same method as for 6.4.19. Yield
88%, m.p. 250-3°C (decomposition), Analysis, found: C, 60.63; H, 4.93;
V, 15.46. $(VC_{17}H_{16}O_4)_2$ requires C, 60.90; H, 4.81; V, 15.20%.

6.4.21 Di-μ-n-propoxo-bis[(dibenzoylmethano)oxovanadium(IV)]

　　　- [VO(dbm)(OPr^n)]$_2$
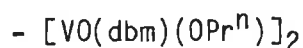
(a)   Following the same procedure as for 6.4.9 (b), an olive-green
product was prepared by the metathesis reaction of (VO(dbm)(OMe)]$_2$ in dry and
degassed n-PrOH. Yield 96%, m.p. 248-50°C (decomposition), Analysis, found:
C, 61.72; H, 5.03; V, 15.17. $(VC_{18}H_{18}O_4)_2$ requires C, 61.90; H, 5.19;
V, 14.59%.

(b)   This was also prepared by method 6.4.19 and identified by its characteristic infrared spectrum.

6.4.22 Di-μ-isopropoxo-bis[(dibenzoylmethano)oxovanadium(IV)]

- [VO(dbm)(OPr^i)]$_2$
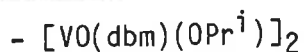
The same metathesis method as for 6.4.9 (b) gave an olive-green product. Yield 95%, m.p. 240-44°C (decomposition), Analysis, found: C, 61.78; H, 4.83; V, 14.29. (VC$_{18}$H$_{18}$O$_4$)$_2$ requires C, 61.90; H, 5.19; V, 14.59%.
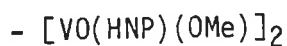
6.4.23 Di-μ-benzyloxo-bis[(dibenzoylmethano)oxovanadium(IV)] - [VO(dbm)(OBz)]$_2$
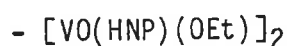
A pale-green product was obtained by the same metathesis method. Yield 87%, m.p. 206-8°C (decomposition), Analysis, found: C, 66.21; H, 4.54; V, 13.12. (VC$_{22}$H$_{18}$O$_4$)$_2$ requires C, 66.50; H, 4.57; V, 12.82%.

6.4.24 Di-μ-methoxo-bis[(2-oxo-1-napthaldehydo)oxovanadium(IV)]
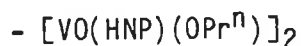
- [VO(HNP)(OMe)]$_2$

A solution of 2-hydroxy-1-napthaldehyde (10 mmol) and Et$_3$N (20 mmol) in dry MeOH (50 ml) was degassed with dinitrogen and added slowly to a degassed solution of VOCl$_2$ (11 mmol) in MeOH (30 ml) when a green precipitate was found almost immediately. The mixture was refluxed for 15 minutes. The precipitate was filtered on cooling, washed with degassed MeOH and petroleum spirit and dried under high vacuum. Yield 92%, m.p. 230-5°C (decomposition), Analysis, found: C, 52.24; H, 3.20; V, 19.21. (VC$_{12}$H$_{10}$O$_4$)$_2$ requires C, 53.55; H, 3.74; V, 18.93%.

6.4.25 Di-μ-ethoxo-bis[(2-oxo-1-napthaldehydo)oxovanadium(IV)]

- [VO(HNP)(OEt)]$_2$

An apple-green product was obtained by following the same method as for 6.4.24. Yield 90%, m.p. 230-5°C (decomposition), Analysis, found: C, 55.02; H, 4.44; V, 18.13. (VC$_{13}$H$_{12}$O$_4$)$_2$ requires C, 55.14; H, 4.27; V, 17.99%.

6.4.26 Di-μ-n-propoxo-bis[(2-oxo-1-napthaldehydo)oxovanadium(IV)]

- [VO(HNP)(OPr^n)]$_2$

(a) A green product was prepared by the same procedure as for 6.4.9(b). The almost insoluble starting [VO(HNP)OMe]$_2$ complex was converted to the n-propoxo dimer on reflux. Yield 96%, m.p. 215-8°C (decomposition), Analysis, found: C, 55.65; H, 4.76; V, 17.25. (VC$_{14}$H$_{14}$O$_4$)$_2$ requires C, 56.58; H, 4.75; V, 17.14%.

(b) This was also prepared by the direct method 6.4.24 and identified by its characteristic infrared spectrum.

6.4.27 Di-μ-isopropoxo-bis[(2-oxo-1-napthaldehydo)oxovanadium(IV)]

- [VO(HNP)(OPr^i)]$_2$
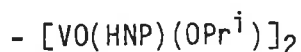
An olive-green product was prepared by the same metathesis method as for 6.4.9 (b). Yield 92%, m.p. 230-3°C (decomposition), Analysis, found: C, 52.79; H, 4.55; V, 17.51. (VC$_{14}$H$_{14}$O$_4$)$_2$ requires C, 56.58; H, 4.75; V, 17.14%.

6.4.28 Di-μ-benzyloxo-bis[(2-oxo-1-napthaldehydo)oxovanadium(IV)]

- [VO(HNP)(OBz)]$_2$

The same metathesis method as for 6.4.9 (b) gave a green product. Yield 80%, m.p. 203-5°C (decomposition), Analysis, found: C, 61.73; H, 3.97; V, 14.91. (VC$_{18}$H$_{14}$O$_4$)$_2$ requires C, 62.62; H, 4.09; V, 14.76%.

6.4.29 Di-μ-methoxo-bis[(2-oxoacetophenone)oxovanadium(IV)] - [VO(HAP)(OMe)]$_2$

A degassed solution of 2-hydroxyacetophenone (10 mmol) and Et$_3$N (20 mmol) in dry MeOH (30 ml) was slowly added to a degassed solution of VOCl$_2$ (11 mmol) in MeOH (20 ml). An olive-green precipitate appeared during stirring at room temperature for about 30 minutes. The mixture was refluxed for 25 minutes. The precipitate was filtered on cooling, washed with degassed methanol and petroleum spirit and dried. Yield 70%, m.p. 218-20°C (decompo-

sition), Analysis, found: C, 43.34; H, 4.22; V, 22.67; [HAP], 58.54. $(VC_9H_{10}O_4)_2$ requires C, 46.37; H, 4.32; V, 21.85; [HAP], 57.97%.

6.4.30 Di-μ-ethoxo-bis[(2-oxoacetophenone)oxovanadium(IV)] - [VO(HAP)(OEt)]$_2$

The same direct method as for 6.4.29 gave a green product. Yield 75%, m.p. 219-21°C (decomposition), Analysis, found: C, 46.76; H, 4.87; V, 20.87; [HAP], 54.52. $(VC_{10}H_{12}O_4)_2$ requires C, 48.60; H, 4.90; V, 20.61; [HAP], 54.68%.
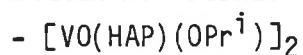
6.4.31 Di-μ-n-propoxo-bis[(2-oxoacetophenone)oxovanadium(IV)]

- [VO(HAP)(OPr^n)]$_2$
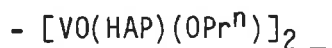
(a) The same metathesis method as for 6.4.9 (b) gave an olive-green product. Yield 83%, m.p. 183-6°C (decomposition), Analysis, found: C, 51.16; H, 5.23; V, 19.46. $(VC_{11}H_{14}O_4)_2$ requires C, 50.59; H, 5.40; V, 19.51%.

(b) This was also prepared by direct method 6.4.29 and identified by its characteristic infrared spectrum.

6.4.32 Di-μ-isopropoxo-bis[(2-oxoacetophenone)oxovanadium(IV)]

- [VO(HAP)(OPr^i)]$_2$

A (bluish) green product was obtained by the metathesis method as described for 6.4.9 (b). Yield 80%, m.p. 127-30°C (decomposition), Analysis, found: [HAP], 51.33; V, 19.67. $V(C_{11}H_{14}O_4)_2$ requires [HAP], 51.74; V, 19.51%.

6.4.33 Di-μ-benzyloxo-bis[(2-oxoacetophenone)oxovanadium(IV)]

- [VO(HAP)(OBz)]$_2$

The same metathesis method as for 6.4.9 (b) gave a light green product. Yield 90%, m.p. 184-7°C (decomposition), Analysis, found: C, 57.41; H, 4.54; V, 16.40. $(VC_{15}H_{14}O_4)_2$ requires C, 58.26; H, 4.56; V, 16.47%.
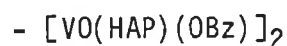
6.4.34 <u>(Acetylacetonato)(2-oxoacetophenone)oxovanadium(IV)</u> - VO(acac)(HAP)

2-Hydroxyacetophenone (1 mmol) in dry toluene (20 ml) was degassed and to it was added [VO(acac)(OEt)]$_2$ (0.5 mmol) under dinitrogen. The colour changed from blue to green in about 10 minutes. The solution was refluxed for 15 minutes and evaporated to dryness under high vacuum. The green solid left was precipitated out from dichloromethane-petroleum spirit, washed with petroleum spirit to remove any free HAP<u>H</u> and dried under vacuum. Yield 85%, Analysis, found, [HAP], 44.2; V, 16.7. VO(acac)(HAP) requires [HAP], 44.9; V, 16.9%. Mass spectrum showed strong peaks for the VO(acac)(HAP) molecular ion (301) along with peaks at 265 and 337 for VO(acac)$_2$ and VO(HAP)$_2$ respectively. The UV spectrum of this compound in 0.5 M H$_2$SO$_4$ in 50% aqueous-ethanol shows absorptions due to both acac<u>H</u> and HAP<u>H</u>. The above compound did not show any spot remaining at the origin in the T.L.C. (in diethylether) plate indicative of the presence of VO(acac)$_2$.

6.5   PREPARATION OF TRIDENTATE LIGANDS

The Schiff base ligands were prepared by condensation reactions following literature methods and their melting point determined. In all cases, the mass spectra and the infrared spectra were taken as evidence for the Schiff base formation. Also the usually quantitative yields and the acceptable micro-analyses of their VL$_2$ and other complexes indicated formation and purity of the ligands. On the basis of the above evidence that the prepared solids were the right Schiff bases, and because of their preparation as intermediates for the preparation of the complexes, no micro-analyses of the ligands were carried out. Thus, although the ligands described below are most probably the right compounds we make no claim, however, for the compounds which we could not find in the literature.

BENZOYLHYDRAZONE SCHIFF BASES

6.5.1 <u>4-Phenylbutane-2,4-dionebenzoylhydrazone</u> - Bzac-BH<u>H</u>$_2$

An equimolar (50 mmol) mixture of benzoylacetone (4-phenylbutane-2,4-dione) and benzoylhydrazine was heated in an oil bath at 120°C for 20 minutes and the oil formed was cooled to a resinous mass which was then treated with a minimum volume of ethanol and refluxed for 1 hour and the precipitate filtered off on cooling. This, on recrystallization from ethanol, gave beautiful white cotton-like product. Yield 75%, m.p. 133°C (lit.[196] 132-3°C), Found: mol. wt. (mass spectrum), 280; Calc. for $C_6H_5COCH_2C(CH_3)(=NNHCOC_6H_5)$: mol. wt., 280.36.

6.5.2 <u>4-Phenylbutane-2,4-dione-p-methoxybenzoylhydrazone</u> - Bzac-p-^{OMe}-BH<u>H</u>$_2$

Following the above procedure, this creamish white compound was prepared by condensing benzoylacetone and p-anisichydrazide. Yield 80%, m.p. 167°C, Found: mol. wt. (mass spectrum), 310; Calc. for $C_6H_5COCH_2C(CH_3)(=NNHCOC_6H_4$-p-$OCH_3)$: mol. wt., 310.34.

6.5.3. <u>4-Phenylbutane-2,4-dione-p-chlorobenzoylhydrazone</u> - Bzac-p^{Cl}-BH<u>H</u>$_2$

This white flaky compound was prepared by the above (6.5.1) procedure. m.p. 158°C (lit.[196] 157-9°C). Yield 80%, Found: mol. wt. (mass spectrum), 314; 316 (for Cl^{37}); Calc. for $C_6H_5COCH_2C(CH_3)(=NNHCOC_6H_4$-p-$Cl)$: mol. wt., 314.77.

6.5.4. <u>4-Phenylbutane-2,4-dione-p-nitrobenzoylhydrazone</u> - Bzac-p^{NO_2}-BH<u>H</u>$_2$

This yellow crystalline compound was prepared by the same method (6.5.1). Yield 85%, m.p. 178-9°C, Found: mol. wt. (mass spectrum), 325; Calc.: mol. wt., 325.35.

6.5.5 1,3-Diphenylpropane-1,3-dionebenzoylhydrazone - dbm-BH$\underline{H}_2$

Following the same procedure (6.5.1) this light creamish white compound was prepared by condensing dibenzoylmethane (1,3-diphenylpropane-1,3-dione) and benzoylhydrazine on heating in an oil bath at 155°C for 40 minutes. m.p. 144°C (lit.[196] 146°C), Found: mol. wt. (mass spectrum), 342; Calc. for $C_6H_5COCH_2C(C_6H_5)(=NNHCOC_6H_5)$: mol. wt., 342.43.

6.5.6 2-Hydroxy-1-napthaldehydebenzoylhydrazone - HNP-BH$\underline{H}_2$

A mixture of 50 mmol each of 2-hydroxy-1-napthaldehyde and benzoylhydrazine in 100 ml of methanol was refluxed for 1 hour when light yellow precipitate appeared. This was filtered on cooling, washed with methanol and recrystallized from hot methanol. Yield 80%, m.p. 211°C (lit.[331] 211-2°C), Found: mol. wt. (mass spectrum), 290; Calc. for 2-OH-$C_{10}H_6CH(=NNHCOC_6H_5)$: mol. wt., 290.37.

6.5.7 2-Hydroxy-1-napthaldehyde-p-chloro-benzoylhydrazone - HNP-p^{Cl}-BH$\underline{H}_2$

This yellow compound was prepared by the above method (6.5.6). m.p. 262°C, Yield 85%, Found: mol. wt., 324, 326 (for Cl^{37}); Calc. mol. wt., 324.77.

6.5.8 2-Hydroxyacetophenonebenzoylhydrazone - HAP-BH$\underline{H}_2$

Fifty mmol of benzoylhydrazine was dissolved in 40 ml of ethanol on heating and 50 mmol of 2-hydroxyacetophenone was added to it and the mixture refluxed for 1 hour. White cotton-like precipitate was obtained on cooling in a refrigerator at about 6°C which, on filtration, was recrystallized from ethanol. Yield 70%, m.p. 180-1°C (lit.[331] 180-1°C), Found: mol. wt. (mass spectrum), 254; Calc. for 2-OH-$C_6H_4C(CH_3)(=NNHCOC_6H_5)$: mol. wt., 254.33.

6.5.9 2-Hydroxyacetophenone-p-chlorobenzoylhydrazone - HAP-p^{Cl}-BH$\underline{H}_2$

This white compound was prepared following the above (6.5.8) procedure.

Yield 80%, m.p. 223°C (lit.[332] 223-5°C), Found: mol. wt. (mass spectrum), 288, 290 (for Cl^{37}); Calc. mol. wt., 288.78.

6.5.10 2-Hydroxypropiophenonebenzoylhydrazone - HPP-BHH$_2$

This white compound was prepared following the procedure for 6.5.1 and recrystallized from ethanol. Yield 70%, m.p. 161-162°C, Found: mol. wt. (mass spectrum), 268; Calc. for 2-OH-C$_6$H$_4$C(C$_2$H$_5$)(=NNHCOC$_6$H$_5$): mol. wt., 268.35.

6.5.11 2,4-Dihydroxybenzophenonebenzoylhydrazone - DHBP-BHH$_2$

The same procedure as for 6.5.1 gave this yellowish white compound. Some insoluble material, possibly the cyclized product, formed during heating/reflux was removed by filtration. Yield 40%, m.p. 246-7°C, Found: mol. wt. (mass spectrum), 332; Calc. for 2,4-(OH)$_2$-C$_6$H$_3$C(C$_6$H$_5$)(=NNHCOC$_6$H$_5$): mol. wt., 332.39.

6.5.12 Salicylaldehydebenzoylhydrazone - Sal-BHH$_2$

Benzoylhydrazine (50 mmol) in methanol (60 ml) was refluxed with salicylaldehyde (50 mmol) in ethanol (60 ml) for 30 minutes and the white precipitate formed was filtered off on cooling, washed with ethanol and petroleum spirit (40-60°C) and dried. Yield 81%, m.p. 182°C (lit.[333] 182°C), Found: mol. wt. (mass spectrum), 240; Calc. for 2-OH-C$_6$H$_4$CH(=NNHCOC$_6$H$_5$): mol. wt., 240.35.

SALICYLOYLHYDRAZONE SCHIFF BASES

6.5.13 4-Phenylbutane-2,4-dionesalicyloylhydrazone - Bzac-SalHH$_2$

A mixture of benzoylacetone and salicyloylhydrazine (20 mmol each) in ethanol (40 ml) was heated for 40 minutes when light yellow precipitate appeared. This was filtered off on cooling and washed with ethanol and dried. Yield 80%, m.p. 206-7°C, Found: mol. wt. (mass spectrum), 296; Calc. for C$_6$H$_5$COCH$_2$C(CH$_3$)(=NNHCOC$_6$H$_4$-2-OH): mol. wt., 296.35.

6.5.14 <u>1,3-Diphenylpropane-1,3-dionesalicyloylhydrazone</u> - dbm-SalHH$_2$

A mixture of dibenzoylmethane and salicyloylhydrazine (20 mmol each) was heated in an oil bath at 150°C for 30 minutes and the creamish white mass obtained was recrystallized twice from hot ethanol. Yield 50%, m.p. 139-40°C, Found: mol. wt. (mass spectrum), 358; Calc. for $C_6H_5COCH_2C(C_6H_5)(=NNHCOC_6H_4-2-OH)$: mol. wt., 358.42.

6.5.15 <u>2-Hydroxy-1-napthaldehydesalicyloylhydrazone</u> - HNP-SalHH$_2$

The same procedure as for 6.5.13 gave this yellow compound. Yield 75%, m.p. 251-2°C, Found: mol. wt. (mass spectrum), 306; Calc. for 2-OH-$C_{10}H_6CH(=NNHCOC_6H_4-2-OH)$: mol. wt., 306.37.

6.5.16 <u>2-Hydroxaycetophenonesalicyloylhydrazone</u> - HAP-SalHH$_2$

This white compound was obtained by the same procedure 6.5.13. Yield 50%, m.p. 282-3°C, Found: mol. wt. (mass spectrum), 270; Calc. for 2-OH-$C_6H_4C(CH_3)(=NNHCOC_6H_4-2-OH)$: mol. wt., 270.32.

6.5.17 <u>2-Hydroxypropiophenonesalicyloylhydrazone</u> - HPP-SalHH$_2$

The same prcoedure as for 6.5.13 gave this white compound. Yield 70%, m.p. 232°C, Found: mol. wt. (mass spectrum), 284; Calc. mol. wt., 284.35.

6.5.18 <u>Salicylaldehydesalicyloylhydrazone</u> - Sal-SalHH$_2$

This white compound was prepared by the same method 6.5.13. Yield 98%, m.p. 275°C, Found: mol. wt. (mass spectrum), 256; Calc. for 2-OH-$C_6H_4CH(=NNHCOC_6H_4-2-OH)$: mol. wt., 256.34.

o-AMINOPHENOL SCHIFF BASES

6.5.19 <u>o-(4-Phenylbutane-4-one-2-)iminomethylphenol</u> - Bzac-OAPH$_2$

Benzoylacetone and o-aminophenol (20 mmol each) in ethanol (50 ml) were

refluxed for 1 hour and the yellowish white crystalline precipitate collected on cooling was recrystallized from ethanol. Yield 70%, m.p. 165°C, Found: mol. wt. (mass spectrum), 253; Calc. for $C_6H_5COCH_2C(CH_3)(=NC_6H_4-2-OH)$: mol. wt., 253.32

6.5.20 o-(1,3-Diphenylpropane-3-one-1-)iminomethylphenol - dbm-OAPH₂

Dibenzoylmethane and o-aminophenol (20 mmol each) were heated in an oil bath at 150°C for 30 minutes and the red mass obtained on cooling was heated for 15 minutes in 80 ml of ethanol. The yellow crystalline precipitate collected on cooling was recrystallized from ethanol. Yield 55%, m.p. 206-7°C, Found: mol. wt. (mass spectrum), 315; Calc. for $C_6H_5COCH_2C(C_6H_5)(=NC_6H_4-2-OH)$: mol. wt., 315.39.

6.5.21 o-(o'-Hydroxynapthyl)iminomethylphenol - HNP-OAPH₂

A mixture of 2-hydroxy-1-napthaldehyde and o-aminophenol (25 mmol each) in ethanol (80 ml) was stirred at 30°C for 1 hour[334] when an orange-yellow precipitate appeared. This was filtered off, washed with and recrystallized from ethanol. Yield 80%, m.p. 254-256°C, Found: mol. wt. (mass spectrum), 263; Calc. for $2-OH-C_{10}H_6CH(=NC_6H_4-2-OH)$: mol. wt., 263.33.

6.5.22 o-(o'-Hydroxynapthyl)iminomethyl-p-methylphenol - HNP-p^Me-OAPH₂

The above procedure (6.5.21) was applied to prepare this orange-yellow compound by condensing 2-hydroxy-1-napthaldehyde and o-amino-p-cresol. Yield 80%, m.p 253-4°C, found: mol. wt. (mass spectrum), 277; Calc. mol. wt., 277.36.

6.5.23 o-(o'-Hydroxynapthyl)iminomethyl-p-chlorophenol - HNP-p^Cl-OAPH₂

The same prcoedure as for 6.5.21 gave this orange compound. m.p. 272°C, Yield 80%, Found: mol. wt. (mass spectrum), 297 (and 299 for Cl^37); Calc., 297.77.

6.5.24 o-(o'-Hydroxphenyl)-1-iminoethylphenol - HAP-OAPH₂

<p>6.5.24 <u>o-(o'-Hydroxphenyl)-1-iminoethylphenol</u> - HAP-OAP$\underline{H_2}$</p>

A mixture of o-aminophenol and 2-hydroxyacetophenone (50 mmol each) in ethanol (100 ml) was stirred at 30°C for 1 hour[334]. The clear solution was concentrated to about 60 ml and left in a refrigerator at ~ 6°C for crystallization. The yellow precipitate separated was filtered off and washed with little ethanol and dried under vaccum. Yield 40%, m.p. 201-2°C (no m.p. given in the above literature), Found: mol. wt. (mass spectrum), 227; Calc. for 2-OH-C₆H₄C(CH₃)(=NC₆H₄-2-OH): mol. wt., 227.29.

6.5.25 <u>o-(o'-Hydroxphenyl)iminomethylphenol</u> - Sal-OAP$\underline{H_2}$

The same procedure as for 6.5.21 gave this orange-red compound by condensing salicylaldehyde and o-aminophenol. Yield 85%, m.p. 184°C (lit.[335] 184.5°C), Found: mol. wt. (mass spectrum), 213; Calc. for 2-OH-C₆H₄CH(=NC₆H₄-2-OH): mol. wt., 213.31.

6.5.26 <u>o-(o'-Hydroxyphenyl)iminomethyl-p-methylphenol</u> - Sal-p^Me-OAP$\underline{H_2}$

The same procedure as for 6.5.21 gave this shining (deep) red compound. Yield 80%, m.p. 151-2°C, Found: mol. wt. (mass spectrum), 227; Calc., 227.34.

6.5.27 <u>o-(o'-Hydroxyphenyl)iminomethyl-p-chlorophenol</u> - Sal-pCl-OAP$\underline{H_2}$

The same procedure, 6.5.21, was applied to prepare this orange compound. Yield 80%, m.p. 152-3°C, Found: mol. wt. (mass spectrum), 247 (and 249 for Cl^{37}); Calc., 247.77.

3-AMINO-2-NAPTHOL SCHIFF BASES

6.5.28 <u>3-(o-Hydroxynapthyl)iminomethyl-2-napthol</u> - HNP-3-am-2-nap-$\underline{H_2}$

This orange-yellow compound was prepared by following the same procedure as for 6.5.21. Yield 80%, m.p. 257-8°C, Found: mol. wt. (mass spectrum), 313; Calc. 2-OH-C₁₀H₆CH(=(3)NC₁₀H₆-2-OH): mol. wt., 313.39.

6.5.29 3-(o-Hydroxyphenyl)iminomethyl-2-napthol - Sal-3-am-2-napH_2

The same procedure, 6.5.21, gave this orange-red compound. Yield 85%, m.p. 197°C, Found: mol. wt. (mass spectrum), 263; Calc., 263.37.

2,2'-DIHYDROXYAZOARENE LIGANDS

The azo dye ligands were formed by coupling of the diazonium salts with various hydroxy aromatic compounds. In cases where substituted phenols were used as the coupling component, the phenolic OH group was protected by methylation. Although the methods for a few preparations are in the literature, they are given here in full because of their use in the subsequent preparations. The compounds, that were not found in the literature were characterized similarly as the Schiff base ligands.

6.5.30 o-Hydroxybenzeneazo-β-napthol - OAP-β-napH_2

o-Aminophenol (15 mmol) was dissolved in H_2O (10 ml) containing concentrated HCl (5 ml) and copper sulphate (5 mg) and the solution cooled to 0-5°C. To this, a cooled (0-5°C) solution (30%) of sodium nitrite (17 mmol) was added slowly, on stirring, when a clear brown-red solution was obtained. Completion of diazotization was checked with KI-starch paper. This cold (0-5°C) solution of the diazonium salt was added slowly to a pre-cooled (0-5°C) and vigorously stirring solution of β-napthol (15 mmol) in NaOH (10%, 30 ml) containing Na_2CO_3 (5.8 g; equivalent to neutralize 5 ml concentrated HCl). After the addition was over, the solution was kept at 0-5°C for about 2 hours with occasional stirring. Then this brown-red-purple solution was acidified with dilute HCl with stirring when brown-red-purplish precipitate separated out. The precipitate was filtered, washed with excess water, dried and then purified by recrystallization from methanol. Yield 90%, m.p. 192°C (lit.[336] 194°C), Found: mol. wt. (mass spectrum), 264; Calc. for $2\text{-}OH\text{-}C_6H_4\text{-}N=N\text{-}C_{10}H_6\text{-}2\text{-}OH$: mol. wt., 264.28.

6.5.31 p-methyl-o-hydroxybenzeneazo-β-napthol - p^{CH_3}-OAP-β-nap$\underline{H_2}$

The same procedure, as detailed above (6.5.30) was followed to prepare this dark magenta-red compound. Yield 90%, m.p. 209-210°C, Found: mol. wt. (mass spectrum), 278; Calc., 278.31.

6.5.32 p-Chloro-o-hydroxybenzeneazo-β-napthol - p^{Cl}-OAP-β-nap$\underline{H_2}$

The same procedure as for 6.5.30 gave this magenta red compound. Yield 85%, m.p. 241-3°C, Found: mol. wt. (mass spectrum), 298 (and 300 for Cl^{37}); Calc., 298.73.

6.5.33 o-Hydroxybenzeneazo-p-cresol - OAP-p-cresol$\underline{H_2}$

For the preparation of this dye, the direct coupling of the diazonium salt of o-aminophenol with p-cresol was not possible. It was, therefore, prepared by hydrolysing the methoxy group of the corresponding o-methoxybenzeneazo-p-cresol dye with aluminium chloride. The o-methoxybenzeneazo-p-cresol dye was prepared from o-anisidine and p-cresol by following the same procedure as for 6.5.30. Yield 90%, m.p. 122°C (lit.[337] 122-3°C).

This dye (6.5 mmol) and anhydrous $AlCl_3$ (3.5 g, excess) in dry benzene (120 ml) were refluxed for 5 hours. The solvent (benzene) was dried off using a rotavapour from this dark red (cloudy) solution. The residue was decomposed with HCl (10%, 40 ml) and extracted with diethylether continuously for about 45 hours using an ether extractor. The ether extract was treated with anhydrous $MgSO_4$ and actived charcoal (to dry and decolourize respectively) for 45 minutes with occasional stirring. The filtrate was dried by distilling off ether. The brown-red residue thus obtained was dissolved in benzene (15 ml) and subjected to column chromatographic separation through an alumina column using 1:1 $CHCl_3$-C_6H_6 solution as eluent. The elution was continued until the colour of the eluted solution was very pale yellow. Then alkaline (NaOH) ethanol was used as an eluent when dark(ish) red eluate (~ 600 ml) was

obtained. This was concentrated to ~ 200 ml using a rotavapour and treated with 6N HCl on stirring until strongly acidic when a yellow precipitate appeared. The mixture was heated for sometime and filtered hot, washed with water and little ethanol, dried and the product recrystallized from ethanol. Yield 50%, m.p. 164°C (lit.[337] 166°C), Found: mol. wt. (mass spectrum), 228; Calc. for $2\text{-OH-C}_6\text{H}_4\text{-N=N-C}_6\text{H}_3\text{-(4-CH}_3)\text{-2-OH}$: mol. wt., 228.25.

6.5.34 o-Hydroxybenzeneazo-p-methoxyphenol - OAP-p^{OCH_3}-phenol$\underline{H_2}$

Following the same method, as detailed for 6.5.33, this chocolate brown compound was prepared by coupling the o-anisidine diazonium chloride with p-methoxyphenol and hydrolysing the o-methoxy group of the resulting o-methoxy-benzeneazo-p-methoxyphenol dye with $AlCl_3$. The I.R. and mass spectral studies showed that the p-methoxy group of the dye was not hydrolysed. Yield 50%, m.p. 145-7°C, Found: mol. wt. (mass spectrum), 244; Calc., 244.25.

6.5.35 o-Hydroxybenzeneazo-p-chlorophenol - OAP-p^{Cl}-phenol$\underline{H_2}$

This yellow brown compound was prepared following the same procedure as described for 6.5.33. Yield 60%, m.p. ~ 185°C, Found: mol. wt. (mass spectrum), 248 (and 250 for Cl^{37}); Calc., 248.66.

6.5.36 1-(2'-Hydroxynapthyl-3'-azo)-2-napthol - 3-am-2-nap-β-nap$\underline{H_2}$

This deep purple compound was prepared by following procedure for 6.5.30 but using 3-amino-2-napthol instead of o-aminophenol. Yield 85%, m.p. 140-2°C, Found: mol. wt. (mass spectrum), 314; Calc., 314.34.

6.6 BIS-(TRIDENTATE) NON-VANADYL VANADIUM(IV) COMPLEXES

The bis-(tridentate) VL_2 complexes were prepared following the general methods described below.

A. FROM VO(acac)$_2$ AND LH$_2$

The dibasic tridentate ligand, LH$_2$ (two molar equivalent) in dry methanol was degassed with dinitrogen and to it VO(acac)$_2$ (one molar equivalent) was added. The mixture was refluxed for about 45 minutes when an intensely coloured precipitate separated out. This was filtered, washed with dry methanol and petroleum spirit (40-60°C) and dried over silica gel under vacuum. This reaction was found to be a versatile reaction for the preparation of VL$_2$ complexes which was possible because of VO(acac)$_2$ being a convenient source of VO^{2+} under the above reaction condition.

B. FROM VO(AA)$_2$.nH$_2$O

VO(AA)$_2$.nH$_2$O (one molar equivalent) [AA = mononegative bidentate ligand, n = 0, 1, 2] in dry methanol was degassed with dinitrogen and to it benzoyl-hydrazine (two molar equivalent) was added. The mixture was refluxed for about 45 minutes when an intensely coloured precipitate of the VL$_2$ complex appeared which was filtered, washed with methanol and petroleum spirit (40-60°C) and dried under vacuum over silica gel.

With o-aminophenol, the reaction of VO(acac)$_2$ did not give the pure VL$_2$ compound. The reaction with VO(Bzac)$_2$ and VO(HNP)$_2$.H$_2$O were very slow and a longer reflux was needed.

C. FROM VOCl$_2$ AND LH$_2$

A mixture of (two molar equivalent each) LH$_2$ and LiOAC (base) in dry methanol was degassed with dinitrogen and to it was added a solution of VOCl$_2$ (one molar equivalent) in methanol. The mixture was refluxed for about 45 minutes and the VL$_2$ precipitate separated was filtered, washed with methanol and petroleum spirit and dried under vacuum.

D. FROM VOLHCl AND LH$_2$

LH$_2$ and LiOAC (one molar equivalent each) in dry MeOH was degassed with

dinitrogen and to it solid VOL.HCl [for preparation see Section 6.7] (one molar equivalent) was added and the mixture was refluxed for about 45 minutes and the product formed was filtered off, washed and dried. Use of a different L'$\underline{H_2}$ gives the mixed ligand VLL' complex.

E.   FROM VOL.OR OR (VOL)$_2$O AND LH_2

VOL.OR or (VOL)$_2$O [for preparations see Sections 6.8 and 6.9], L$\underline{H_2}$ [or L'H_2 for mixed-ligand VLL' complexes] and benzoylhydrazine [acting as a reducing agent] (one molar equivalent each) in dry MeOH was degassed with dinitrogen and refluxed for about an hour and the separated product was filtered, washed and dried.

Below are the methods employed for the preparation of the individual VL$_2$ complexes.

BENZOYLHYDRAZONE SCHIFF BASE COMPLEXES

6.6.1   Bis[pentane-2,4-dionebenzoylhydrazonato(2-)]vanadium(IV) - V(acac-BH)$_2$

VO(acac)$_2$ (2.5 mmol) in dry MeOH (40 ml) was degassed with dinitrogen and to it benzoylhydrazine (5 mmol) was added. The mixture was refluxed for 40 minutes, the solution turning dark in about 10 minutes. The deep purple precipitate formed was filtered, washed with MeOH and petroleum spirit (40-60°C). It was purified on an Al$_2$O$_3$ column using CH$_2$Cl$_2$ as the eluent. Some light green material stayed back on top of the column. The eluted purple solution was concentrated and mixed with an approximately equal volume of petroleum spirit (60-80°C) and heated for a short time to remove some of the CH$_2$Cl$_2$. Beautiful deep purple crystals, formed on standing overnight in a refrigerator at ~ 6°C, was filtered, washed with petroleum spirit (40-60°C) and dried under vacuum over silica gel. Yield 60%. This was identified from its characteristic infrared and E.S.R.[73] spectra and vanadium content.

6.6.2 Bis[4-phenylbutane-2,4-dionebenzoylhydrazonato(2-)]vanadium(IV)

- V(Bzac-BH)$_2$

(a) The tridentate ligand 4-phenylbutane-2,4-dionebenzoylhydrazone (4 mmol) in dry MeOH (60 ml) was thoroughly degassed with dinitrogen and to this clear yellow solution VO(acac)$_2$ (2 mmol) was added and the mixture was refluxed for 45 minutes when lots of dark (purple) green precipitate appeared. This was filtered hot, washed with methanol and petroleum spirit (40-60°C) and dried under vacuum over silica gel. Yield 90%, m.p. > 250°C, Analysis found: C, 67.18; H, 4.61; N, 9.08; V, 8.31. VC$_{34}$H$_{28}$N$_4$O$_4$ requires C, 67.21; H, 4.64; N, 9.22; V, 8.38%.

(b) This was also prepared following the procedure for 6.6.1 and identified from its characteristic infrared and E.S.R. spectra.

(c) A mixture of Bzac-BHH$_2$ (2 mmol) and LiOAC (2 mmol) in dry MeOH (60 ml) was degassed with dinitrogen. A VOCl$_2$ solution (1 mmol) was added to this when the colour changed to red-brown-purple immediately. This was refluxed for 35 minutes and the dark purplish-green precipitate formed was filtered hot, washed with hot methanol and petroleum spirit (40-60°C), dried and characterized as above. Yield 96%.

(d) This was also prepared following the general methods 6.6 D and E and characterized similarly.

6.6.3 Bis[4-phenylbutane-2,4-dione-p-methoxybenzoylhydrazonato(2-)]vanadium

(IV) - V(Bzac-p^{OMe}-BH)$_2$

The same procedure as for 6.6.2 (a) gave this dark purplish-green compound. Yield 90%, m.p. > 250°C, Analysis, found: C, 64.81; H, 4.83; N, 8.44; V, 7.51. VC$_{36}$H$_{32}$N$_4$O$_6$ requires C, 64.77; H, 4.83; N, 8.39; V, 7.63%.

6.6.4 Bis[4-phenylbutane-2,4-dione-p-chlorobenzoylhydrazonato(2-)]vanadium

(IV) - V(Bzac-p^{Cl}-BH)$_2$

The same procedure as for 6.6.2 (a) gave a dark purplish-green product.

Yield 98%, m.p. > 250°C, Analysis, found: C, 60.29; H, 4.07; N, 8.37; Cl, 10.07; V, 7.42. $VC_{34}H_{26}N_2O_4Cl_2$ requires C, 60.37; H, 3.87; N, 8.28; Cl, 10.48; V, 7.53%.

6.6.5 Bis[4-phenylbutane-2,4-dione-p-nitrobenzoylhydrazonato(2-)]vanadium(IV)

- $V(Bzac-p^{NO_2}-BH)_2$

A dark purplish-green product was obtained following the same procedure 6.6.2 (a). Yield 100%, m.p. > 250°C, Analysis, found: C, 58.58; H, 3.77; N, 12.08; V, 7.21. $VC_{34}H_{26}N_6O_8$ requires C, 58.54; H, 3.76; N, 12.05; V, 7.30%.

6.6.6 Bis[1,3-diphenylpropane-1,3-dionebenzoylhydrazonato(2-)]vanadium(IV)

- $V(dbm-BH)_2$

The tridentate ligand dbm-BHH_2 (2 mmol) in dry MeOH (40 ml) was degassed with dinitrogen. VO(acac)$_2$ (1 mmol) was added to this and the mixture was refluxed for 1 hour when a dark purplish green precipitate separated out. This was filtered hot, washed with hot methanol and petroleum spirit and dried under vacuum. Yield 65%, m.p. > 250°C, Analysis, found: C, 72.18; H, 4.49; N, 7.65; V, 6.98. $VC_{44}H_{32}N_4O_4$ requires C, 72.23; H, 4.41; N, 7.66; V, 6.96%.

6.6.7 Bis[2-oxo-1-napthaldehydebenzoylhydrazonato(2-)]vanadium(IV)

- $V(HNP-BH)_2$

(a) The same procedure and quantities as for 6.6.6 gave a dark purple product. Yield 96%, m.p. > 250°C, Analysis, found: C, 68.60; H, 3.85; N, 8.89; V, 8.19. $VC_{36}H_{24}N_4O_4$ requires C, 68.90; H, 3.85; N, 8.93; V, 8.12%.

(b) VO(HNP)$_2$.H$_2$O [for preparation see Section 6.1.6] (1 mmol) in dry MeOH (25 ml) was degassed and benzoylhydrazine (2 mmol) was added when the mixture immediately started turning brown-purple. The mixture was refluxed for 30 minutes and the product formed was filtered hot, washed, dried and identified from its characteristic infrared and E.S.R. spectra.

6.6.8 Bis[2-oxo-1-napthaldehyde-p-chlorobenzoylhydrazonato(2-)]vanadium(IV)
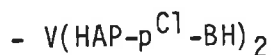#### - V(HNP-p^{Cl}-BH)$_2$
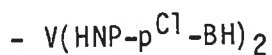
The same procedure as for 6.6.2 (a) gave a dark purple product. Yield 98-100%, m.p. > 250°C, Analysis, found: C, 61.56; H, 3.26; N, 7.95; Cl, 9.60; V, 7.47.   VC$_{36}$H$_{22}$N$_4$O$_4$Cl$_2$ requires C, 62.09; H, 3.18; N, 8.04; Cl, 10.18; V, 7.31%.

6.6.9 Bis[2-oxo-acetophenonebenzoylhydrazonato(2-)]vanadium(IV) - V(HAP-BH)$_2$

The same procedure as for 6.6.2 (a) gave a dark purple product. Yield 80%, m.p. > 250°C, Analysis, found: C, 64.88; H, 4.44; N, 9.97; V, 9.10. VC$_{30}$H$_{24}$N$_4$O$_4$ requires C, 64.87; H, 4.35; N, 10.09; V, 9.17%.

6.6.10 Bis(2-oxo-acetophenone-p-chlorobenzoylhydrazonato(2-))vanadium(IV)
- V(HAP-p^{Cl}-BH)$_2$

A dark purple product was obtained by the same procedure as for 6.6.2 (a).   Yield 85%, m.p. > 250°C, Analysis, found: C, 57.56; H, 3.70; N, 8.90; Cl, 11.11; V, 8.10.   VC$_{30}$H$_{22}$N$_4$O$_4$Cl$_2$ requires C, 57.71; H, 3.55; N, 8.97; Cl, 11.36; V, 8.16%.

This was also prepared by the method as described for 6.6.2 (c).

6.6.11 Bis[2-oxo-propiophenonebenzoylhydrazonato(2-)]vanadium(IV) - V(HPP-BH)$_2$

The same procedure as for 6.6.2 (a) gave a dark purple product. Yield 75%, m.p. 204-6°C, Analysis, found: C, 65.84; H, 5.01; N, 9.61; V, 8.84. VC$_{32}$H$_{28}$N$_4$O$_4$ requires C, 65.86; H, 4.84; N, 9.60; V, 8.73%.

6.6.12 Bis[2-oxo-4-hydroxybenzophenonebenzoylhydrazonato(2-)]vanadium(IV)
- V(DHBP-BH)$_2$

The procedure described for 6.6.2 (a) was followed to prepare this compound. This reaction seemed to be a little slower. The clear dark purple

solution on cooling in a refrigerator at ~ 6°C gave dark (green) purple precipitate which was filtered, washed and dried as usual. Yield 70%, m.p. 208°C, Analysis found: C, 66.99; H, 4.17; N, 7.52; V, 7.05. $VC_{40}H_{28}N_4O_6$ requires C, 67.51; H, 3.97; N, 7.87; V, 7.16%.

6.6.13 Bis[salicylaldehydebenzoylhydrazonato(2-)]vanadium(IV) - V(Sal-BH)$_2$

A dark green-purple product was obtained by the same method as for 6.6.2 (a). Yield 90%, m.p. > 250°C, Analysis, found: C, 63.84; H, 3.75; N, 10.66; V, 9.80. $VC_{28}H_{20}N_4O_4$ requires C, 63.76; H, 3.82; N, 10.62; V, 9.66%.

SALICYLOYLHYDRAZONE SCHIFF BASE COMPLEXES

6.6.14 Bis[pentane-2,4-dionesalicyloylhydrazonato(2-)]vanadium(IV)

- V(acac-SalH)$_2$
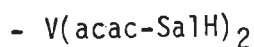
The same procedure as for 6.6.1, but using salicyloylhydrazine, gave a dark purple product which was filtered hot, washed with methanol and dried under vacuum. Yield 70%, m.p. 228-9°C, Analysis found: C, 55.91; H, 4.95; N, 10.85; V, 9.80. $VC_{24}H_{24}N_4O_6$ requires C, 55.93; H, 4.69; N, 10.87; V, 9.88%.

6.6.15 Bis[4-phenylbutane-2,4-dionesalicyloylhydrazonato(2-)]vanadium(IV)

- V(Bzac-SalH)$_2$
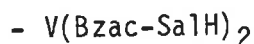
A dark purplish green product was obtained by the same procedure as for 6.6.2 (a). Yield 96%, m.p. > 250°C, Analysis, found: C, 63.60; H, 4.56; N, 8.75; V, 7.91. $VC_{34}H_{28}N_4O_6$ requires C, 63.85; H, 4.41; N, 8.76; V, 7.96%.

6.6.16 Bis[1,3-diphenylpropane-1,3-dionesalicyloylhydrazonato(2-)]vanadium(IV)

- V(dbm-SalH)$_2$
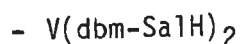
This dark purple-green compound was prepared similarly as for 6.6.2 (a).

Yield 80%, m.p. > 250°C, Analysis, found: C, 68.86; H, 4.25;N, 7.26; V, 6.79. $VC_{44}H_{32}N_4O_6$ requires C, 69.20; H, 4.22; N, 7.34; V, 6.67%.

6.6.17 Bis[2-oxo-1-napthaldehydesalicyloylhydrazonato(2-)]vanadium(IV)

- $V(HNP-SalH)_2$

The same procedure as for 6.6.2 (a) gave a dark green product. Yield 98%, m.p. > 250°C, Analysis, found: C, 65.13; H, 3.72; N, 8.44; V, 7.64. $VC_{36}H_{24}N_4O_6$ requires C, 65.56; H, 3.67; N, 8.49; V, 7.72%.

6.6.18 Bis[2-oxo-acetophenonesalicyloylhydrazonato(2-)]vanadium(IV)

- $V(HAP-SalH)_2$

The same procedure as for 6.6.2 (a) gave a dark purple product. Yield 98%, m.p. > 250°C, Analysis, found: C, 61.24; H, 3.99; N, 9.49; V, 8.61. $VC_{30}H_{24}N_4O_6$ requires C, 61.33; H, 4.12; N, 9.54; V, 8.67%.

6.6.19 Bis[2-oxo-propiophenonesalicyloylhydrazonato(2-)]vanadium(IV)

- $V(HPP-SalH)_2$

A dark purple product was obtained by the same method as for 6.6.2 (a). Yield 70%, m.p. 220-2°C, Analysis, found: C, 59.34; H, 4.32; N, 10.36; V, 8.48. $VC_{32}H_{28}N_4O_6$ requires C, 62.44; H, 4.58; N, 9.10; V, 8.28%.
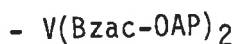
6.6.20 Bis[salicylaldehydesalicyloylhydrazonato(2-)]vanadium(IV)

- $V(Sal-SalH)_2$

The same method as for 6.6.2 (a) gave a dark green-purple product. Yield 80%, m.p. > 250°C, Analysis, found: C, 59.51; H, 3.73; N, 9.87; V, 9.10. $VC_{28}H_{20}N_4O_6$ requires C, 60.12; H, 3.60; N, 10.01; V, 9.11%.

o-AMINOPHENOL SCHIFF BASE COMPLEXES

6.6.21 Bis[o-(4-phenylbutane-4-one-2-)iminomethylphenolato(2-)]vanadium(IV)

- V(Bzac-OAP)$_2$

The ligand Bzac-OAPH$_2$ (3 mmol) in dry MeOH (80 ml) was degassed with dinitrogen. VO(acac)$_2$, (1.5 mmol) was added and the mixture was refluxed for 1 ½ hours. The dark purple-green precipitate that separated out during reflux, was filtered hot, washed with methanol and petroleum spirit (40-60°C) and dried under vacuum. Yield 85%, m.p. 232-5°C, Analysis, found: C, 69.33; H, 4.89; N, 5.06; V, 9.11. VC$_{32}$H$_{26}$N$_2$O$_4$ requires C, 69.44; H, 4.73; N, 5.06; V, 9.20%.

6.6.22 Bis[o-(1,3-diphenylpropane-3-one-1-)iminomethylphenolato(2-)]vanadium

(IV) - V(dbm-OAP)$_2$
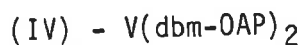
The same procedure as for 6.6.21 was followed to prepare this dark purple-green compound. Yield 50%, m.p. > 250°C, Analysis, found: C, 75.11; N, 4.06; V, 7.59. VC$_{42}$H$_{30}$N$_2$O$_4$ requires C, 74.44; H, 4.46; H, 4.65; N, 4.13; V, 7.52%.

6.6.23 Bis[o-(o'-oxonapthyl)iminomethylphenolato(2-)]vanadium(IV)
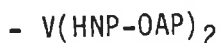
- V(HNP-OAP)$_2$

(a) The same procedure as for 6.6.21 gave a dark purple green product. Yield 70%, m.p. > 250°C, Analysis, found: C, 71.06; H, 3.75; N, 4.84; V, 8.88. VC$_{34}$H$_{22}$N$_2$O$_4$ requires C, 71.21; H, 3.87; N, 4.88; V, 8.88%.

(b) The ligand HNP-OAPH$_2$ (1.05 mmol) was added to VO(HNP-OAP).H$_2$O [prepared by published procedure[37] and identified by its vanadium content and infrared spectrum] (1 mmol) in degassed MeOH (30 ml) and the mixture was refluxed for 1 ½ hours and the dark (purple) green compound formed was collected and identified by its I.R. and E.S.R. spectra and vanadium content.

(c) This was also prepared by following procedures as described for 6.6.2 (c) and 6.6.7 (b) and identified similarly.

6.6.24 Bis[o-(o'-oxonapthyl)iminomethyl-p-methylphenolato(2-)]vanadium(IV)
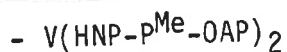
- V(HNP-p^{Me}-OAP)$_2$

A dark purple-green product was obtained by the same procedure as for 6.6.21. Yield 96%, m.p. > 250°C, Analysis, found: C, 71.30; H, 4.54; N, 4.66; V, 8.40. VC$_{36}$H$_{26}$N$_2$O$_4$ requires C, 71.88; H, 4.36; N, 4.66; V, 8.47%.

6.6.25 Bis[o-(o'-oxonapthyl)iminomethyl-p-chlorophenolato(2-)]vanadium(IV)

- V(HNP-p^{Cl}-OAP)$_2$
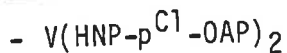
A dark purple-green product was obtained by the same method as for 6.6.21. Yield 98%, m.p. 228-9°C, Analysis, found, C, 63.94; H, 3.14; N, 4.24; Cl, 11.60; V, 8.10. VC$_{34}$H$_{20}$N$_2$O$_4$Cl$_2$ requires C, 63.57; H, 3.14; N, 4.36; Cl, 11.04; V, 7.93%.

6.6.26 Bis[o-(o'-oxophenyl)-1-iminoethylphenolato(2-)]vanadium(IV)

- V(HAP-OAP)$_2$
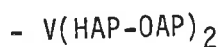
The procedure as described for 6.6.21 was used to prepare this compound. On reflux, the resulting dark red-purple solution was cooled in a refrigerator at ~ 6°C when a dark red-purple precipitate separated out. This was filtered, washed and dried as usual. Yield 60%, m.p. 206-8°C, Analysis, found: C, 66.62; H, 4.73; N, 5.53; V, 10.30. VC$_{28}$H$_{22}$N$_2$O$_4$ requires C, 67.07; H, 4.42; N, 5.59; V, 10.16%.

6.6.27 Bis[o-(o'-oxophenyl)iminomethylphenolato(2-)]vanadium(IV) - V(Sal-OAP)$_2$

The same method as for 6.6.21 was used to prepare the dark green purple compound. Yield 94%, m.p. > 250°C, Analysis, found: C, 65.78; H, 3.72; N, 5.88; V, 10.90. VC$_{26}$H$_{18}$N$_2$O$_4$ requires C, 65.97; H, 3.83; N, 5.92; V, 10.76%.

6.6.28 Bis[o-(o'-oxophenyl)iminomethyl-p-methylphenolato(2-)]vanadium(IV)

- V(Sal-p^{Me}-OAP)$_2$
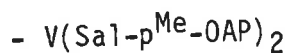
The same method as for 6.6.21 gave a dark green-purple product. Yield 98%, m.p. > 250°C, Analysis, found: C, 66.41; H, 4.52; N, 5.47; V, 10.28. VC$_{28}$H$_{22}$N$_2$O$_4$ requires C, 67.07; H, 4.42; N, 5.59; V, 10.16%.
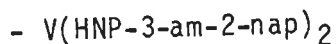
6.6.29 Bis[o-(o'-oxophenyl)iminomethyl-p-chlorophenolato(2-)]vanadium(IV)

- V(Sal-p^{Cl}-OAP)$_2$
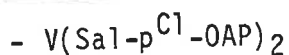
A dark green-purple product was obtained by the same procedure as for 6.6.21. Yield 98%, m.p. > 250°C, Analysis, found: C, 56.87; H, 2.91; N, 4.96; Cl, 12.74; V, 9.52. VC$_{26}$H$_{16}$N$_2$O$_4$Cl$_2$ requires C, 57.59; H, 2.97; N, 5.17; Cl, 13.08; V, 9.39%.

3-AMINO-2-NAPTHOL SCHIFF BASE COMPLEXES

6.6.30 Bis[3-(o'-oxonapthyl)iminomethyl-2-naptholato(2-)]vanadium(IV)

- V(HNP-3-am-2-nap)$_2$

The same procedure as for 6.6.21 gave a dark green-purple compound. Yield 96%, m.p. > 250°C, Analysis, found: C, 74.16; H, 4.16; N, 4.11; V, 7.51. VC$_{42}$H$_{26}$N$_2$O$_4$ requires C, 74.89; H, 3.89; N, 4.16; V, 7.56%.

6.6.31 Bis[3-(o'-oxophenyl)iminomethyl-2-naptholato(2-)]vanadium(IV)
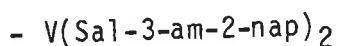
- V(Sal-3-am-2-nap)$_2$

A dark green-purple product was obtained by following the same procedure as for 6.6.21. Yield 96%, m.p. > 250°C, Analysis, found: C, 70.96; H, 3.77; N, 4.84; V, 8.96. VC$_{34}$H$_{22}$N$_2$O$_4$ requires C, 71.21; H, 3.87; N, 4.88; V, 8.88%.

2,2'-DIHYDROXYAZOARENE COMPLEXES

6.6.32 Bis[o-oxobenzeneazo-β-naptholato(2-)]vanadium(IV) - V(OAP-β-nap)$_2$

The tridentate ligand o-hydroxybenzeneazo-β-napthol (2 mmol) in dry methanol (80 ml) was degassed with dinitrogen. VO(acac)$_2$ (1 mmol) was added to this and the mixture was refluxed for 1 hour when a dark green precipitate separated out. This was filtered hot, washed with methanol and petroleum spirit (40-60°C) and dried under vacuum. Yield 90%, m.p. > 250°C, Analysis, found C, 65.88; H, 3.64; N, 9.53; V, 8.93. VC$_{32}$H$_{20}$N$_4$O$_4$ requires C, 66.79; H, 3.50; N, 9.74; V, 8.85%.

6.6.33 Bis[p-methyl-o-oxobenzeneazo-β-naptholato(2-)]vanadium(IV)

   - V(p^{Me}-OAP-β-nap)$_2$

The above procedure (6.6.32) with p-methyl-o-hydroxybenzeneazo-β-napthol as the ligand, gave a dark green product. Yield 65%, m.p. > 250°C, Analysis, found: C, 66.55; H, 4.05; N, 8.96; V, 8.40. VC$_{34}$H$_{24}$N$_4$O$_4$ requires C, 67.66; H, 4.01; N, 9.28; V, 8.44%.

6.6.34 Bis[p-chloro-o-oxobenzeneazo-β-naptholato(2-)]vanadium(IV)

   - V(p^{Cl}-OAP-β-nap)$_2$
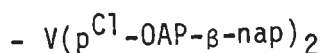
A dark green product was obtained by following the same procedure as for 6.6.32. Yield 95%, m.p. > 250°C, Analysis, found: C, 58.28; H, 2.74; N, 8.51; Cl, 11.01; V, 8.03. VC$_{32}$H$_{18}$N$_4$O$_4$Cl$_2$ requires C, 59.65; H, 2.82; N, 8.69; Cl, 11.00; V, 7.91%.

6.6.35 Bis(o-oxobenzeneazo-p-cresolato(2-)] vanadium (IV) - V(OAP-p-cresol)$_2$

The same procedure as for 6.6.32 gave a dark green product. Yield 60%, m.p. 208-10°C (decomposition), Analysis, found: C, 62.01; H, 4.07; N, 10.56; V, 10.08. VC$_{26}$H$_{20}$N$_4$O$_4$ requires C, 62.03; H, 4.00; N, 11.13; V, 10.12%.

6.6.36 <u>Bis[o-oxobenzeneazo-p-methoxyphenolato(2-)]vanadium(IV)]</u>

    - V(OAP-p^{OMe}-phenol)$_2$

The same procedure (6.6.32) gave a dark green product. Yield 65%, m.p. 212-5°C (decomposition), Analysis, found: C, 58.95; H, 4.02; N, 9.63; V, 9.37. VC$_{26}$H$_{20}$N$_4$O$_6$ requires C, 58.33; H, 3.76; N, 10.46; V, 9.51%.

6.6.37 <u>Bis[o-oxobenzenazo-p-chlorophenolato(2-)]vanadium(IV)</u>

    - V(OAP-p^{Cl}-Phenol)$_2$
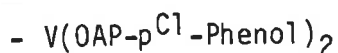
This dark green compound was prepared by the same method (6.6.32). Yield 30%, m.p. > 250°C, Analysis, found: V, 9.69; VC$_{24}$H$_{14}$N$_4$O$_4$Cl$_2$ requires V, 9.36%.

6.6.38 <u>Bis(1-(2'-oxonapthyl-3'-azo)-2-naptholato(2-)]vanadium(IV)</u>

    - V(3-am-2-nap-β-nap)$_2$
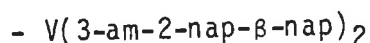
The same procedure as for 6.6.32 and using 1-(2'-hydroxynapthyl-3'-azo)-2-napthol gave a dark green product. Yield 86%, m.p. > 250°C, Analysis, found: C, 68.25; H, 3.78; N, 8.22; V, 7.46. VC$_{40}$H$_{24}$N$_4$O$_4$ requires C, 71.11; H, 3.58; N, 8.29; V, 7.54%.

6.6.39 <u>Bis[sodium-1-(1-oxo-2-napthylazo)-6-nitro-2-naptholato-4-sulphonate</u>

    <u>(2-)]vanadium(IV)</u> - V(Erio T)$_2$

The same procedure as for 6.6.32 gave this dark green compound. Yield 95%, m.p. > 250°C, Analysis, found: C, 45.38; H, 2.54; N, 7.85; S, 6.10; V, 5.12. Na$_2$VC$_{40}$H$_{20}$N$_6$O$_{14}$S$_2$ requires C, 49.55; H, 2.08; N, 8.67; S, 6.61%, V, 5.25%. (The experimental values fit the formula VL$_2$.5 H$_2$O).

MIXED-LIGAND COMPLEXES

6.6.40 <u>[(2-oxo-1-napthaldehydebenzoylhydrazonato(2-))(4-phenylbutane-2,4-</u>

    <u>dionebenzoylhydrazonato(2-))] vanadium (IV)</u> - V(HNP-BH)(Bzac-BH)

    (a) A mixture of Bzac-BH<u>H$_2$</u> (1 mmol) and LiOAC (1 mmol) in dry MeOH

(30 ml) was rigorously degassed with dinitrogen. Monochloro(2-oxo-1-napthalde-hydebenzoylhydrazonato)oxovanadium(IV), VO(HNP-BH$\underline{H}$)Cl [for preparation see Section 6.7.2] (1 mmol) was added to this solution (yellow) when almost instantly the colour changed to dark green. The mixture was refluxed for 45 minutes when a dark green (purple with reflected light) precipitate separated out. This was filtered hot, washed with methanol and petroleum spirit (40-60°C) and dried under vacuum. Yield 85%, m.p. 212-4°C, Analysis, found: C, 68.12; H, 4.27; N, 9.06; V, 8.30. VC$_{35}$H$_{26}$N$_4$O$_4$ requires C, 68.07; H, 4.24; N, 9.07; V, 8.25%.

(b) This compound was also prepared from VO(HNP-BH).OMe [for preparation see Section 6.8.4] in the following way. A mixture of VO(HNP-BH).OMe (1 mmol), BH(1 mmol) and Bzac-BH$\underline{H}_2$ (1 mmol) in dry and degassed MeOH (30 ml) was refluxed for 1 hour when a dark green-purple precipitate separated out. This was filtered hot, washed and dried as usual and identified by its characteristic infrared spectrum and vanadium content. [Note: Use of [VO(HNP-BH)]$_2$0 (for preparation see Section 6.9.4) in place of VO(HNP-BH).OMe also gave this compound].

6.6.41 [(2-oxoacetophenonebenzoylhydrazonato(2-))(4-phenylbutane-2,4-dione-benzoylhydrazonato(2-))]vanadium(IV) - V(HAP-BH)(Bzac-BH)

(a) The same method as detailed for 6.6.40 (a) and use of VO(HAP-BH$\underline{H}$)Cl (Section 6.7.3) in this case gave a dark purple mixed-ligand complex. Yield 80%, m.p. 233-4°C, Analysis, found: C, 66.09; H, 4.45; N, 9.65; V, 8.73. VC$_{32}$H$_{26}$N$_4$O$_4$ requires C, 66.09; H, 4.51; N, 9.63; V, 8.76%.

(b) This was also prepared following the method as for 6.6.40 (b) and characterized by its infrared spectra. Yield 80%.

6.6.42 [(2-oxoacetophenonebenzoylhydrazonato(2-))(2-oxo-1-napthaldehydebenz-oylhydrazonato(2-))]vanadium(IV) - V(HAP-BH)(HNP-BH)

Following the same method as for 6.6.40 (a) and refluxing HNP-BH$\underline{H}_2$, LiOAC

and VO(HAP-BHH)Cl (see Section 6.7.3) (1 mmol each) in dry and degassed MeOH (30 ml), a dark purple compound was obtained. Yield 80%, m.p. 230-1°C, Analysis, found: C, 67.06; H, 4.07; N, 9.29; V, 8.57. $VC_{33}H_{24}N_4O_4$ requires C, 67.01; H, 4.09; N, 9.47; V, 8.61%.

6.6.43 [(2-oxoacetophenonebenzoylhydrazonato(2-))(4-phenylbutane-2,4-dione-salicyloylhydrazonato(2-))]vanadium(IV) - V(HAP-BH)(Bzac-SalH)

A dark purple product was obtained following the procedure described for 6.6.40 (a) and refluxing Bzac-SalHH$_2$, LiOAC and VO(HAP-BHH)Cl [see Section 6.7.3] (1 mmol each) in dry and degassed MeOH (30 ml) for 45 minutes. Yield 80%, m.p. 252-3°C, Analysis Found: C, 64.11; H, 4.38; N, 9.28; V, 8.59. $VC_{32}H_{26}N_4O_5$ requires C, 64.32; H, 4.38; N, 9.38; V, 8.53%.

6.6.44 [(2-oxo-1-napthaldehydebenzoylhydrazonato(2-))(o-oxobenzeneazo-β-naptholato(2-))]vanadium(IV) - V(HNP-BH)(OAP-β-nap)

A dark purple solid was obtained following the same procedure as for 6.6.40 (a) and refluxing OAP-β-napH$_2$, LiOAC and VO(HNP-BHH)Cl [see Section 6.7.2] (1 mmol each) in dry and degassed MeOH (40 ml) for 45 minutes. Yield 90%, m.p. 242-4°C, Analysis, found, C, 67.63; H, 3.75; N, 9.29; V, 8.56. $VC_{34}H_{22}N_4O_4$ requires C, 67.89; H, 3.69; N, 9.31; V, 8.46%.

6.7 MONOCHLORO[TRIDENTATE(-1)]OXOVANADIUM(IV) COMPLEXES

6.7.1 Monochloro[4-phenylbutane-2,4-dione-p-chlorobenzoylhydrazonato(-1)] oxovandium(IV)] - VO(Bzac-p^{Cl}-BHH)Cl

Bzac-p^{Cl}-BHH$_2$ (2 mmol) in dry acetone (A.R., 40 ml) was degassed with dinitrogen on a vacuum line and cooling the Schlenk container in liquid nitrogen. It was then brought to room temperature slowly under a constant flow of dinitrogen. The clear yellowish solution was added to a rigorously degassed schlenk flask containing dry VOCl$_2$ (3 mmol, high excess to prevent

formation of any VL_2 compound) in MeOH ($\sim$ 1 ml) when green precipitate was formed in about a minute. The mixture was stirred at room temperature for 30 minutes and the product filtered, washed with excess acetone, petroleum spirit (40-60°C) and dried under vacuum. Yield 95%, Analysis, found: C, 49.14; H, 3.60; N, 6.59; Cl, 16.75; V, 12.36. $VC_{17}H_{13}N_2O_3Cl_2$ requires C, 49.06; H, 3.39; N, 6.73; Cl, 17.04; V, 12.24%.

6.7.2 Monochloro[2-oxo-1-napthaldehydebenzoylhydrazonato(-1)]oxovanadium(IV)

- VO(HNP-BHH)Cl

A yellowish green compound was obtained by following the above procedure (6.7.1) and using HNP-BHH$_2$ as the ligand. In this preparation, the reaction mixture was refluxed for 40 minutes when the precipitate separated out. Yield 70%, Analysis, found: C, 55.02; H, 3.41; N, 7.08; Cl, 9.05; V, 13.17. $VC_{18}H_{12}N_2O_3Cl$ requires C, 55.19; H, 3.35; N, 7.15; Cl, 9.05; V, 13.00%.

6.7.3 Monochloro[2-oxoacetophenonebenzoylhydrazonato(-1)]oxovanadium(IV)

- VO(HAP-BHH)Cl

This green compound was obtained by following the same method as for 6.7.1. Yield 85%, Analysis, found: C, 51.05; H, 4.00; N, 7.71; Cl, 9.85; V, 14.17. $VC_{15}H_{12}N_2O_3Cl$ requires C, 50.65; H, 3.68; N, 7.88; Cl, 9.97; V, 14.32%.

6.7.4 Monochloro[salicylaldehydebenzoylhydrazonato(-1)]oxovanadium(IV)

- VO(Sal-BHH)Cl

The same procedure as detailed for 6.7.1 and use of Sal-BHH$_2$ as the ligand gave a green product. Yield 80%, Analysis, found: C, 49.14; H, 3.43; N, 8.17; Cl, 10.43; V, 14.97. $VC_{14}H_{10}N_2O_3Cl$ requires C, 49.22; H, 3.25; N, 8.20; Cl, 10.38; V, 14.91%.

6.8   (ALKOXO)OXO[TRIDENTATE(2-)]VANADIUM(V) COMPLEXES

6.8.1   (Ethoxo)oxo[4-phenylbutane-2,4-dionebenzoylhydrazonato(2-)]vanadium(V)

- VO(Bzac-BH).OEt

To $VOCl_2$ (3 mmol) and LiOAC (5 mmol) in ethanol (30 ml), Bzac-BHH$_2$ (2.5 mmol) was added. The green solution turned brown immediately. Air was bubbled through the solution for 15 minutes, and the solution was then refluxed for 1 hour. On standing overnight, a brilliant dark brown crystalline precipitate was obtained. It was washed with ethanol and pretroleum spirit (40-60°C) and dried. Yield 70%, m.p. 198-9°C, Analysis, found: C, 58.52; H, 5.04; N, 7.16; V, 13.05. $VC_{19}H_{19}N_2O_4$ requires C, 58.47; H, 4.91; N, 7.18; V, 13.05%.

6.8.2   (Methoxo)oxo[4-phenylbutane-2,4-dione-p-chlorobenzoylhydrazonato(2-)]

vanadium(V) - VO(bzac-p^{Cl}-BH).OMe

This dark brown compound was prepared following the above method (6.8.1) and using Bzac-p^{Cl}-BHH$_2$ as the ligand and MeOH as the solvent. In this preparation most of the precipitate appeared during bubbling air through the solution to cause oxidation. Yield 75%, m.p. 158-60°C, Analysis, found: C, 52.46; H, 4.08; N, 6.81; Cl, 8.45; V, 12.46. $VC_{18}H_{16}N_2O_4Cl$ requires C, 52.64; H, 3.93; N, 6.82; Cl, 8.63; V, 12.40%.

6.8.3   (Methoxo)oxo[1,3-diphenylpropane-1,3-dionebenzoylhydrazonato(2-)]

vanadium(V) - VO(dbm-BH).OMe

The same procedure as for 6.8.1 gave a dark brown product. Yield 75%, m.p. 133-5°C, Analysis, found: C, 63.15; H, 4.48; N, 6.43; V, 11.50. $VC_{23}H_{19}N_2O_4$ requires C, 63.02; H, 4.37; N, 6.39; V, 11.62%.

6.8.4   (Methoxo)oxo[2-oxo-1-napthaldehydebenzoylhydrazonato(2-)]vanadium(V)

- VO(HNP-BH).OMe

The same procedure as for 6.8.1 gave this dark brown compound. Yield

80%, m.p. 282-3°C, Analysis, found: C, 57.76; H, 3.56; N, 7.15; V, 13.08. $VC_{19}H_{15}N_2O_4$ requires C, 59.08; H, 3.91; N, 7.25; V, 13.19%.

6.8.5   (Methoxo)oxo[2-oxo-1-napthaldehyde-p-chlorobenzoylhydrazonato(2-)] vanadium(V) - VO(HNP-p^{Cl}-BH).OMe

A magenta-brown compound was obtained following the same method as for 6.8.1.   Yield 80%, m.p. 198-9°C, Analysis, found: C, 54.17; H, 3.43; N, 6.69; Cl, 8.35; V, 12.23. $VC_{19}H_{14}N_2O_4Cl$ requires C, 54.24; H, 3.35; N, 6.66; Cl, 8.43; V, 12.11%.

6.8.6   (Methoxo)oxo[2-oxoactophenonebenzoylhydrazonato(2-)]vanadium(V) - VO(HAP-BH).OMe

The same procedure (6.8.1) gave a dark brown product.   Yield 70%, m.p. > 250°C, Analysis, Found: C, 54.66; H, 4.42; N, 7.96; V, 14.41. $VC_{16}H_{15}N_2O_4$ requires C, 54.87; H, 4.32; N, 8.00; V, 14.54%.

6.8.7   (Methoxo)oxo[salicylaldehydebenzoylhydrazonato(2-)]vanadium(V) - VO(Sal-BH).OMe

A dark brown product was obtained by the same method as for 6.8.1.   Yield 80%, m.p. 106-8°C, Analysis, found: C, 53.52; H, 3.52; N, 8.64; V, 14.94. $VC_{15}H_{13}N_2O_4$ requires C, 53.59; H, 3.90; N, 8.33; V, 15.15%.

6.9   μ-OXO-BIS[OXO(TRIDENTATE(2-))VANADIUM(V)] COMPLEXES

These oxo-bridged dimers were prepared in good yield by hydrolysing the VOL.OR complexes (for preparations see Section 6.8) in chloroform.

6.9.1   μ-Oxo-bis[oxo(4-phenylbutane-2,4-dionebenzoylhydrazonato(2-))vanadium (V)] - [VO(Bzac-BH)]$_2$O

VO(Bzac-BH).OEt (1 mmol) was dissolved in chloroform (30 ml), and filtered.   Water (10 ml) was added to the filtrate, and the mixture was vigorously

stirred and boiled gently to remove the chloroform and the ethanol formed in the reaction. Fresh chloroform was added and the procedure repeated. The chocolate-brown precipitate was separated, washed with water, dried and cryst-allized from chloroform and petroleum spirit (60-80°C). m.p. 221-2°C, Analysis, found: C, 56.92; H, 4.17; N, 7.78; V, 14.56. $V_2C_{34}H_{28}N_4O_7$ requires C, 57.80; H, 3.99; N, 7.93; V, 14.42%.

6.9.2 μ-Oxo-bis[oxo(4-phenylbutane-2,4-dione-p-chlorobenzoylhydrazonato(2-)) vanadium (V)] - [VO(Bzac-p^{Cl}-BH)]$_2$O

The same method (6.9.1) gave a magenta-red compound. m.p. 230-2°C, Analysis, found: C, 52.50; H, 3.59; N, 7.11; Cl, 9.15; V, 13.29. $V_2C_{34}H_{26}N_4O_7Cl_2$ requires C, 52.67; H, 3.38; N, 7.23; Cl, 9.14; V, 13.14%.

6.9.3 μ-Oxo-bis[oxo(1,3-diphenylpropane-1,3-dionebenzoylhydrazonato(2-)) vanadium(V)] - [VO(dbm-BH)]$_2$O

The same method (6.9.1) gave a brown-red product. m.p. 235-7°C, Analysis, found: C, 63.24; H, 3.73; N, 6.52; V, 12.42. $V_2C_{44}H_{32}N_4O_7$ requires C, 63.62; H, 3.88; N, 6.74; V, 12.27%.

6.9.4 μ-Oxo-bis[oxo(2-oxo-1-napthaldehydebenzoylhydrazonato(2-))vanadium(V)] - [VO(HNP-BH)]$_2$O

The same method (6.9.1) gave a yellow-brown product. m.p. > 250°C, Analysis, found: C, 58.52; H, 3.48; N, 7.56; V, 14.10. $V_2C_{36}H_{24}N_4O_7$ requires C, 59.52; H, 3.33; N, 7.71; V, 14.02%.

6.9.5 μ-Oxo-bis[oxo(2-oxo-1-napthaldehyde-p-chlorobenzoylhydrazonato(2-)) vanadium(V)] - [VO(HNP-p^{Cl}-BH)]$_2$O

The same method as for 6.9.1 gave this magenta-brown compound. m.p. > 250°C, Analysis, found: C, 53.27; H, 2.83; N, 6.89; Cl, 9.02; V, 13.01. $V_2C_{36}H_{22}N_4O_7Cl_2$ requires C, 54.36; H, 2.79; N, 7.04; Cl, 8.91; V, 12.81%.

6.9.6 <u>μ-Oxo-bis[oxo(2-oxoacetophenonebenzoylhydrazonato(2-))vanadium(V)]</u>
- [VO(HAP-BH)]$_2$O

The same method as for 6.9.1 gave a chocolate-brownish product. m.p. 230-2°C, Analysis, found: C, 54.49; H, 3.77; N, 8.61; V, 15.45. $V_2C_{30}H_{24}N_4O_7$ requires C, 55.06; H, 3.70; N, 8.56; V, 15.57%.

6.9.7 <u>μ-Oxo-bis[oxo(salicylaldehydebenzoylhydrazonato(2-))vanadium(V)]</u>
- [VO(Sal-BH)]$_2$O

The same method as for 6.9.1 gave this brown compound. m.p. > 250°C, Analysis found: C, 53.39; H, 3.32; N, 8.88; V, 16.43. $V_2C_{28}H_{20}N_4O_7$ requires C, 53.69; H, 3.22; N, 8.94; V, 16.27%.

6.10 PHYSICAL MEASUREMENTS

(a) SPECTRAL MEASUREMENTS

Infrared spectra were determined on a Perkin-Elmer 683 infrared spectro-photometer in nujol mulls or KBr discs. Electronic absorption spectra were recorded on a Varian DMS 100 UV-visible spectrophotometer and a Zeiss DMR-10 recording spectrophotometer. Mass spectra were measured using an AEI-MS30 double focus spectrometer operating at 70ev ionizing energy. The E.S.R. spectra were recorded on a Varian E.P.R. E-9 spectrometer. Proton N.M.R. spectra were recorded relative to TMS on Varian T-60 spectrometer and Jeol JNM-PMX 60 N.M.R. spectrometer (for routine spectra) and Bruker WP-80 spectro-meter (for accurate measurements).

(b) MOLECULAR WEIGHT

Molecular weights were determined using a Knauer vapour pressure osmo-metry - universal temperature measuring instrument.

(c) MAGNETIC MEASUREMENTS

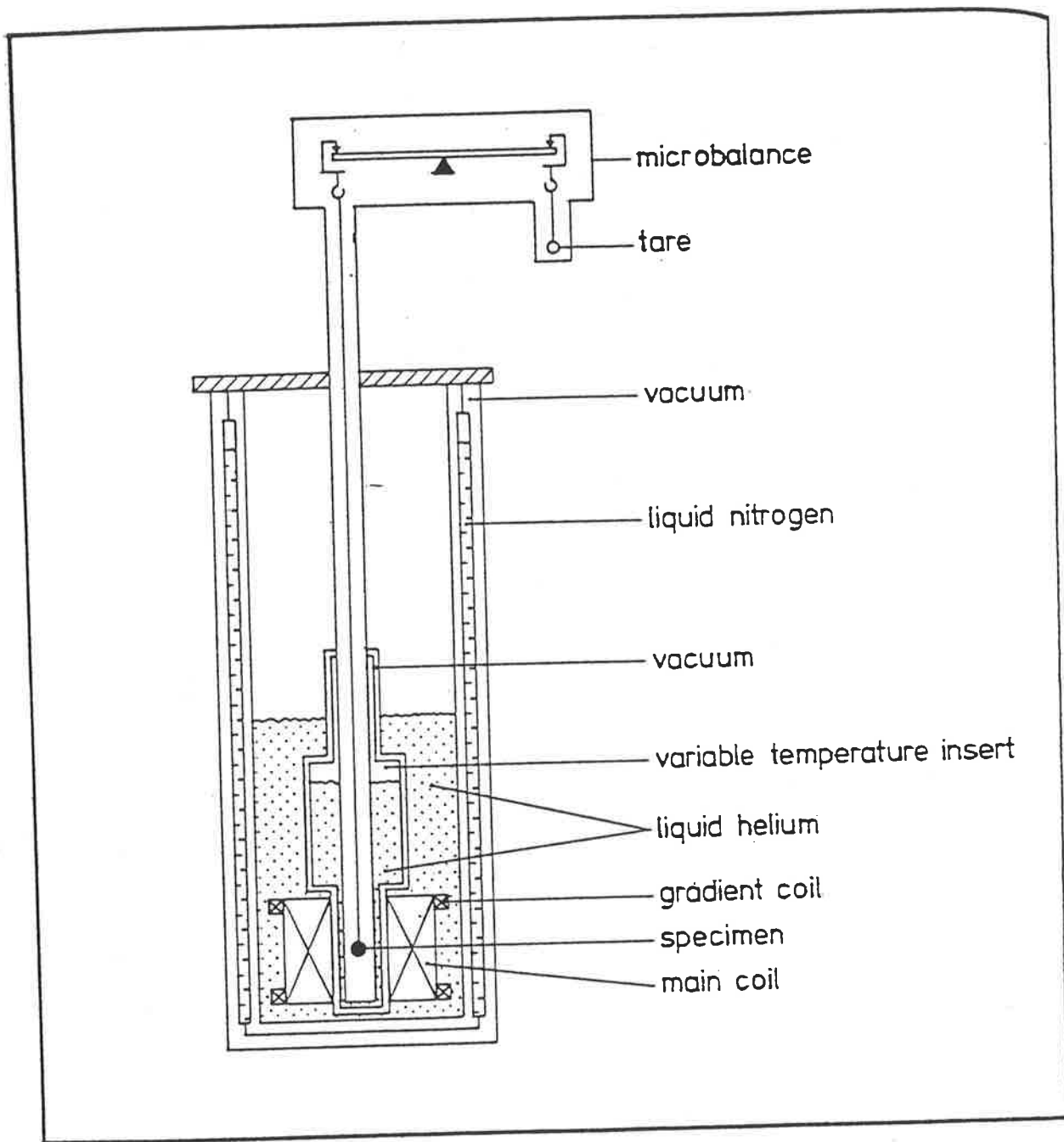The room temperature magnetic moments were determined by the Gouy method.

Figure 6.10.1: Schematic representation of the cryostat including the microbalance.

Tubes were calibrated with $Hg[Co(NCS)_4]$ as a standard. Diamagnetic correct-ions for the metal and ligand atoms were computed using a standard source[159e].

The magnetic susceptibility measurements of the solid alkoxo-bridged complexes over the temperature range 4.2 - 300K were made in the Department of Chemistry at the Monash University, Victoria on an extensively modified Oxford Instruments Faraday Magnetometer with main fields of 10 kG and/or 40 kG and a gradient field of 1000 G cm^{-1}. This novel Faraday balance system incorporated a superconducting solenoid and an automatic data-logging facility. The cryo-stat carrying the microbalance (Figure 6.10.1) keeps the superconducting coils immersed in a bath of liquid helium and allows the specimen temperature to be varied in a wide range. Samples weighing between 20 and 50 mg were placed in a gold bucket and suspended from a Sartorius electronic microbalance by a fine quartz fibre down into the cryostat with its position coinciding with the centre of the magnet system. Special vacuum techniques and care were employed to charge pure liquid helium into the cryostat to avoid any solidification of previously charged liquid nitrogen (used for pre-cooling) which must be exhausted completely before helium insertion. Samples were checked for any unusual field dependence at both 4.2 and 300K and none were found to be present. Temperatures below 30K were measured using a carbon resistor while above this a copper/constantan thermocouple was employed. The temperatures were accurately calibrated by means of a gallium arsenide diode suspended in the sample position[338]. The exchange integral, J values were computed by measuring the susceptibilities of the dimer as a function of temperature and fitting the observed data by least squares methods to the Bleaney-Bowers equation (1) (Section 2.8) allowing for the presence of monomer impurity[156].

(d)   ELECTROCHEMISTRY

Voltammetry work was carried out using a three-electrode system consist-ing of a circular platinum working electrode, a platinum counter electrode and a modified saturated calomel reference electrode. Depending on solvents, the

electrolyte in the reference electrode was Et_4NCl. The electrodes were fitted into a cell of approximately 50 cm^3 capacity such that the working electrode was in close proximity to the reference electrode. Argon was bubbled through the solution to purge dissolved oxygen. A supporting electrolyte of 0.1 M Et_4NBF_4 (also Et_4NClO_4 or Et_4NCl) was used.

Cyclic voltammograms (CV) were determined using an RDE 3 Potentiostat from Pine Instrument Company connected to a Hewlett Packard 7015B X-Y recorder (for routine work) and a BAS-100 Electrochemical Analyzer (manufactured by Bioanalytical Systems Inc., West Lafayette, Indiana) connected to a Houston Instrument HIPLØT DMP-40 series Digital Plotter or a printer (Amust P88-2). The controlled potential bulk electrolysis was carried out using BAS-100 and by applying a fixed voltage (determined from CV) to an electrode with a large surface area (platinum gauze).

The half-wave potentials and the reversibility of the system (as measured by peak separation, ΔEp) were determined using the standard procedure and equations.

CONCLUSION

This work explored the formation and chemistry of alkoxo-bridged vanadyl dimers and the novel bis-tridentate non-vanadyl vanadium(IV) complexes. A number of ligand systems have been developed which stabilize these less common types of vanadium complexes.

As regards the formation of the alkoxo-bridged oxovanadium(IV) $[VO(AA)(OR)]_2$ complexes, it appears that the singly charged bidentate ligands (AA^-) having at least one phenyl ring or quasi-aromatic nature through delocalization are necessary to form such complexes. Isolation is difficult unless the ligands are capable of yielding dimer products of low-solubility. Electron-attracting phenyl rings help stabilize the +4 oxidation state thus preventing oxidation to vanadium(V) under 'normal' oxygen-free conditions. These complexes have been successfully used as model compounds to investigate (i) the electronic interaction between the VO^{2+} centres based on the strong antiferromagnetism observed and (ii) the type of E.S.R. response characteristic of a dimer configuration. These properties proved to be the most significant consequences of the presence of two VO^{2+} centres per molecule as compared to those of the monomeric complexes.

The bis-tridentate VL_2 complexes are limited to ligands that can stabilize the +4 oxidation state of vanadium without the oxo group. It seems that the substitution of the stable oxo ligand takes place only with ligands which themselves are strongly electron-donating (σ- as well as π-). Such ligands contain two strongly basic oxygens of an enolic and/or phenolic nature and an imine nitrogen which together fulfil the σ-donation requirement. In

addition, the near planarity of the two contiguous chelate rings provide occupied delocalized π-orbitals capable of π-donation into the d-orbitals of the metal. Other dinegative tridentate ligands without an extended π-system, e.g. pyridine-2,6-dicarboxylic acid and Schiff bases of amino acids do not form VL_2 complexes. Both σ- and π- ligand to metal bonding, stability associated with the chelation as well as ready separation of the neutral VL_2 product from the reaction mixture must be important in determining the ligand type favouring VL_2 formation.

Bidentate ligands such as catechol, salicylic acid and benz-hydroxamic acid which form non-vanadyl vanadium(IV) complexes with oxygen donors support the above idea that strong σ- and π-donations are needed to form such non-oxo complexes. However, these complexes are less stable as one bidentate ligand can be replaced by a strongly donating oxo ligand to form VO-complexes. The exceptional stability of the VL_2 complexes lies in the fact that a strongly donating tridentate ligand bound to the metal through two chelate rings need to be removed to give a VO-complex. A simplistic explanation of the extra-stability of the VL_2 complexes is that the two tridentate ligands provide the electron density, needed to stabilize the non-vanadyl vanadium(IV) moiety, from four strongly basic oxygens arranged in a flattened tetrahedron.

The isolation of $V^{IV}OL\underline{H}Cl$, $(V^{IV}OL)_2/V^{IV}OLX$ and of $V^VOL.OR$ and $(V^VOL)_2O$ complexes, depending on reaction condition, suggests stepwise formation of the VL_2 chelates via '$V^{IV}OL$' intermediates. However, except in cases of high insolubility, such intermediates are difficult to prevent from oxidizing. This is consistent with the strong electron donation from the ligand which when combined with that due to the oxo ligand leads to a very electron rich

centre. The charge-transfer spectra and electrochemical studies suggest that one tridentate ligand transfers less electronic charge than one doubly bonded oxo ligand making the fully substituted VL_2 product more stable towards oxidation than the intermediates.

Of striking characteristic of the VL_2 complexes is that they display a trigonal prismatic (in one case, severely distorted) coordination geometry. Low occupancy of the d-orbitals is equally favourable for octahedral and trigonal prismatic coordination with the suggestion that the latter may be actually preferred[233]. However, the fact that the catecholato complexes are octahedral suggests that factors other than the d- configuration are important. Kepert has rationalized the stereochemical arrangement of many complexes by using arguments based solely on energy minimization and chelate bite sizes. Our results and the structure of the catecholato complex are consistent with his explanation and the bite sizes of the chelates to the extent of even predicting a most unusually distorted trigonal prismatic structure. Surprisingly, two titanium complexes with the same ligands, which form trigonal prismatic VL_2 complexes, were found to be octahedral. This is quite contrary to the Kepert's theory and suggest that factors other than electrostatic repulsion must be determinant. One such factor may be π-donation which would be expected to be less important in titanium than in vanadium. It could be that the π-donation stabilizes a trigonal prismatic arrangement of the ligands.

* * * * * * *

REFERENCES

1. N.D. Chasteen, Structure and Bonding **53**, 105, 1983.

2. T. Thanabal and V. Kirshnan, Inorg. Chem. **21**, 3606, 1982.

3. J. Selbin, L.H. Holmes and S.P. McGlynn, J. Inorg. Nucl. Chem. **25**, 1359, 1963.

4. J. Selbin, Chem. Rev. **65**, 153, 1965.

5. J. Selbin, Coord. Chem. Rev. **1**, 293, 1966.

6. A. Syamal, Coord. Chem. Rev. **16**, 309, 1975.

7. D. Nicholls, Coord. Chem. Rev. **1**, 379, 1966.

8. D.A. Rice, Coord. Chem. Rev. **37**, 61, 1981.

9. E.M. Page, Coord. Chem. Rev. **57**, 237, 1984.

10. M.R. Caira, J.M. Haigh and L.R. Nassimbeni, J. Inorg. Nucl. Chem. **34**, 3171, 1972.

11. N.S. Al-Niami, A.R. Al-Karaghouli, S.M. Aliwi and M.G. Jalhoom, J. Inorg. Nucl. Chem. **36**, 283, 1974.

12. M.R. Caira, J.M. Haigh and L.R. Nassimbeni, Inorg. Nucl. Chem. Letts. **8**, 109, 1972.

13. T.L. Riechel and D.T. Sawyer, Inorg. Chem. **14**, 1869, 1975.

14. C.J. Hawkins, University of Queensland - private communication.

15. J. Reuben and D. Fiat, Inorg. Chem. **6**, 579, 1967.

16. K. Wüthrich and R.E. Connick, Inorg. Chem. **6**, 583, 1967.

17. A.E. Martell, Ed., A.C.S. Monograph 174, 'Coordination Chemistry', Vol. 2, 1978, Figure 1-1 at p. 20, American Chemical Society.

18. J.L. Burdett and M.T. Rogers, J. Am. Chem. Soc. **86**, 2105, 1964.

19. R.C. Mehrotra, R. Bohra and D.P. Gaur, 'Metal β-Diketonates and Allied Derivatives', Academic Press, 1978, p. 31.

20. R.P. Dodge, D.H. Templeton and A. Zalkin, J. Chem. Phys. **35**, 55, 1961.

21. P.K. Hon, R.L. Belford and C.E. Pfluger, J. Chem. Phys. **43**, 1323, 3111, 1965.

22. K. Nakamoto, Y. Morimoto and A.E. Martell, J. Am. Chem. Soc. **83**, 4533, 1961.

23. C.J. Popp, J.H. Nelson and R.O. Ragsdale, J. Am. Chem. Soc. **91**, 610, 1969.

24. S. Ikeda, A. Yamamoto, S. Kurita, K. Takahashi and T. Watanabe, Inorg. Chem. **5**, 611, 1966.

25. B.B. Adeleke and K.S. Patel, J. Coord. Chem. **11**, 201, 1982.

26. K.S. Patel, J. Inorg. Nucl. Chem. **43**, 667, 1981.

27. M.A. Nawi and T.L. Riechel, Inorg. Chem. **20**, 1974, 1981.

28. R.J. Baker, Ph.D. Thesis, University of Adelaide, 1966.

29. A.P. Summerton, A.A. Diamantis and M.R. Snow, Inorg. Chim. Acta **27**, 123, 1978.

30. A. Van den Bergen, K.S. Murray, B.O. West and A.N. Buckley, J. Chem. Soc. A, 2051, 1969.

31. R.H. Holm and G.W. Everett Jr., Progr. Inorg. Chem. **7**, 83, 1966.

32. L. Sacconi and U. Campigli, Inorg. Chem. **5**, 606, 1966.

33. V.V. Zelentsov, Dokl. Akad. Nauk. SSSR **139**, 1110, 1961; C.A. **56**, 1442c, 1962.

34. V.V. Zelentsov, Russ. J. Inorg. Chem. **7**, 670, 1962.

35. V.V. Zelentsov, Zh. Strukt. Khim. **5**, 714, 1964; C.A. **62**, 3515a, 1965.

36. A.P. Ginsberg, E. Koubek and H.J. Williams, Inorg. Chem. **5**, 1656, 1966.

37. A. Syamal and L.J. Theriot, J. Coord. Chem. **2**, 193, 1973.

38. G.O. Carlisle and D.A. Crutchfield, Inorg. Nucl. Chem. Lett. **8**, 443, 1972.

39. G.O. Carlisle, D.A. Crutchfield and M.D. McKnight, J. Chem. Soc., Dalton Trans. 1703, 1973.

40. B.R. Havinale and I.B. Pujar, J. Inorg. Nucl. Chem. **43**, 2689, 1981.

41. A. Syamal and K.S. Kale, Inorg. Chem. **18**, 992, 1979.

42. A. Syamal and K.S. Kale, Ind. J. Chem. **15A**, 431, 1977.

43. A. Syamal, E.F. Carey and L.J. Theriot, Inorg. Chem. **12**, 245, 1973.

44. A.A. Diamantis, J.M. Frederiksen, Md. Abdus Salam, M.R. Snow and E.R.T. Tiekink, Aust. J. Chem. (in press).

45. C.J. Ballhausen and H.B. Gray, Inorg. Chem. **1**, 111, 1962.

46. D.K. Rastogi, S.K. Sahni, V.B. Rana, K. Dua and S.K. Dua, J. Inorg. Nucl. Chem. **41**, 21, 1979.

47. G.A. Kolawole and K.S. Patel, J. Chem. Soc., Dalton Trans. 1241, 1981.

48. V.H. Kulkarni, B.R. Patil and B.K. Prabhakar, Curr. Sci. **50**, 585, 1981.

49. M.M. Patel, M.R. Patel and M.N. Patel, Ind. J. Chem. **20A**, 623, 1981.

50. D. Bruins and D.L. Weaver, Inorg. Chem. **9**, 130, 1970.

51. U. Casellato and P.A. Vigato, Inorg. Chim. Acta **49**, 173, 1981.

52. B.E. Bridgland, G.W.A. Fowles and R.A. Walton, J. Inorg. Nucl. Chem. **27**, 383, 1965.

53. R.J.H. Clark, 'The Chemistry of Titanium and Vanadium', Elsevier Publishing Co., 1968, p. 160.

54. R.J.H. Clark, J. Lewis and R.S. Nyholm, J. Chem. Soc. 2460, 1962.

55. D.C. Bradley and M.L. Mehta, Canad. J. Chem. **40**, 1183, 1962.

56. E.C. Alyea and D.C. Bradley, J. Chem. Soc., A. 2330, 1969.

57. R. Eisenberg, Progr. Inorg. Chem. **12**, 295, 1970.

58. R. Eisenberg, E.I. Steifel, R.C. Rosenberg and H.B. Gray, J. Am. Chem. Soc. **88**, 2874, 1966.

59. R. Eisenberg and H.B. Gray, Inorg. Chem. **6**, 1844, 1967.

60. E.I. Steifel, Z. Dori and H.B. Gray, J. Am. Chem. Soc. **89**, 3353, 1967.

61. D.C. Bradley, I.F. Rendall and K.D. Sales, J. Chem. Soc., Dalton Trans. 2228, 1973.

62. O. Piovesana and G. Cappuccili, Inorg. Chem. **11**, 1543, 1972.

63. M. Pasquali, A. Torres-Filho and C. Floriani, J. Chem. Soc., Chem. Comm. 534, 1975.

64. M. Pasquali, F. Marchetti and C. Floriani, Inorg. Chem. **18**, 2401, 1979.

65. C. Floriani and F. Calderazzo, J. Chem. Soc., A. 3665, 1971.

66. A. Jezierski and J.B. Raynor, J. Chem. Soc., Dalton Trans. 1, 1981.

67. P. Richard, J.L. Poulet, J.M. Barbe, R. Guilard, J. Groulou, D. Rinaldi, A. Cartier and P. Tola, J. Chem. Soc., Dalton Trans. 1451, 1982.

68. M. Tirant and T.D. Smith, Inorg. Chim. Acta **90**, 111, 1984.

69. R.B. Van Dreele and R.C. Fay, J. Am. Chem. Soc. **94**, 7935, 1972.

70. R.P. Henry, P.C.H. Mitchell and J.E. Prue, J. Chem. Soc. A. 3392, 1971.

71. S.R. Cooper, Y.B. Koh and K.N. Raymond, J. Am. Chem. Soc. **104**, 5092, 1982.

72. T.J. Hörr, Honours Report, The University of Adelaide, 1983.

73. A.A. Diamantis, M.R. Snow and J.A. Vanzo, J. Chem. Soc. Chem. Comm. 264, 1976. [Also, J.A. Vanzo, Honours Report, The University of Adelaide, 1975].

74. D. Fairlie, Honours Report, The University of Adelaide, 1977.

75. I.W. Roberts, Honours Report, The University of Adelaide, 1978.

76. A. Giacomelli, C, Floriani, A.O.D.S. Duarte, A. Chiesi-villa and C. Guastini, Inorg. Chem. **21**, 3310, 1982.

77. A.E. Patrovic, B. Ribar, D.M. Petrovic, V.M. Leovac and N.V. Gerbeleu, J. Coord. Chem. **11**, 239, 1982.

78. Y. Jeannin, J.P. Launay and M.A.S. Sedjadi, J. Coord. Chem. **11**, 27, 1981.

79. W.R. Scheidt, D.M. Collins and J.L. Hoard, J. Am. Chem. Soc. **93**, 3873, 1971.

80. K.P. Srivastava, R. Dutta and I.K. Jain, J. Inorg. Nucl. Chem. **43**, 1155, 1981.

81. L.M. Dyagileva, O.S. Morozov and N.M. Vyshinskii, Zh. Obsch. Khim. **50**, 1859, 1980.

82. H.L. Krauss and G. Gnatz, Chem. Ber. **95**, 1023, 1962.

83. H. Funk, W. Weiss and M. Zeising, Z. Anorg. Allg. Chem. **296**, 36, 1958.

84. K. Pande and S.G.R. Tandon, J. Inorg. Nucl. Chem. **42**, 1509, 1980.

85. C.N. Caughlan, H.M. Smith and K. Watenpaugh, Inorg. Chem. **5**, 2131, 1966.

86. W.R. Scheidt, Inorg. Chem. **12**, 1758, 1973.

87. R.L. Dutta and A. Syamal, J. Ind. Chem. Soc. **44**, 381, 1967.

88. K.L. Chawla, P. Prashar and J.P. Tandon, J. Ind. Chem. Soc. **49**, 553, 1972.

89. H. Mimoun, P. Chaumette, M. Mignard, L. Saussine, J. Fischer and R. Weiss, Nouv. J. Chim. **7**, 467, 1983.

90. L. Saussine, H. Mimoun, A. Mitschler and J. Fisher, Nouv. J. Chim. **4**, 235, 1980.

91. S. Yamada, C. Katayama, J. Tanaka and M. Tanaka, Inorg. Chem. **23**, 253, 1984.

92. U. Casellato, P.A. Vigato, R. Graziani, M. Validi, F. Milani and M.M. Musiani, Inorg. Chim. Acta **61**, 121, 1982.

93. K. Wieghardt, W. Holzbach and J. Weiss, Inorg. Chem. **20**, 3436, 1981.

94. A. Yuchi, Y. Yagishita, S. Yamada and M. Tanaka, Bull. Chem. Soc. Japan **54**, 200, 1981.

95. W.R. McWhinnie, J. Inorg. Nucl. Chem. **27**, 1063, 1965.

96. B. Chiari, O. Piovesana, T. Tarantelli and P.F. Zanazzi, Inorg. Chem. **23**, 3398, 1984.

97. H.R. Fischer, J. Glerup, D.J. Hodgson and E. Pedersen, Inorg. Chem. **21**, 3063, 1982.

98. M.M. Musiani, F. Milani, R. Graziani, M. Vidali, U. Casellato and P.A. Vigato, Inorg. Chim. Acta **61**, 115, 1982.

99. A.A. Diamantis, private communications.

100. D.J. Hodgson, Progr. Inorg. Chem. **19**, 173, 1975.

101. W.R. McWhinnie, J. Chem. Soc. 2959, 1964.

102. K. Watenpaugh and C.N. Caughlan, Inorg. Chem. **5**, 1782, 1966.

103. C.S. Wu, G.R. Rossman, H.B. Gray, G.S. Hammond and H.J. Schugar, Inorg. Chem. **11**, 990, 1972.

104. N.T. Moxon, J.H. Moffett and A.K. Gregson, J. Inorg. Nucl. Chem. **43**, 2695, 1981.

105. D.C. Bradly, R.C. Mehrotra and D.P. Gaur, 'Metal Alkoxides', Academic Press, 1978, pp. 61, 90.

106. C.L. O'Young, J.C. Dewan, J.R. Lilienthal and S.J. Lippard, J. Am. Chem. Soc. **100**, 7291, 1978.

107. K.S. Murray, Symposium Lecture (SL-2) in the R.A.C.I. COMO-12 Conference in Hobart, January, 1984.

108. W. Mazurek. K.J. Berry, K.S. Murray, M.J. O'Connor, M.R. Snow and A.G. Wedd. Inorg. Chem. **21**, 3071, 1982.

109. J. Elguero, R. Jacquier et. Mme H.C.N. Tien Duc, Bull. Soc. Chim. Fr. **12**, 3727, 1966.

110. M.D. Fitzroy, G.D. Fallon and K.S. Murray, A paper on Molybdenum Chemistry sent for publication in Inorg. Chem.

111. T.R. Ortolano, J. Selbin and S.P. McGlynn, J. Chem. Phys. **41**, 262, 1964.

112. D.P. Graddon, Coord. Chem. Rev. **4**, 1, 1969.

113. J.H. Weber, Synth. Reac. Inorg. Metal Org. Chem. **7**, 243, 1975.

114. B. Morosin and H. Montogomery, Acta Cryst. **25B**, 1354, 1969.

115. M. Mathew, A.J. Carty and G.J. Palenik, J. Am. Chem. Soc. **92**, 3197, 1970.

116. M. Pasquali, F. Marchetti, C. Floriani and S. Merlino, J. Chem. Soc., Dalton Trans. 139, 1977.

117. J. Konarski, J. Mol. Structure **13**, 45, 1972.

118. R.S. Rasmussen, D.D. Tunnicliff and R.R. Brattain, J. Am. Chem. Soc. **71**, 1068, 1949.

119. L.J. Bellamy, C.S. Spicer and J.D.H. Strickland, J. Chem. Soc. 4653, 1952; L.J. Bellamy and R.F. Branch, J. Chem. Soc. 4491, 1954.

120. S. Pinchas, B.L. Silver and I. Laulicht, J. Chem. Phys. **46**, 1506, 1967.

121. G.T. Behnke and K. Nakamoto, Inorg. Chem. **6**, 443, 1967.

122. G.T. Behnke and K. Nakamoto. Inorg. Chem. **6**,. 440, 1967.

123. H. Junge and H. Musso, Spectrochim. Acta **A24**, 1219, 1968.

124. R.C. Fay and T.J. Pinnavaia, Inorg. Chem. **7**, 508, 1968.

125. C.G. Barraclough, D.C. Bradley, J. Lewis and I.M. Thomas, J. Chem. Soc. 2601, 1961.

126. C.T. Lynch, K.S. Mazdiyasni, J.S. Smith and W.J. Crawford, Anal. Chem. **36**, 2332, 1964.

127. F.K. Butcher, W. Gerrard, E.F. Mooney, R.C. Rees and H.A. Willis, Spectrochim. Acta **20**, 51, 1964.

128. C. Furlani, Ricerca. Scient. **27**, 1141, 1957.

129. R.D. Feltham, Thesis, University of California, UCRL-3867, 1957.

130. C.K. Jorgensen, Acta Chem. Scand. **11**, 73, 1957.

131. R.E. Tapscott and R.L. Belford, Inorg. Chem. **6**, 735, 1967.

132. J. Selbin, G. Maus and D.L. Johnson, J. Inorg. Nucl. Chem. **29**, 1735, 1967.

133. J. Selbin and T.R. Ortolano, J. Inorg. Nucl. Chem. **26**, 37, 1964.

134. J. Selbin. L.H. Holmes Jr. and S.P. McGlynn, J. Inorg. Nucl Chem. **25**, 1359, 963.

135. J. Selbin and L. Morpurgo, J. Inorg. Nucl. Chem. **27**, 673, 1965.

136. L.G. Vanquickenborne and S.P. McGlynn, Theoret. Chim. Acta **9**, 390, 1968.

137. H.J. Stoklosa, J.R. Wasson and B.J. McCormic, Inorg. Chem. **13**, 592, 1974.

138. J.E. Drake, J. Vekis and J.S. Wood, J. Chem. Soc., (A) 1000, 1968.

139. H.A. Kuska and P.H. Yang, Inorg. Chem. **13**, 1090, 1974.

140. C.C. Lee, A. Syamal and L.J. Theriot, Inorg. Chem. **10**, 1669, 1971.

141. J.C. Donini, B.R. Hollebone, G. London, A.B.P. Lever and J.C. Hempel, Inorg. Chem. **14**, 455, 1977.

142. J.C. Donini, B.R. Hollebone and A.B.P. Lever, Progr. Inorg. Chem. **22**, 225, 1976.

143. T.R. Felthouse and D.N. Hendrickson, Inorg. Chem. **17**, 444, 1978.

144. A. Syamal, Ind. J. Chem. **11**, 363, 1973.

145. T.R. Felthouse, E.J. Laskowski and D.N. Hendrickson, Inorg. Chem. **16**, 1077, 1977.

146. R.L. Belford, N.D. Chasteen, H. So and R.E. Tapscott, J. Am. Chem. Soc. **91**, 4675, 1969.

147. R.H. Dunhill and T.D. Smith, J. Chem. Soc., (A) 2189, 1968.

148. P.D.W. Boyd, T.D. Smith, J.H. Price and J.R. Pilbrow, J. Chem. Phys. **56**, 1253, 1972.

149. T.D. Smith and J.R. Pilbrow, Coord. Chem. Rev. **13**, 173, 1974.

150. C.P. Slichter, Phys. Rev. **99**, 479, 1955.

151. B.N. Figgis and R.L. Martin, J. Chem. Soc. 3837, 1956.

152. H.A. Kramers, Physicia **1**, 182, 1934.

153. M. Kato, H.B. Jonassen and J.C. Fanning, Chem. Rev. **64**, 99, 1964.

154. K.S. Murray, Coord. Chem. Rev. **12**, 1, 1974.

155. J.B. Goodenough, 'Magnetism and the Chemical Bond', Interscience, N.Y. 1963, Chapter II; (a) Chapter III.

156. A.P. Ginsberg, Inorg. Chim. Acta Rev. **5**, 45, 1971.

157. P.W. Anderson, Phys. Rev. **115**, 2, 1959.

158. R.L. Martin, in E.A.V. Ebsworth, A.G. Maddock and A.G. Sharpe (Eds.), 'New Pathways in Inorganic Chemistry', Cambridge Univ. Press, Cambridge, 1968, Chapter 9 and references therein.

159. F.E. Mabbs and D.J. Machin, 'Magnetism and Transition Metal Complexes', Chapman and Hall, London, 1973; (a) p. 8; (b) p. 174; (c) p. 179; (d) p. 171; (e) p. 5.

160. B. Bleaney and K.D. Bowers, Proc. Royal Soc. (London) **A214**, 451, 1952.

161. A. Gaines, L.P. Hammett and G.H. Walden, J. Am. Chem. Soc. **58**, 1668, 1936.

162. A. Bose, Proc. Indian Acad. Sci., Sect. A, **1**, 754, 1934.

163. J.N. Van Niekerk and F.K.L. Schöning, Acta Cryst. **6**, 227, 1953.

164. A. Earnshaw and J. Lewis, J. Chem. Soc. 396, 1961.

165. J. Lewis, F.E. Mabbs and A. Richards, Nature **207**, 855, 1965.

166. J. Lewis, F.E. Mabbs and A. Richards, J. Chem. Soc. 1014, 1967.

167. B.N. Figgis and J. Lewis, in 'Modern Coordination Chemistry', Edtd. by J. Lewis and R.G. Wilkins, Interscience, N.Y., 1964; (a) p. 436.

168. G.M. Klesova, V.V. Zelentsov and V.I. Spitsyn, Dokl. Akad. Nauk. SSSR **208**, 642, 1973; C.A. **78**, 116937a, 1973.

169. I.Y. Kasparova and V.V. Zelentsov, Dokl. Akad. Nauk. SSR **173**, 127, 1967; C.A. **67**, 27322 b, 1967.

170. A.P. Ginsberg, R.C. Sherwood and E. Koubek, J. Inorg. Nucl. Chem. **29**, 353, 1967.

171. G.N. Rao and S.C. Rustagi, Indian J. Chem. **11**, 1181, 1973.

172. M.D. Revenko and N.V. Gerbeleu, Russ. J. Inorg. Chem. **17**, 529, 1972.

173. N.V. Gerbeleu and M.D. Revenko, Zh. Neorg. Khim. **18**, 2397, 1973; C.A. **79**, 132408e, 1973.

174. V.T. Kalinnikov, V.V. Zelentsov, O.D. Ubozhenko and T.G. Aminov, Dokl. Akad. Nauk. SSSR **206**, 627, 1972; C.A. **78**, 21723, 1973.

175. R.C. Agarwal and B. Prasad, Indian J. Chem. **10**, 1182, 1972.

176. A. Hodge, K. Nordquest and E.L. Blinn, Inorg. Chim. Acta **6**, 491, 1972.

177. R.L. Dutta and G.P. Sengupta, J. Indian Chem. Soc. **44**, 738, 1967 and **48**, 33, 1971.

178. Y. Kuge and S. Yamada, Bull. Chem. Soc. Japan **45**, 799, 1972.

179. K.S. Murray, Monash University, Victoria.

180. J.E. Andrew, A.B. Blake and L.R. Fraser, J. Chem. Soc., Dalton Trans. 477, 1976.

181. C.G. Barraclough, R.W. Brookes and R.L. Martin, Aust. J. Chem. **27**, 1843, 1974.

182. D. Kivelson and S.K. Lee, J. Chem. Phys. **41**, 1896, 1964.

183. F.A. Cotton and M.J. Millar, J. Am. Chem. Soc. **99**, 7886, 1977.

184. F.A. Cotton, G.E. Lewis and G.N. Mott, Inorg. Chem. **22**, 560, 1983.

185. M. Julve, M. Verdaguer, M.F. Charlot, O. Khan and R. Claude, Inorg. Chim. Acta **82**, 5, 1984.

186. M.J. Heeg, J.L. Mack, M.D. Glick and R.L. Lintvedt, Inorg. Chem. **20**, 833, 1981.

187. H. Matschiner, H, Tanneberg and H.H. Ruettinger, Zl. Phys. Chem. **260**, 538, 1979.

188. A.D. Jannakoudakis, C. Tsiamis, P.D. Jannakoudakis and E. Theordoridou, J. Electroanal. Chem. **184**, 123, 1985.

189. R.F. Handy and R.L. Lintvedt, Inorg. Chem. **13**, 893, 1974.

190. G.S. Patterson and R.H. Holm, Inorg. Chem. **11**, 2285, 1972.

191. K. Wieghardt, U. Bossek, K. Volckmar, W. Swiridoff and J. Weiss, Inorg. Chem. **23**, 1387, 1984.

192. R.M. Issa, M.F. El-Shazly and M.F. Iskander, Zl. Anorg. Allg. Chem. **354**, 90, 1967.

193. J. Chatt, J.R. Dilworth, G.J. Leigh and V.D. Gupta, J. Chem. Soc. (A). 2631, 1971.

194. M.D. Fitzroy, J.M. Frederiksen. K.S. Murray and M.R. Snow, Inorg. Chem. **24**, 3265, 1985.

195. J.F. Alcock, R.J. Baker and A.A. Diamantis, Austr. J. Chem. **25**, 289, 1972.

196. L. Sacconi, Zl. Anorg. Allg. Chem. **275**, 249, 1954.

197. J.P. Wilshire and D.T. Sawyer, J. Am. Chem. Soc. **100**, 3972, 1978.

198. C. Hedbom and E. Helgstrand, Acta Chem. Scand. **24**, 1744, 1970.

199. Beilsteine 10^3, 161, 115.

200. M.F. Iskander, S.E. Zayan, M.A. Khalifa and L. El-Sayed, J. Inorg. Nucl. Chem. **36**, 551, 1974.

201. S.C. Shome and H.R. Das, Anal. Chim. Acta **32**, 400, 1964.

202. R.L. Dutta and A.K. Pal, Ind. J. Chem. **21(A)**, 1130, 1982.

203. R. Grieb and A. Niggli, Helv. Chim. Acta **48**, 317, 1965.

204. H.D.K. Drew and R.E. Fairbairn, J. Chem. Soc. 823, 1939.

205. H. Pfitzner, Angew Chem. **62**, 242, 1950.

206. R.L.M. Allen. 'Colour Chemistry', Appleton-Century-Crofts, N.Y. 1971, (a) p. 48; (b) p. 64.

207. G. Schetty, Helv. Chim. Acta **53(6)**, 1437, 1970.

208. H. Pfitzner and H. Schweppe, Zl. Anal. Chem. **268(5)**, 337, 1974.

209. T. Misono, K. Sawamura, Y. Nagao and Y. Abe, Shikizai Kyokaishi, **57(4)**, 186, 1984 (C.A. **101**, 91988w); T. Misono, Y. Abe, Y. Nagao and K. Nigor-ikawa, ibid **56(3)**, 143, 1983 (C.A. **99**, 39780Y) and ibid **55(2)**. 76, 1982 (C.A. **96**, 164110u); T. Misono, Y. Abe. Y. Nagao and T. Kajima, ibid **54(1)**, 15, 1981 (C.A. **95**, 26592f).

210. J.D. Roberts and M.C. Caserio, 'Basic Principles of Organic Chemistry', W.A. Benzamine Inc., N.Y., 1964, p. 893.

211. G. Hilgetag and A. Martini, Ed., 'Preparative Organic Chemistry', 4th Edition (English Translation), John Wiley and Sons, 1972, p. 439.

212. L.C. Anderson and M.J. Roedel, J. Am. Chem. Soc. **67**, 955, 1945.

213. J.D.C. Anderson and R.J.W. Le Févre, Nature **162**, 450, 1948.

214. J.D.C. Anderson, R.J.W. Le Févre and I.R. Wilson, J. Chem. Soc. 2082, 1949.

215. R. Willstätter and M. Benz, Ber. **39**, 3492, 1906.

216. E.J. Gonzales and H.B. Jonassen, J. Inorg. Nucl. Chem. **24**, 1595, 1962.

217. L.F. Feiser and M. Feiser, 'Organic Chemistry', 3rd Edn., Reinhold Publishing Corp., N.Y., 1956, p. 627.

218. H.D. Becker, Acta Chem. Scand. **16**, 78, 1962.

219. J.P. Collman and D.A. Buckingham, J. Am. Chem. Soc. **85**, 3039, 1963; D.A. Buckingham, J.P. Collman. D.A.R. Happer and L.G. Marzilli, _ibid_ **89**, 1082, 1967; A. Nakahara, K. Hamada, Y. Nakao and T. Higashiyama, Coord. Chem. Rev. **3**, 207, 1968.

220. A.K. Babko, Talanta **15**, 721, 1968; R.M. Dagnall, M.T. EL-Ghamry and T.S. West, _ibid_ **15**, 1353, 1968; B.W. Bailey, J.E. Chester, R.M. Dagnall and T.S. West, _ibid_ **15**, 1359, 1968.

221. A.S. Mildvan and M. Cohn, J. Biol. Chem. **241**, 1178, 1966; E.J. Peck Jr. and W.J. Ray, _ibid_ **244**, 3754, 1969.

222. S. Kida, Bull. Chem. Soc. Japan **34**, 962, 1961.

223. D.L. Kepert, Progr. Inorg. Chem. **23**, 1, 1973.

224. D.L. Kepert, 'Inorganic Stereochemistry', Springer-Verlag, N.Y., 1982; Chapters 8 and 9; (a) p. 103, (b) p. 101.

225. D.L. Kepert, Inorg. Chem. **11**, 1561, 1972; **12**, 1944, 1973.

226. K.R. Butler, Ph.D. Thesis, University of Adelaide, 1973.

227. E.I. Steifel and G.F. Brown, Inorg. Chem. **11**, 434, 1972.

228. M. Calligaris, G. Nardin and L. Randaccio, Coord. Chem. Rev. **7**, 385, 1972.

229. A.F. Wells, 'Structural Inorganic Chemistry', 3rd Edn., Oxford University Press 1962, p. 616.

230. C. Pelizzi. G. Pelizzi, G. Predieri and F. Vitali, J. Chem. Soc., Dalton Trans. 2387, 1985.

231. R.A.D. Wentworth, Coord. Chem. Rev. **9**, 171, 1972.

232. R. Huisman, R. de Jonge, C. Haas and F. Jellinek, J. Solid State Chem. **3**, 56, 1971.

233. R. Hoffmann, J.M. Howell and A.R. Rossi, J. Am. Chem. Soc. **98**, 2484, 1976.

234. C.G. Pierpont and R. Eisenbeg, J. Chem. Soc., (A) 2285, 1971.

235. M.C. Favas, D.L. Kepert, A.H. White and A.C. Willis, J. Chem. Soc., Dalton Trans. 1350, 1977.

236. M.C. Favas and D.L. Kepert, J. Chem. Soc., Dalton Trans. 793, 1978,

237. D.L. Kepert, J. Organometallic Chem. **107**, 49, 1976.

238. R.E. Tapscott, R.L. Belford and I.C. Paul, Inorg. Chem. **7**, 356, 1968.

239. R.C. Pattersen and L.E. Alexander, J. Am. Chem. Soc. **90**, 3873, 1968.

240. R. Krishnamurthy and W.B. Schaap, J. Chem. Ed. **46**, 799, 1969 and **47**, 433, 1970.

241. G.C. Percy and D.A. Thornton, J. Inorg. Nucl. Chem. **34**, 3357, 3369, 1972; **35**, 2319, 1973.

242. N.H. Chromwell, F.A. Millar, A.R. Johnson, R.L. Franck and D.J. Wallace, J. Am. Chem. Soc. **71**, 3337, 1949.

243. H.F. Holtzclaw Jr., J.P. Collman and R.M. Alire, J. Am. Chem. Soc. **80**, 1100, 1958.

244. K. Ueno and A.E. Martell, J. Phys. Chem. **59**, 998, 1955.

245. A.E. Martell, R.L. Belford and M. Calvin. J. Inorg. Nucl. Chem. **5**, 170, 1958.

246. K. Ueno and A.E Martell, J. Phys. Chem. **61**, 257, 1957; (a) G.O. Dudek and R.H. Holm, J. Am. Chem. Soc. **83**, 2099, 1961.

247. K. Nakamoto, 'Infra-red and Raman Spectra of Inorganic and Coordination Complexes', John Wiley and Sons, N.Y., 3rd Edn., 1978.

248. L.J. Bellamy, 'The Infra-red Spectra of Complex Molecules', John Wiley and Sons Inc., N.Y., 2nd Edn., 1960.

249. B.D. Sharma and J.C. Bailar Jr., J. Am. Chem. Soc. **77**, 5476, 1955.

250. R.G.R. Bacon and W.S. Lindsay, J. Chem. Soc. 1382, 1958.

251. W.J. Strattan and D.H. Busch, J. Am. Chem. Soc. **82**, 4834, 1960.

252. G.C. Percy and J.S. Stenton, J. Inorg. Nucl. Chem. **38**, 1255, 1976.

253. G.C. Percy and H.S. Stenton, Spectrochim. Acta **32A**, 1615, 1976.

254. P.L. Pickard and G.W. Polly, J. Am. Chem. Soc. **76**, 5169, 1954.

255. P. Teyssie and J.J. Charette, Spectrochim. Acta **19**, 1407, 1963.

256. G. Dudek and E. Dudek, Inorg. Nucl. Chem. Lett. **3**, 241, 1967.

257. A. Bigotto, V. Galasso and G. De Alti, Spectrochim. Acta **28A**, 1581, 1972.

258. S. Satapathy and B. Sahoo, J. Inorg. Nucl. Chem. **32**, 2223, 1970.

259. Sutherland, Discuss. Faraday Soc. **9**, 274, 1950.

260. H. Okawo, T. Tokii, N. Nonaka, Y. Muto and S. Kida, Bull. Chem. Soc. Japan **46**, 1462, 1973.

261. J.A. Carroll, D.R. Fisher, G.W.R. Canham and D. Sutton, Canad. J. Chem. **52**, 1914, 1974.

262. A.L. Belch and D. Petridis, Inorg. Chem. **8**, 2247, 1969.

263. B.L. Haymore, J.A. Ibers and D.W. Meek, Inorg. Chem. **14**, 541, 1975.

264. J.A. Faniran, K.S. Patel and J.C. Bailar Jr., J. Inorg. Nucl. Chem. **36**, 1547, 1974.

265. J.R. Kincaid and K. Nakamoto, Spectrochim. Acta **32A**, 277, 1976.

266. K.S. Patel and G.A Kolawole, J. Coord. Chem. **11**, 231, 1982.

267. C.P. Prabhakaran and C.C. Patel, J. Inorg. Nucl. Chem. **31**, 3316, 1969.

268. B.C. Sharma and C.C. Patel, Ind. J. Chem. **8**, 747, 1970.

269. M. Mikami, I. Nakagawa and T. Shimanouchi, Spectrochim. Acta **25A**, 365, 1969.

270. K.E. Lawson, Spectrochim. Acta **17**, 249, 1961.

271. L.E. Orgel, Quart. Rev. **8**, 422, 1954.

272. J.N. Murrel, _ibid_ **15**, 191, 1961.

273. C.K. Jorgensen, Progr. Inorg. Chem. **12**, 101, 1970.

274. R.J.H. Clark, J. Chem. Soc. 5699, 1965.

275. G.S. Kyker and E.P. Schram, Inorg. Chem. **8**, 2313, 1969.

276. D.C. Bradley and M.H. Gitlitz, J. Chem. Soc.. (A) 1152, 1969.

277. F.W. Moore and R.E. Rice. Inorg. Chem. **7**, 2510, 1968.

278. P.S. Moritz, Honours Report, University of Adelaide, 1980.

279. J.N. Murrel, 'The Theory of the Electronic Spectra of Organic Molecules', Methuen and Co. Ltd., London, 1963, p. 183.

280. S.F. Mason, Quart. Rev. **15**, 287, 1961.

281. E.I. Steifel, R. Eisenberg, R.C. Rosenberg and H.B. Gray, J. Am. Chem. Soc. **88**, 2956, 1966.

282. G.N. Schrauzer and V.P. Mayweg, J. Am. Chem. Soc. **88**, 3235, 1966.

283. A. Desideri, J.B. Raynor and A.A. Diamantis, J. Chem. Soc., Dalton Trans. 423, 1978.

284. B.A. Goodman and J.B. Raynor, Adv. Inorg. Chem. Radiochem. **13**, 135, 1970.

285. D.W. Pratt, Nucl. Sc. Abs. **21**, 34254, 1967.

286. G.F. Kokoszka, H.C. Allen Jr. and G. Gordon, Inorg. Chem. **5**, 91, 1966.

287. D.C. Bradley, R.H. Moss and K.D. Sales, Chem. Commun. 1255, 1969.

288. C.E. Holloway, F.E. Mabbs and W.R. Smail, J. Chem. Soc., (A) 2980, 1968.

289. C.P. Stewart and A.L. Porte, J. Chem. Soc., Dalton Trans. 722, 1973.

290. S. Sabo, R. Choukroun and D. Gervais, J. Chem. Soc., Dalton Trans. 2695, 1983.

291. A. Davison, N. Edelstein, R.H. Holm and A.H. Maki, Inorg. Chem. **4**, 55, 1965.

292. N.M. Atherton and C.J. Winscom, Inorg. Chem. **12**, 383, 1973.

293. W. Kwik and E.I. Stiefel. Inorg. Chem. **12**, 2337, 1973.

294. A.A. DIamantis, J.B. Raynor and P.H. Rieger, J. Chem. Soc., Dalton Trans. 1731, 1980.

295. P.B. Ayscough in 'Spectroscopic Methods in Organometallic Chemistry', Edited by W.O. George, Butterworths, London, 1970, Chapter 5.

296. A. Davison, N. Adelstein, R.H. Holm and A.H. Maki, J. am. Chem. Soc. **86**, 2799, 1964.

297. R. Hämäläinen, U. Turpeinen and M. Ahlgren, Acta Cryst. **C41**, 1726, 1985.

298. S.J. Miles and J.D. Wilkins, J. Inorg. Nucl. Chem. **37**, 2271, 1975.

299. H.J. Seifert and W. Sauertig, ZL Anorg. Allg. Chem. **376**, 245, 1970.

300. G.W.A. Fowles, D.A. Rice and J.D. Wilkins, Inorg. Chim. Acta **7**, 642, 1973.

301. R.J.H. Clark and W. Errington, Inorg. Chem. **5**, 650, 1966.

302. N.J.H. Hawkins and D.R. Carpenter, J. Chem. Phys. **23**, 1700, 1955.

303. M.N. Mookerjee, R.V. Singh and J.P. Tandon, Trans. Metal Chem. **10**, 66, 1985.

304. H.J. Bielig and E. Bayer, Annalen **584**, 96, 1953.

305. M. Kitamura, K. Yamashita and H. Imai, Bull. Chem. Soc. Japan **49**, 97, 1976.

306. Y. Israel and L. Meites, J. Electroanal. Chem. **8**, 99, 1964.

307. M. Kitamura, K. Yamashita and H. Imai, Chem. Lett. 1071, 1975.

308. M.D. Stallings, M.M. Morrison and D.T. Sawyer, Inorg. Chem. **20**, 2655, 1981.

309. P.J. Bosserman and D.T. Sawyer, Inorg. Chem. **21**, 1545, 1982.

310. A. Kapturkiewicz, Inorg. Chim. Acta **53**, L77, 1981.

311. A.M. Bond, A.T. Casey and J.R. Thackeray, J. Chem. Soc., Dalton Trans. 773, 1974.

312. A.M. Bond, A.T. Casey and J.R. Thackeray, Inorg. Chem. **12**, 887, 1973.

313. T.L. Riechel, L.J. De Hayes and D.T. Sawyer, Inorg. Chem. **15**, 1900, 1976.

314. A.M. Bond and R.L. Martin, Coord. Chem. Rev. **54**, 23, 1984.

315. M.A. Hepler and T.L. Riechel, Inorg. Chim. Acta **54**, L255, 1981.

316. R.L. Lintvedt, in 'Copper Coordination Chemsitry: Biochemical and Inorganic Perspectives', Edtd. by K.D. Karlin and J. Zubieta, Adenine Press, N.Y., 1983, p. 129.

317. E.R. Brown and R.F. Large, in 'Physical Methods of Chemical Analysis, Part IIA - Electrochemical methods', Edtd. by A. Weissberger and B.W. Rossiter, Wiley-Interscience, N.Y., 1971, p. 423.

318. R.S. Nicholson and I. Shain, Anal. Chem. **36**, 706, 1964.

319. M. Nishizawa, K. Hirotsu, S. Ooi and K. Saito, J. Chem. soc. Chem. Comm. 707, 1979.

320. H. Taguchi, K. Isobe, Y. Nakamura and S. Kawaguchi, Bull. Chem. soc. Japan **52**, 452, 1979.

321. R.A. Rowe and M.M. Jones, Inorg. synth. **5**, 115, 1975.

322. J.J.R. Frausto da Silva, R. Wotton and R.D. Gillard, J. Chem. Soc., (A) 3369, 1970.

323. Beil. **9**, 319.

324. A.I. Vogel, 'Text Book of Practical Organic Chemistry'. 4th Edn., Longman, 1978.

325. I. Heilburn and H.M. Bunburry Edtd., 'Dictionary of Organic Compounds', Vol. 1, Eyre and Spottiswoode, London, 1953, p. 471.

326. I. Heilburn and H.M. Bunburry Edtd., 'Dictionary of Organic Compounds', Vol. 1, Eyre and Spottiswoode, London, 1953, p. 639.

327. M.S. Kachhawaha and A.K. Bhattacharya, J. Inorg. Nucl. Chem. **25**, 361, 1963.

328. D.T. Sawyer and J.L. Roberts Jr., 'Experimental Electrochemistry for Chemists', John Wiley and Sons, N.Y., 1974, p. 212.

329. D.D. Perrin, W.L.F. Armarego and D.R. Perrin, 'Purification of Laboratory Chemicals', 2nd Edn., Pergamon Press, 1980.

330. I.M. Kolthof and P.J. Elving, 'Treatise on Analytical Chemistry', Part II, Vol. 8, Interscience Publishers, 1963, p. 234.

331. L. Sacconi, J. Am. Chem. Soc. **75**, 5434, 1953.

332. L. Sacconi, P. Paoletti and F. Maggio, J. Am. Chem. Soc. **79**, 4067, 1957.

333. Beil, **2**, 648.

334. W.E. Rudzinski, T.M. Aminabhabi, N.S. Biradar and C.S. Patil, Inorg. Chim. Acta **69**, 83, 1983.

335. E. Czerwinska, Zł. Eckstein, R. Kowalik, H. Krzywicka and E. Zwierz, Dissert. Pharm. **15**, 369, 1964 (C.A. **61**, 3007b, 1964).

336. G. Schetty and W. Kuster, Helv. Chim. Acta **44**, 2193, 1961.

337. G. Schetty, Helv. Chim. Acta **53**, 1437, 1970.

338. D.J. Mackey, S.V. Evans and R.L. Martin, J. Chem. Soc., Dalton Trans. 1515, 1976.